INFORMATION TO USERS

This manuscript has been reproduced from the microfilm master. UMI films the text directly from the original or copy submitted. Thus, some thesis and dissertation copies are in typewriter face, while others may be from any type of computer printer.

The quality of this reproduction is dependent upon the quality of the copy submitted. Broken or indistinct print, colored or poor quality illustrations and photographs, print bleedthrough, substandard margins, and improper alignment can adversely affect reproduction.

In the unlikely event that the author did not send UMI a complete manuscript and there are missing pages, these will be noted. Also, if unauthorized copyright material had to be removed, a note will indicate the deletion.

Oversize materials (e.g., maps, drawings, charts) are reproduced by sectioning the original, beginning at the upper left-hand corner and continuing from left to right in equal sections with small overlaps.

Photographs included in the original manuscript have been reproduced xerographically in this copy. Higher quality 6" x 9" black and white photographic prints are available for any photographs or illustrations appearing in this copy for an additional charge. Contact UMI directly to order.

Bell & Howell Information and Learning
300 North Zeeb Road, Ann Arbor, MI 48106-1346 USA

UMI®
800-521-0600

DEVELOPMENT OF AN EFFECTIVE MODEL FOR PARTICLE SIZE DISTRIBUTION IN SUSPENSION COPOLYMERIZATION OF STYRENE/DIVINYLBENZENE

By

EDUARDO VIVALDO-LIMA, B. Sc., M. Eng.

A Thesis

Submitted to the School of Graduate Studies

in Partial Fulfilment of the Requirements

for the Degree of

Doctor of Philosophy

McMaster University

PSD IN SUSPENSION COPOLYMERIZATION OF STYRENE/DIVINYLBENZENE

DOCTOR OF PHILOSOPHY (1998)
(Chemical Engineering)

McMaster University
Hamilton, Ontario

TITLE: Development of an Effective Model for Particle Size Distribution in Suspension Copolymerization of Styrene/Divinylbenzene.

AUTHOR: Eduardo Vivaldo-Lima,
B. Sc. (Universidad Nacional Autónoma de México, UNAM)
M. Eng. (McMaster University)

SUPERVISORS: Professors Philip E. Wood, Archie E. Hamielec, and Alexander Penlidis
(University of Waterloo)

NUMBER OF PAGES: xiv, 221

ABSTRACT

An effective mathematical model for estimation of the Particle Size Distribution (PSD) in suspension copolymerization of styrene/divinylbenzene has been developed. Its effectiveness is shown as a compromise between a sound theoretical basis and the simplest possible mathematical structure, which makes possible the solution of the governing equations using conventional computational tools.

In building the model, a comprehensive and systematic approach was undertaken. The first stage of this approach was to critically review and analyse the literature in suspension polymerization. The most important weaknesses and deficiencies of the existing models and the approaches used to build them were identified, and a strategy to overcome them was designed and implemented. The second stage of the approach was to identify the key factors that control the PSD, and build mechanistic mathematical models of an intermediate and balanced degree of complexity. The third stage consisted of incorporating these mechanistic models into a macro-scale model of the PSD. Using novel experimental design techniques, the relative importance of the different factors on the PSD, and the aspects of the model that needed refinement were determined. The final stage consisted of implementing changes to the model in a balanced and effective way. The result was an improved model for PSD that assigns adequate weight to the importance of each key factor, with similar degree of complexity as the best models reported in the literature, but better performance and increased reliability of predictions.

Some of the contributions of this thesis to the field of Polymer Science and Engineering include: the development and validation of an effective model for crosslinking free-radical copolymerization kinetics; the establishment of prescriptions to guide the efforts in the acquisition and interpretation of information aimed at improving our understanding and modelling capabilities of suspension polymerization reactors; the inclusion, for the first time in suspension polymerization modelling, of non-homogeneous mixing in the stirred tank reactor into the PSD model; the development of

mathematical models for breakage and coalescence in liquid-liquid dispersions, and the systematic and effective use of mechanistic modelling for experimental design purposes in polymer production studies.

ACKNOWLEDGEMENTS

After several years of mixed emotions and experiences, this thesis finally comes to an end. I could not have accomplished this important objective of my professional and academic life without the help or influence from several individuals, to whom I am deeply and sincerely grateful. Some of them are acknowledged here:

Professors Philip E. Wood, Archie E. Hamielec, and Alexander Penlidis, my thesis supervisors. The three of them provided continuous guidance, encouragement and support. Even though sometimes it was difficult to come to terms with four different points of view (mine included), I consider myself lucky for having been able to be supervised by three individuals who are known and recognized as leading authorities in their disciplines.

Professors Harald Stöver (Chemistry Department) and Shiping Zhu, members of my Ph.D. Supervisory Committee, for their interest in this project, their valuable insights and comments, and their technical assistance throughout the development of this project.

Greg Emery, Doug Keller and Kris Kostanski (MIPPT); Elizabeth Takacs (CAPPA-D); Wen-Hui Li and Brian Sayer (Chemistry Department); Justyna Derkach, J. Maiolo, and Paul Gatt (Research Staff, Dept. of Chemical Engineering); Shaffiq Jaffer; and Jun Gao and Neil McManus (IPR, Dept. of Chemical Engineering, University of Waterloo), for their technical assistance in the different experimental stages of this thesis. I also thank Sara Gallo O'Toole, Barb Owen, and Gord Slater for their assistance with many frequent administrative issues.

Professors John MacGregor, Andy Hrymak and Robert Pelton, for their helpful comments or suggestions with some different aspects of the theoretical and experimental issues of this thesis. Coincidently, the three of them (and Professor Zhu) had a positive influence on my increased attraction towards teaching and learning. I was lucky to have worked for them as teaching assistant in some of their undergraduate courses. Also influential in my increased interest on teaching and learning are Mr.

Dale Roy (Instructional Development Centre, McMaster University), and Professor Don Woods.

Consejo Nacional de Ciencia y Tecnología (CONACYT), Mexico; Departments of Chemical Engineering, McMaster University and University of Waterloo, for their financial support.

Drs. Enrique Saldívar and Leonardo Rios for their positive influence in some of my career choices. I also thank them, along with Drs. Luis García-Rubio and Marco A. Villalobos, for their interest in my research work and their help, advice and recommendations during my job search.

My wife Adry, who provided me with the best moments and memories of my stay in Canada, and who shared most of the frustrating moments and feelings that were frequent during the execution of this thesis.

I thank very specially my original (mother, sister, brothers, sisters in law, nephews and nieces) and extended (my wife's parents, sister, brother and relatives) families for their continuous and unconditional love, encouragement, and moral support.

Finally, although we were never close, I wish to use this thesis as a small tribute to the memory of my father, Lauro Vivaldo, who died while I was in Canada. There is a lot of you in each and everyone of us, your "children". Descanse en Paz.

TABLE OF CONTENTS

LIST OF FIGURES

LIST OF TABLES

Chapter 1

GENERAL INTRODUCTION

1.1 Opening Remarks and Problem Definition

Like it or not, synthetic polymers are present almost everywhere we look at in any place of today's world. Even at the most remote places on Earth you may be able to find a non-pleasant reminder of the presence of the "most civilized" members of the "most evolved" species in nature (the human being): polymer waste (empty bottles which used to contain "pure" water, cracker's packaging waste, etc.). As with any technological improvement, what we get from synthetic polymers depends on how we use them. Polymers can be used to produce useless and senseless "commodities" but, on the other hand, polymers can and are being used to produce the materials that can save lives (countless applications in medicine and biotechnology), take us to previously unthinkable places (e.g., space), improve our quality of life, etc.

Polymers are very large macromolecules made out of smaller units, monomers, which are attached to each other by chemical covalent bonds. The size (number of units), type of monomer(s) and spatial configuration of these macromolecules can lead to an immense range of physical and chemical properties and applications. Crosslinked polymers (polymer networks) are very important in technology, medicine, biotechnology, and agriculture (as construction materials, polymer glasses with high mechanical strength and high thermal stability, rubbers, ion-exchange resins and sorbents, insoluble polymer reagents, etc.). Poly(styrene-divinylbenzene) is a crosslinked polymer used for chromatographic applications and as precursor for ion-exchange resins, among other uses. It is also a model system in the study of network formation via crosslinking free-radical copolymerization.

Suspension polymerization is a fairly old and relatively simple process used to produce low volume demand polymers (compared to the production volumes of continuous processes). Its description and review of the state of the art on modelling of this process are detailed on Chapter 2 of this thesis.

This Ph.D. thesis is intended to consolidate and expand the previous theoretical and practical knowledge about suspension polymerization processes. More specifically, it is intended to focus on the polymer particle size distribution design and prediction in the free-radical suspension copolymerization of water insoluble monomers, where the initiator is soluble in the monomer/polymer phase and a stirred tank reactor operated in a batch mode is used.

Consolidation is meant to put together and improve, when necessary, the present theories of mixing, rheological, surface and polymerization phenomena as applied to this situation. Expansion is meant to remove, modify or adapt their present limitations or restrictions, so that a general mathematical model with predictive power capabilities can be developed.

Put it briefly, this project is intended to effectively quantify what we already know (mainly qualitative) about this process, to propose or try new ideas that have not been considered or implemented in this context, and to build a stronger framework which may facilitate the incorporation of major new changes in suspension polymerization technologies.

1.2 Research Goal and Objectives

The main goal of this thesis is to develop effective mathematical models for the estimation and design of the polymer particle size distribution obtained in suspension copolymerization processes. These models should aid in the development of more rational and less expensive strategies for the design of new technologies or modifications of the present ones in the manufacture of resins via suspension polymerization. To accomplish our goal, the following objectives were stated:

a) Identify the factors that control the PSD and quantify their relative importance, using carefully designed experiments and critical analysis of the existing literature in the field.

b) Develop an effective (namely, accurate and simple) model for the free-radical crosslinking copolymerization kinetics of vinyl/divinyl monomers.

c) Develop effective models for the breakage and coalescence phenomena involved in suspension polymerization.

d) Incorporate the effect of non-homogeneous mixing into the PSD model in a balanced and effective way.

e) Insert or couple the previous models into a population balance equation, and model different copolymerization conditions.

f) Test the predictive power of the PSD model.

1.3 Thesis Outline

Most of the research undertaken and reported in this thesis has been already published or submitted to publications in specialized journals of the polymer and chemical engineering areas. Each chapter is made out of one of such papers and, therefore, it has its own structure, objectives, conclusions and references. This thesis format, known as "the Sandwich Thesis", is officially accepted by the School of Graduate Studies of McMaster University. Although the papers are self-structured and self-contained, there is a logical structure and sequence in this thesis. Figure 1.1 shows a schematic representation of the structure of this thesis. Each box describes a major component of the thesis. The chapter(s) associated to each of these components are indicated in brackets. The sequence and inter-relation among different components are indicated with arrow-ended lines. The broken lines indicate flow of information and activities among components that do not flow through the other components. A more specific description of each chapter is offered below.

Chapter 1 provides a research context. The main goal and objectives of the thesis are explained, as well as its structure and outline. The description of the different factors that influence the particle size distribution in suspension polymerization and the selection of factors and responses considered in this study are also offered in this chapter.

Chapter 2 offers a comprehensive and critical review of the state of the art in modelling of particle size distribution in suspension polymerization reactors. A systematic research approach to the study of suspension polymerization is proposed in this chapter. The execution of several of the activities proposed in this approach is the scope of the remaining chapters of this thesis. The paper reproduced in this chapter was published in *Industrial and Engineering Chemistry Research*. This paper was coauthored by my research supervisors. The author of this thesis, the main author of the paper, designed the structure of the paper, carried out the literature review, uncovered the strengths and weaknesses of the existing models, and proposed the research approach described in the paper. Professor P.E. Wood suggested making significant changes to section 2.2.2 (Mixing Phenomena) of the original manuscript, provided valuable insight and some key references as to what aspects of this section were weak in the early version of the paper. Professor A.E. Hamielec provided expert insight about section 2.2.6 (Polymerization Effects). Finally, Professor A. Penlidis continuously brought to the authors' attention several recent publications about all aspects of the contents of the paper, and suggested writing a review paper out of my original Ph.D. research proposal. The three supervisors read the finished manuscript and made critical and editorial comments.

As observed in Figures 1.1 and 1.2, the polymerization kinetics has a major effect on the evolution of the particle size distribution. The M. Eng. thesis of the author dealt with the development of an effective model for the crosslinking free-radical copolymerization kinetics of the polymerization system used in the present thesis. In Chapter 3, the kinetic model developed in the M. Eng. thesis was used to design the recipe and polymerization conditions to be used herein. With the designed conditions, the synthesis in glass ampoules of a copolymer of styrene and divinylbenzene and the characterization of its properties were carried out.

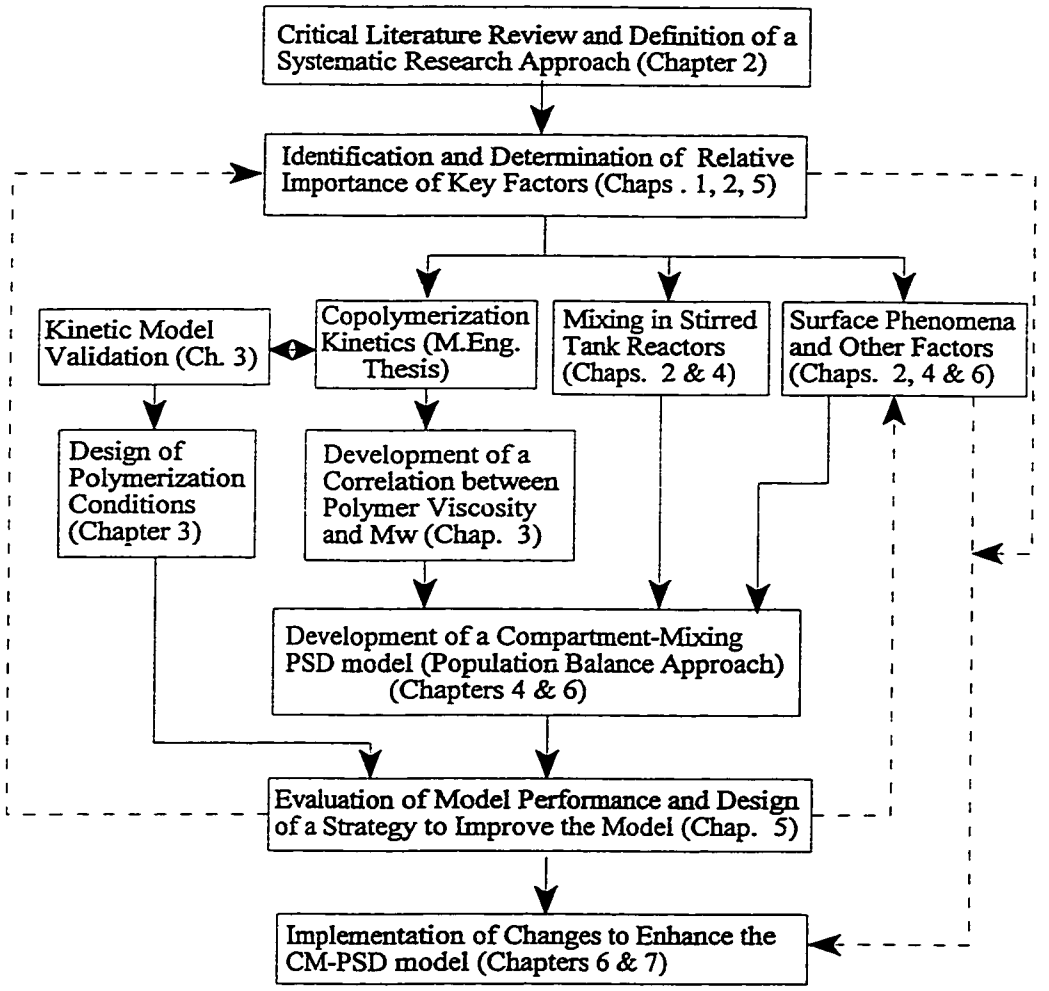

Figure 1.1 Thesis Structure.

The experimental data obtained in Chapter 3 were used to test the predictive power of the copolymerization kinetic model. The polymerization conditions designed in this chapter were used in the suspension polymerization experiments in a pilot plant reactor reported in Chapters 4, 5 and 6. A correlation between zero-shear polymer viscosity and weight-average molecular weight was also developed in this chapter. The contents of this chapter were accepted for publication in the *Journal of Polymer Science, Part A: Polymer Chemistry*. The author of this thesis designed the experiments, carried out the synthesis and characterization of the polymer product, and tested the predictive power of the kinetic model. Professors Wood, Hamielec and Penlidis made critical and editorial comments to the manuscript. Professor Penlidis also made arrangements to carry out several of the characterization measurements at the University of Waterloo.

Chapter 4 is devoted to the development of a mathematical model for PSD in suspension polymerization. The emphasis of this model is on the effect of non-homogeneous mixing in the tank reactor. An adequate balance of the complexity of the mathematical equations that model the effect of the key factors that control the PSD was sought. The copolymerization kinetic model and the viscosity correlation developed in Chapter 3 are used in the model developed in Chapter 4. The model developed here is tested against experimental data in a pilot plant reactor from the literature, as well as experimental data generated as part of this thesis. The contents of this chapter were accepted for publication in *The Canadian Journal of Chemical Engineering*. The author of this thesis developed the mathematical model, developed a computer program to solve the model equations, carried out the pilot plant experiments, and performed the data analysis and comparison of results. Some concepts and characteristics of the mixing model were influenced by ideas from Professor P.E. Wood. He and Professors Hamielec and Penlidis read the manuscript and provided critical and editorial comments.

In Chapter 5, a strategy to improve the predictive power of the PSD model developed in Chapter 4 is proposed and implemented. The strategy consists of determining the relative importance of the factors that control the PSD using a Bayesian design of experiments where the prior knowledge needed for this technique is generated with the PSD model developed in Chapter 4.

A pilot plant reactor is used to carry out the suspension copolymerization experiments of Chapter 5. The statistical analyses of results from these experiments provide valuable information as to which aspects of the model are weak, and how much degree of complexity on the model equations for the factors that need improvement should be sought. The contents of this paper were submitted to *AIChE Journal*. The author of this thesis proposed use of the approach to guide the refinement of the PSD model, designed and carried out the experiments, and performed the required statistical analyses. Professor A. Penlidis provided detailed reports where the use of the Bayesian experimental design technique in a similar context was documented, and provided the author of this thesis with a computer program for Bayesian design of experiments developed by his research group at the University of Waterloo. Professors Wood and Hamielec read the manuscript and provided critical and editorial comments.

Chapter 6 reports the development of an improved model for PSD based on the results from chapters 4 and 5. The emphasis is placed on the insufficiently explained factors that were detected in Chapter 5. The contents of this chapter have not been published yet. The objectives of this thesis have already been fulfilled with the results of Chapters 1 to 6. A publishable paper that follows up on the guidelines established in Chapters 6 and 7 is being prepared by the author of this thesis as one of the first fruits from his work as an independent researcher.

Finally, in Chapter 7, overall conclusions, a summary of contributions to knowledge derived from the development of this thesis, and some recommendations for future research in this area are offered.

1.4 Selection of Factors and Responses

Suspension polymerization is a complex process whose PSD is affected by many factors. As shown in Chapter 2, there have been many studies related to the study of the effects of these parameters on the PSD, although few of them have been complete and systematic. These factors, listed in the first column of Table 1.1, can be classified into four categories: polymerization kinetics, surface phenomena, intensity of mixing, and dispersion concentration, as shown in Figure 1.2.

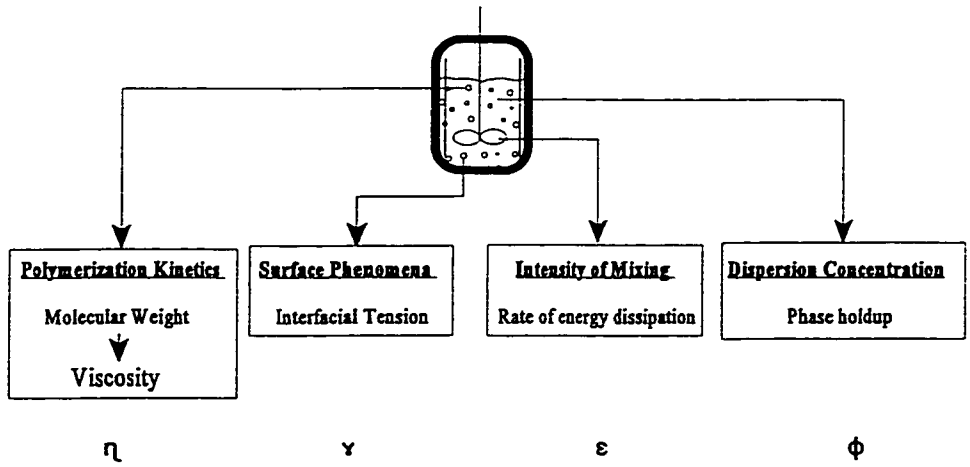

Figure 1.2 Important Factors for Modelling of Particle Size Distribution in Suspension Polymerization.

Some of the responses that can be related to the PSD in suspension polymerization are listed in the second column of Table 1.1. The responses related to the polymerization kinetics were measured independently from batch experiments in glass ampoules, as documented in Chapter 3. This is possible due to the insolubility of the monomer, polymer and initiator in the continuous phase (water). In Chapters 4, 5 and 6, mean particle size (MPS), coefficient of variation (CV), or measurement of the full PSD were used as responses.

The values of some of these factors can be fixed *a priory*. It is known that the kinetics of polymerization strongly affects the particle size distribution (PSD), but this dependence goes in only one direction (namely, the PSD does not affect the kinetics of polymerization in bead suspension polymerization). The link between the polymerization kinetics and the PSD is the zero-shear viscosity of the disperse phase, which depends on the molecular weight of the polymer. The effect of the kinetic factors on molecular weight development are reasonably well understood and can be studied independently.

The only need to change the values of the kinetic factors is to generate different molecular weight evolution profiles (thus, different viscosity evolution profiles). A known and adequate evolution profile can be obtained by choosing appropriate values for crosslinker concentration, temperature, initiator concentration, and concentration of chain transfer agent. To choose these values, the kinetic model developed in the author's M.Eng. Thesis (1993) was used (see Chapter 3). The remaining kinetic factors were fixed to their design values, as explained in Chapter 3 of this thesis.

Table 1.1 Important Factors and Responses in Suspension Polymerization.

Factors	Responses
Polymerization Kinetics Monomer Type Monomer Concentration Crosslinker Concentration (Comonomer Concentration) Temperature Initiator Type (mono- or bi-functional) Initiator Concentration Presence or Absence of Chain Transfer Agent CTA Concentration Inhibitor Type Inhibitor Concentration Intensity of Mixing Gravity Effect (Froude Number) Agitator Design Impeller Diameter Agitation Speed Agitation Time Off-bottom clearance Distance of separation between impellers Presence or Absence of Baffles Vessel Configuration (Geometry of the tank) Reactor Volume Surface Phenomena Stabilizer type (protective colloid or inorganic powder) Stabilizer Concentration Dispersion Concentration Disperse Phase Holdup	Main Responses Mean Diameter Particle Size Distribution Identity Point Secondary Responses Conversion Dispersed Phase Viscosity Viscoelasticity Molecular Weight Averages Interfacial Tension

Chapter 2

An Updated Review on Suspension Polymerization[1]

Eduardo Vivaldo-Lima, Philip E. Wood*, and Archie E. Hamielec
McMaster Institute for Polymer Production Technology, Department of Chemical Engineering, McMaster University, Hamilton, Ontario, Canada, L8S 4L7.

Alexander Penlidis
Institute for Polymer Research, Department of Chemical Engineering, University of Waterloo, Waterloo, Ontario,Canada, N2L 3G1.

Abstract

An updated review on suspension polymerization is presented. The time period from 1991 to 1995 is stressed, as well as research articles or reports not considered in previous reviews. Our review is aimed at providing a sound basis for the theoretical background required to build an effective model for the particle size distribution (PSD) in suspension polymerization. All major phenomena that affect the PSD are considered, and a proposed approach to develop an accurate, yet simple model is included. Most of the experimental information in this review is related to the styrene/divinylbenzene copolymerization system, although the ideas and models are not exclusive to this system.

2.1 Introduction

Several detailed and complete literature reviews on Suspension Polymerization have already been published (Hamielec and Tobita, 1992; Arshady, 1992; Yuan et al., 1991; Brooks, 1990; Dawkins, 1989; Villalobos, 1989; Vivaldo-Lima, 1989; Mitchell, 1986). What will be stressed in the present review is information not considered in the previous reviews, or information that is believed to be of importance for the adequate understanding of a more detailed and effective modelling of this process. This literature review will be separated into "Modelling" and "Experimental studies", for convenience.

---

[1]Reprinted with permission from *Ind. Eng. Chem. Res.* **1997**, 36, 939-965.

The term suspension polymerization describes a process in which monomer(s), relatively insoluble in water, is (are) dispersed as liquid droplets with steric stabilizer and vigorous stirring (which is maintained during polymerization) to produce polymer particles as a dispersed solid phase. Initiators soluble in the liquid monomer phase are employed in this polymerization process. The terms pearl and bead polymerization are also used for the suspension polymerization process when particle porosity is not required. The major aim in suspension polymerization is the formation of as uniform as possible dispersion of monomer droplets in the aqueous phase with controlled coalescence of these droplets during the polymerization process. The interfacial tension, the degree of agitation, and the design of the stirrer/reactor system govern the dispersion of monomer droplets, typically with diameters in the range of 10 μm to 5 mm. The presence of suspending agents (e.g. stabilizers) hinder the coalescence of monomer droplets and the adhesion of partially polymerized particles during the course of polymerization, so that the solid beads may be produced in the same spherical form in which the monomer was dispersed in the aqueous phase. Many (but not all) important commercial suspension polymers yield bead sizes above 10 μm, and so these relatively large particles (compared with emulsion particles) are simply isolated by filtration and/or sedimentation (Dawkins, 1989). A clear distinction among the terms "suspension", "emulsion", "dispersion", and "precipitation" as used in reference to heterogeneous polymerization systems was made by Arshady (1992).

Non-aqueous suspension agents such as paraffin oils have been developed to polymerize polar monomers, such as acrylic acid. The so-called water-in-oil (W/O) suspension polymerization (reversed phase suspension polymerization) comprises an aqueous solution containing the hydrophillic monomer(s) and initiator(s), which are dispersed in a liquid paraffin oil or other non-polar hydrocarbon media and polymerized. The use of perfluorocarbon fluids has extended the scope of the suspension polymerization method to monomers and initiators that can not be used due to their high solubility and reactivity in conventional suspension media (Zhu, 1996).

The reactor vessel is usually a stirred tank. The monomer phase is subjected either to turbulent pressure fluctuations or viscous shear forces, which break it into small droplets that assume a spherical

shape under the influence of interfacial tension. These droplets undergo constant collisions (collision rate≥ 1 s^{-1}), with some of the collisions resulting in coalescence. Eventually, a dynamic equilibrium is established, leading to a stationary mean particle size. Individual drops do not retain their unique identity, but instead undergo continuous breakup and coalescence. In some cases, an appropriate dispersant can be used to induce the formation of a protective film on the droplet surface. As a result, pairs of clusters of drops that tend to coalesce are broken up by the action of the stirrer before the critical coalescence period elapses. A stable state is ultimately reached in which individual drops maintain their identities over prolonged periods of time (Hamielec and Tobita, 1992).

In the case of a polymer that is miscible in all proportions with its monomer (e.g. styrene and methyl methacrylate), a very large variation of the range of the dispersed phase viscosity is observed during the course of polymerization. The initially low viscosity liquid monomer is transformed gradually into an increasingly viscous polymer in monomer solution and, as conversion increases, the dispersed phase acquires the characteristics of a solid particle. Particularly in the "tacky" intermediate stage, individual polymer particles tend to form incompletely fused clumps. Agglomeration at this critical stage of conversion is somewhat inhibited by the action of the dispersant, but other effective measures to reduce coalescence may also be taken, including adjusting the densities of the two phases to make them more similar, or increasing the viscosity of the aqueous continuous phase. Rapid polymerization during the sticky stage minimizes the number of effective collisions among polymer particles and thus should reduce coagulation (Hamielec and Tobita, 1992).

The most important issue in the practical operation of suspension polymerization is the control of the final particle size distribution. The size of the particles will depend on the monomer type, the viscosity change of the dispersed phase with time, the type and concentration of stabilizer, and the agitation conditions in the reactor. The particle morphology is an important characteristic for the application of the polymer product, particularly in the cases of expandable polystyrene, ion-exchange resins, and poly(vinyl chloride) (Yuan et al., 1991). The polymerization kinetics and the mechanism of primary particle aggregation in the polymerization of vinyl chloride are rather different to the ones

present in bead polymerization. The differences are mainly due to the insolubility of polyvinyl chloride in vinyl chloride. Modelling of the polymerization kinetics and particle size distribution (using a population balance equation) in vinyl chloride polymerization has been addressed by the group of Kiparissides (e.g., Dimadopoulos et al., 1990, and Kiparissides, 1990).

Suspension polymerization has the following advantages compared with the other polymerization processes (bulk, solution, and emulsion): easy heat removal and temperature control; low dispersion viscosity; low levels of impurities in the polymer product (compared with emulsion); low separation costs (compared with emulsion); and final product in particle form. On the other hand, among the disadvantages of suspension polymerization one may refer to: lower productivity for the same reactor capacity (compared to bulk); wastewater problems; polymer build-up on the reactor wall, baffles, agitators, and other surfaces; no commercial continuous process operable yet; difficult to produce homogeneous copolymer composition during batch suspension polymerization (Yuan et al., 1991). Semi-batch operation is more difficult with suspension versus emulsion polymerization because of the lower interfacial area (particle/water).

A number of important commercial resins are manufactured by suspension polymerization, including poly(vinyl chloride) and copolymers, styrene resins (general purpose polystyrene, expandable polystyrene (EPS), high impact polystyrene (HIPS), poly(styrene-acrylonitrile) (SAN), poly(acrylonitrile-butadiene-styrene) (ABS), styrenic ion-exchange resins), poly(methyl methacrylate) and copolymers, and poly(vinyl acetate) (Yuan et al., 1991).

No continuous suspension polymerization process is known to be employed on a commercial scale, but such processes have been carried out in the laboratory and on pilot-plant scale. Some of the problems with continuous suspension polymerization are: deposition of polymer on the wall of the reactor during polymerization (which will affect the heat transfer through the reactor jacket), deposition of viscous monomer-polymer particles on the pipes and pumps, and difficulty to achieve high conversions (Yuan et al., 1991).

In the last decade, most manufacturers of suspension polymers and copolymers have faced a decrease on profits due to technological improvements on rival processes and other unfavourable economic factors. This situation led Villalobos (1993) to recommend that suspension polymerization technologies should be focused to the manufacturing of specialty copolymers (of low-volume, high-value added type). Although the analysis presented by Villalobos (1993) is valid, it should also be pointed out that the lack of deep and effective understanding on the fundamentals and therefore, practical issues (operation/modification of present processes) concerning the suspension polymerization technologies has also promoted the replacement of technologies.

The inadequacy of traditional suspension polymerization processes to produce polymer of narrow particle size distribution (mainly in the ion-exchange and chromatographic material production applications) motivated the development of a technology using an encapsulation step of monomer droplets (Matsumoto et al., 1989), previous to the polymerization step (which can then be carried out in suspension without using stabilizers). Other examples of replacement of technologies are the proposal of a circular loop reactor to carry out the suspension polymerization, which was reported to be superior for the production of the polymer (polystyrene) particles of uniform size than the conventional suspension polymerization process (Tanaka and Hosogai, 1990), the development of a method for the production of large spherical monosized polymer particles where monosized droplets of 2-hydroxyethyl methacrylate (HEMA) and glycerol monomethacrylate (GMA) were made by passing the monomers under pressure through a nozzle coupled to an energized piezoelectric crystal (Colvin et al., 1990), the use of a suspension polymerization (of methyl methacrylate) in a "gelled" solution of water and agarose (which immobilizes the polymerizing particles all along the reaction) (Polacco et al., 1994), and the use of a Shirasu porous glass (SPG) membrane emulsifier to generate styrene drops of uniform size which would later polymerize in an agitated tank reactor (Hatate et al., 1995).

The step of scaling up a reactor from pilot plant to industrial scale, is an issue where much empiricism is still used and where expensive and time consuming experimental programs are usually

required. Okufi et al. (1990) concluded that complete geometric, kinematic, dynamic, chemical and thermal similarity cannot be simultaneously achieved in a scale up procedure and that differences should be allowed at some point. Other researchers have arrived at this same conclusion independently, after several months of experimental and theoretical work (e.g. Villalobos, 1989; Chylla, 1994). Indeed, this same issue has taken commercial producers years of experience, which most of the time is not shared due to secrecy policies.

Although the suspension polymerization process has been widely studied over more than 50 years, the present situation is that its understanding is still limited and a lot of experimental effort and empirical knowledge are still used to design new resins and to scale their production up from a pilot scale reactor to an industrial level one. The least developed issues in the suspension polymerization process are related to the changing rheological behaviour of the reacting mass during polymerization, the non-homogeneous flow and rate of energy dissipation field distributions within the tank reactor, and the relationship among them and the polymerization kinetics with the breakage/coalescence phenomena that ultimately determine the particle size distribution.

2.2 Modelling

2.2.1 Population Balance Equation

Polymerization processes can be classified in several levels on which modelling is important. These levels are: Microscale Chemical Kinetics (chain growth, chain branching, end group formation, and multifunctional sites), Mesoscale Physical Phenomena (interphase equilibria, interphase heat and mass transfer, intraphase heat and mass transfer, fluid mechanics and micromixing, polymer morphology), and Macroscale Reactor Phenomena (macromixing residence time distribution, overall material and energy balances, particle population balances, heat and mass transfer from the reactor, and reactor dynamics and control). Usually, separate models are required at each level and simplified versions of the smaller scale models are incorporated as the scale grows larger. In this way the level of detail is appropriate to the task at hand (Ray, 1991).

For the suspension polymerization case, the microscale chemical kinetics is reasonably well understood. The macroscale has been considered independently from the other scales, so that effective interconnection has not been obtained to date. It seems that the least understood scale is the mesoscale (breakage/coalescence phenomena).

Modelling the PSD requires a start from the macroscale stage. The model at this stage is usually represented by a population balance equation. An excellent review on the status of population balances was presented by Ramkrishna (1985). A Monte Carlo Technique can also be used to model the drop interactions (Ramkrishna, 1985; Das, 1996). The Monte Carlo techniques are extremely flexible, powerful and free of convergence problems, but they require so much computer time that they are not practical for many purposes (Laso et al., 1987a). In this review a population balance model will be considered. The population balance equation for a suspension polymerization system can be expressed as shown in equation (1) (Alvarez et al., 1994a), where F(u,t)= drop volume distribution, r_p= polymerization rate referred to dimensionless monomer concentration, u,v= monomer/polymer droplet volume, t= time, β= breakage rate distribution, κ= coalescence rate distribution, v= number of daughter drops after breakage of a mother drop, ξ= normalized daughter drop distribution, and ψ= polymerization volume contraction factor.

$$\frac{\partial F}{\partial t} = \psi r_p\left(F + u\,\frac{\partial F}{\partial u}\right) + \int_u^{\infty}\beta(v)\,v(v)\,\xi(v,u)\,F(v,t)\,dv + \int_0^{\frac{u}{2}}\kappa(u-v,v)\,F(u-v,t)\,F(v,t)\,dv - \int_0^{\infty}\kappa(u,v)\,F(u,t)\,F(v,t)\,dv - \beta(u,t)\,F(u,t) \qquad (1)$$

What is basically needed to obtain the PSD, or F(u,t) in equation (1), is to develop effective models for each one of the terms in the kernels of the integrals and to solve the equation. In the following subsections we will review some of the most important modelling approaches available in the literature to take into account the polymerization, surface, rheological and turbulent mixing phenomena in these functions.

Before proceeding into an independent analysis of each phenomenon, it should be pointed out that equation (1) implicitly assumes that the PSD does not depend on position within the tank reactor, namely, homogeneous flow and rate of energy dissipation fields are being assumed. If a non-homogeneous flow field was to be assumed, an external physical variable should be considered in the population balance equation, in addition to the internal one (droplet volume). A more general population balance equation that considers an external variable (position) is described in Randolph (1964). The issue of non-homogeneity in the tank will be discussed further in Section 2.4 of this paper (Suggested Research Approach). Also important at this point is to note the approaches that have been implemented to approximate F(u,t) itself (what will be discussed in the following subsections deals mainly with the other terms of equation (1)), and the numerical methods used to solve equation (1).

The population balance equation, as applied to different situations, has been solved by different methods, such as Finite Differences (e.g. Mikos et al., 1986; Kiparissides, 1990; Ribeiro et al., 1995; Baldyga et al., 1995b), Orthogonal Collocation, Method of Weighted Residuals using problem-specific polynomials generated by an orthogonalization process with a suitable weight function in the definition of the inner product (e.g. Valadez-González, 1988), Method of Moments (e.g. Aduna-Espinoza, 1991), Method of Classes (Chatzi and Kiparissides, 1992), Collocation on Finite Elements (e.g. Saldívar-Guerra, 1986; Saldívar Guerra et al., 1989; Zamora, 1990; Alvarez et al., 1991 and 1994a), Self-Preserving Distributions or Similarity Solutions (Ramkrishna, 1985), and a wavelet-Galerkin method which converts the problem of solving scaled differential and integro-differential equations to one of soiving a linear system of equations for unknown wavelet series coefficients (Chen et al., 1996). Section 6 on Ramkrishna's review (1985) provides descriptions of some of the techniques, and a detailed compilation of references on the solution of population balance equations.

Other researchers (e.g. Hounslow et al., 1988; Lister et al., 1995; Hill and Ng, 1995; Kumar and Ramkrishna, 1996a, 1996b) have used discretized population balances (DPB) where the PSD function is assumed to be constant within each interval, and a linear or adjustable geometric size discretizations of the size domain are used. Smit et al. (1994, 1995) used a DPB to predict

mathematical gelation (which is manifest in a divergence of the sixth moment and in a decrease in the third moment of the PSD), and used this concept to develop a method to reduce the number of kernels that one might consider as candidates for use in modelling experimental data (their method is summarised by the following rule: "do not use gelling kernels if physical gelation does not occur and use them if it does").

Some of the previous methods present numerical ill-conditioning and all of them, except for the method of moments, transform the size domain from an infinite one to a finite one. In general, these methods involve many equations and require a lot of computational time. The method of moments is usually more attractive for the case where the distribution function is unimodal (Aduna-Espinoza, 1991).

Regarding the estimation of F(u,t), the method of moments does not impose a specific functionality to the PSD, but it implies that the density function is unimodal. Some of the orthogonal collocation and collocation with finite elements techniques use a weighted residual function which contains a weight function "similar" in shape to the function being estimated. In this regard, Valadez-González (1988), Saldívar Guerra et al. (1989), and Alvarez et. al. (1991 and 1994a) used a gamma function as the weight function. It has also been assumed that the PSD has a specific known function and this function is immersed into the population balance. Mikos et al. (1986) assumed that the initial PSD was a logarithmic normal distribution. Vivaldo-Lima (1989) assumed that the PSD could be represented by a gamma density distribution function and estimated the parameters of the gamma distribution that produced the same mode as the experimental PSD. Other researchers have used specific analytical functions to approximate F(u,t) (either for unimodal or bimodal distributions), although not necessarily within a population balance context (e.g., Kalfas and Ray, 1993b; Nishikawa et al., 1994; Moreira et al., 1995).

Laso et al. (1987a) developed a model for liquid-liquid dispersions which was based on a geometrically discretized version of the population balance equation. Assuming that breakage is a first order process where only breakage into equally sized drops is considered, that coalescence is a second

order process where only coalescence between equally size drops is considered, and that breakage and coalescence at each class are characterized by a pair of constants, they reduced the population balance equation to a set of differential equations for the number of drops in each of the discretized classes.

2.2.2 Mixing Phenomena

2.2.2.1 Importance of Mixing on Suspension Polymerization

It has long been recognized that some of the important factors that influence the PSD in a suspension polymerization are: geometry and size of the vessel, type of stirrer, stirrer diameter (relative to the reactor dimensions), bottom clearance of the stirrer, presence or absence of internal fittings (such as baffles), and amount of energy supplied to the fluid through the impeller rotation (Hamielec and Tobita, 1992). All these factors will determine the flow and energy fields inside the tank. In the presence of electrolytes electrical effects are also important, as pointed out by Tobin et al. (1992).

All the modelling studies which have used the population balance approach, equation (1), have assumed that the Kolmogorov theory of local isotropy (Shinnar and Church, 1960; Shinnar, 1961), as applied to stirred tanks, is valid. Even though the theory of local isotropy does not necessarily imply that a single value for the rate of energy dissipation should be used, most of the models for PSD in suspension polymerization do use a single average value for the whole vessel (as will be mentioned later, there have been some exceptions). Doing so, allows for equation (1) to be independent of position within the tank reactor. In other words, all the modelling studies on suspension polymerization that we are aware of, have considered a homogeneous energy (rate of energy dissipation) field. Some of them have been aware of the fact that the impeller zone is highly energetic (where most breakage of droplets take place), and the bulk is much less energetic (most coalescence takes place in the bulk of the tank) (e.g. Yuan et al., 1991), but nonetheless, that fact has not been incorporated properly into their models.

If one were to characterize the role of mixing in a suspension polymerization with a single

"parameter", that should be the rate of energy dissipation, ϵ (as will become clear later, this importance comes from turbulence theory). In the following subsections on mixing, some highlights on turbulence theory and modelling of the rate of energy dissipation will be briefly outlined. A section on scaling-up of tank reactors, a summary of the most recent trends and developments on modelling of stirred tank reactors, and a suggested approach for modelling that is aimed at establishing a compromise between the highly sophisticated computational fluid dynamics (CFD) techniques and the unrealistic homogeneous modelling approach, will also be included.

2.2.2.2 Highlights about Turbulence Theory

This subsection is not intended to provide a detailed introduction to turbulence theory. The intention is to stress some of the important concepts and limitations of the theory, in the context of a stirred tank reactor. Turbulent fluid motion is an irregular condition of flow in which various components show a random variation with time and space coordinates so that statistically distinct average values can be determined (Hinze, 1987). The fluctuations on velocity due to the random character of a turbulent flow will result in a range of frequencies. These frequencies reflect different "scales" of turbulent motion. Because of the stochastic nature of turbulence, the local fluid velocity, $v_x(x,t)$, can be expressed as the contributions of a mean velocity, $\langle V(x) \rangle$, and a instantaneous velocity fluctuation, $v'_x(x,t)$, as expressed in equation (2) (x in equation (2) denotes the "x-direction" in a Cartesian coordinate system).

$$v_x(x,t) = \langle V(x) \rangle + v_x'(x,t) \qquad (2)$$

The turbulent flow field in a stirred tank reactor (and in any flow system) can be described by the Navier-Stokes governing equations. These equations for momentum and continuity can be represented by (tensorial) equations (3) and (4), where v is velocity, x is direction (in a coordinate system), t is time, p is pressure, ρ is density, and ν is kinematic viscosity (viscosity/density, μ/ρ). Strictly speaking the problem is solvable. There are four unknowns (three components of velocity and

pressure), and four equations (equation (3) for each coordinate, and equation (4)). However, there is a problem of resolving all the scales of fluid motion. The Navier-Stokes equations are usually solved numerically, although the non linear term (second in equation (3)) complicates the numerical solution. In order to resolve for the smallest motions (smallest eddies), very fine numerical grids would be needed (and thus, prohibitive computational demands). Even if these equations were solved, the solution would provide much more information than is useful for this flow field. The usual way to proceed is to use average values. To obtain an equation that describes the average (on time) velocity, equation (2) is plugged into equation (3), and averaged. The result is (tensorial) equation (5), which describes a steady flow (on the mean).

$$\frac{\partial v_i}{\partial t} + v_j \frac{\partial v_i}{\partial x_j} = -\frac{1}{\rho}\frac{\partial p}{\partial x_i} + \nu \frac{\partial^2 v_i}{\partial x_j^2} \qquad (3)$$

$$\frac{\partial v_i}{\partial x_i} = 0 \qquad (4)$$

$$\rho \overline{v_j} \frac{\partial \overline{v_i}}{\partial x_j} = -\frac{\partial \overline{p}}{\partial x_i} + \mu \frac{\partial^2 \overline{v_i}}{\partial x_j \partial x_j} - \frac{\partial}{\partial x_j}\{\rho \overline{v_i' v_j'}\} \qquad (5)$$

The term in brackets on the right hand side of equation (5) is a turbulent flux of i-momentum in the j-direction, and is called turbulent stress, or "Reynolds" stress. There is a problem because now we have 10 variables (six components of the Reynolds stress tensor, three components of velocity, and pressure), and still four equations (equations (5), and a continuity equation). The simplest approach to close equation (5) is to assume that the Reynolds stress is proportional to a strain. The constant of proportionality for that relationship between turbulent stress and strain is called a turbulent or eddy viscosity (μ_t). This eddy viscosity is usually approximated using "mixing lengths", and "characteristic velocities" (e.g. Prandtl's model). For details on this classic approach to turbulence, the reader is

referred to any textbook on turbulence or fluid dynamics (e.g. Hinze, 1987, or Warsi, 1993).

When an equation for mean velocities (first order quantity) was derived (equation (5)), a second order term appeared (the "Reynolds" stress tensor). Therefore, in order to calculate mean velocities, a model for the "Reynolds" stress tensor in terms of velocities (and their derivatives and related quantities) is needed. An equation for the "Reynolds" stress tensor can be constructed from equations (2) through (5) to give equation (6) (Wood, 1994).

$$\frac{\partial}{\partial t}\{\overline{v_i'v_j'}\} + \overline{v_k}\frac{\partial \overline{v_i'v_j'}}{\partial x_k} = -\{\overline{v_i'v_k'}\frac{\partial \overline{v_j}}{\partial x_k} + \overline{v_j'v_k'}\frac{\partial \overline{v_i}}{\partial x_k}\} + \overline{\frac{p'}{\rho}\{\frac{\partial v_i'}{\partial x_j} + \frac{\partial v_j'}{\partial x_i}\}} - \frac{\partial}{\partial x_k}\{\frac{1}{\rho}[\delta_{jk}\overline{p'v_i'} + \delta_{ik}\overline{p'v_j'}] + \overline{v_i'v_j'v_k'} - \nu\frac{\partial \overline{v_i'v_j'}}{\partial x_k}\} - 2\nu\overline{\frac{\partial v_i'}{\partial x_k}\frac{\partial v_j'}{\partial x_k}} \quad (6)$$

Equation (6) is the cornerstone for all turbulence closure methods. In general there are six components but usually only four are important (the mean values of $\langle v_1'v_1'\rangle$, $\langle v_2'v_2'\rangle$, $\langle v_3'v_3'\rangle$, and $\langle v_1'v_2'\rangle$). Equation (6) describes the transport of "Reynolds" stresses. The last term in equation (6) represents the viscous dissipation of energy into heat. However, it is also noticed that developing an equation for a second order term resulted in the appearance of a third order term, and second order terms involving correlations between fluctuating pressure and velocity, and a correlation between derivatives of velocities. What is usually done to close the equations is to model the higher order correlations in terms of Reynolds stresses (second order correlation between fluctuating velocities), derivatives of mean velocities, and the characteristic scales of length and velocity. A rigorous method to close the problem is the Mean (or Algebraic) Reynolds Stress (MRS) closure technique. Other less rigorous methods to close the equations are the so called "zero equation" modelling, where the streamwise diffusion terms from the Navier-Stokes equations are neglected (Pelletier et al., 1994, provide of an example of the application of the "zero-equation" model), the "one equation" modelling (which assumes that the eddy viscosity depends on the turbulence kinetic energy, k), and the "two equation" modelling (k-ϵ model). Some assumptions and limitations of the k-ϵ model are: (i) the constitutive equation is assumed isotropic, (ii) the flow is assumed nearly homogeneous, (iii) the flow

is at very high Reynolds numbers (no wall or viscosity effects considered), and (iv) the dissipation of energy is obtained assuming local isotropy, a single integral length scale, and equilibrium between energy transfer from large scale eddies and dissipation. A short description of these techniques is available in Warsi (1993). Gibson and Dafa'Alla (1994) proposed a modified two equation model (two variables are defined in terms of k and ϵ, that behave better at the wall). Some general reviews on turbulence modelling are available in Reynolds (1976), Rodi (1982), Lumley (1983), and Speziale (1991).

As a solid boundary is approached in a turbulent flow field (say the tank wall, the baffles, and the impeller blades), viscous effects become important, and the assumption of turbulent flow becomes invalid. There are two basic approaches to handling wall bounded flows, when using a k-ϵ model. In the first the equations for k and ϵ are modified to account for the decreasing Reynolds number and increasing viscosity effects, as the wall is approached (so called "wall functions"). In the second approach a universal logarithmic velocity profile is assumed. Discussions about the near wall effect and development, use or comparison of models are available in Patel et al. (1985), Cho and Goldstein (1994), Hrenya et al. (1995), and Nagano and Shimada (1995).

2.2.2.3 Rate of Energy Dissipation (ϵ)

The last term in equation (6) is the rate of energy dissipation, usually represented as ϵ (epsilon). If it is assumed that the flow field is locally isotropic, then the rate of energy dissipation will be given by:

$$\epsilon = 2\nu\overline{\left[\frac{\partial u_i'}{\partial x_j}\right]^2} \qquad (7)$$

This term, ϵ, turns out to be the most important term in the description of turbulence, at least from the point of view of process modelling. It is the point in the dynamic equations where most of the dissipation occurs; where limiting length scales are determined, and where most of the productive

process work is accomplished.

There are several ways to estimate the rate of energy dissipation. It can be calculated by difference from either the integral kinetic energy balance or the differential kinetic energy balance. The assumption of local isotropy provides special properties for the correlation functions, which can thus be used to provide a starting point for determinations of ϵ based on length scales. These length scales can be calculated from the dissipation spectrum, from the autocorrelation function, or from the time derivative of the velocity using the Taylor's frozen turbulence hypothesis; they can be approximated based on physical arguments (dimensional arguments); or they can be predicted using turbulence models. Once ϵ is known, any other length scale of interest can be estimated. Details on each of these estimation routes for ϵ have been reviewed by Kresta (1991) and Kresta and Wood (1993b).

Baldyga and Bourne (1995) presented a multifractal formalism to describe the intermittency (large variability of the instantaneous energy dissipation rate field) of the turbulence variables (mainly ϵ), and deduced their distributions. The starting point for their analysis was the use of the Navier-Stokes equations (equation (3) in this paper) in terms of re-scaled transformations. Based on their analysis they derived corrections to the traditional equations describing micromixing, concentration spectra, rates of particle encounter, turbulent rupture of flocs and drop breakage in both the inertial and viscous subranges of the turbulence spectrum. Among their findings, they reported that coalescence (of drops or flocs) is not too much affected by intermittency, but breakage is (in the inertial subrange).

2.2.2.4 Scale-Up Procedures

The droplet size in a polymerization reactor is influenced by turbulence fluctuation, interfacial tension, viscous stress due to droplet deformation, and adhesion forces. A list of correlations proposed for scale up purposes, which consider the effect of these forces, is included in the review by Yuan et al. (1991). Oldshue et al. (1982) studied the difference in behaviour between pilot scale and plant scale

agitated tank reactors using retreat blade impellers, and different types of tank bottom (dish, flat, and sloping-side). They concluded that it is necessary to sensitize the pilot plant by using non-geometric techniques to obtain blend time, circulation time, and other phenomena approximate with what is happening in the plant-size unit. Unless this is done, Oldshue et al. (1982) warned, the effect of chemical reaction and polymerization variables can be missed completely in the laboratory and pilot plant, and "funny things" could happen on the way to the large-size reactor. Villalobos (1989) developed a procedure for scaling down and up suspension polymerization reactors which implied establishing a compromise between increasing (decreasing) the stabiliser concentration, and decreasing (increasing) the phase hold-up when scale-down (scale-up) is required. The reason for that change on those physical conditions is that the ratio of relative area per unit volume decreases greatly as the volume of the reactor is increased. Özkaya et al. (1993) developed a recipe-dependent semi-empirical correlation that relates the mean particle size of poly(vinyl chloride) (PVC), obtained in suspension, to the geometric and interfacial properties and the speed of agitation of the system.

There is no simple rule or procedure to scale up suspension polymerization reactors. In fact, there is no simple rule for scaling-up in most mixing situations. Recent examples of different situations where the same conclusion comes up are scale-up of stirred vessels with (solid) suspensions (Geisler et al., 1993), and scale-up of jet (tank) reactors (Baldyga et al., 1995a). This is due to the non-homogeneous character of the turbulent flow field (using a local isotropy assumption does not imply that the turbulence quantities are homogeneously distributed in the tank reactor), coupled with the complex surface and rheological phenomena that take place in the dispersed phase. The rigorous and detailed analysis of turbulent flows using CFD techniques is a major step forward into that direction. What is needed is the ability to extract the necessary information from a CFD simulation (the results would be too detailed for inclusion into another level of modelling, namely the population balance equation). In order to do so, the invaluable practical experience from practitioners of the field is most helpful, not only for modelling purposes, but also for better every day operation of chemical processes. A good source of practical expertise on scale-up and design of industrial mixing processes is available

in Tatterson (1994). Other important references that address the issue of scaling-up are Okufi et al. (1990), Villalobos (1989), Fasano and Penney (1991a, 1991b), Dickey (1993), Larsson et al. (1993), Obot (1993), Oldshue (1993), Tipnis (1993), Tatterson (1993), and Chylla (1994).

2.2.2.5 State of the Art on Modelling of Stirred Tank Reactors

Reviews on the state of the art of turbulent flow in stirred tanks up to 1991 are available in Kresta (1991) and Kresta and Wood (1991). In this subsection, we will emphasize publications appeared afterwards. Unless otherwise stated, the fluid used in the simulations mentioned in this section is water (single phase situation).

The many recent publications on modelling of stirred tanks can be classified on 7 categories, depending on the focus of the research studies. These categories, their relevant characteristics or associated ideas and references are described in Table 2.1.

2.2.2.6 Degree of Sophistication about Mixing required to model Particle Size Distribution in Suspension Polymerization

In this subsection some situations where macromixing is coupled with other phenomena will be described, as well as the approaches followed to model those systems. The intention is to get ideas (from similar situations) that might be useful for application in suspension polymerization. At the end, some recommendations on how to address the modelling of a suspension polymerization case will be offered.

Jaworski et al. (1991) measured the turbulent flow in a baffled vessel agitated by a pitched blade turbine (using laser Doppler anemometry), and proposed using a two-region model (one for the impeller and outflow stream, one for the remainder of the vessel) for the distribution of the fluctuating velocities within the agitated vessel. In studying precipitation processes and the factors that determine the form and size distribution of the precipitate, Garside (1991) addressed the role of mixing by using a single average rate of energy dissipation. However, in his analysis he recognized that the rate of

energy dissipation varies in the order of a hundred-fold difference (between the impeller and the bulk zones), and that this variation should be considered. Parthasarathy and Ahmed (1994) used an empirical correlation (based on the theory of local isotropy) to calculate the Sauter mean and maximum bubble diameters in aerated stirred vessels. They suppressed coalescence by adding a surface active agent. What is interesting from this paper is that the rate of energy dissipation (ϵ) for their correlations was not based on the total volume of the tank, but on the impeller swept volume (which was calculated assuming a cylinder with dimensions of the impeller). By doing so, they were dividing the tank in two zones: one at the impeller (the one they used for their calculations), and one at the bulk, with a negligible value of ϵ. Nambiar et al. (1994) also proposed and used a two-zone model (for breakage) (the main aspects of that model are mentioned in section 2.2.3.1).

On studying the insect cellular response to agitation in stirred tanks, Aloi and Cherry (1996) calculated the rate of energy dissipation for the turbulent zone surrounding a 6-bladed Rushton impeller. They used local-isotropy theory, but the dissipation volume was defined by the volume of the trailing vortices emanating from the impeller tips. In this way they were accounting for the non-homogeneous distribution of the rate of energy dissipation, ϵ.

The approach followed by Tosun (1992) in modelling mixing and polymerization in a semibatch stirred-tank reactor (a "segregated-feed-zone" model for mixing and a "lumped chain concentration" model for kinetics were coupled to model the system), serves as an example on how a complex system can be modelled by using simplified models of the most important phenomena that rule the behaviour of the system (in this case mixing and polymerization). Baldyga et al. (1995b) provide another interesting example on how to address the modelling of a complex problem. They modelled a double feed semibatch precipitation system where both mixing and precipitation were important. The interactions between mixing at various scales (macro-, meso- and micromixing) were coupled with a population balance for crystallization (similar problem structure to suspension polymerization). Among the important information obtainable from that paper, some aspects are worth mentioning here: (i) different time scales were calculated to determine the controlling mechanism, and

(ii) a simplified distribution of the rate of energy dissipation (ϵ) was used (one value for the impeller zone, and other for the bulk of the tank).

Table 2.1 State of the art in modelling turbulent flow in stirred tanks.

Modelling tools	Comments or details	References
Energy spectrum function (ESF)	- Used to evaluate turbulence variables, and applied to study solid-liquid dispersions.	Nonaka (1990).
	- Use of "similar ESF" as a scale-up criterion.	Ogawa (1992).
Compartment-mixing models	The flow is divided into different regions. Useful approach for scale-up applications.	Mann and El-Hamouz (1995) and their references, Mayr et al. (1994), Cui et al. (1996).
Experimental-CFD model building	- Qualitative studies of flow behaviour for better understanding of mixing phenomena (e.g. effects of hydrodynamic variables on circulation patterns, etc.).	Kresta and Wood (1993a), Abid et al. (1994), Roberts et al. (1995), Moore et al. (1995).
	- Experimental determination of the boundary conditions for turbulence variables at the impeller region.	Kresta and Wood (1991, 1993b) and their references, Ranade et al. (1992), Fokema et al. (1994), Sahu and Joshi (1995), Armenante and Chou (1996).
	- Reviews on CFD	Harris et al. (1996), Ranade (1996).
Turbulence models	Comparison between "k-ϵ" and "ASM" (Algebraic Stress Model) turbulence models. ASM is reported to behave better than k-ϵ.	Bakker and Van den Akker (1994a, b), Armenante and Chou (1996).
Rotating frame of reference	- Suggestion to use this technique.	Ranade et al. (1992).
	- A moving grid (including the impeller zone) rotates and the other grid remains stationary. Steady and unsteady simulations have been presented.	Luo et al. (1993) (steady and unsteady), Yuan Perng and Murthy (1993) (unsteady), Dong et al. (1994b) (steady), Harvey et al. (1995) (for laminar flow, steady), Harvey (1995) (unsteady), Skeldon (1995).
Micromixing theory	- Important when mixing and chemical reaction times are of same order of magnitude. Interaction between micro- and macromixing is measured in terms of mixing times.	Thoma et al. (1991), Geisler et al. (1991), Baldyga and Bourne (1992), Baldyga and Pohorecki (1995) (a review).
	- Micromixing models (e.g. "E" and cylindrical-stretching-vortex (CSV) models).	Baldyga and Bourne (1989) (E-model), Bakker and Van den Akker (1994d) (CSV).
	- Coupling of macromixing (CFD with ASM turbulence model) and micromixing (CSV model).	Bakker and Van den Akker (1994c).
Software or expert systems for stirred-tank (or more general) applications.	- AgDesign: a knowledge based system of Chemineer, which is described to be capable of selecting an agitator, designing an impeller for it, and generating a tank sketch.	In Howlett (1995).
	- MIXES: another knowledge based system for preliminary design of mixing equipment.	Koiranen et al. (1995).

In situations where chemical reaction and mixing phenomena, as carried out in stirred tanks, take place at similar rates, the assumption of perfect mixing is inappropriate. Several models such as the two-zone, three-zone, four-zone, and network-of-zones have been used to model this type of system (Mann and El-Hamouz, 1995). These multi-zone models are also known as "compartment-mixing-models" (Cui et al., 1996). As a matter of fact, these modelling approaches can be considered as simplifications of, or approximations to, a rigorous three-dimensional CFD calculation (Mann et al., 1995). Although suspension polymerization is not a system of this kind (kinetics is usually unaffected by the mixing homogeneity within the tank), breakage and coalescence are very much affected by the degree of homogeneity in the tank. Therefore, even though these multi-zone models are not necessary to model the kinetic behaviour of the system, the idea of considering several zones (as an alternative to a rigorous coupling of the fluid mechanics Navier-Stokes equations with space-dependant population balance equation) could be useful to model the particle size distribution in suspension polymerization.

Some comments are pertinent at this point. Detailed modelling of the turbulent flow in a stirred tank reactor is a very complex issue. Nonetheless, enormous progress has been made in the last decade, and nowadays it is possible to model the flow in an agitated tank very accurately (at least to a degree of accuracy much higher than it is needed to build our models for suspension polymerization), but the calculations are still expensive. It is also possible to measure experimentally the turbulence characteristics very precisely. On the other hand, it can be said that representing the rate of energy dissipation in an agitated tank as a single average value over the whole domain of the vessel, is inappropriate for modelling purposes. It does not help much to complicate the breakage and coalescence models (which will be reviewed in the next section) if the mixing model is inaccurate. The rigorous way to couple macromixing and the population balance models would be by calculating the distribution of the rate of energy dissipation (ϵ) (using CFD tools) and inputting this profile into a space-dependant population balance equation (an external coordinate -position- should be considered in equation (1)). However, even with the availability of much more powerful computers (than were

available in the previous years), the numerical task would be enormous and, most likely, the information obtained would be much more detailed than needed. Therefore, an intermediate approach should be used. The most immediate choice (and perhaps enough) would be to consider two zones, one for the impeller region, and other for the bulk of the tank. The idea is not new, but it seems that it has not been exploited enough in suspension polymerization modelling. Even though the information gained using CFD calculations would be too detailed, it would serve to obtain accurate estimates for the ϵ values to be used in a simplified model (a two-zone or multi-zone model).

2.2.3 Breakage and Coalescence

2.2.3.1 Breakage

The first approaches to model the breakage of droplets in a liquid-liquid suspension assumed that a minimum and a maximum diameter existed for a droplet to be stable. Based on the Weber Number theory those extreme values can be estimated (Hinze, 1955; Shinnar, 1961). These models are limited, however, to very low dispersed phase viscosity and holdup fraction. Doulah (1975) proposed a correction to these correlations to account for the holdup fraction, whereas Arai et al. (1977) derived an expression for the maximum droplet diameter incorporating the suspension viscosity in such expression. A similar correlation was used by Konno et al. (1982). Other correlations were developed by Leng and Quarderer (1982) (no coalescence considered), Calabrase et al. (1986) (viscosity of the dispersed phase considered), and Borwankar et al. (1986) (for non-coalescing dispersions). For users of the Weber Number theory, Bourne and Baldyga (1994) recommended to use an exponent of -1 on the Weber number (based on the derivation by Shinnar (1961)), instead of -1/3 (based on the original derivation of Kolmogorov). All these models are mainly phenomenological in nature.

In contrast to the previous empirical models, other models have been developed where the breakage frequency is considered. Valentas and Amundson (1966) assumed the breakage frequency, ω_b, to be proportional to the droplet surface area. By drawing an analogy between droplet breakage

and molecular decomposition, Ross et al. (1978) obtained equation (8),

$$\omega_b \propto ND^{2/3}d^{-2/3}\exp\left[- \frac{K\sigma}{\rho_c N^2 D^{4/3} d^{5/3}} \right] \qquad (8)$$

where K is a constant, N is agitation speed, D is agitator diameter, d is droplet diameter, σ is interfacial tension, and ρ_c is continuous phase density. A very similar expression to equation (8) was obtained by Coulaloglou and Tavlarides (1977), but their derivation was made from an analysis of the hydrodynamics of the dispersion. Mikos et al. (1986) used a model for the breakage probability based on the droplet breakage due to oscillation resulting from the relative velocity fluctuations.

Valadez-González (1988) proposed a model where the efficiency for breakage is determined by energy and time, namely, that a minimum amount of energy should be provided to the droplet in order for it to be broken, and that energy must be provided for at least a minimum given time. He proposed that the breakage frequency should be given as shown in equation (9),

$$\omega_b(u) = \omega_r(u)\lambda_t(u)\lambda_e(u) \qquad (9)$$

where ω_r is collision frequency, u is droplet volume, and λ_t, λ_e are time and energy efficiencies. The time efficiency was proposed to be a function of the time required for deformed polymer droplet to flow a distance equal to its (original) radius, and the time where enough energy to break the droplet is available. The energy efficiency is obtained from an energy balance considering the surface energy (energy required to overcome the interfacial tension), and the energy required to promote viscous internal flow. To account for the monomer/polymer flow, Valadez-González (1988) used a power law viscosity model and assumed the flow to be equivalent to the flow of monomer/polymer mixture through a circular duct of diameter equal to the droplet diameter, and pressure drop of the order of magnitude of the available kinetic energy. Based on these assumptions, he obtained equations (10) to (12) for collision frequency, time and energy efficiencies, respectively,

$$\omega_r = C_1 \frac{ND^{2/3}}{(1+\phi)u^{2/9}} \qquad (10)$$

$$\lambda_t = \exp[-C_5 \frac{3n+1}{n} (\frac{2\rho_d}{Re_d \rho_c})^{1/n} \frac{D^{2(1+1/n)/3}}{u^{2(1+1/n)/9}} (1+\phi)^{(2-n)/n}] \quad (11)$$

$$\lambda_e = \exp[-(1+\phi)^2 (C_2 \frac{D^{5/3}}{(We)u^{5/9}} + C_3 \frac{D^{2/3}}{Re_0 u^{2/9}} + C_4 \frac{D^{2(n+1)/3}}{Re_d u^{2(n+1)/n}} (\frac{\rho_d}{\rho_c})^{1-n/2} (1+\phi)^{-n})] \quad (12)$$

where C_1 through C_5 are adjustable parameters, n is the power law index, τ is shear stress, γ is shear rate, η is viscosity, and the Weber (We) and Reynolds (Re_0, Re_d) numbers are defined by equations (13) to (15) (subscript "0" accounts for zero shear conditions, and subscript "d" represents the dispersed phase).

$$We = \frac{\rho_c N^2 D^3}{\sigma} \quad (13)$$

$$Re_0 = \frac{\rho_c N^2 D^2}{\tau_0} \quad (14)$$

$$Re_d = \frac{\rho_d N^{2-n} D^2}{\eta_0 \dot{\gamma}_0^{1-n}} \quad (15)$$

Alvarez et al. (1991, 1994a) used the same approach as Valadez-González (1988), but instead of using a power law viscosity model, they assumed the polymer flow to behave as a Maxwell fluid and only one breakage efficiency was used. The efficiency expression they obtained was rather more complex than those obtained by Valadez-González (1988), but less adjustable parameters were required (two, instead of five). For the breakage rate distribution Alvarez et al. (1994a) obtained equation (16).

$$\beta(u) = \omega_b(u) \exp[-\lambda_b(u)] \quad (16)$$

where

$$\omega_b(u) = \frac{k_b \epsilon^{1/3}}{(1+\phi) d_u^{2/3}} \tag{17}$$

$$\lambda_b(u) = \frac{6a_b}{Re(d_u)[1+Re(d_u)V_e(d_u)]} + \frac{1}{We(d_u)} \tag{18}$$

k_b and a_b are constants, ϵ is rate of energy dissipation, Re(d) and We(d) are Reynolds and Weber numbers for a drop of diameter d_u (and volume u), and $V_e(d_u)$ is a dimensionless function that accounts for elasticity. The explicit expression for $V_e(d_u)$ is presented in the paper of Alvarez et al. (1994a).

Kumar et al. (1992) proposed a model for drop breakage which considered the possibility of multiple drop-eddy interactions. The model was aimed at explaining the behaviour of systems with high dispersed phase viscosity and low interfacial tension. In their model the stirred vessel was divided in two zones: a deformation zone near the impeller, and a relaxation zone comprising the rest of the vessel. The drop was assumed to circulate continuously along with the bulk fluid. As it passed through the deformation zone, it would get deformed due to intense turbulent fluctuations present there, but might not break. The deformed and unbroken drops would then entered the relaxation zone, where it would begin to relax back. If the drop did not relax back completely, it would reach the deformation zone in a deformed state. Thus, the drop would increase its deformation with each cycle until broken, or it would reach a "steady" state. Based on this model, a simplified graphical procedure to estimate the maximum stable drop diameter, d_{max}, in a liquid-liquid dispersion was developed by Kumar et al. (1993).

Chatzi and Kiparissides (1992) assumed the breakage frequency to depend on the average number of eddies arriving on the surface of the drop per unit time and on the probability that the arriving eddy will have energy greater than or equal to the minimum increase in the surface energy required to break a droplet of diameter d. They indeed used the same principle as Valadez-González (1988), but only considered surface energy to be overcome and, therefore, their model is limited to low viscosities. An interesting issue in the model of Chatzi and Kiparissides (1992), however, is the

proposal of considering breakage of the drops into one daughter and several "satellite" drops. This concept of satellite drops allows the prediction of bimodal distributions, which is common in suspension polymerizations carried out in small reactors (Konno et al., 1982; Mitchell, 1986; Villalobos, 1989). According to Chatzi and Kiparissides (1992, 1994, 1995) the breakage frequency is given by equations (19) and (20).

$$\omega(d) = C_{VII}\, erfc\left[\frac{C_{VIII}\left(\frac{\sigma}{\rho_d}\right)^{\frac{1}{2}}}{d^{\frac{5}{6}} N^{*} (D_I)^{\frac{2}{3}}}\right] \qquad (19)$$

$$C_{VIII} = C'_{VIII}\sqrt{\frac{N_{da} x^{\frac{2}{3}} + N_{sa}}{(N_{da} x + N_{sa})^{\frac{2}{3}}} - 1} \qquad (20)$$

where C_{VII} and C_{VIII}' are constants, D_I is impeller diameter, N^* is speed of agitation, N_{da} and N_{sa} are the number of daughter and satellite drops, respectively, and x is the ratio of volume of daughter to volume of satellite drops. The calculations of Sathyagal et al. (1996) on the average number of daughter drops formed upon breakage of drops of carbon tetrachloride in benzene in the range of 50 to 450 μm and a dispersed viscosity of 0.74 cP (very low if compared to the range of dispersed viscosities found in suspension polymerization) (from figure 14 of that paper, the number of daughter drops lies between 3 and 8), seem to coincide with the proposal of Chatzi and Kiparissides (1992).

Although there is experimental evidence that the breakage of a droplet produces a large number of daughter droplets of different sizes (Tavlarides and Stamatoudis, 1981), most researchers assume this number to be fixed, and usually equal to two (e.g. Coulaloglou and Tavlarides, 1976, 1977; Delichatsios and Probstein, 1976; Saldívar-Guerra et al., 1989; Alvarez et al., 1991, 1994a). The daughter drop volume distribution has been adequately represented as a normal distribution (Valentas et al., 1966; Coulaloglou and Tavlarides, 1977; Alvarez et al., 1991, 1994a).

Ayazi Shamlou et al. (1994) developed a model for breakage frequency of protein precipitates in turbulently agitated bioreactors. The rate of breakage of aggregates was expressed as the product of an eddy-aggregate collision frequency, a probability of collision leading to breakage, and a number concentration of aggregates. To model collision frequency the local isotropic turbulence theory of Kolmogorov was used, and an exponential distribution law of probability was assumed valid to represent the probability of collisions.

Stone (1994) presented a review on the dynamics of drop deformation and breakup in viscous flows at low Reynolds numbers. Although that situation is not exactly the same as the one present in suspension polymerization (where Reynolds numbers are high), there are some concepts and ideas that are useful. It is important to note that rigorous modelling of droplet deformation and breakup leads to very complex models (which usually require computational fluid dynamics methods and tools). To this complexity one can also add the already difficult problems of modelling the non-homogeneous mixing, the coalescence of droplets, and the polymerization kinetics (which may be non-trivial, particularly when crosslinking is considered), and realize that modelling the particle size distribution is an extremely challenging problem.

Tjahjadi et al. (1992) studied the shape evolution and eventual breakup of a highly extended fluid filament completely immersed in a second immiscible fluid. In that study they concluded that the number of satellite droplets and their relative sizes depended strongly on the ratio, p, of viscosity of the dispersed phase to viscosity of the continuous phase. At low values of p ($0.01<p<2.8$), for the system they studied, the centre drop always experienced further breakups, generating 3 satellites at $p=2.8$ up to 19 visible satellites at $p=0.01$. Although this result is valid for a system very much different from a suspension polymerization environment, the result is meaningful. This result would suggest that as polymerization proceeds (and p increases), the number of satellite drops would decrease, and at some point the assumption of only two droplets being formed from the breakage of a mother droplet (quite common in modelling breakage in suspension polymerization) might be considered valid. Considering that bimodal particle size distributions are obtained in suspension

polymerization when coalescence becomes important (usually at rather high values of p), it seems likely that reasons other than the formation of satellite droplets (as suggested by Chatzi and Kiparissides, 1992, 1995) could be responsible for this behaviour. It is our feeling that the non-homogeneity of mixing within the vessel is a more likely cause for the bimodal PSD observed in suspension polymerization reactors (usually at the pilot plant scale, where the volumes of the impeller zone and the bulk of the tank are rather similar). It is possible that the satellite-drops formation model has worked well for Chatzi and Kiparissides (1992, 1995) because they have applied it to systems with low to moderate values of p (compared to values of p in suspension polymerization at intermediate or high conversions). However, a combined effect of both mechanisms could be the responsible for the bimodal (or even multimodal) PSD obtained in suspension polymerization, since the small satellite droplets obtained at low conversion levels could remain well stabilized and retain their identities during the whole course of polymerization, thus having an important role on the PSD development.

Varanasi et al. (1994) investigated the characteristics of deformation and breakup of model viscoelastic drops suspended in immiscible purely viscous Newtonian fluids undergoing simple shear flow. Although the situation again is different from suspension polymerization, the results are meaningful. In that study the results were compared with data obtained on purely viscous Newtonian drops under similar conditions. The ratio of viscous forces to interfacial tension forces at breakup (ϵ_b) was found to depend on the ratio of the viscosity of the dispersed phase to that of the continuous phase (p), the shear stress prevailing in the continuous phase at breakup, and the primary normal stress difference. At any fixed shear rate, a characteristic viscosity ratio (p^*) was observed above which model viscoelastic drops were easier to breakup than purely viscous Newtonian drops. For this specific system, the mode of deformation and breakup of the model viscoelastic drops was observed to depend on the magnitude of the shear rate applied to the system (in a suspension polymerization system this shear rate would be characterized by the degree of turbulence present in the vessel). In general, the mode of breakup was due to extension of the drops into long threadlike filaments which became unstable as the critical shear rate was approached. The filament then ruptured into many smaller

(satellite) drops. When more than two drops were formed upon the breakup of these threads, at low shear rates, the main drops were not necessarily appreciably larger than the satellite drops. On the other hand, at high critical shear rates, the appearance of a Rayleigh interfacial wave on the surface of the thread (Rayleigh instability) was usually observed prior to breakup. In this case, the fine threadlike region joining any two bulblike regions of the wave was very thin and, consequently, the satellite drops formed were much smaller than the satellite drops formed from purely viscous Newtonian drops. According to these results, in suspension polymerization (where there is a high degree of turbulence) it would be expected that the satellite drops formed from rupture of a mother drop were significantly smaller than the mother drop. Considering the environment surrounding the drops in suspension polymerization (rather high holdup fractions, random like movement of the drops, and high frequency of collision with other drops), it would be less likely for the drops to elongate significantly before being broken. This would suggest that small and not numerous satellite drops might be produced from breakup of a mother drop, and that the particle size distribution would be affected by the formation of satellite drops at the low size range. Therefore, it is unlikely that formation of satellite drops could be the main cause leading to the development of bimodal distributions when coalescence is important (namely, when the viscosity of the dispersed phase is high).

Tsouris and Tavlarides (1994) developed an interesting model for drop breakage rate. As most authors have done, they assumed that (i) the turbulent flow in a stirred tank is isotropic, (ii) the drop size is in the inertial subrange, and (iii) drops can break only by collisions with smaller eddies, or the same size, since larger eddies have the tendency to transport the drop rather than breaking it. Based on these assumptions they obtained equation (21),

$$\omega(d) = k_8 D(\phi)\epsilon_i^{\frac{1}{3}}\left[\int_{\frac{2}{d}}^{\frac{2}{d_{e,min}}} \left(\frac{2}{k}+d\right)^2 \left(\sqrt{\frac{8.2}{k^{2/3}}+1.07d^{\frac{2}{3}}}\right)k^2 \exp\left[-\frac{E_c}{c_1 e}\right]dk\right] n_d \qquad (21)$$

where k_g is a geometric factor which also takes into account the ratio of impeller volume to total volume, d is drop diameter, $d_{c,min}$ is an eddy size taken as half the size of the critical drop size, k is eddy wavenumber, ϵ_i is the energy dissipation rate at the impeller region, E_c is the energy required for breakage [equation (40) in the paper of Tsouris and Tavlarides (1994)], c_1 is a constant, n_d is the number of drops, ϕ is volume fraction of the dispersed phase, and $D(\phi)$ is a damping factor defined in equation (22).

$$D(\phi) = [1 + 2.5\,\phi\,(\frac{\mu_d + 0.4\mu_c}{\mu_d + \mu_c})]^2 \qquad (22)$$

μ_c and μ_d in equation (22) are viscosities of the continuous and dispersed phases, respectively. Even though Tsouris and Tavlarides (1994) assumed the flow to be isotropic, they accounted for the non-homogeneity of the tank by using an energy dissipation rate at the impeller zone, and another energy dissipation rate at the bulk of the tank. They used a value at the impeller which is 5.1 times the value at the bulk.

Nambiar et al. (1994) proposed a two-zone model of breakage frequency of drops in stirred dispersions. They divided the vessel into the deformation and recirculation zones. The drop was assumed not to be broken in the recirculation zone and the time spent in it was supposed to be infructuous as far as breakage was concerned. They assumed the drop to follow a given circulation pattern in the stirred vessel, and it was also assumed to interact with only one eddy in the deformation zone. If the drop did not break, it had to pass through the recirculation zone before another interaction with an eddy became possible. They assigned the residence time of a drop in the deformation zone to be a fraction of the mean cycle time of a fluid element in the stirred vessel. That fraction was assumed to be the volume fraction where breakage was observed to occur (they used 10% in their model). Their model assumed a low viscosity dispersed phase, and therefore no deformation was considered to take place in the circulation zone. However, this is not a serious limitation as their model could accommodate a different initial condition for deformation on entry to the breakage zone. This idea of

considering the different mixing environment at the impeller in the breakage model is a clear advantage over most precedent models, based on a homogeneous isotropic medium.

Lachaise et al. (1995) proposed a model for simulation of the formation of moderately concentrated oil-in-water emulsions generated by turbulent stirring using an anionic surfactant as emulsifier. Although this situation is not exactly the same as suspension polymerization, it is worth mentioning. Breakup and coalescence are modelled by probability functions. In their development they consider that during an elementary period of time, each droplet is submitted to a random event transition with a probability P_b to break into two equal volume droplets, a probability P_c to coalesce with another droplet of the same volume, and a probability P_{iv} to remain unaltered. The breakup probability is based partly on isotropic turbulence theory, and the influence of the emulsifier is introduced through an efficiency factor which takes into account the competition between turbulent and capillary forces. The coalescence probability is derived from molecular collision theory, and again the effect of the emulsifier is introduced through an efficiency factor which quantifies the balance between collisional turbulent forces and capillary forces.

Sathyagal et al. (1995, 1996) applied a mathematical and computational procedure, called the inverse problem, to determine the drop breakage rate and daughter drop distribution from experimental transient size distributions. Their technique uses a similarity transformation of the population balance equation. A test for similarity must be made and, if positive, the breakage rate and daughter drop distribution can then be calculated. They found that the breakage rate increases sharply with the drop size and the stirrer speed while decreasing sharply with increase in the interfacial tension. They also found the breakage rate to decrease with increase in the dispersed phase viscosity, though the dependence on viscosity was weaker than on the other variables (they used a dispersed viscosity range of 0.74 to 134 cP, which might be considered low, if compared to a suspension polymerization situation), (Sathyagal et al., 1996).

2.2.3.2 Coalescence

Coalescence has been modelled assuming that the suspended droplets move randomly and that their collision mechanism is similar to the one for ideal gas molecules (Kinetic Theory of Gases). Different expressions for collision frequency have been proposed (Howarth, 1964; Abrahamson, 1975; Coulaloglou and Tavlarides, 1977; Das et al., 1987).

Howarth (1964) developed an expression for the frequency of coalescence on the basis of the turbulent nature of the dispersion. He obtained the frequency of collision by assuming that the collision between randomly moving drops is analogous to collision between particles encountered in smoke and colloidal suspensions. For obtaining the efficiency of coalescence, he assumed coalescence to be a single-shot process. If the velocity of approach between two drops along the line of their centres exceeds a critical value, immediate coalescence results; otherwise the collision does not end up in coalescence of drops. Coulaloglou and Tavlarides (1977) calculated the probability of coalescence by using the argument that for coalescence to occur, the time of contact between drops must exceed the time required for coalescence. Shiloh et al. (1973) assumed that coalescence efficiency is inversely proportional to the ratio of drainage time to life time of an eddy. Das et al. (1987) modelled the film drainage between two colliding drops as a stochastic process driven by a suitably idealized random process for the fluctuating force. The group of Alvarez (Valadez-González, 1988; Saldívar-Guerra et al., 1989; Martínez-Gómez, 1990; Hernández-Valdez, 1993; Alvarez et al., 1991, 1994a), as previously mentioned, also used the Kinetic Theory for Gases to calculate the coalescence frequency, but they proposed different expressions for the coalescence efficiency that take into consideration the rheological behaviour of the reacting mass (increase in viscosity as monomer polymerizes). Valadez-González (1988) and Saldívar-Guerra et al. (1989) proposed this efficiency to depend on a deformation efficiency, a film drainage efficiency, and a time for deformation efficiency. In developing expressions for these efficiencies, they used a power law rheological model. Alvarez et al. (1991) proposed that the overall coalescence efficiency was the product of four different efficiencies, namely an efficiency for droplet-droplet approach, a deformation efficiency, a film drainage efficiency

before the film is broken, and a film drainage efficiency once it has been broken. In developing these efficiencies, they included the effect of the dispersion agent, and a Maxwell fluid model was used to characterize the rheological behaviour of the droplets. In a simplified version of their model, Alvarez et al. (1994a) considered only two efficiencies, a deformation efficiency and a film drainage efficiency. The main features of their model (Maxwell fluid rheological approach and consideration of the stabilizer presence) were preserved, however.

Wright and Ramkrishna (1992) developed a mathematical and computational technique, called the inverse problem, to determine the particle coalescence rate from experimental transient size distributions. They used this technique to investigate how various physical factors such as the dispersed-phase fraction and the impeller speed affect the droplet coalescence frequency (Wright and Ramkrishna, 1994).

Danov et al. (1993) have presented a detailed model for film thinning between two colliding particles in the context of emulsion droplets. By using appropriate expressions for the droplet interaction and boundary conditions of Smoluchowski type, they calculated the distance at which the droplet deformation takes place, the non-equilibrium (but steady) radial distribution function, and the total force (including the averaged Brownian force) acting between the droplets. As a result the particle flux toward a given "central" droplet, i.e. the coalescence rate, was determined.

Kumar et al. (1993) developed a model for drop coalescence efficiency in stirred vessels that considered drop collisions at all possible angles of approach. In their model, the drops were permitted to rotate while approaching each other. For coalescence to occur, the drops were assumed to approach each other under a squeezing force acting over the life time of an eddy, which could vary with time, depending upon the angle of approach. The model accounted for the change in the shape of two approaching drops and the dependence of the critical thickness of film rupture on various parameters. The coalescence efficiency was defined as the ratio of the range of angles resulting in coalescence to the total range of all possible approach angles. The model seemed to reconcile some contradictory results obtained with other models, although its structure is rather complex (considering that in the

modelling of a suspension polymerization the coalescence model has to be immersed into a population balance equation).

Chatzi and Kiparissides (1994, 1995) defined an overall efficiency, which considered two different types of deformation behaviour, namely, deformable droplets, and rigid spheres.

Tsouris and Tavlarides (1994) also used the Kinetic Theory of Gases to model collision frequency, but they developed a model for coalescence efficiency that accounts for the effects of film drainage for drops with partially mobile interfaces. The expression that they obtained for coalescence efficiency, $\lambda(d_i, d_j)$, is given below:

$$\lambda(d_1,d_2) = \exp\left[- \frac{6\pi\mu_c c_2 \zeta}{\rho_c \epsilon^{*2/3}(d_1+d_2)^{2/3}} \frac{31.25 N D_i}{(T^2 H)^{1/3}}\right] \qquad (23)$$

where

$$\epsilon^* = [D(\phi)]^{\frac{3}{2}} \qquad (24)$$

$$\zeta = 1.872 \ln\left[\frac{\sqrt{h_1}+1.378q}{\sqrt{h_2}+1.378q}\right] + 0.127 \ln\left[\frac{\sqrt{h_1}+0.312q}{\sqrt{h_2}+0.312q}\right] \qquad (25)$$

$$q = \frac{\mu_c}{\mu_d}\sqrt{\frac{r_1 r_2}{r_1+r_2}} \qquad (26)$$

c_2 is a constant, h is film thickness, r is radius of droplet, d is diameter of a droplet, ϕ is volume fraction of dispersed phase, T is vessel diameter, H is tank height, and $D(\phi)$ is defined in equation (22).

Li (1994) developed a model to predict coalescence time between two small bubbles or drops with different radii (the time required for the thinning and rupture of the liquid film formed between them). The analysis considered the effects of van der Waals and electrostatic double layer forces, a situation different from the one present in suspension polymerization. However, the approach to

address the problem is useful. To model the dynamics of the thinning film, use was made of the appropriate continuity and Navier-Stokes equations describing the flow of the liquid film separating the two drops. The effects of the van der Waals and electrostatic forces were considered in the pressure term of the Navier-Stokes equations. In suspension polymerization other forces should be considered (e.g. viscous, surface, and kinetic).

Danov et al. (1994) developed a kinetic model for the simultaneous processes of flocculation and coalescence in emulsion systems. They considered a complete kinetic scheme accounting for the possibilities of flocculation and coalescence in and between the aggregates. A rate constant to each elementary act was assigned, and thus a full set of kinetic differential equations describing the system was defined. That system of equations represented a balance on the formation and disappearance of aggregates comprising from 1 to n particles. Although there was a count on number of particles, no distinction on particle size was made. The rate constants for coalescence were modelled in terms of the probability for rupture of a single film. The model turned out to be characterized by the rate constant for coalescence of two drops into a single one, and that value was regarded as a model parameter (their model considers coalescence of aggregates of n particles into aggregates of i particles, where $i<n$, and where the lowest values for i and n are 1 and 2, respectively).

Whitesides and Ross (1995) studied the limited coalescence process (process by which a colloidal, surface active stabilizer is used to prepare an emulsion, usually of an oil-in-water type), also known as "Pickering emulsions". Their dispersion system consisted of a fine emulsion of dodecyl phthalate in water, using sodium laureate as emulsifying agent. The emulsion was then acidified in the presence of silica and a promoter, under which conditions a normal limited coalescence process occurs. They presented calculations of the rate of change of the number concentration of particles, n, assuming a kinetic scheme involving the formation of dimeric agglomerates that could either coalesce or break up into the original monomer agglomerates under the influence of hydrodynamic forces. By assuming a monodisperse system they obtained that the mentioned rate was of first order in n. They also presented the case where the particles are not monodispersily sized, and a population balance

equation was derived. A particle size distribution function, n(x,y,t) was introduced, where x is particle volume, y denotes the covered fraction of particle surfaces, and t is time. They modelled the effect of the surfactant by assuming that the probability that two colliding particles coalesce is equal to the product of the fractions of their surfaces that are uncovered. However, they were interested in the PSD at long times, so that the population balance equation was solved only for a simple situation (assuming a delta initial distribution function which transforms the population balance equation into a system of ordinary differential equations), and a Monte Carlo Method was used, instead, to obtain the PSD.

Mousa and van de Ven (1995) proposed an empirical expression to model the coalescence efficiency for emulsion droplets in simple shear, which was assumed to depend on the radius ratio of the two colliding droplets. They followed the time evolution of the emulsion droplets by using a Monte Carlo simulation. They also used a moments method, and concluded that the agreement between the results using both methods was excellent, but the moments method was computationally preferred.

2.2.4 Rheological Phenomena

2.2.4.1 Relationship between viscosity and molecular weight

Adam and Delsanti (1979) studied the relationship between Newtonian viscosity, η, molecular weight, M, and monomer concentration, c, for semidilute polystyrene-benzene solutions. They obtained the following relationship:

$$\eta \sim M^{3\pm0.5} c^{4.5\pm0.1} \qquad (27)$$

where η is given in Poises, and c in g/g.

Adam et al. (1979) reported some viscosity measurements taken during the copolymerization of styrene-divinylbenzene, near the gel point. The dependence of the viscosity η on the reaction time t was found to be:

$$\eta \sim \left[\frac{t_c - t}{t_c}\right]^{-0.78\pm0.1} \quad ; \; when \; \frac{t_c - t}{t_c} \leq 2x10^{-2} \qquad (28)$$

where t_c is the reaction time at which gelation occurs.

Adam et al. (1981) measured the mechanical properties (viscosity and elasticity) of two polymeric systems, namely, styrene-divinylbenzene (radical copolymerization), and polycondensation of hexamethyl di-isocianate with n-hexane triol. From their measurements they obtained the following relationships:

$$\eta \sim \frac{1}{(x_c - x)^{0.78}} \tag{29}$$

$$E \sim (x_c - x)^t \tag{30}$$

where E is elasticity, x is conversion (subscript "c" accounts for gelation point), and t=2.1 for radical copolymerization (t=3.2 for polycondensation).

Baillagou and Soong (1985) proposed the following equation to calculate viscosity of a polymer/monomer solution (in the concentrated region), based on free-volume and coil-coil interaction theories:

$$\eta\,(M, c_p, T) = \eta_m(T) + K' M^n c_p^{\,m} \exp[\frac{B}{f}] \tag{31}$$

where η is viscosity of the polymer solution, η_m is viscosity of the monomer, M is molecular weight of the polymer, T is temperature, c_p is polymer concentration, f is fractional free volume, B is a constant of the order of 1, and K', n and m are adjustable parameters (n is of the order of 3.4 in the concentrated region).

Based on a free-volume theory, Alvarez et al. (1990, 1994b) obtained the following expression to calculate the zero shear viscosity of the dispersed phase:

$$\mu(\frac{g}{cm\text{-min}}) = a_\mu T^{b_\mu} \exp[\frac{-2.3 m c_\mu}{A(T) + a_E m}] \tag{32}$$

$$A(T) = b_A - a_A(T - T_g)^2 \qquad (33)$$

where a_μ, a_A, a_E, b_A, b_μ and c_μ are constants; T is temperature in °K, T_g is glass transition temperature of the polymer (in °K), and m is dimensionless monomer concentration.

As mentioned in Xie (1994), the relationship between intrinsic viscosity and molecular weight can be represented by the Mark-Houwink-Sakurada (MHS) equation, shown below:

$$[\eta] = K M_w^{\alpha} \qquad (34)$$

or the empirical Dondos-Benoit (DB) equation, if in the low molecular weight region:

$$\frac{1}{[\eta]} = -A_2 + \frac{A_1}{\sqrt{M_w}} \qquad (35)$$

where $[\eta]$ is intrinsic viscosity (in cm^3/g), M_w is molecular weight (in g/mol), and K, α, A_1 and A_2 are constants for a defined condition, which are related to the particular polymer-solvent system, temperature and the molecular weight range employed. For polystyrene in tetrahydrofuran (THF) at 40 °C and $1.91 \times 10^4 \le M_w \le 1.11 \times 10^6$, K= 0.0131, α= 0.719, A_1= 11.6 $g^{3/2}cm^{-3}mol^{-1/2}$, and A_2= 0.0206 $g\ cm^{-3}$.

Wang et al. (1995) used the following correlation for zero shear viscosity of polystyrene/styrene mixture during batch free-radical polymerization:

$$\eta_o = \exp\left\{ -12.116 + \frac{1496}{T(^oC)} + M_w^{0.2845}\left[8.679 w_p - 15.024 w_p^2 + \left(2.828 + \frac{4500}{T(^oC)}\right) w_p^3 \right] \right\} \qquad (0 < w_p < 0.6) \qquad (36)$$

where η_o is zero shear viscosity, T is temperature, and w_p is weight fraction of polymer.

Zubarev (1992) derived an expression to estimate the viscosity of colloids in the hydrodynamic vicinity of the critical point of the sol-gel transition. To derive that expression, the space occupied by a colloidal suspension was divided into cells, and a strain-stress equation was used. The expression obtained was considered to be a very simple scaling equation for viscosity at the gelation point.

Several research groups have focused their efforts on the estimation of the molecular weight distribution (MWD) of a polymer from the viscosity function. Yu (1991) proposed a numerical method to calculate the polymer molecular weight and its distribution curve from the plateau modulus G_n°, and the terminal zone of the stress relaxation modulus function, G(t). The method was illustrated with a series of monodisperse polystyrenes, and the agreement between predictions and experimental data obtained by light scattering and sedimentation methods was reported to be very good (less than 10% error was claimed). By using shift factors of the relaxation times (for binary blends of two monodisperse polymers with the same chemical structure), the suggested numerical method was used to calculate the molecular weight and molecular weight distribution of polystyrene from the terminal zone of the storage modulus (Yu, 1993). In order to handle polydisperse systems, the double reptation model (des Cloizeaux, 1988, 1990, 1992) has been used. Essentially, the double reptation model is a well conceived mixing rule which works very well in practice. Mead (1994) developed numerical and analytical methods to invert the double reptation mixing rule to determine the molecular weight distribution. It was found that the MWDs calculated from rheological data for polybutadiene and polypropylene were in close agreement with the corresponding GPC data and that they were very sensitive to small amounts of high molecular weight material present (Mead, 1994). On addressing criticism made to the viscosity-MWD conversion problem (it has been reported that this problem is ill-posed, from a mathematical point of view), Shaw and Tuminello (1994) argued that the inversion of the viscosity function to the MWD function is possible if the viscosity data are precise and complete. They mentioned that if the data are sufficiently numerous, the inversion appears to be quite resistant to random noise, although they acknowledged that the inversion involves a loss of resolution. Wasserman (1995) developed other numerical algorithms to calculate the MWD from the linear viscoelastic response of polymer melts, also based on the double reptation theory. Mead (1995) used the double reptation mixing rule to model the MWD and linear viscoelastic properties of an extrusion process. To estimate the process parameters, viscoelastic mechanical properties of the melt were measured, and the double reptation mixing rule was inverted. The estimation of polymer molecular

weight, and MWD, from rheological measurements can be useful in developing a correlation between molecular weight and viscosity, that could be used for the modelling of the PSD in suspension polymerization. However, the limitations and uncertainties of the numerical methods just mentioned should be considered.

2.2.4.2 Effects of rheological properties on breakage and coalescence

As mentioned previously, the increasing viscosity of the suspended droplets as polymerization proceeds, makes the quantitative analysis of suspension polymerization a complex problem. Most of the modelling studies on suspension polymerization have focused on liquid-liquid dispersions of low to moderate viscosities.

Hinze (1955) established a basis for data correlation when both surface and dispersed phase viscous forces contribute to drop stability. He proposed that two independent dimensionless groups were required and chose them to be a generalized Weber number, and a Viscosity Group, both based on drop diameter. Calabrase et al. (1986) used this viscosity group to study the effect of the dispersed viscosity on drop size. However, the range of viscosity they used was very low (up to 10 Pa-s). In studying a non-Newtonian mixture of monomers, their copolymer and pigment dispersed into water with emulsifier, Chaffey et al. (1991) described the drop's rheology with the Herschel-Bulkley Law (a power-law model). However, their analysis of the dispersion phenomena was performed semi-empirically using dimensionless-group correlations.

It seems that the first attempt to include the viscosity effects in a more realistic way and within the population balance approach was undertaken by the group of Alvarez (Valadez-González, 1988; Saldívar-Guerra et al., 1989; Martínez-Gómez, 1990; Hernández-Valdez, 1993; Alvarez et al., 1991, 1994a). As mentioned previously, they assumed that the material flow when a drop is broken or when two drops are coalescing, can be represented by flow of monomer/polymer through a circular duct of diameter equal to the diameter of the drop and a pressure drop term equal to the available kinetic energy. In one version of their model they used a power law rheology and a Scale-Law Theory to

correlate weight average molecular weight with zero shear viscosity (Valadez-González, 1988; Saldívar-Guerra et al., 1989; Vivaldo-Lima, 1989). In another version of their model the zero shear viscosity was still calculated using a Scale-Law Theory, but the flow problem was addressed as if the monomer/polymer mass behaved as a Maxwell fluid (Martínez-Gómez, 1990 and Alvarez et al., 1991). In the last version of their model, they calculated the zero shear viscosity using Free-Volume Theory (Alvarez et al., 1994a) and the internal flow was still envisioned as a Maxwell fluid (Hernández-Valdez, 1993 and Alvarez et al., 1994a).

2.2.5 Surface Phenomena

2.2.5.1 Protective Colloid Dispersants

It can be claimed that the suspending agent increases the viscosity of the continuous aqueous phase thus improving dispersion. However, there is evidence that the suspension stabilizer forms a film or skin around the droplet/particle surface, and so it is this layer which prevents coalescence and agglomeration by a mechanism analogous to steric stabilization, which is known to protect particles produced by dispersion and emulsion polymerization against flocculation. Some suspension polymerizations use low levels of protective colloid (~0.1 wt.%) with little increase in the viscosity of the aqueous phase, and the addition of water insoluble inorganic compounds is not likely to raise this viscosity significantly. Consequently, suspension stabilizers are largely effective when present in the interfacial layers between the water and the monomer droplets, and the tendency for interfacial adsorption is more important than the increase in viscosity of the aqueous phase when choosing a suitable stabilizer. (Dawkins, 1989).

The thin protecting film is generally regarded as adsorbed on to the surface of the generated droplet. The protective action of this adsorbed layer by steric stabilization operates by preventing the approach of the droplets (so "tacky" particles can not touch and aggregate). A good steric stabilizer is one which adsorbs strongly and quickly, is well anchored and provides a thick steric barrier. For a multiblock copolymer $(AB)_n$ in which A is an anchoring component on the droplet surface and B is

a steric stabilizer component, A should be organic compatible and B water compatible, giving a train-loop chain arrangement. Stabilization will be improved with longer A and B segments, but the length of the A segment should not prevent solubility of the copolymer in the aqueous phase. Studies by interferometry indicate that the thickness of the surface layer formed by the copolymer and the viscosity of this layer contribute to stabilization by the protective colloid, (Dawkins, 1989).

The stabilizing ability of suspension stabilizers depends not only on the decrease in the interfacial tension, but also on the mechanical properties of the protective film. When reducing the interfacial tension by means of surface active compounds, one should consider their chemical nature. The larger the hydrophobic part of the molecule, the higher the surface activity of the compound (or the larger the decrease in the interfacial tension caused by it), (Horák et al., 1981).

The intensive search for the best hydrophillic polymeric suspending agents for different monomers and different conditions of polymerization, keeping emulsion polymerization to a minimum and giving easily separated polymer beads at the same time, has resulted in a large patent literature. Besides natural and synthetic water-dispersible polymers and derivatives of the latter, many mixtures have been evaluated as well as additions of very small amounts of true surface active or soaplike micelle-forming agents, (Munzer and Trommsdorff, 1977).

When organic soluble polyvinyl acetate is hydrolysed so that less than about 20 mol% of the acetate groups are left, a water soluble copolymer containing acetate and alcohol groups is produced. Because of water solubility these suspending agents are often grouped under the generic name polyvinyl alcohol (PVA). Their behaviour as protective colloids will be influenced not only by molecular weight and degree of hydrolysis, but also by the method of manufacture, positioning of monomer units (whether head-to-head or head-to-tail), stereochemistry, degree of branching and distribution of acetate and hydroxyl groups. Industrially synthesized polyvinyl acetate has a wide molecular weight distribution and since the acid hydrolysis process is essentially random, control of block length is impossible. Alkaline hydrolysis using methanol is often preferred industrially, because of easy control of hydrolysis and few waste products. This alkaline product has a more blocky

structure where sequences are longer, but it would be expected that anchoring would be poorer because of the shorter sequences of acetate groups. It is presumed therefore that the acetate groups have affinity to the dispersed monomer phase and that the hydroxyl groups are directed towards the aqueous phase. The best suspending agents will require optimization of the degree of hydrolysis together with the number and length of the hydrophillic and hydrophobic sequences, (Dawkins, 1989; Fabini et al., 1994).

Winslow and Matreyek (1951) investigated the effect of a range of stabilizers, including PVA, on the particles formed during the suspension polymerization of divinylbenzene. They showed that under comparable conditions, (i) high molecular weight grades, (ii) partially hydrolysed grades, and (iii) high concentrations of stabilizer were associated with beads of lower mean diameter. The decrease of interfacial tension with increasing molecular weight, concentration and degree of hydrolysis can be used to explain the previous observations (Dawkins, 1989).

The issue of developing a method for selection of the type of PVA as stabilizer in suspension polymerization was addressed by Mendizabal et al. (1992). They proposed a method where it is not needed to carry out the polymerization at this stage (the stability analysis of the suspension is made based on the behaviour of the non-reacting system).

Other common stabilizers used for suspension polymerization are hydroxyethylcellulose (HEC) and hydrophobically modified HEC (HMHEC). The use of hydrophobically modified water soluble polymers as stabilizers in suspension polymerization shows some distinct advantages over conventional water soluble polymers used as stabilizers. These polymers strongly adsorb at the droplet interface and seem to act as barrier for migration of monomer and radicals from the monomer droplets to the continuous aqueous phase, thereby greatly reducing the formation of emulsion particles (Ahmed, 1984).

Hydroxypropyl methylcellulose (HPMC) is also used commonly as suspension stabilizer (Cheng and Langsam, 1984; Chung and Wasan, 1988; Zilberman et al., 1993). Cheng and Langsam (1984) found that the particle structure of polyvinyl chloride produced by suspension polymerization

using HPMC as stabilizer is controlled by the substitution and molecular weight of HPMC while the molecular weight distribution shows no apparent effect.

The use of only one dispersant is often not enough to provide the necessary dispersing power of the aqueous phase during the polymerization of vinyl chloride. Therefore, such dispersants as PVA and HPMC are used together with some additives. Many manufacturers use dispersing systems containing both PVA and HPMC. According to the patent literature, during polymerization in the presence of PVA-HPMC systems, the overall concentration of both polymers in water may be less than that during polymerization in the presence of individual dispersants. It is also known that the PVC particle properties greatly depend on the ratio between the components of the dispersing system; and the ability of the system is not an additive function of the ones related to PVA and HPMC alone. HPMC makes it possible to regulate the viscosity of the aqueous solutions and PVA, if necessary, secures low interfacial tension (Zilberman et al., 1993).

Macho et al. (1994) modified PVA to different degrees by acetalization reactions with different aldehydes in the presence of hydrochloric acid as "catalyst". By manipulating the degree of acetalization it is possible to prepare a suitable dispersant to produce PVC powder (in suspension polymerization) with the required morphology, and characterized by porosity, absorbtion of plasticizer and bulk density.

2.2.5.2 Powdered Dispersants (Pickering Emulsifiers)

Solid dispersants must be wet by two immiscible liquids, and they must also exhibit a certain degree of self-adhesion. The wettability can be modified by adsorption of low molecular mass surfactants. This technique is referred to as modulation and it has much in common with techniques used in mineral flotation processes (Hamielec and Tobita, 1992).

The wettability of a solid S by a liquid such as water (W) in the presence of a gas G depends upon the wetting angle α, which results from equilibrium between three interfacial tensions:

$$\sigma_{SW} + \sigma_{WG} \cdot \cos\alpha = \sigma_{SG} \qquad (37)$$

An angle α=0° corresponds to total wetting. For α=90°, σ_{SW}=σ_{SG}, and at α=180° no wetting occurs. In a three phase emulsion, two immiscible liquids compete for wetting a solid S: monomer M and water W. The equilibrium condition for this three phase emulsion is:

$$\sigma_{SW} + \sigma_{WM} \cdot \cos\alpha = \sigma_{SM} \qquad (38)$$

Taking the example of barium sulphate as the dispersant in a styrene-water bead polymerization, the barium sulphate is at first wetted more effectively by water than by styrene, so σ_{SW}<σ_{SM}. Water wets the barium sulphate with a small contact angle α and cos(α) is positive. Addition of a surfactant whose polar groups are adsorbed on the barium sulphate makes the surface more hydrophobic (or lipophilic). As a result, σ_{SW} increases and σ_{SM} decreases. In the limiting case, the particle is fully immersed in the monomer phase and loses its effectiveness as a dispersant. A good Pickering dispersant must possess amphipatic characteristics, (Hamielec and Tobita, 1992).

In studying the morphology of the layer of hydroxyapatite (TCP) that surrounded the polymer beads during the suspension polymerization of a random copolymer of styrene and butadiene, Deslandes (1987) found that the layer was actually composed of two distinct parts: a thin layer made of very uniformly distributed TCP primary particles and a second layer, usually much thicker, which was made of agglomerates of TCP which were loosely packed. He suspected that at the beginning of the reaction, when the monomer beads, which are still fluid, coalesce and reseparate, only the thin layer is sufficient to keep the suspension from collapsing. But as the reaction proceeds and the beads become more viscous and tacky, the second layer probably plays an important role in keeping the beads separated and in hindering coalescence. He pointed out that it could be possible that the thick layer was more efficient in acting as shock absorber and stabilizing the suspension late in the process.

2.2.5.3 Steric Stabilization

Stability of dispersion is one of the most important physical properties required for industrial suspension products. A review on stability of dispersions (DLVO and Steric Stabilization Theories) was prepared by Sato (1993). In it, he points out that the mechanism of the steric stabilization is

sufficiently complicated, and that a universal theory has not yet been established. A number of equations for calculating the steric repulsion energy have been derived theoretically from various points of view, e.g., from thermodynamics of polymer solutions, from statistical thermodynamics, from mechanical analysis, etc. However, it is difficult to confirm the validity of the equations experimentally since these equations involve various parameters such as segment density of adsorbed molecules, segment distribution, molar volume of the segment, etc., which can not be measured experimentally by the present technology (Sato, 1993). A very complete description and modelling of steric stabilization can be obtained from Napper and Hunter (1972).

2.2.5.4 Conventional Modelling

As applied to suspension polymerization, the effect of the stabilizer (either "protective colloid" or "pickering powder") is usually modelled in terms of the equilibrium interfacial tension between the water and organic (monomer/polymer) phases. This interfacial tension, σ_{WM}, is usually assumed constant and immersed in empirical correlations ("Weber number" models), (Dawkins, 1989; Yuan et. al, 1991; Hamielec and Tobita, 1992).

Alvarez et al. (1994a) used a population balance approach to model the Particle Size Distribution (PSD) in suspension polymerization. This model considers the viscoelastic effects of the dispersed phase, and the effect of the stabilizer (PVA) is modelled in terms of the amount of surface coverage, assuming a Langmuir-type interfacial tension. The expressions they used are the following:

$$\sigma = \sigma_o - k_\sigma \theta \tag{39}$$

$$\theta = \frac{k_a C_a}{1 + k_a C_a} \tag{40}$$

$$C_a = C_s - a\theta C_m \tag{41}$$

where σ is interfacial tension, σ_0 is interfacial tension in the absence of the suspending agent, θ is surface coverage, a is interfacial area per unit volume of water, k_a and k_σ are constants, and C_a, C_s, and C_∞ are concentrations of stabilizer in aqueous phase, total, and at $\theta=1$, respectively.

2.2.5.5 Dynamic Interfacial Properties

It has been proposed that the rheology of emulsions (and suspensions) may be influenced by the interfacial rheology of the emulsifier film (or suspension stabilizer) surrounding the droplets (Tadros, 1994), and the dynamic nature of the interfacial tension (Janssen et al., 1994).

The magnitude of the deviation from uniform (equilibrium) interfacial properties (interfacial tension, viscosity and elasticity) depends on the ratio of the time scale of the interfacial deformation and that of its relaxation toward adsorption equilibrium. In particular, the use of the equilibrium interfacial tension is believed to be adequate only when the relaxation is very effective (Janssen et al., 1994).

Chung and Wasan (1988) measured the dynamic interfacial properties (interfacial tension, shear viscosity and shear modulus) for a mixture with physical properties analogous to vinyl chloride, and concluded that the dynamic interfacial properties, and not the equilibrium interfacial tension, are the controlling parameters in droplet dynamic stability (although it should be considered that their analysis was made at a low viscosity of the dispersed phase, which may not make this conclusion applicable for suspension polymerization). There has been development of techniques to measure the dynamic interfacial tension, such as the "breaking thread method" (Elemans et al., 1990), "shape evolution of short fibers" (Carriere et al., 1989), and estimation via relaxation of drop shapes and filament breakup (Tjahjadi et al., 1994).

Some research groups, such as Stone and Leal (1990) and Tjahjadi et al. (1994), have studied the effect of surfactants on drop deformation and breakup using rigorous fluid mechanics equations and computational fluid dynamics (CFD) tools. They have been able to calculate the surfactant

distribution and drop shape evolution (using a simple linear correlation between interfacial tension and surface coverage), but the method is complex and limited to simple flow situations (suspension polymerization would be extremely difficult to model using those ideas), and Newtonian fluids (which is not the case in suspension polymerization).

A good review paper on the importance, modelling, and measurement techniques of dynamic interfacial rheology was published recently (Tadros, 1994). In it, he defined several interfacial properties (Gibbs dilational elasticity, interfacial shear viscosity, surface yield stress, etc.), a relaxation time (associated to stress relaxation experiments), a strain or compliance (associated to strain relaxation experiments), and a complex modulus (associated to dynamic oscillatory experiments). He described the equipment and techniques used to measure such properties, and tried to find a correlation of interfacial rheology with emulsion stability. He concluded that although interfacial rheology is a powerful tool to understand macromolecular films, other factors are more important in stabilization (such as film drainage and thickness).

2.2.6 Polymerization Effects

Initiators used in suspension polymerization are oil-soluble, and polymerization takes place within the monomer droplets. Typical initiator concentrations are 0.1-0.5 wt % based on monomer. A simple calculation shows that the monomer droplets are large enough to contain a very large number of free radicals (~10^5) (Kalfas and Ray, 1993a). Therefore, the kinetic mechanism is the same as that of bulk polymerization (Munzer and Trommsdorff, 1977), and the same kind of dependence of polymerization rate on initiator concentration and temperature is observed. Bead suspension processes are considered to be water-cooled micro-bulk polymerizations in the monomer droplets.

As mentioned previously, polymerization kinetics belongs to the microscale stage for modelling purposes. The link between this stage and the macroscale one (represented by the population balance equation) is established by the zero shear viscosity of the monomer/polymer droplets. Complete descriptions on the different stages of polymerization (characterized by the viscosity of the droplets)

and their effect on the breakage/coalescence rates are offered elsewhere (Hamielec and Tobita, 1992; Yuan et al., 1991; Villalobos, 1989; Mitchell, 1986).

It is important to realize that the more accurate (the predictions) and simple (the mathematical structure) the kinetic model is, the more reliable and simple the predictions of breakage/coalescence rates would be. Important kinetic studies which are being used by our group are those conducted by Vivaldo-Lima et al. (1994a) in the case of free radical homopolymerization, Vivaldo-Lima et al. (1994b) for free radical copolymerization with crosslinking, and Villalobos et al. (1991, 1993) for free radical homopolymerization with bifunctional initiators. Other models for free-radical polymerization and copolymerization have been reviewed elsewhere (e.g., Vivaldo-Lima et al., 1994a, 1994b). A recent general review on polymerization reactor modelling was presented by Kiparissides (1996). Additional recent contributions follow in this section.

Kalfas and Ray (1993a) studied the kinetics of aqueous suspension polymerization processes. They modelled polymerization of partially soluble monomers, and concluded that if adequate modelling of the equilibrium partition and transport of monomers between the two phases is made, universal models built on the common kinetic mechanism of free radical polymerization can be used for either case (namely, no different kinetic constants should be required for the case of partially soluble monomers).

Tefera et al. (1994) developed a model for the free-radical suspension polymerization kinetics of styrene up to high conversions. Their model was based on free volume theory, it considered the initiator's efficiency to decrease with a free-volume dependence (as per Vivaldo-Lima et al. (1994a) and other references cited in Vivaldo-Lima et al.'s paper), and made use of two different bimolecular termination kinetic rate constants, one for polymerization rate, and the other for molecular weights (number and weight average molecular weights). In their paper, Tefera et al. (1994) questioned the proposal of Zhu and Hamielec (1989) regarding the use of different averages for the bimolecular termination kinetic rate constant (different averages of the distribution of termination rate constants), and the implicit suggestion that polymerization rate and number average molecular weight can be

modelled with the same termination kinetic constant, namely the number average termination kinetic constant, k_m. They based their postulates on the fact that their model could not simultaneously predict rate and number average molecular weight using the same termination kinetic constant (an overestimation of Mn at low and intermediate conversions was observed in their predicted profiles), whereas a better fit was obtained by using a different k_t for molecular weight calculations. However, Vivaldo-Lima et al. (1994a) developed a model where a single k_m gives good predictions of rate and number average molecular weight, and where a weight average termination constant, k_{tw}, is defined and used without additional parameters to the model. This weight average termination constant is used to model weight average molecular weight. It seems that the overestimation of molecular weights at low and intermediate conversions in the paper of Tefera et al. (1994) comes from using a kinetic model with a "parallel" structure, instead of a "series" one (for details on the "parallel" and "series" approaches for modelling free-radical polymerization, the reader is referred to the paper of Vivaldo-Lima et al., 1994a).

O'Shaughnessy and Yu (1994) presented a theory for the auto-acceleration effect in free-radical polymerization. According to their theory, the termination rate constant (k_t) between two macroradicals ("living chains") is dominated by the length, N, of the shortest chain, $k_t \sim N^{-\alpha}$, where α is a characteristic exponent that depends on the (polymer) concentration regime. This leads to the result that polymerization rates, R_p, are independent of initiation rates, R_i, in contrast to the classical $R_i^{1/2}$ result. Although the theory of O'Shaughnessy and Yu (1994) is sound and elegant, it is realistic for sufficiently high temperatures or sufficiently low conversions. For practical engineering purposes it is still more adequate to use other models.

Panke (1995) presented a model for the diffusion-controlled initiation, propagation and bimolecular termination in free-radical polymerization. The model was based on free-volume theory, considered that the kinetic rate constants could be modelled with a "parallel" structure to take into account the chemical and diffusional phenomena, considered the effect of instantaneous and accumulated molecular mass on the translational termination constant, and also reaction diffusion

termination. The model was tested using conversion-time data. According to the analysis presented by Vivaldo-Lima et al. (1994a), there are some potential disadvantages with Panke's model. Firstly, the model assumes a "parallel" structure, which Vivaldo-Lima et al. (1994a) demonstrated to be uncertain for systems with moderate gel effect (for instance, the conversion-time profiles included in Panke's paper show an exaggerated gel effect prediction for MMA polymerization in the presence of dodecyl mercaptan). Secondly, only conversion-time data were used for the parameter estimation, which explains the very good predictions of conversion-time profiles without solvent or chain transfer agents. Finally, only a single average is used for the termination kinetic constant, namely k_m (according to Zhu and Hamielec, 1989, and Vivaldo-Lima et al., 1994a, it would be expected that Panke's model can provide good predictions of conversion and number average molecular weight for bulk polymerizations, but weight average molecular weight might be underpredicted at intermediate and high conversions).

Seth and Gupta (1995/6) developed a model for auto-acceleration effect in free-radical polymerization. Their model followed the approach of Achilias and Kiparissides (1992) (based on a "parallel" structure for diffusion-controlled kinetic rate constants), but non-isothermal and semi-batch conditions were considered. As expected (from the analysis of Vivaldo-Lima et al., 1994a), predictions of conversion are overestimated and those for weight average molecular weight are underestimated, when the model of Seth and Gupta (1995/6) is used to model a solution homopolymerization (of methyl methacrylate).

Beuermann et al. (1995) investigated the low and intermediate solution polymerization kinetics of methyl methacrylate (MMA) in toluene and in 2-butanone. They described an experimental technique (using laser pulse initiation and infrared spectroscopy to determine MMA concentrations) to measure the coupled values of the rate coefficients for propagation and termination (k_p and k_m). As k_p was known experimentally from other measurements, k_m could be estimated directly. They found that at low conversions, k_m is a strong function of solvent concentration, and that the variation of k_m with conversion is significantly affected by the starting fraction of solvent. They modelled the

evolution of k_m with conversion using a model with a "parallel" structure, and a viscosity dependent expression to take into account the diffusion-controlled nature of termination. By using a single adjustable parameter, they were able to obtain good predictions of k_m in the ranges of conversion and experimental conditions considered in their study.

Buback and Kuchta (1995) determined experimentally the propagation rate coefficient, k_p, of the free-radical polymerization of styrene between 30 and 90 °C, and up to a maximum pressure of 2800 bar. Their data from pulsed-laser polymerization and product analyses by gel-permeation chromatography were reported to be adequately represented by the expression:

$$k_p(L\,mol^{-1}s^{-1})] = 17.14 - 1.873x10^{-4}p\,(bar) - \frac{3748}{T(^0K)} + 0.202\frac{p\,(bar)}{T(^0K)} \qquad (42)$$

Anseth and Bowman (1994) presented a kinetic gelation simulation of the network microstructure (simulation of the structure in space using a percolation-type simulation) during homopolymerization of tetrafunctional monomers and the copolymerization of tetrafunctional and difunctional monomers. They studied network inhomogeneities, relative functional group reactivities, and cyclization versus crosslinking tendencies. The kinetic gelation simulations (using a percolation model) were used to study highly crosslinked systems. These same authors defined a heterogeneity index to measure the heterogeneous distribution of species during the polymerization of tetrafunctional monomers. To do so, kinetic gelation simulation predictions were obtained (Anseth and Bowman, 1995).

The group of Okay developed a model for gel formation in free-radical crosslinking copolymerization. A summary of this model and some experiments on the equilibrium swelling and gel fraction for the methyl methacrylate/ethylene glycol dimethacrylate (MMA/EGDMA) and styrene/p-divinylbenzene systems, are discussed in Naghash et al. (1995). That model consists of rate equations for the concentration of various species and the moment equations for branched molecules and primary chains. The model considers three types of vinyl groups with different reactivities, neglects cyclization reactions, uses an empirical model for bimolecular termination (which is assumed

to be diffusion-controlled only during the post-gelation period), uses the steady-state hypothesis for the radical concentration, and assumes the validity of the limitations following from the Flory lattice theory and the theory of rubber elasticity. In another version of their model, cyclization and substitution effects were considered (Okay et al., 1995).

Luo et al. (1995) presented a model for molecular weight development in the vinyl chloride-divinyl monomer suspension copolymerization during the pre-gelation period. This model can be considered as an adaptation of the Tobita-Hamielec model (e.g., Tobita and Hamielec, 1989) to a two phase copolymerization with crosslinking.

Finally, Capek (1996) presented a review on the kinetics of heterogeneous (emulsion, dispersion and suspension) free-radical crosslinking polymerization. This review and the paper of Vivaldo-Lima et al. (1994b) provide a complete overview of the state of the art on modelling of free-radical crosslinking polymerization kinetics.

2.3 Experimental Studies

2.3.1 Particle Size Distribution and Breakage/Coalescence Phenomena

This subsection will briefly summarize the experimental studies on PSD of either styrene or styrene/divinylbenzene (co)-polymerizations (reactive systems) available in the literature. There will also be some mention to recent experimental studies on particle size distributions of suspended droplets for non-reactive systems, and a summary of techniques to measure the particle size distribution in liquid-liquid dispersions. The reactive and non-reactive situations are described in Table 2.2.

The techniques to measure particle size distributions can be classified in: (i) bulk separation methods (sieving), (ii) sedimentation, (iii) centrifugation, (iv) electrical sensing, (v) spectroscopy and microscopy, and (vi) laser diffraction (light scattering). Some relevant characteristics of each of them are given below (Hildebrand and Row, 1995).

Bulk separation methods (used for solid particles) were preferred in the past. They eliminated

much of the problems associated with sampling (obtaining a representative sample). Sieving afforded a major reduction in analysis time (and cost) over microscopy, but the tradeoff for this increase in speed was a loss of resolution. A limitation on the minimum size that could be determined restricted its use for some applications. The minimum size measurable with this technique is of the order of 38 μm.

Table 2.2 Experimental studies on PSD and breakage/coalescence phenomena.

Type of system	Remarks	References
Reactive systems (homo- or copolymerizations of styrene and divinylbenzene).	Effects of hydrodynamic (type of agitator and size of impeller, presence of baffles, etc.), surface (type and concentration of stabilizers), and kinetic factors have been studied following different experimental approaches ("once at a time" variation of each factor, and factorial designs with few factors). PSD measurements have been made using different techniques (sieving, micro-photography, use of Coulter Counter, etc.).	Winslow and Matreyek (1951), Watters and Smith (1979), Langner et al. (1979, 1980), Leng and Quarderer (1982), Konno et al. (1982), Balakrishnan and Ford (1982), Schröder and Protowski (1982), Hatate and Ikari (1985), Mitchell (1986), Villalobos (1989), Apostolidou and Stamatoudis (1990), Erbay et al. (1992).
Non reactive systems.	- Model systems (e.g. styrene - without initiator-, ethylbenzene, carbon tetrachloride in n-heptane or 1-octanol, etc.) have been used to study breakage and coalescence. Photographic, imaging, laser light scattering, and other techniques have been used.	Borwankar et al. (1986), Laso et al. (1987b), Söhnel and Mullin (1991), Chatzi and Kiparissides (1992, 1995).
	- An interesting videotechnique to measure transient drop-size distributions (during phase inversion in chlorobenzene-water or glycerol-water solutions) has been presented recently. It requires a high speed video camera, a low magnification stereo microscope, a super VHS videorecorder, and a stroboscopic lighting system.	Pacek et al. (1993, 1994a, 1994b), Pacek and Nienow (1995).

Sedimentation is based on the principle that particles of different sizes have different rates of fall through a fluid of known viscosity (Stokes law). This technique extended the lower end of the size range to 2 μm, while retaining the benefit of examining large number of particles. Centrifugation separates particles based on the particles' responses to physical forces as a function of their size. The lower end of size is around 0.05 μm but, as with sieving and sedimentation, results are strongly influenced by particle shape.

Particle size analyzers using the electrical sensing zone method directly determine the volume of a particle by measuring the change in electrical impedance across an aperture of known dimensions through which the particle is made to flow. This is a high resolution technique and it is extremely accurate across its 0.4-1200 μm range. However, samples with a dynamic range greater than 30:1 by diameter require multiple-aperture measurements. the Coulter Counter size counter can be classified in this group.

Photon correlation spectroscopy (PCS) and electron microscopy measure particles from a few nanometres up to a few microns. PCS analyzers are inherently low resolution instruments. Electron microscopes offer high resolution but require complicated sample preparation.

The interaction of light and a particle results in a combination of the optical phenomena known as diffraction, transmission, absorption and reflection. Light-scattering particle size analyzers vary widely in design and execution, but all are sensitive to at least one of these optical phenomena. Laser diffraction measurements are based on the phenomenon of diffraction. A laser light scattering particle sizer measures the flux pattern (of light diffracted by particles) accurately enough to determine the populations of particles in different size classes. Some advantages of laser light scattering (over the other methods) are: (i) results are accurate and highly reproducible, (ii) a wide range of particle sizes can be sized in a single measurement (50,000:1, depending on the sample transport system design), (iii) measurements are fast (typically 60-90 seconds), (iv) any transparent fluid (including air) can be used to deliver the sample to the sensing zone, (v) field calibration is unnecessary, and (vi) the instrumentation is easy to use.

2.3.2 Mixing Effects

In characterizing flow fields, one important experimental technique is Laser Doppler Anemometry (LDA), or Laser Doppler Velocimetry (LDV) (for measuring of individual velocity components). Other experimental techniques in this area are Laser Sheet Illumination (LSI) (for qualitative visualization of flow patterns inside the vessel), Laser Induced Fluorescence (LIF), and Coherent Anti-Stokes Raman Spectroscopy (CARS). These techniques, combined with detailed (yet computationaly time-demanding) CFD calculations, are among the most important tools to address mixing phenomena. A description of the practical use of some of these kinds of measurements is available in Kresta (1991), who studied turbulent flow in stirred tanks using pitched blade impellers (PBT) (Kresta and Wood, 1991). Some recent experimental studies on mixing in stirred tanks are presented in Table 2.3. This kind of experimental studies can be used to characterize the type of mixing in a given system, and quantify the turbulent kinetic energy and its dissipation rate, for the tank. These values could be obtained using CFD tools, and from the results, divide the tank in two or more zones with appropriate ϵ average values.

2.3.3 Rheological Phenomena

Due to the reactive and sensitive nature of the monomer/polymer mixture, the determination of zero shear viscosity is usually made from mixtures of monomer and polymer in such proportion that an equivalent conversion value is represented. Shumsky et al. (1994) measured the viscosity evolution of a reacting step growth system (hexamethylene diisocyanate, HMDI, and oligomeric epoxy rubber, ER, which leads to the formation of a polymer network), using a rheoviscometer in a cone and plate configuration. However, for free-radical systems such direct monitoring is not possible with conventional viscometers, due to the toxicity of the monomers, the inhibition effect of oxygen from air on the polymerization reaction, and the extremely high viscosities obtained when crosslinking reactions are involved. Other techniques used or of potential use are discussed below.

Table 2.3 Experimental studies on characterization of flow fields in stirred tanks.

Type of technique	Remarks	References
Laser Doppler Anemometry (LDA)	Many studies have been reported. Effects of type, dimensions and location of impeller on velocities, turbulent kinetic energy, flow number, hydraulic efficiency and pumping effectiveness have been considered. Also considered have been the effects of geometric modifications to the vessel, and the presence of two or more (multiple) impellers.	Jaworski et al. (1991), Ranade et al. (1992), Nouri and Whitelaw (1992), Mishra and Joshi (1993), Bakker and Van den Akker (1994a), Dong et al. (1994a), Mishra and Joshi (1994), Stoots and Calabrase (1995), Armenante and Chou (1996), Jaworski et al. (1996), Rutherford et al. (1996).
Flow visualization techniques	- Tuft flow visualization.	Chapple and Kresta (1994).
	- Laser sheet illumination (LSI).	Horio and Kuroki (1994), Rutherford et al. (1996).
	- Laser induced fluorescence (LIF)	Bakker and Van den Akker (1994d).
	- Tracer visualization and video techniques.	Janzon and Theliander (1994), Mann et al. (1995), Lamberto et al. (1996).
	- Flow follower techniques.	Bodemeier et al. (1992), Roberts et al. (1995).
	- Electrical impedance tomography.	Williams et al. (1993).
	- "Dye-streak" technique.	Hoyt and Sellin (1995).
	- Fluorescence tracer pulse response technique.	Cui et al. (1996), Jones et al. (1996).
Measurement of power number	Power numbers for stirred tanks using different types and number of impellers, have been determined using strain-gauge techniques.	Distelhoff et al. (1995), Ibrahim and Nienow (1995), Rutherford et al. (1996).
Other techniques	- Determination of time-averaged specific kinetic energy of turbulence using a stirring-intensity-meter (SIM).	Fořt and Libal (1991), Fořt et al. (1992, 1993).
	- Development of a mechanical device to measure the frequency of turbulent macro-instabilities in agitated systems.	Brůha et al. (1995).

Adam and Delsanti (1979), and Adam et al. (1979, 1981) used a magnetic sphere rheometer to measure viscosity of styrene-benzene in situ (Adam and Delsanti, 1979), and styrene-divinylbenzene (Adam et al., 1979, 1981). A magnetic sphere was introduced with each sample (5 cm^3) into a glass tube which was then degassed under vacuum and sealed. The magnetic sphere experienced a force F due to a non-uniform magnetic field created by an external coil. The sphere was imaged on two photodiodes by an optical system. The differential photo-current P_1-P_2 was fed to a monitor which adjusted the voltage V applied to the magnetic coil in such a way that the sphere remained at the same position on the coil axis. Thus, the force F acting on the magnetic sphere was proportional to the voltage V. By measuring V, the magnetic force that counteracts the viscous or elastic forces, could be known.

In McClusky et al. (1994) there is mention of several viscometers used to measure the viscosity build-up of a reacting polyurethane or other foam formulation systems. Some of them include a vibrating ball viscometer (which was a heat sink that altered the chemical and morphological development of the polymer), a pulse rheometer using an aluminum paddle, with bottom and side edges sharpened to a knife edge, as a sensor (however, the cooling effect of the paddle on the polymer presented a major problem), and a vibrating needle curemeter (which appears to be useful in following the later stages of foam cure). McClusky et al. (1994) used a vibrating rod viscometer to follow and understand the development of reacting polyurethane formulations. The sensor rod of the vibrating rod viscometer oscillated about its vertical axis, tracing out a circle with a controlled radius. Thus, the rod created a shear wave which was absorbed by the liquid. Two coil sensors in the viscometer head measured the amplitude of oscillation, and drove the rod to replace the energy absorbed by the liquid. It was the current required to power the drive coil which was measured by the viscometer (since not all the energy transferred from the rod to the polymer is absorbed, this viscometer measured the complex viscosity, instead of the nominal one).

The dependence of rheological properties on molecular weight has been used to develop molecular weight determination techniques. Dynamic properties, such as the storage modulus and

viscosity, can be measured with a conventional parallel-plate rheometer. Using numerical methods, the MWD can be obtained from the rheological data (Yu, 1993; Wasserman, 1995).

Horita et al. (1993) measured intrinsic viscosity and weight average molecular weight for solutions of atactic polystyrene in trans-decalin at 21 °C, in methyl ethyl ketone at 35° C, and in benzene at 25 °C. Their measurements were obtained with conventional capillary viscometers, of the Ubbelohde type. These results could be used to develop a correlation between number average molecular weight and viscosity (other experimental data could be added or obtained, in order to get better estimates of the correlation parameters).

2.3.4 Surface Phenomena

Methods to measure interfacial tension include the Ring Method (Hiemenz, 1977), and the Drop Dimensions Measurement Technique (Manning, 1976). Chatzi and Kiparissides (1994) measured the interfacial tension of a n-butyl chloride/water system at different times and concentrations of stabilizer, using the Wilhelmy plate method. They used PVA at 73, 80, and 88 mol% degree of hydrolysis. From the measurements of PSD in the system studied, it was observed that changing the agitation level had a greater impact on PSD when a low degree of hydrolysis PVA (73 mol%) was used than was the case when a high degree of hydrolysis PVA (88 mol%) was used.

Finally, Castellanos et al. (1991) proposed a method for the selection of the type of PVA as stabilizer. In this method it is not needed to carry out the polymerization at the selection stage.

2.4 Suggested Research Approach

2.4.1 Theoretical/Modelling Approach

As mentioned in the introduction of this paper, one of the major deficiencies in the understanding and development of suspension polymerization technologies is the interconnection between the different stages of modelling (micro-, meso-, and macroscales). Also, the scale up of polymerization reactors is an issue not adequately understood. With these issues in mind, the following

recommendations can be made for future directions:

a) The non-homogeneous flow field in the reactor should be considered in the population balance equation. A 3-dimensional analysis would lead to a very complex problem of limited practical use. Instead, advantage should be taken of what is known about the process. It is well known that the homogeneous approach reasonably predicts experimental data, except for the fact that most models can not predict the bimodal PSD which is rather common is suspension polymerizations at the pilot plant scale. It is also known that the flow field has two main regions: the one around the impeller where most breakage occurs, and the bulk of the tank, where most coalescence takes place. Therefore, a practical proposal is to use a two zone (or multi-zone) model, where different kinetic energy and energy dissipation values in the kernels of the integrals of the population balance are used for each zone.

b) To estimate which values (or profiles) for kinetic energy and rate of energy dissipation should be used, 2-dimensional simulations of a simplified system with the same hydrodynamic conditions and main physical properties could be performed. Although simplified, this approach is not straightforward, as the determination of the boundary conditions for impellers other than the disk-turbine is not a trivial issue, even in the 2-dimensional case. Other possible approaches could be to experimentally measure the rate of energy dissipation distribution using water, and the same reactor configuration, or perform a rigorous 3-dimensional CFD simulation of the non-reactive system (water). In both of these two cases, corrections (or inclusion) due to the presence of a dispersed phase should be done.

c) It is known that the PSD for systems where coalescence is not present (or where it is negligible) can be well represented with a normal or log-normal distribution (e.g., Mitchell, 1986). Coalescence causes the distribution to be broadened and deviate from normality, even producing multimodal distributions. Therefore, it is proposed that in the initial stages of modelling (since this approach is rather empirical) this behaviour could be captured adequately and the solution to the population balance equations simplified, if it is assumed that breakage

and coalescence have different analytical density distributions that, when superimposed, produce the PSD of size encountered experimentally. A similar approach has been taken by Moreira et al. (1995), in the context of animal cell aggregates in stirred vessels. They assumed that a bimodal distribution could be represented by a linear combination of two modified β-distributions. Nishikawa et al. (1991, 1994) also modelled breakage, coalescence, and mixing with aeration as phenomena with individual size distributions (normal distributions with different parameters), and the overall PSD was considered to be a linear combination of the individual normal distributions.

d) It is known that the Maxwell fluid model for viscoelesticity is a widely used model in the rheology area, mainly for academic purposes. It is known that it is one of the poorest models to predict elongational viscosity, since it predicts constant shear viscosity at all shear rates, which is known to be in disagreement with actual polymer behaviour (Vlachopoulos, 1994). One of the best models available to date for rupture/coalescence phenomena uses this model (Alvarez et al., 1991, 1994a). Therefore, the rheology of the droplets would have to be reconsidered, if an effective model (one which possesses predictive power) is desired. Obtaining a general viscoelastic model is yet a theoretical challenge; therefore, developing a semi-empirical model might be the most appropriate choice.

e) Using an adequate polymerization kinetic model is very important. It is recommended to use a "series" approach for modelling diffusion-controlled kinetics in free-radical (co)-polymerization, since the use of a "parallel" structure has been shown to produce rather uncertain predictions of conversion and molecular weight evolution, at least for the styrene and styrene/divinylbenzene polymerization cases (Vivaldo-Lima et al., 1994a, 1994b).

2.4.2 Experimental Approach

a) Suspension polymerization has been widely studied experimentally to present, hence one may consider that the main factors affecting the PSD are already known. What is not fully clear,

however, is the effect obtained when those factors interact. Inadequate experimental design strategies sometimes lead to incorrect conclusions on this regard. In order to identify and estimate the relative importance of the different factors, it is suggested to exploit the information available in the literature (this review can be a guide in that direction), and use rigorous statistical experimental design techniques. A good example on how to address a difficult problem such as this one is given by Scott et al. (1993a, 1993b).

b) The phenomena involved in suspension polymerization are so varied and complex, that a model validation using a single measurement (namely particle size distribution) would be clearly insufficient. As pointed out by Laso et al. (1987a), most models for rupture and coalescence phenomena involve a number of parameters that have to be determined from experimental data. Due to the complexity of the models, the design of those experiments is not always the most adequate and the statistical significance of those parameters is usually very low. Besides, in order to propose adequate models for the rupture and coalescence phenomena, a good physical understanding and evidence of what is going on inside the vessel is needed. Therefore, it is strongly recommended to perform experimental studies that can capture the main mechanistic behaviour of the rupture and coalescence phenomena. To do so, adaptations from techniques similar to the ones described in sections 2.3.1 and 2.3.2 of this paper can be made and tested. These techniques would be expected to provide valuable insight into the mechanistic behaviour of the rupture and coalescence phenomena, and hopefully some basis for quantitative parameter estimation. Some of the issues that would be desired to highlight in this way include: number and distribution of "daughter" droplets when a mother droplet is broken, type of "flow behaviour" dominant in the formation of a droplet when a collision results in coalescence of smaller droplets, assessment of changes in the mechanistic behaviour for rupture and coalescence of droplets as polymerization proceeds (as viscosity changes), etc.

c) If impellers other than the Rushton turbine and the pitched blade turbine are used, it would be necessary to carry out flow visualization studies, and perhaps experimental determination of

kinetic energy and rate of energy dissipation profiles in the tank, using Laser Doppler anemometry techniques.

d) For parameter estimation purposes, optimal Bayesian experimental designs may be used in order to take advantage of the previous information and minimize the experimental effort, and the associated costs and time (see, for instance, Dubé et al., 1996).

2.5 Concluding Remarks

Even though suspension polymerization has been studied for more than 50 years, the present review and the industrial problems that practitioners are continuously faced with their processes in controlling the particle size distribution, show that the main issues are still far from solved. This situation is not surprising if one takes into account all the complex phenomena (polymerization kinetics, rheological behaviour of the polymer/monomer particles, interfacial properties, suspension stability, and the inhomogeneity of the tank, to name a few) that occur simultaneously in a suspension polymerization reactor.

With such a diversity of phenomena occurring simultaneously, it is not uncommon to overemphasize some effects and neglect others when a model is being developed. The best way to discriminate among models is to perform carefully designed experiments. However, before using statistical tools, one has to make sure that the experimental techniques being used are adequate in terms of providing enough information and insight on the mechanism under consideration. It is our opinion that much effort must be placed on developing experimental techniques that can provide (not just infer) information on the rupture and coalescence mechanisms.

Some key issues in modelling suspension polymerization are (i) free-radical polymerization kinetics, (ii) rheological evolution of the monomer/polymer droplets during the polymerization, (iii) mixing effects, and (iv) surface phenomena effects. From these issues item (i) has been the most studied (and yet can not be considered fully covered, particularly when phenomena such as crosslinking take place inside the droplets), item (ii) has only recently being considered in a more

systematic way (e.g., the models of Alvarez et al., 1991, 1994a), and item (iii) is assumed to be well represented by a homogeneous model. Modelling of surface phenomena has been addressed from simple and rather more sophisticated points of view (considering dynamic interfacial rheology), leading to the conclusion that there is a need for more fundamental research in this area. In addressing complex phenomena such as suspension polymerization the present simple surface phenomena models seem to still be more adequate. Regarding the mixing environment, the experimental evidence shows that at least two zones are observed in a stirred tank reactor (the impeller and bulk zones). Therefore, it is our opinion that the homogeneity approach can no longer be accepted as a standard valid assumption for realistic (reliable) modelling studies on PSD in suspension polymerization.

Some guidelines on what is believed to be an adequate way to address the modelling and control of the particle size distribution in suspension polymerization reactors have been offered in this paper. Some of them are being used by our research groups, and results will be communicated in the near future.

Acknowledgement

One of the authors (E. Vivaldo-Lima) wishes to acknowledge partial financial support from the Mexican Science and Technology National Council (CONACYT) and the Department of Chemical Engineering of McMaster University.

2.6 References

Abid, M.; Xuereb, C.; Bertrand, J. Modeling the 3D hydrodynamics of 2-blade impellers in stirred tanks filled with a highly viscous fluid. *Can. J. Chem. Eng.*, **1994**, 72, 185-193.

Abrahamson, J. Collision rates of small particles in a vigorously turbulent fluid. *Chem. Eng. Sci.*, **1975**, 30(11), 1371-1379.

Achilias, D.S.; Kiparissides, C. Development of a general mathematical framework for modelling diffusion-controlled free-radical polymerization reactions. *Macromolecules*, **1992**, 25, 3739-3750.

Adam, M.; Delsanti, M. Viscosity and reptation time in polystyrene-benzene semidilute solutions. *J. Phys. Lett.*, **1979**, 40, 523-527.

Adam, M.; Delsanti, M.; Okasha, R.; Hild, G. Viscosity study in the reaction bath of the radical copolymerization of styrene divinylbenzene. *J. Phys. Lett.*, **1979**, 40, 539-542.

Adam, M.; Delsanti, M.; Durand, D.; Hild, G.; Munch, J.P. Mechanical properties near gelation threshold, comparison with classical and 3d percolation theories. *Pure & Appl. Chem.*, **1981**, 53, 1489-1494.

Aduna-Espinoza, E. Solución de balances de población mediante aproximación con función gama. M. Eng. Thesis (in Spanish), Unidad de Ciencias Básicas e Ingeniería, Universidad Autónoma Metropolitana, Plantel Iztapalapa, México D.F., Mexico, 1991.

Ahmed, S.M. Effects of agitation, and the nature of protective colloid on particle size during suspension polymerization. *J. Dispersion Science and Technology*, **1984**, 5(3&4), 421-432.

Aloi, L.E.; Cherry, R.S. Cellular response to agitation characterized by energy dissipation at the impeller tip. *Chem. Eng. Sci.*, **1996**, 51(9), 1523-1529.

Alvarez, J., Suárez, R.; Sánchez, A. Nonlinear decoupling control of free-radical polymerization continuous stirred tank reactors. *Chem. Eng. Sci.*, **1990**, 45(11), 3341-3357.

Alvarez, J.; Alvarez, J.J.; Martínez, R.E. Conformation of the particle size distribution in suspension polymerization. The role of kinetics, polymer viscosity and suspension agent. *J. Appl. Polym. Sci.: Appl. Polym. Symp.*, **1991**, 49, 209-221.

Alvarez, J.; Alvarez, J.J.; Hernández, M. A population balance approach for the description of particle size distribution in suspension polymerization reactors. *Chem. Eng. Sci.*, **1994a**, 49(1), 99-113.

Alvarez, J., Suárez, R.; Sánchez, A. Semiglobal nonlinear control based on complete input-output linearization and its application to the start-up of a continuous polymerization reactor. *Chem. Eng. Sci.*, **1994b**, 49(21), 3617-3630.

Anseth, K.S.; Bowman, C.N. Kinetic gelation model predictions of crosslinked polymer network microstructure. *Chem. Eng. Sci.*, **1994**, 49(14), 2207-2217.

Anseth, K.S.; Bowman, C.N. Kinetic gelation predictions of species aggregation in tetrafunctional monomer polymerizations. *J. Polym. Sci. Part B: Polym. Phys.*, **1995**, 33, 1769-1780.

Apostolidou, C.; Stamatoudis, M. On particle size distribution in suspension polymerization of styrene. *Collect. Czech. Chem. Commun.*, **1990**, 55, 2244-2251.

Apostolidou, C.; Stamatoudis, M. Transient behaviour of drop sizes in stabilized agitated dispersions. *Chem. Ing. Tech.*, **1991**, 63(1), 66-68.

Arai, K.; Konno, M.; Matunaga, Y.; Saito, S. Effect of dispersed-phase viscosity on the maximum stable drop size for breakup in turbulent flow. *J. Chem. Eng. Japan*, **1977**, 10(4), 325-330.

Armenante, P.M.; Chou, C.-C. Velocity profiles in a baffled vessel with single or double pitched-blade turbines. *AIChE J.*, **1996**, 42(1), 42-54.

Arshady, R. Suspension, emulsion, and dispersion polymerization: A methodological survey. *Colloid Polym. Sci.*, **1992**, 270, 717-732.

Ayazi Shamlou, P.; Stavrinides, S.; Titchener-Hooker, N.; Hoare, M. Growth-independent breakage frequency of protein precipitates in turbulently agitated bioreactors. *Chem. Eng. Sci.*, **1994**, 49(16), 2647-2656.

Bae, J.H.; Tavlarides, L.L. Laser capillary spectro-photometry for drop-size concentration measurements. *AIChE J.*, **1989**, 35, 1073-1084.

Baillagou, P.E.; Soong, D.A. A viscosity constitutive equation for PMMA-MMA solutions. *Chem. Eng. Commun.*, **1985**, 33, 125-134.

Bakker, R.A.; Van Den Akker, H.E.A. Single phase flow in stirred reactors. *Trans. Inst. Chem. Eng.*, **1994a**, 72, Part A, 583-593.

Bakker, R.A.; Van Den Akker, H.E.A. A computational model for the gas-liquid flow in stirred reactors. *Trans. Inst. Chem. Eng.*, **1994b**, 72, Part A, 594-606.

Bakker, R.A.; Van Den Akker, H.E.A. A computational study of chemical reactors on the basis of micromixing models. *Trans. Inst. Chem. Eng.*, **1994c**, 72, Part A, 733-738.

Bakker, R.A.; Van Den Akker, H.E.A. A cylindrical stretching vortex model of micromixing in chemical reactors. In *ICHEME Symp. Series*, 1994d; No. 136, 275-282.

Balakrishnan, T.; Ford, W.T.; Particle size control in suspension copolymerization of styrene, chloromethyl-styrene, and divinylbenzene. *J. Appl. Polym. Sci.*, **1982**, 27, 135-138.

Bałdyga, J.; Bourne, J.R. Simplification of micromixing calculations. I. Derivation and application of new model. *Chem. Eng. J.*, **1989**, 42, 83-92.

Bałdyga, J.; Bourne, J.R. Interactions between mixing on various scales in stirred tank reactors. *Chem. Eng. Sci.*, **1992**, 47(8), 1839-1848.

Bałdyga, J.; Bourne, J.R. Interpretation of turbulent mixing using fractals and multifractals. *Chem. Eng. Sci.*, **1995**, 50(3), 381-400.

Bałdyga, J.; Bourne, J.R.; Dubuis, B.; Etchells, A.W.; Gholap, R.V.; Zimmermann, B. Jet reactor scale-up for mixing-controlled reactions. *Trans. Inst. Chem. Eng.*, **1995a**, 73, Part A, 497-502.

Bałdyga, J.; Podgórska, W.; Pohorecki, R. Mixing-precipitation model with application to double feed semibatch precipitation. *Chem. Eng. Sci.*, **1995**b, 50(8), 1281-1300.

Bałdyga, J.; Pohorecki, R. Turbulent micromixing in chemical reactors - a review. *Chem. Eng. J. Biochem. Eng. J.*, **1995**, 58, 183-195.

Beuermann, S.; Buback, M.; Russell, G.T. Kinetics of free radical solution polymerization of methyl methacrylate over an extended conversion range. *Macromol. Chem. Phys.*, **1995**, 196, 2493-2516.

Bilgiç, T.; Karalı, M.; Savaşçı, Ö.T. Effect of the particle size of the solid protective agent tricalcium phosphate and its in-situ formation on the particle size of suspension polystyrene. *Die Angewandte Makromol. Chem.*, **1993**, 213, 33-42.

Bodemeier, S.; Claas, W.; Lübbert, A. Measuring techniques to characterize multiphase reactors. In *AIChE Symp. Ser.*, 1992; Vol. 88, No. 286, 109-113.

Borwankar, R.P.; Chung, S.I.; Wasan, D.T. Drop sizes in turbulent liquid-liquid dispersions containing polymeric suspension stabilizers. I. The breakage mechanism. *J. Appl. Polym. Sci.*, **1986**, 32, 5749-5762.

Bourne, J.R.; Baldyga, J. Drop breakage in the viscous subrange: a source of possible confusion. *Chem. Eng. Sci.*, **1994**, 49(7), 1077-1078.

Brooks, B.W. Basic aspects and recent developments in suspension polymerisation. *Makromol. Chem., Macromol. Symp.*, **1990**, 35/36, 121-140.

Brůha, O.; Fořt, I.; Smolka, P. Phenomenon of turbulent macro-instabilities in agitated systems. *Collect. Czech. Chem. Commun.*, **1995**, 60, 85-94.

Buback, M.; Kuchta, F.-D. Variation of the propagation rate coefficient with pressure and temperature in the free-radical bulk polymerization of styrene. *Macromol. Chem. Phys.*, **1995**, 196, 1887-1898.

Calabrase, R.V.; Chang, T.P.K.; Dang, P.T. Drop breakup in turbulent stirred-tank contactors. Part I: Effect of dispersed-phase viscosity. *AIChE J.* **1986**, 32(4), 657-666.

Capek, I. On the kinetics of heterogeneous free radical crosslinking polymerization, *J. Dispersion Sci. Technol.*, **1996**, 17(2), 139-244.

Carriere, C.J.; Cohen, A.; Arends, C.B. Estimation of interfacial tension using shape evolution of short fibers. *J. Rheol.*, **1989**, 33(5), 681-689.

Castellanos, J.R.; Mendizabal, E.; Puig, J.E. A quick method for choosing a protecting colloid for suspension polymerization. *J. Appl. Polym. Sci.: Appl. Polym. Symp.* **1991**, 49, 91-101.

Chaffey, C.E.; Tasalloti, S.; Paine, A.J. Emulsification of a viscous monomer mix: particle size and size distribution. *Can. J. Chem. Eng.*, **1991**, 69, 639-646.

Chapple, D.; Kresta, S. The effect of geometry on the stability of flow patterns in stirred tanks. *Chem. Eng. Sci.*, **1994**, 49, 3651-3660.

Chatzi, E.G.; Kiparissides, C. Dynamic simulation of bimodal drop size distributions in low-coalescence batch dispersion systems. *Chem. Eng. Sci.*, **1992**, 47(2), 445-456.

Chatzi, E.G.; Kiparissides, C. Drop size distributions in high holdup fraction dispersion systems: effect of the degree of hydrolysis of PVA stabilizer. *Chem. Eng. Sci.*, **1994**, 49(24B), 5039-5052.

Chatzi, E.G.; Kiparissides, C. Steady-state drop-size distributions in high holdup dispersion systems. *AIChE J.*, **1995**, 41(7), 1640-1652.

Chen, M.-Q.; Hwang, C.; Shih, Y.-P. A wavelet-Galerkin method for solving population balance equations. *Computers Chem. Eng.*, **1996**, 20(2), 131-145.

Cheng, J.T.; Langsam, M. Effect of cellulose suspension agent structure on the particle morphology of PVC. Part II. Interfacial properties. *J. Macromol. Sci.-Chem.*, **1984**, A21(4), 395-409.

Cho, H.H.; Goldstein, R.J. An improved low-Reynolds number k-ϵ turbulence model for recirculating flows. *Int. J. Heat & Mass Transfer*, **1994**, 37, 1495-1508.

Chung, S.I.; Wasan, D.T. Dynamic stability of liquid-liquid dispersions containing polymeric suspension stabilizers. *Colloids and Surfaces*, **1988**, 29, 323-336.

Chylla, R. W. Scaleup of transport phenomena in polymer stirred tank reactors: A review. 44th Canadian Society for Chemical Engineering Conference, Calgary, Alberta, Canada, October 1994.

Colvin, M.; Chung, S.K.; Hyson, M.T.; Chang, M.; Rhim, W.K. A new method for the production of large spherical monosized polymer particles for biomedical and chromatographic applications. *J. Polym. Sci. Part A: Polym. Chem.*, **1990**, 28, 2085-2095.

Coulaloglou, C.A.; Tavlarides, L.L. Drop size distributions and coalescence frequencies of liquid-liquid dispersions in flow vessels. *AIChE J.*, **1976**, 22(2), 289-297.

Coulaloglou, C.A.; Tavlarides, L.L. Description of interaction processes in agitated liquid-liquid dispersions. *Chem. Eng. Sci.*, **1977**, 32, 1289-1297.

Cui, Y.Q.; Van der Lans, R.G.J.M.; Noorman, H.J.; Luyben, K.Ch.A.M. Compartment mixing model for stirred reactors with multiple impellers. *Trans. Inst. Chem. Eng.*, **1996**, 74, Part A, 261-271.

Danov, K.D.; Denkov, N.D.; Petsev, D.N.; Ivanov, I.B.; Borwankar, R. Coalescence dynamics of deformable Brownian emulsion droplets. *Langmuir*, **1993**, 9(7), 1731-1740.

Danov, K.D.; Ivanov, I.B.; Gurkov, T.D.; Borwankar, R.P. Kinetic model for the simultaneous processes of flocculation and coalescence in emulsion systems. *J. Colloid Interface Sci.*, **1994**, 167, 8-17.

Das, P.K. Monte Carlo simulation of drop breakage on the basis of drop volume. *Computers Chem. Eng.*, **1996**, 20(3), 307-313.

Das, P.K.; Kumar, R.; Ramkrishna, D. Coalescence of drops in stirred dispersion. A white noise model for coalescence. *Chem. Eng. Sci.*, **1987**, 42(2), 213-220.

Dawkins, J.V. Chapter 14. Aqueous suspension polymerizations. In Volume 4 (Chain Polymerization II) of *Comprehensive Polymer Science. The Synthesis, Characterization & Applications of Polymers*; Geoffrey, A., Bevington, J.C., Eds.; Pergamon Press: Great Britain, 1989.

Delichatsios, M.A.; Probstein, R.F. The effect of coalescence and the average drop size in liquid-liquid dispersions. *Ind. Eng. Chem. Fundam.*, **1976**, 15(2), 134.

des Cloizeaux, J. Double reptation vs. simple reptation in polymer melts. *J. Europhys. Lett.*, **1988**, 5, 437-442.

des Cloizeaux, J. Relaxation of entangled polymers in melts. *Macromolecules*, **1990**, 23, 4678-4687.

des Cloizeaux, J. Relaxation of entangled and partially entangled polymers in melts: Time dependent reptation. *Macromolecules*, **1992**, 25, 835-841.

Deslandes, Y. Morphology of hydroxyapatite as suspension stabilizer in the polymerization of poly(styrene-co-butadiene). *J. Appl. Polym. Sci.*, **1987**, 34, 2249-2257.

Diamadopoulos, E.; Zoubourtikoudis, I.; Kiparissides, C. Aggregation phenomena in the suspension polymerization of VCM. *Colloid Polym. Sci.*, **1990**, 268, 306-314.

Dickey, D.S. Dimensional analysis, similarity and scale-up. In *AIChE Symp. Ser.*, 1993; Vol. 89, No. 293, 143-150.

Distelhoff, M.F.W.; Laker, J.; Marquis, A.J.; Nouri, J.M. The application of a strain gauge technique to the measurement of the power characteristics of five impellers. *Exp. Fluids*, **1995**, 20, 56-58.

Dong, L.; Johansen, S.T.; Engh, T.A. Flow induced by an impeller in an unbaffled tank-I. Experimental. *Chem. Eng. Sci.*, **1994a**, 49(4), 549-560.

Dong, L.; Johansen, S.T.; Engh, T.A. Flow induced by an impeller in an unbaffled tank-II. Numerical modelling. *Chem. Eng. Sci.*, **1994b**, 49(20), 3511-3518.

Doulah, M.S. The effect of hold-up on drop sizes in liquid-liquid dispersions. *Ind. Eng. Chem. Fundam.*, **1975**, 14(2), 137.

Dubé, M.A.; Penlidis, A.; Reilly, P.M. A systematic approach to the study of multicomponent polymerization kinetics: the butyl acrylate/methyl methacrylate/vinyl acetate example. IV. Optimal Bayesian design of emulsion terpolymerization experiments in a pilot plant reactor. *J. Polym. Sci., Polym. Chem.*, **1996**, 34, 811-831.

Elemans, P.H.M., Janssen, J.M.H.; Meijer, H.E.H. The measurement of interfacial tension in polymer/polymer systems: the breaking thread method. *J. Rheol.*, **1990**, 34(8), 1311-1325.

Erbay, E.; Bilgiç, T.; Karali, M.; Savaşçi, Ö.T. Polystyrene suspension polymerization: the effect of polymerization parameters on particle size and distribution. *Polym.-Plast. Technol. Eng.*, **1992**, 31(7&8), 589-605.

Fabini, M.; Bobula, S.; Rusina, M.; Macho, V.; Harustiak, M. Preparation of poly(vinyl alcohol) as the dispersant for suspension vinyl chloride polymerizations. *Polymer*, **1994**, 35(10), 2201-2204.

Fasano, J.B.; Penney, W.R. Avoid blending mix-ups. *Chem. Eng. Prog.*, **1991a**, 87(10), 56-63.

Fasano, J.B.; Penney, W.R. Cut reaction by-products by proper feed blending. *Chem. Eng. Prog.*, **1991b**, 87(10), 56-63.

Fokema, M.D.; Kresta, S.M.; Wood, P.E. Importance of using the correct impeller boundary conditions for CFD simulations of stirred tanks. *Can. J. Chem. Eng.*, **1994**, 72(2), 177-183.

Fořt, I.; Ettler, P.; Kolín, F.; Vanags, J.; Rikmanis, M.A. Study of spatial distribution of kinetic energy of turbulence in a cylindrical system with turbine impellers and radial baffles. *Collect. Czech. Chem. Commun.*, **1992**, 57, 1053-1064.

Fořt, I.; Líbal, J.; Vanags, J.; Rickmanis, M.A.; Viesturs, U. Distribution of kinetic energy of turbulence in agitated system with axial high-speed impeller and baffles. ACHEMA Congress, Frankfurt am Main, FRG, 1991.

Fořt, I.; Machoň, V.; Kadlec, P. Distribution of energy dissipation rate in an agitated gas-liquid system. *Chem. Eng. Technol.*, **1993**, 16, 389-394.

Garside, J. Tailoring crystal products in precipitation processes and the role of mixing. In *AIChE Symp. Series*, 1991; Vol. 87, No. 284, 16-25.

Geisler, R.K.; Buurman, C.; Mersmann, A.B. Scale-up of the necessary power input in stirred vessels with suspensions. *Chem. Eng. J.*, **1993**, 51, 29-39.

Geisler, R.; Mersmann, A.; Voit, H. Macro- and micromixing in stirred tanks. *Int. Chem. Eng.*, **1991**, 31(4), 642-653.

Gibson, M.M.; Dafa'Alla, A.A. Two equation model for turbulent wall flow. *AIAA J.*, **1994**, 33(8), 1514-1518.

Hamielec, A.E.; H. Tobita, H. Polymerization Processes. In Vol. A21 of *Ullmann's Encyclopedia of Industrial Chemistry*; VCH Publishers, Inc., 305-428, 1992.

Harris, C.K.; Roekaerts, D.; Rosendal, F.J.J.; Buitendijk, F.G.J.; Daskopoulos, Ph.; Vreenegoor, A.J.N.; Wang, H. Computational fluid dynamics for chemical reactor engineering. *Chem. Eng. Sci.*, **1996**, 51(10), 1569-1594.

Harvey, A.D. Steady and unsteady computation of impeller stirred reactors. Submitted for publication in *AIChE J.*, 1995.

Harvey, A.D.; Lee, C.K.; Rogers, S.E. Steady-state modelling and experimental measurement of a baffled impeller stirred tank. *AIChE J.*, **1995**, 41(10), 2177-2186.

Hatate, Y.; Ikari, A. Change of size distribution of polymer droplets with time in styrene suspension polymerization under ultrasonic irradiation. *Chem. Eng. Commun.*, **1985**, 34, 325-333.

Hatate, Y.; Uemura, Y.; Ijichi, K.; Kato, Y.; Hano, T.; Baba, Y.; Kawano, Y. Preparation of GPC packed polymer beads by a SPG membrane emulsifier. *J. Chem. Eng. Japan*, **1995**, 28(6), 656-659.

Hernández-Valdez, J.M. Dinámica de reactores de polimerización en suspensión. M. Eng. Thesis (in Spanish), Unidad de Ciencias Básicas e Ingeniería, Universidad Autónoma Metropolitana, Plantel Iztapalapa, México D.F., Mexico, 1993.

Hiemenz, P.C. Principles of colloid and surface science; Marcel Dekker: New York, 1977.

Hildebrand, H.; Row, G. Laser light scattering in particle size analysis. *American Ceramic Soc. Bull.*, **1995**, 74(7), 49-52.

Hill, P.J.; Ng, K.M. New discretization procedure for the breakage equation. *AIChE J.*, **1995**, 41(5), 1204-1216.

Hinze, J.O. Fundamentals of the hydrodynamics mechanism of splitting in dispersion processes. *AIChE J.*, **1955**, 1, 950-956.

Hinze, J.O. *Turbulence: an introduction to its mechanism and theory*; 2nd edition, McGraw Hill: Toronto, 1987.

Horák, D.; Pelzbauer, Z.; Švec, F.; Kálal, J. Reactive polymers. XXXIII. The influence of the suspension stabilizer on the morphology of a suspension polymer. *J. Appl. Polym. Sci.*, **1981**, 26, 3205-3211.

Horio, M.; Kuroki, H. Three-dimensional flow visualization of dilutely dispersed solids in bubbling and circulating fluidized beds. *Chem. Eng. Sci.*, **1994**, 49(15), 2413-2421.

Horita, K.; Abe, F.; Einaga, Y.; Yamakawa, H. Excluded-volume effects on the intrinsic viscosity of oligo- and polystyrenes. Solvent effects. *Macromolecules*, **1993**, 26(19), 5067-5072.

Hounslow, M.J.; Ryall, R.L.; Marshall, V.R. A discretized population balance for nucleation, growth, and aggregation. *AIChE J.*, **1988**, 34(11), 1821.

Howarth, W.J. Coalescence of drops in a turbulent flow field. *Chem. Eng. Sci.*, **1964**, 19, 33-38.

Howlett, L. Getting mixed up about agitation?. *Process Eng.*, **1995**, 76(3), 39-42.

Hoyt, J.W.; Sellin, R.H.J. A turbulent-flow dye-streak technique. *Exp. Fluids*, **1995**, 20, 38-41.

Hrenya, C.M.; Bolio, E.J.; Chakrabarti, D.; Sinclair, J.L. Comparison of low Reynolds number k-ε turbulence models in predicting fully developed flow. *Chem. Eng. Sci.*, **1995**, 50(12), 1923-1941.

Ibrahim, S.; Nienow, A.W. Power curves and flow patterns for a range of impellers in Newtonian fluids: $40<Re<5x10^5$. *Trans. Inst. Chem. Eng.*, **1995**, 73, Part A, 485-491.

Janssen, J.J.; Boon, A.; Agterof, W.G.M. Influence of dynamic interfacial properties on droplet breakup in simple shear flow. *AIChE J.*, **1994**, 40(12), 1929-1939.

Janzon, J.; Theliander, H. On the suspension of particles in an agitated vessel. *Chem. Eng. Sci.*, **1994**, 49(20), 3522-3526.

Jaworski, Z.; Nienow, A.W.; Koutsakos, E.; Dyster, K.N.; Bujalski, W. An LDA study of turbulent flow in a baffled vessel agitated by a pitched blade turbine. *Trans. Inst. Chem. Eng.*, **1991**, 69, Part A, 313-320.

Jaworski, Z.; Nienow, A.W.; Dyster, K.N. An LDA study of the turbulent flow field in a baffled vessel agitated by an axial, down-pumping hydrofoil impeller. *Can. J. Chem. Eng.*, **1996**, 74, 3-15.

Jones, M.C.; Nassimbene, R.D.; Wolfe, J.D.; Frederick, N.V. Mixing and dispersion measurements on packed bed flows using a fiber optic probe array. *Chem. Eng. Sci.*, **1996**, 51(7), 1009-1021.

Kalfas, G.; Ray, W.H. Modelling and experimental studies of aqueous suspension polymerization processes. 1. Modeling and simulations. *Ind. Eng. Chem. Res.*, **1993a**, 32(9), 1822-1830.

Kalfas, G.; Ray, W.H. Modelling and experimental studies of aqueous suspension polymerization processes. 2. Experiments in batch reactors. *Ind. Eng. Chem. Res.*, **1993b**, 32(9), 1831-1838.

Kiparissides, C. Prediction of the primary particle size distribution in vinyl chloride polymerization. *Makromol. Chem., Macromol. Symp.*, **1990**, 35/36, 171-192.

Kiparissides, C. Polymerization reactor modeling: a review of recent developments and future directions. *Chem. Eng. Sci.*, **1996**, 51(10), 1637-1659.

Koiranen, T.; Kraslawski, A.; Nyström, L. Knowledge-based system for the preliminary design of mixing equipment. *Ind. Eng. Chem. Res.*, **1995**, 34(9), 3059-3067.

Konno, M.; Arai, K.; Saito, S. The effect of stabilizer on coalescence of dispersed drops in suspension polymerization of styrene. *J. Chem. Eng. Japan*, **1982**, 15(2), 131-135.

Kresta, S.M. Characterization, measurement and prediction of the turbulent flow in stirred tanks. Ph.D. Thesis, Department of Chemical Engineering, McMaster University, Hamilton, Ontario, Canada, 1991.

Kresta, S.M.; Wood, P.E. Prediction of the three-dimensional turbulent flow in stirred tanks. *AIChE J.*, **1991**, 37(3), 448-460.

Kresta, S.M.; Wood, P.E. The Mean Flow Field Produced by a 45° Pitched Blade Turbine: Changes in the Circulation Pattern Due to Off Bottom Clearance. *Can. J. Chem. Eng.*, **1993a**, 71(1), 45-53.

Kresta, S.M.; Wood, P.E. The Flow Field Produced by a Pitched Blade Turbine: Characterization of the Turbulence and Estimation of the Dissipation Rate. *Chem. Eng. Sci.*, **1993b**, 48(10), 1761-1774.

Kumar, S.; Kumar, R.; Gandhi, K.S A multi-stage model for drop breakage in stirred vessels. *Chem. Eng. Sci.*, **1992**, 47, 971-980.

Kumar, S.; Kumar, R.; Gandhi, K.S. A new model for coalescence efficiency of drops in stirred dispersions. *Chem. Eng. Sci.*, **1993a**, 48(11), 2025-2038.

Kumar, S.; Kumar, R.; Gandhi, K.S. A simplified procedure for predicting d_{max} in stirred vessels. *Chem. Eng. Sci.*, **1993b**, 48(17), 3092-3096.

Kumar, S.; Ramkrishna, D. On the solution of population balance equations by discretization -I. A fixed pivot technique. *Chem. Eng. Sci.*, **1996**a, 51(8), 1311-1332.

Kumar, S.; Ramkrishna, D. On the solution of population balance equations by discretization -II. A moving pivot technique. *Chem. Eng. Sci.*, **1996**b, 51(8), 1333-1342.

Lachaise, J.; Mendiboure, B.; Dicharry, C.; Marion, G.; Bourrel, M.; Cheneviere, P.; Salager, J.L. A simulation of emulsification by turbulent stirring. *Colloids Surfaces A: Physicochem. Eng. Aspects*, **1995**, 94, 189-195.

Lamberto, D.J.; Muzzio, F.J.; Swanson, P.D.; Tonkovich, A.L. Using time-dependent rpm to enhance mixing in stirred vessels. *Chem. Eng. Sci.*, **1996**, 51(5), 733-741.

Langner, F.; Moritz, H.; Reichert, K.-H. On particle size of suspension polymers II. Polymerizing two-phase system. *Ger. Chem. Eng.*, **1979**, 2, 329-336.

Langner, F.; Moritz, H.; Reichert, K.-H. Reactor scale-up for polymerization in suspension. *Chem. Eng. Sci.*, **1980**, 35, 519-525.

Larsson, G.; George, S.; Enfors, S.-O. Scale-down reactor model to simulate insufficient mixing conditions during fed batch operation using a biological test system. In *AIChE Symp. Ser.*, 1993; Vol. 89, No. 293, 151-157.

Laso, M.; Steiner, L.; Hartland, S. Dynamic simulation of liquid-liquid agitated dispersions - I. Derivation of a simplified model. *Chem. Eng. Sci.*, **1987**a, 42(10), 2429-2436.

Laso, M.; Steiner, L.; Hartland, S. Dynamic simulation of liquid-liquid agitated dispersions - II. Experimental determination of breakage and coalescence rates in a stirred tank. *Chem. Eng. Sci.*, **1987**b, 42(10), 2437-2445.

Launder, B.E. Second moment closure: present ... and future?. *Int. J. Heat & Fluid Flow*, **1989**, 10, 282-300.

Leng, D.E.; Quarderer, G.J. Drop dispersion in suspension polymerization. *Chem. Eng. Commun.*, **1982**, 14, 177-201.

Li, D. Coalescence between two small bubbles or drops. *J. Colloids Interface Sci.*, **1994**, 163, 108-119.

Lister, J.D.; Smit, D.J.; Hounslow, M.J. Adjustable Discretized Population Balance for Growth and Aggregation. *AIChE J.*, **1995**, 41(3), 591-603.

Lumley, J.L. Turbulence modelling. *J. Appl. Mech.*, **1983**, 50, 1097-1103.

Luo, J.Y.; Gosman, A.D.; Issa, R.I.; Middleton, J.C.; Fitzgerald, M.K. Full flow field computation of mixing in baffled stirred vessels. *Trans. Inst. Chem. Eng.*, **1993**, 71, Part A, 342-344.

Luo, Y.; Pan, Z.; Wang, Z..; Huang, Z. A molecular weight model in vinyl chloride-divinyl monomer suspension copolymerization before the gel point. *J. Appl. Polym. Sci.*, **1995**, 56, 1221-1230.

Macho, V.; Fabíni, M.; Rusina, M.; Bobula, S.; Harustiak, M. Modified poly(vinyl alcohol) as a dispersant in suspension polymerization of vinyl chloride: 3. Acetalized poly(vinyl alcohol). *Polymer*, **1994**, 35(26), 5773-5777.

Mann, R.; El-Hamouz, A.M. A product distribution paradox on scaling up a stirred batch reactor. *AIChE J.*, **1995**, 41(4), 855-867.

Mann, R.; Pillai, S.K.; El-Hamouz, A.M.; Ying, P.; Togatorop, A.; Edwards, R.B. Computational fluid mixing for stirred vessels: progress from seeing to believing. *Chem. Eng. J.*, **1995**, 59, 39-50.

Manning, C.D. Measurement of ultralow interfacial tensions in surfactant-brine-oil systems. M.Eng. Thesis, University of Minnesota, 1976.

Martínez-Gómez, R.E. Conceptualización y modelado de la polimerización en suspensión. M. Eng. Thesis (in Spanish), Unidad de Ciencias Básicas e Ingeniería, Universidad Autónoma Metropolitana, Plantel Iztapalapa, México D.F., Mexico, 1990.

Matsumoto, S.; Takeshita, K; Koga, J.; Takashima, Y. A production process for uniform-size polymer particles. *J. Chem. Eng. Japan*, **1989**, 22(6), 691-693.

Mayr, B.; Nagy, E.; Horvat, P.; Moser, A. scale-up on basis of structured mixing models: A new concept. *Biotech. and Bioeng.*, **1994**, 43, 195-206.

McClusky, J.V.; O'Neill, R.E.; Priester Jr., R.D.; Ramsey, W.A. Vibrating rod viscometer: a valuable probe into polyurethane chemistry. *J. Cellular Plastics*, **1994**, 30, 224-241.

Mead, D.W. Determination of molecular weight distributions of linear flexible polymers from linear viscoelastic material functions. *J. Rheol.*, **1994**, 38(6), 1797-1827.

Mead, D.W. Evolution of the molecular weight distribution and linear viscoelastic rheological properties during the reactive extrusion of polypropylene. *J. Appl. Polym. Sci.*, **1995**, 57, 151-173.

Mendizabal, E.; Castellanos-Ortega, J.R.; Puig, J.E. A method for selecting polyvinyl alcohol as stabilizer in suspension polymerization. *Colloids and Surfaces*, **1992**, 63, 209-217.

Mikos, A.G.; Takoudis, C.G.; Peppas, N.A. Reaction engineering aspects of suspension polymerization. *J. Appl. Polym. Sci.*, **1986**, 31, 2647-2659.

Mishra, V.P.; Joshi, J.B. Flow generated by a disc turbine: Part III: effect of impeller diameter, impeller location and comparison with other radial flow turbines. *Trans. Inst. Chem. Eng.*, **1993**, 71, Part A, 563-573.

Mishra, V.P.; Joshi, J.B. Flow generated by a disc turbine: Part IV: multiple impellers. *Trans. Inst. Chem. Eng.*, **1994**, 72, Part A, 657-668.

Mitchell, G.B. Effect of agitator geometry and speed on suspension polystyrene particle formation. M. Eng. Thesis, Department of Chemical Engineering, McMaster University, Hamilton, Ontario, Canada, 1986.

Moore, I.P.T.; Cossor, G.; Baker, M.R. Velocity distributions in a stirred tank containing a yield stress fluid. *Chem. Eng. Sci.*, **1995**, 50(15), 2467-2481.

Moreira, J.L.; Cruz, P.E.; Santana, P.C.; Aunins, J.G.; Carrondo, M.J.T. Formation and disruption of animal cell aggregates in stirred vessels: mechanisms and kinetic studies. *Chem. Eng. Sci.*, **1995**, 50(17), 2747-2764.

Mousa, H.; van de Ven, T.G.M. Solutions of the shear-induced coalescence equations for polydisperse emulsion droplets using Monte Carlo and moments techniques. *Colloids Surfaces A: Physicochem. Eng. Aspects*, **1995**, 95, 221-228.

Munzer, M.; Trommsdorff, E. Polymerization in suspension. In *Polymerization Processes*, Schildknecht, C.E., Skeist, I., Eds.; Wiley, pp 106, 1977.

Nagano, Y.; Shimada, M. Rigorous modeling of dispersion-rate equation using direct simulations. *JSME Int. J.*, **1995**, Series B, 38(1), 51-59.

Naghash, H.J.; Okay, O.; Yildirim, H. Gel formation in free-radical crosslinking copolymerization. *J. Appl. Polym. Sci.*, **1995**, 56, 477-483.

Nambiar, D.K.R.; Kumar, R.; Das, T.R.; Gandhi, K.S. A two-zone model of breakage frequency of drops in stirred dispersions. *Chem. Eng. Sci.*, **1994**, 49(13), 2194-2198.

Napper, D.H.; Hunter, R.J. Hydrosols. In *Surface Chemistry and Colloids*. Buckingham, A.D., Kerker, M., Eds.; MTP International Review of Science, Physical Chemistry, Series One, Volume 7: Butterworth, 1972.

Nishikawa, M.; Mori, M.; Kayama, T.; Nishioka, S. J. *Chem. Eng. J.*, **1991**, 24, 88.

Nishikawa, M.; Kayama, T.; Nishioka, S.; Nishikawa, S. Drop size distribution in mixing vessel with aeration. *Chem. Eng. Sci.*, **1994**, 49(14), 2379-2384.

Nonaka, M. Optimum design of a solid-liquid stirred system by taking into account the propagation of turbulent energy. *Sep. Sci. Technol.*, **1990**, 25(6), 753-779.

Nouri, J.M.; Whitelaw, J.H. Particle velocity characteristics of dilute to moderately dense suspension flows in stirred reactors. *Int. J. Multiphase Flow*, **1992**, 18(1), 21-33.

Obot, N.T. Designing mixing processes using frictional law of corresponding states. *Chem. Eng. Prog.*, **1993**, 89(7), 47-53.

Ogawa, K. Evaluation of common scaling-up rules for a stirred vessel from the viewpoint of energy spectrum function. *J. Chem. Eng. Japan*, **1992**, 25(6), 750-752.

Okay, O.; Naghash, H.J.; Pekcan, Ö. Critical properties for gelation in free-radical crosslinking copolymerization. *Makromol. Theory Simul.*, **1995**, 4, 967-981.

Okufi, S.; Pérez de Ortíz, E.S.; Sawistowski, H. Scale-up of liquid-liquid dispersions in stirred tanks. *Can. J. Chem. Eng.*, **1990**, 68, 400-406.

Oldshue, J.Y. Geometric relationships for scale-up of diverse mixing processes. In *AIChE Symp. Ser.*, 1993; Vol. 89, No. 293, 159-163.

Oldshue, J.Y.; Mechler, D.O.; Grinnell, D.W. Fluid Mixing Variables in Suspension and Emulsion Polymerization. *Chem. Eng. Prog.*, **1982**, 78, 68-74.

O'Shaughnessy, B.; Yu, J. Auto-acceleration in free radical polymerization. 1. Conversion. *Macromolecules*, **1994**, 27(18), 5067-5078.

Özkaya, N.; Erbay, E.; Bilgiç, T.; Savaşçı, Ö.T. Agitation scale-up model for the suspension polymerization of vinyl chloride. *Die Angew. Makromol. Chem.*, **1993**, 211(3649), 35-51.

Pacek, A.W.; Moore, I.P.T.; Calabrese, R.V.; Nienow, A.W. Evolution of drop size distributions and average drop diameter in liquid-liquid dispersions before and after phase inversion. *Trans. Inst. Chem. Eng.*, **1993**, 71, Part A, 340-341.

Pacek, A.W.; Moore, I.P.T.; Nienow, A.W.; Calabrese, R.V. Video technique for measuring dynamics of liquid-liquid dispersion during phase inversion. *AIChE J.*, **1994a**, 40(12), 1940-1949.

Pacek, A.W.; Nienow, A.W.; Moore, I.P.T. On the structure of turbulent liquid-liquid dispersed flows in an agitated vessel. *Chem. Eng. Sci.*, **1994b**, 49(20), 3485-3498.

Pacek, A.W.; Nienow, W. Measurement of drop size distribution in concentrated liquid-liquid dispersions: video and capillary techniques. *Trans. Inst. Chem. Eng.*, **1995**, 73, Part A, 512-518.

Panke, D. Modelling the free-radical polymerization of methyl methacrylate over the complete range of conversion. *Macromol. Theory Simul.*, **1995**, 4, 759-772.

Parthasarathy, R.; Ahmed, N. Sauter mean and maximum bubble diameters in aerated stirred vessels. *Trans. Inst. Chem. Eng.*, **1994**, 72, Part A, 565-572.

Patel, V.C.; Rodi, W.; Scheuerer, G. Turbulence models for near-wall and low Reynolds number flows: a review. *AIAA J.*, **1985**, 23, 1308-1319.

Pelletier, D.; Ilinca, F.; Hétu, J.-H. Adaptive finite element method for turbulent flow near a propeller. *AIAA J.*, **1994**, 32(11), 2186-2193.

Polacco, G.; Semino, D.; Rizzo, C. Feasibility of methyl methacrylate polymerization for bone cement by suspension polymerization in a gel phase. *J. Mat. Sci., Mat. Medicine*, **1994**, 5, 587-591.

Ranade, V.V. Computational fluid dynamics for reactor engineering. *Comp. Fluid Dynamics Reactor Eng.*, **1995**, 11(3), 229-289.

Ranade, V.V.; Mishra, V.P.; Saraph, V.S.; Deshpande, G.B.; Joshi, J.B. Comparison of axial flow impellers using a laser doppler anemometer. *Ind. Eng. Chem. Res.*, **1992**, 31, 2370-2379.

Randolph, A.D. A population balance for countable entities. *Can. J. Chem. Eng.*, **1964**, 280-281.

Ray, W.H. Modelling of Addition Polymerization Processes. Free Radical, Ionic, Group Transfer, and Ziegler-Natta Kinetics. *Can. J. Chem. Eng.*, **1991**, 69, 626-629.

Reynolds, W.C. Computation of turbulent flows. *Annual Rev. Fluid Mech.*, **1976**, 8, 183-208.

Ribeiro, L.M.; Regueiras, P.F.R.; Guimarães, M.M.L.; Madureira, C.M.N.; Cruz-Pinto, J.J.C. The dynamic behaviour of fluid liquid-liquid agitated dispersions. I. The hydrodynamics. *Computers Chem. Eng.*, **1995**, 19(3), 333-343.

Roberts, R.M.; Gray, M.R.; Thompson, B.; Kresta, S.M. The Effect of Impeller and Tank Geometry on Circulation Time Distributions in Stirred Tanks. *Trans. IChem.*, **1995**, 73(A), 79-86.

Rodi, W. Examples of turbulence models for incompressible flows. *AIAA J.*, **1982**, 20, 872-879.

Ross, S.L.; Verkhoff, F.H.; Curl, R.L. Droplet breakage and coalescence processes in an agitated dispersion. *Ind. Eng. Chem. Fundam.*, **1978**, 17(2), 101.

Rutherford, K.; Lee, K.C.; Mahmoudi, S.M.S.; Yianneskis, M. Hydrodynamic characteristics of dual Rushton impeller stirred vessels. *AIChE J.*, **1996**, 42(2), 332-346.

Sahu, A.K.; Joshi, J.B. Simulation of flow in stirred vessels with axial flow impellers: effects of various numerical schemes and turbulence model parameters. *Ind. Eng. Chem. Res.*, **1995**, 34, 626-639.

Saldívar-Guerra, E. Elemento Finito con Malla Adaptable en el Modelado de Sistemas de Polimerización. M. Sc. Thesis (in Spanish), Universidad Nacional Autónoma de México (UNAM), Ciudad Universitaria, Mexico, 1986.

Saldívar-Guerra, E.; Vivaldo-Lima, E.; Gómez-Cadena, L.E. Simulación de la distribución de tamaños de partícula en polimerización en suspensión empleando colocación con splines. Comparación con datos industriales. (In Spanish). X Encuentro Anual AMIDIQ (Mexican Academy for Research and Docence in Chemical Engineering), Universidad de Guadalajara, Guadalajara, Jalisco, Mexico, 1989.

Sathyagal, A.N.; Ramkrishna, D.; Narsimhan, G. Solution of inverse problems in population balances. II. Particle break-up. *Computers Chem. Eng.*, **1995**, 19(4), 437-451.

Sathyagal, A.N.; Ramkrishna, D.; Narsimhan, G. Droplet breakage in stirred dispersions. Breakage functions from experimental drop-size distributions. *Chem. Eng. Sci.*, **1996**, 51(9), 1377-1391.

Sato, T. Stability of dispersion. *J. Coatings Technol.*, **1993**, 65(825), 113-121.

Schröder, R.; Piotowski, B. On particle formation during suspension polymerization of styrene. *Ger. Chem. Eng.*, **1982**, 5, 139-146.

Scott, P.J.; Penlidis, A.; Rempel, G.L. Ethylene-vinyl acetate semi-batch emulsion copolymerization: experimental design and preliminary screening experiments. *J. Polym. Sci. Part A: Polym. Chem.*, **1993a**, 31, 403-426.

Scott, P.J.; Penlidis, A.; Rempel, G.L. Ethylene-vinyl acetate semi-batch emulsion copolymerization: use of factorial experiments for improved process understanding. *J. Polym. Sci. Part A: Polym. Chem.*, **1993b**, 31, 2205-2230.

Seth, V.; Gupta, S.K. Free radical polymerizations associated with the Trommsdorff effect under semibatch reactor conditions: an improved model. *J. Polym. Eng.*, **1995/6**, 15(3&4), 283-326.

Shaw, M.T. ; Tuminello, W.H. A closer look at the MWD-viscosity transform. *Polym. Eng. Sci.*, **1994**, 34(2), 159-165.

Shiloh, K.; Sideman, S.; Resnick, W. Coalescence and breakup in dilute polydispersions. *Can. J. Chem. Eng.*, **1973**, 51, 542-549.

Shinnar, R. On the behaviour of liquid dispersions in mixing vessels. *J. Fluid Mech.*, **1961**, 10, 259-275.

Shinnar, R.; Church, J.M. Predicting particle size in agitated dispersions. *Ind. & Eng. Chem.*, **1960**, 52(3), 253-256.

Shumsky, V.F.; Getmanchuk, I.P.; Kramarenko, V.Y.; Privalko, V.P. Kinetics of formation of heterocyclic polymer networks: II. Rheological study. *J. Polym. Eng.*, **1994**, 13(3), 241-247.

Skeldon, P. Going stir crazy. *Process Eng.*, **1995**, 76(12), 24-25.

Smit, D.J.; Paterson, W.R.; Hounslow, M.J. Aggregation and gelation: II. Mixing effects in continuous flow vessels. *Chem. Eng. Sci.*, **1994**, 49(18), 3147-3167.

Smit, D.J.; Hounslow, M.J.; Paterson, W.R. Aggregation and gelation: III. Numerical classification of kernels and case studies of aggregation and growth. *Chem. Eng. Sci.*, **1995**, 50(5), 849-862.

Speziale, C.G. Analytical methods for the development of Reynolds-stress closures in turbulence. *Annual Rev. Fluid Mech.*, **1991**, 23, 107-157.

Stone, H.A. Dynamics of drop deformation and breakup in viscous fluids. *Annu. Rev. Fluid. Mech.*, **1994**, 26, 65-102.

Stone, H.A.; Leal, L.G. The effects of surfactants on drop deformation and breakup. *J. Fluid Mech.*, **1990**, 220, 161-186.

Stoots, C.M.; Calabrase, R.V. Mean velocity field relative to a Rushton turbine blade. *AIChE J.*, **1995**, 41(1), 1-11.

Tadros, Th. F. Fundamental principles of emulsion rheology and their applications. *Colloids Surfaces A: Physicochem. Eng. Aspects*, **1994**, 91, 39-55.

Tanaka, M.; Hosogai, K. Suspension polymerization of styrene with circular loop reactor. *J. Appl. Polym. Sci.*, **1990**, 39, 955-966.

Tatterson, G.B. Scaling based upon process similarity and scale matching concepts. In *AIChE Symp. Ser.*, 1993; Vol. 89, No. 293, 165-168.

Tatterson, G.B. *Scaleup and design of industrial mixing processes*; McGraw Hill, Inc.: U.S.A., 1994.

Tavlarides, L.L.; Stamatoudis, M. The analysis of interphase reactions and mass transfer in liquid-liquid dispersions. *Adv. Chem. Eng.*, **1981**, 11, 199-273.

Tefera, N.; Weickert, G.; Bloodworth, R.; Schweer, J. Free radical polymerization kinetics of styrene up to high conversion. *Macromol. Chem. Phys.*, **1994**, 195, 3067-3085.

Thoma, S.; Ranade, V.V.; Bourne, J.R. Interaction between micro- and macro-mixing during reactions in agitated tanks. *Can. J. Chem. Eng.*, **1991**, 69, 1135-1141.

Tipnis, S.K.; Penney, W.R.; Fasano, J.B. An experimental investigation to determine a scale-up method for fast competitive parallel reactions in agitated vessels. AIChE Annual Meeting, St. Louis, 1993; Paper 1f.

Tjahjadi, M.; Ottino, J.M.; Stone, H.A. Estimating interfacial tension via relaxation of drop shapes and filament breakup. *AIChE J.*, **1994**, 40(3), 385-394.

Tjahjadi, M.; Stone, H.A.; Ottino, J.M. Satellite and subsatellite formation in capillary breakup. *J. Fluid Mech.*, **1992**, 243, 297-317.

Tobin, T.; Ramkrishna, D.; Muralidhar, R. An investigation of drop charge effects on coalescence in agitated liquid-liquid dispersions. In *AIChE Symp. Ser.*, 1992; Vol. 88, No. 286, 61-64.

Tobita, H.; Hamielec, A.E. Crosslinking kinetics in free-radical copolymerization. In *Polymer Reaction Engineering*; Reichert, K.-H., Geiseler, W., Eds.; VCH Publishers: New York, 1989, 43-83.

Tosun, G. A mathematical model of mixing and polymerization in a semibatch stirred-tank reactor. *AIChE J.*, **1992**, 38(3), 425-437.

Tsouris, C.; Tavlarides, L.L. Breakage and Coalescence Models for Drops in Turbulent Dispersions. *AIChE J.*, **1994**, 40(3), 395-406.

Valadez-González, A. Evolución de la distribución de tamaños de partículas en una polimerización en suspensión. M. Eng. Thesis (In Spanish), Unidad de Ciencias Básicas e Ingeniería, Universidad Autónoma Metropolitana, Plantel Iztapalapa, México D.F., Mexico, 1988.

Valentas, K.J.; Amundson, N.R. Breakage and coalescence in dispersed phase systems. *I & EC Fundamentals*, **1966**, 5(4), 533-542.

Valentas, K.J.; Bilous, O.; Amundson, N.R. Analysis of breakage in dispersed phase systems. *I & EC Fundamentals*, **1966**, 5(2), 271-279.

Varanasi, P.P.; Ryan, M.E.; Stroeve, P. Experimental study on the breakup of model viscoelastic drops in uniform shear flow. *Ind. Eng. Chem. Res.*, **1994**, 33, 1858-1866.

Villalobos, M.A. Suspension polymerization of styrene through bifunctional initiators. M. Eng. Thesis, Department of Chemical Engineering, McMaster University, Hamilton, Ontario, Canada, 1989.

Villalobos, M.A. Synthesis and modelling of high Tg copolymers through suspension co-polymerization with bifunctional initiators. Ph.D. Thesis, Department of Chemical Engineering, McMaster University, Hamilton, Ontario, Canada, 1993.

Villalobos, M.A.; Hamielec, A.E.; Wood, P.E. Kinetic model for short-cycle bulk styrene polymerization through bifunctional initiators. *J. Appl. Polym. Sci.*, **1991**, 42, 629-641.

Villalobos, M.A.; Hamielec, A.E.; Wood, P.E. Bulk and suspension polymerization of styrene in the presence of n-pentane. An evaluation of monofunctional and bifunctional initiation. *J. Appl. Polym. Sci.*, **1993**, 50, 327-343.

Vivaldo-Lima, E. Simulación del proceso de polimerización de estireno via suspensión. B.Sc. Thesis (in Spanish), Facultad de Química, Universidad Nacional Autónoma de México, Ciudad Universitaria, México D.F., Mexico, 1989.

Vivaldo-Lima, E.; Hamielec, A.E.; Wood, P.E. Auto-acceleration effect in free radical polymerization. A comparison of the CCS and MH models. *Polym. React. Eng.*, **1994a**, 2(1&2), 17-86.

Vivaldo-Lima, E.; Hamielec, A.E.; Wood, P.E. Batch reactor modelling of the free radical copolymerization kinetics of styrene/divinylbenzene up to high conversions. *Polym. React. Eng.*, **1994b**, 2 (1&2), 87-162.

Vlachopoulos, J. Ch. E. 772 Polymer Rheology Course Notes, Department of Chemical Engineering, McMaster University, Hamilton, Ontario, Canada, 1994.

Wang, Z.L.; Pla, F.; Corriou, J.P. Nonlinear adaptive control of batch styrene polymerization. *Chem. Eng. Sci.*, **1995**, 50(13), 2081-2091.

Warsi, Z.U.A. *Fluid dynamics: theoretical and computational approaches*; CRC Press, Inc.: Boca Raton, Florida, USA, 1993.

Wasserman, S.H. Calculating the molecular weight distribution from linear viscoelastic response of polymer melts. *J. Rheol.*, **1995**, 39(3), 601-625.

Watters, J.C.; Smith, T.G. Pilot-scale synthesis of macroporous styrene-divinylbenzene copolymers. *Ind. Eng. Chem. Process Des. Dev.*, **1979**, 18(4), 591-594.

Whitesides, T.H.; Ross. D.S. Experimental and theoretical analysis of the limited coalescence process: stepwise limited coalescence. *J. Colloid Interface Sci.*, **1995**, 169, 48-59.

Williams, R.A.; Mann, R.; Dickin, F.J.; Ilyas, O.M.; Ying, P.; Edwards, R.B.; Rushton, A. Application of electrical impedance tomography to mixing in stirred vessels. *AIChE Symp. Ser.* No. 293, **1993**, 89, 8-15.

Winslow, F.H.; Matreyek, W. Particle size in suspension polymerization. *Ind. & Eng. Chem.*, **1951**, 43(5), 1108-1112.

Wood, P.E. Chem. Eng. 730 Fluid mechanics course notes. Department of Chemical Engineering, McMaster University, Hamilton, Ontario, Canada, 1994.

Wright, H.; Ramkrishna, D. Solutions of inverse problems in population balances I. Aggregation kinetics. *Computers Chem. Eng.*., **1992**, 16, 1019-1038.

Wright, H.; Ramkrishna, D. Factors affecting coalescence frequency of droplets in a stirred liquid-liquid dispersion. *AIChE J.*, **1994**, 40(5), 767-776.

Xie, J. Viscometric constants for small polystyrenes and polyisobutenes by gel permeation chromatography. *Polymer*, **1994**, 35(11), 2385-2389.

Yu, T.-L. Molecular weight of linear polymer from transient viscoelasticity. *J. Polym. Eng.*, **1991**, 10(4), 345-359.

Yu, T.-L. Polymer molecular weight from dynamic viscoelastic properties. *J. Polym. Eng.*, **1993**, 12(4), 331-352.

Yuan, H.G.; Kalfas, G.; Ray, W.H. Suspension Polymerization. *JMS-Rev. Macromol. Chem. Phys.*, **1991**, C31(2&3), 215-299.

Yuan Perng, C.; Murthy, J.Y. A moving-deforming technique for simulation of flow in mixing tanks. In *AIChE Symp. Ser.*, 1993; Vol. 89, No. 293, 37-41.

Zamora, J.M. Solución Numérica del Balance de Población para Sistemas de Partículas con el Método de Elemento Finito con Colocación Nodal y Malla Adaptable. M. Eng. (In Spanish), Unidad de Ciencias Básicas e Ingeniería, Universidad Autónoma Metropolitana, Plantel Iztapalapa, México D.F., Mexico, 1990.

Zhu, D.-W. Perfluorocarbon fluids: universal suspension polymerization media. *Macromolecules*, **1996**, 29(8), 2813-2817.

Zhu, S.; Hamielec, A.E. Chain-length-dependent termination for free radical polymerization. *Macromolecules*, **1989**, 22(7), 3093-3098.

Zilberman, E.N.; Lerner, F.; Joseph, H.M.; Alon, M. Properties of Hydroxypropyl Methylcellulose-Polyvinyl Alcohol Water Systems, Dispersants in Vinyl Chloride Suspension Polymerization. *J. Appl. Polym. Sci.*, **1993**, 48, 435-442.

Zubarev, A.Y. Viscosity of colloids in the hydrodynamic vicinity of the critical point of the sol-gel transition. Colloid *Journal of the Russian Academy of Sciences*, **1992**, 54(1), 49-53 (63-68 in original *Kolloidnyi Zhurnal*).

Chapter 3

Kinetic Model-Based Experimental Design of the Polymerization Conditions in Suspension Copolymerization of Styrene/Divinylbenzene[1]

Eduardo Vivaldo-Lima[†], Philip E. Wood[†*], Archie E. Hamielec[†], and Alexander Penlidis[‡]

[†]McMaster Institute for Polymer Production Technology, Department of Chemical Engineering, McMaster University, Hamilton, Ontario, L8S 4L7, Canada.
[‡]Institute for Polymer Research, Department of Chemical Engineering, University of Waterloo, Waterloo, Ontario, N2L 3G1, Canada.

ABSTRACT: The use of a mechanistic model-based experimental design technique to determine the polymerization conditions and polymer properties in suspension copolymerization of styrene and divinylbenzene is reported. The technique consists of using a mathematical model to design the polymerization conditions of a copolymer with characteristics specified beforehand. The properties (conversion, gel content, molecular weight averages and copolymer composition) of the copolymer synthesized using this approach agree very well with the calculated properties for the pre-gelation period, but accurate prediction of properties during the post-gelation period is still uncertain. It is demonstrated that the use of mechanistic modelling for experimental design purposes can be more adequate (when the model is sound, yet simple to solve) than other design techniques (e.g., factorial designs).

Keywords: copolymerization, crosslinking, polystyrene-divinylbenzene, experimental designs.

3.1 Introduction

This paper represents an intermediate stage of a systematic study on suspension polymerization processes undertaken by our research groups at McMaster and Waterloo. A critical review on suspension polymerization was presented recently (Vivaldo-Lima et al., 1997). The selection of the polymerization conditions to be used in the experimental stages of this study is addressed in this paper. Earlier stages of the study have dealt with the development of mathematical models for copolymerization kinetics (Vivaldo-Lima et al., 1994a, 1994b), and will be followed by studies on the particle size distribution in suspension polymerization (Vivaldo-Lima et al., 1998).

The main objective herein was to design the polymerization conditions (temperature, initiator concentration and crosslinker concentration) required to study the rupture and coalescence phenomena in suspension copolymerization of styrene and divinylbenzene (DVB). These conditions should fulfil the following requirements:

a) Cause gelation in 3 - 5 h after the polymerization is started. This period of time should be long enough to allow for monitoring of the particle size distribution (PSD) evolution during the pre-gelation period. Gelation in this paper is understood as the time when a polymer network is obtained. This is characterized by a huge increase (toward infinity) of the weight average molecular weight, and the formation of an "insoluble in all solvents" phase. Gelation time should not be confused with the "onset" of the auto-acceleration effect, which takes place much sooner.

b) Yield maximum conversion (as close as possible to 100%) in less than 8 h (typical duration of a batch).

A second objective of this study was to test the predictive power of the kinetic model developed by Vivaldo-Lima et al. (1994a) and fine-tune the parameters of the model, if needed.

3.2 Selection of Initiator and Temperature Range

The most commonly used initiators in free-radical polymerization are peroxide- and azo-type initiators. Some of the peroxide-type of initiators which are (commercially) available include diacyl peroxides (one of which is dibenzoyl peroxide, BPO), acetyl alkylsulfonyl peroxides, dialkyl peroxy dicarbonates, *tert*-alkyl peroxy esters, O,O-di-*tert*-alkyl O-alkyl monoperoxy carbonates, bis(*tert*-alkyl) peroxy ketals, di-*tert*-alkyl peroxides, *tert*-alkyl hydro peroxides, ketone peroxides, and other structures. Both symmetrical and unsymmetrical organic azo-compounds can be used. By far the most widely used azo-initiator is 2,2'-azo-bis-isobutyronitrile (AIBN) (Sandler and Karo, 1992).

For purposes of selecting an initiator for a polymerization, the half-life (time) of the initiator at a given temperature is a major factor. Usually only temperature is considered to determine the half-life of the initiator, although the solvent used may have an important effect and should also be

specified. By choosing an initiator with a suitable half-life under the conditions employed (or using a semi-batch addition of a rapidly decomposing initiator), reasonably constant radical production rate can be achieved.

The free-radical copolymerization of styrene/divinylbenzene has been studied using mostly BPO and AIBN in mass (bulk) and suspension. Experimental copolymerization studies in bulk are reported in the literature using AIBN (Okasha et al., 1979; Hild and Okasha, 1985; Hild et al., 1985; Batch and Macosko, 1992) and BPO (Storey, 1965; Malinsky et al., 1971), and in suspension using BPO (Winslow and Matreyek, 1951; Balakrishnan and Ford, 1982; Leng and Quarderer, 1982; Watters and Smith, 1979).

The half-lives for BPO at 70, 80 and 90 °C are, respectively, 12, 5, and 1.5 h. For AIBN the half-lives at 60, 70, 80 and 90 °C are, respectively, 15, 4.5, 1.1, and 0.2 h (Sandler and Karo, 1992). If a total polymerization time of 8 h is considered, and it is desired to have an initiator concentration high enough as to maintain the quasi-constant radical production rate, but low enough as to have minimum content of unreacted initiator in the final product, then a polymerization temperature around 80 °C for BPO or 65° C for AIBN should be used. Higher temperatures will translate into higher productivity (higher polymerization rate), provided that the molecular weight is not too low (considering that gelation will occur, this may not be a major concern). Therefore, in our experimental studies on suspension copolymerization of styrene/divinylbenzene, BPO at 80 °C was used.

3.3 Experimental Design

3.3.1 Strategy

To design the experimental conditions required to produce a copolymer of styrene and divinylbenzene which gels at a desired time and polymerizes completely at a time specified in advance, the mathematical model developed by Vivaldo-Lima et al. (1994a) was used. The design steps were the following:

a) Selection of the initiator to be used. On the basis of the arguments given in the preceding section, BPO was chosen.

b) Selection of the polymerization temperature, or temperature range. As shown before, an adequate temperature for the purposes of this application is 80 °C.

c) Selection of the initiator and crosslinker concentrations. To choose these concentrations a computer program based on the model of Vivaldo-Lima et al. (1994a) was used. Lower and upper bounds for these concentrations were obtained from experimental studies reported already in the literature (Vivaldo-Lima et al., 1994a; Winslow and Matreyek, 1951; Balakrishnan and Ford, 1982; Leng and Quarderer, 1982; Watters and Smith, 1979). Figures 3.1 and 3.2 are simulated profiles that illustrate how this design stage was developed. Some of the profiles in those two figures might not be quantitatively accurate. Since this could not necessarily be known *a priori* during the design stage, they are included here to emphasize the sequence and type of decisions that the experimenter has to make during the development of a mechanistic model-based experimental design.

3.3.2 Simulation Program and Designed Conditions

The mathematical model developed by Vivaldo-Lima et al. (1994a) is based on the Tobita-Hamielec (1989) model for crosslinking kinetics for the pre-gelation period, an improved version of the Marten-Hamielec model for diffusion-controlled kinetics in free-radical polymerization (Vivaldo-Lima et al., 1994b) (which incorporates the recommendations of Zhu and Hamielec (1989) on the use of different number and weight average termination constants), and a simple phenomenological approach for the termination kinetic constant during the post-gelation period (although simple, this approach takes into account the unequal reactivity of vinyl groups and cyclization reactions). Some features and characteristics of the kinetic model are described in the next three paragraphs.

The model consists of a set of ordinary differential and algebraic equations that describe the most important reactions that take place during the copolymerization: initiation, inhibition, propagation, propagation through pendant double bonds (crosslinking, primary and secondary

cyclizations), chain transfer to monomers, chain transfer to other small molecules (either solvent or chain transfer agents), and bimolecular termination. These equations are listed in Table 3.1.

The kinetic scheme can be treated as if it was a homopolymerization by making use of the "pseudo-kinetic rate constants method", developed by Hamielec and MacGregor (1983). The method of moments is used to follow the molecular weight development. Initiation, propagation and termination reactions are considered to be diffusion-controlled, and are modelled using a free-volume theory from the start of the polymerization. Two averages, number- and weight-average termination rate constants , are used to model the mechanism of termination by combination. The number average termination kinetic constant, k_{tn}, is used to calculate polymerization rate and number average molecular weight. The weight average termination kinetic constant, k_{tw}, is used to calculate the weight average molecular weight. These averages depend on polydispersity and conversion, and are defined in such a way that no additional parameters are needed in the model.

All diffusion-controlled reactions are modelled using a series structure for the effective kinetic constants, as opposed to the rather common parallel approach. The differences between these two modelling approaches are explained in detail in Vivaldo-Lima et al. (1994b). The model equations can be solved using the steady-state-hypothesis (SSH) for polymer radicals, but this is reliable only during the pre-gelation period. The simulations for the experimental design stage presented in this paper were obtained using the SSH. The selected conditions for experimental study were simulated with and without use of the SSH.

Cyclization reactions are modelled using the equations proposed by Tobita and Hamielec (1989), although only average cyclization densities are calculated, instead of the full density distributions. Likewise, only the average crosslinking density as function of time is calculated. Tobita and Hamielec (1989) generalized Flory's theory for the post-gelation period by using a crosslinking density distribution. Instead, we used the original Flory-Stockmayer equation for sol fraction, but his simplifying assumptions regarding equal reactivity of double bonds, absence of cyclization and independence of double bonds were removed.

Table 3.1 Free-radical copolymerization kinetics of vinyl/divinyl monomers.

Initiation	$\frac{d(V[I])}{Vdt} = -k_d[I]$
Overall conversion	$\frac{dx}{dt} = (k_p + k_{fm})(1-x)[R^\bullet]$
Moment equations for polymer radicals	$\frac{d(VY_0)}{Vdt} = 2fk_d[I] - (\bar{k}_{tcn} + \bar{k}_{td})Y_0^2$ $\frac{d(VY_1)}{Vdt} = 2fk_d[I] + (k_{fm}[M] + k_{fT}[T]) + k_p^\bullet Y_0 Q_2 + k_p[M]Y_0$ $-\{k_{fm}[M] + k_{fT}[T] + (\bar{k}_{tcn} + \bar{k}_{td})Y_0 + k_{fp}([Y_1 + Q_1] - Y_1)\}Y_1$
Moment equations for total polymer concentration	$\frac{d(V[Y_0 + Q_0])}{Vdt} = 2fk_d[I] + (k_{fm}[M] + k_{fT}[T])Y_0 - k_p^\bullet Y_0([Y_1 + Q_1] - Y_1) - \frac{1}{2}\bar{k}_{tcn}Y_0^2$ $\frac{d(V[Y_1 + Q_1])}{Vdt} = 2fk_d[I] + (k_{fm}[M] + k_{fT}[T])Y_0 + k_p[M]Y_0$ $\frac{d(V[Y_2 + Q_2])}{Vdt} = 2fk_d[I] + (k_{fm}[M] + k_{fT}[T])Y_0 + k_p[M]Y_0 + 2k_p[M]Y_1$ $+2k_p^\bullet Y_1[Y_2 + Q_2] + \bar{k}_{tcw}Y_1^2$
Divinyl monomer consumption	$\frac{df_2}{dt} = \frac{f_2 - F_2}{1-x}$
Accumulated copolymer composition	$\overline{F_2} = \frac{f_{20} - f_2(1-x)}{x}$
Crosslink density	$\frac{d[x\bar{\rho}(x)]}{dt} = \frac{k_p^{\bullet 0}[2\overline{F_2}(x)(1-k_{cp}) - \bar{\rho}(x)(1+k_{cs})]x}{k_p(1-x)}\frac{dx}{dt}$
Transfer to small molecule	$\frac{d(V[T]_i)}{Vdt} = -k_{fTi}[T_i][R^\bullet]$
Temperature	$\frac{dT}{dt} = \frac{(-\Delta H)_r R_p}{n_m Cp_m} - \frac{n_w Cp_w}{n_m Cp_m}\frac{dT_w}{dt} - \frac{UA}{n_m Cp_m}(T - T_w)$

Table 3.2 Kinetic and physical parameters (Vivaldo-Lima et al., 1994a)

Parameter	Value or functionality
k_d, s^{-1}	$2.06 \times 10^{12} \exp [-13612/T(^oK)]$
f^0_{BPO}	0.7
k^o_{11}, L mol^{-1} s^{-1}	$275.38 \exp [-4267.24 (1/T(^oK) - 1/333.15)]$
k^o_{22}, L mol^{-1} s^{-1}	$(k_{22}/k_{11})_m$=0.95, $(k_{22}/k_{11})_p$= 1.9
k_{fi}, L mol^{-1} s^{-1}	0.18 k^o_{11}, @ 80 °C [Bamford and Tipper (1976)]
k_{fm}, L mol^{-1} s^{-1}	$2.31 \times 10^6 \exp [- 6376.95/T(^oK)]$
k_{fp}, L mol^{-1} s^{-1}	0.0
k^o_{tc}, L mol^{-1} s^{-1}	$1.223 \times 10^8 \exp [- 3586.81/(1/T(^oK) - 1/333.15)]$
k^o_{td}, L mol^{-1} s^{-1}	$2.19 \times 10^5 \exp [- 13810/T(^oK)]$
k_{fT1}, k_{fT2}, L mol^{-1} s^{-1}	0.0133 k_{11}
k_{fT3}, L mol^{-1} s^{-1}	2 k_{11}
$(r_1)_m$	$(k_{11}/k_{12})_m$= 0.4
$(r_2)_m$	$(k_{22}/k_{21})_m$= 1.0
$(r_1)_p$	$(k_{11}/k_{12})_p$= 0.13
$(r_2)_p$	$(k_{22}/k_{21})_p$= 2.0
$(r_1)_{mix}$, $(r_2)_{mix}$	$(r_i)_{mix} = [n^0_{p\text{-}DVB} (r_i)_p + n^0_{m\text{-}DVB} (r_i)_m]/(n^0_{p\text{-}DVB} + n^0_{m\text{-}DVB})$, i= 1,2
k_{3i}, L mol^{-1} s^{-1}	$(k_{31})_m$= 0.0067 k_{11} $(k_{31})_p$= 0.109 k_{11} $k_{32}/k_{31} = r_2$
k^*_{i3}, L mol^{-1} s^{-1}	$(k^*_{i3}/k_{11})_m = 2 (k^*_{i3}/k_{11})_p$ $(k^*_{i3}/k_{11})_p = 0.0626 + 1.245 \times 10^{-3}/f_{20}$ $(k^*_{i3})_{mix} = [n^0_{p\text{-}DVB} (k^*_{i3})_p + n^0_{m\text{-}DVB} (k^*_{i3})_m]/(n^0_{p\text{-}DVB} + n^0_{m\text{-}DVB})$
k_{cp}	0.25 @ $[CCl_4]$= 0.0, 0.335 @ $[CCl_4]$= 0.125 mole/L
k_{cs}	0.0

Table 3.3 Free-volume and reaction-diffusion termination parameters [Vivaldo-Lima et al., (1994a)]

Parameter	Value
A	0.465
V_{fcr2}	0.036
D	0.001
C^0_{rd}, L/mol	135
C_1, C_2	0
C_3	1
α_i, $^oC^{-1}$	0.001, Styrene 0.0008, Divinylbenzene 0.007, Carbon tetrachloride
Tg_i, ^oC	-88.1, Styrene -90.0, Divinylbenzene -110.0, Carbon tetrachloride 93.5, Polymer

The dominant mechanism for termination during the post-gelation period was considered to be "reaction-diffusion" termination, and each phase was considered to have different rates of termination. In Tables 3.2 and 3.3 the values for all the parameters of the model are summarized. The details of the derivation, solution and use of the model equations are provided in the papers of Vivaldo-Lima et al. (1994a, b).

The kinetic model of Vivaldo-Lima et al. (1994a) can provide detailed information on the polymerization conditions and polymer properties during the reaction. For this study, the information that we monitored and recorded were total conversion, number and weight average molecular weights, copolymer composition, gel fraction, and zero-shear viscosity.

Using BPO as the initiator in a concentration range of 0.01 to 0.05 mole/litre, a temperature of 80 ^oC, and divinyl benzene (it was known at this point that the DVB that we had available for the subsequent experimental stage was an Aldrich technical mixture with 54% m-DVB, 24% p-DVB, 20% ethylvinylbenzene, 1% diethyl benzene and 1% naphthalene) in a concentration range of 0.001 to 0.78

(in terms of mole fraction), the simulations shown in Figure 3.1 were obtained. Figure 3.1(a) shows the effect of initial initiator concentration on overall conversion (at a crosslinker mole fraction of 0.001). One can see that the higher the initiator concentration, the longer it takes to obtain the gelation point, but the faster the polymerization proceeds. Also noticed in Figure 3.1(a) is a discontinuity in the conversion versus time profile. This change of slope takes place at the gelation point and is a consequence of using two different models for the termination kinetic constant (one model is valid for the pre-gelation period and the other for the post-gelation period). As mentioned before, gelation should not be understood as the "onset" of the auto-acceleration effect, which occurs sooner. At initial BPO concentrations of 0.03, 0.04 and 0.05 mole per litre, the predicted behaviour during the post-gelation period may be unreliable (the change in slope is too abrupt).

Figure 3.1(b) shows the effect of crosslinker initial concentration on conversion at constant initial initiator concentration ([BPO]=0.01 mole/litre). As expected, it is observed that the higher the crosslinker concentration, the faster the polymerization proceeds, and the sooner gelation occurs. From Figures 3.1(a) and 3.1(b), it is observed that the profile at [BPO]=0.02 mole/litre and f_{20}=0.001 seems the most adequate for our purposes. At these conditions, gelation is predicted to occur at approximately 2 hours (long enough to monitor the viscosity change during the pre-gelation period in a suspension polymerization), and the final conversion is predicted to occur at approximately six hours. Figure 3.1 was obtained using the computer program developed by Vivaldo-Lima (1993), assuming a steady state hypothesis (SSH) for the concentration of polymer radicals. As demonstrated by Zhu and Hamielec (1993), the SSH is valid as long as k_p/k_m (ratio of propagation to number-average termination kinetic constants) is lower than 10^{-3}. This condition applies during most of the polymerization in our simulations. To further prove that these profiles are valid, transient calculations (removal of the SSH) for the selected conditions from Figure 3.1 were carried out. No deviations were observed during the pre-gelation period, and little deviation (no larger than 5%) was observed during the post-gelation period.

Even though gelation was predicted to occur at approximately 2 hours, it was reasonable to

expect that the particle identity point (PIP) in the suspension copolymerization occurred before gelation and thus, it would be convenient to delay gelation even further. The PIP in a suspension polymerization is the time when an equilibrium between the breakage and coalescence of droplets is established. At this time the mean particle size of the droplets stops increasing (a slight decrease is observed due to volume contraction). Choosing a lower crosslinker fraction would imply using very small quantities of crosslinker, thus likely increasing the reproducibility error. Using a chain transfer agent permits to obtain the same result (delaying gelation) without reducing the amount of crosslinker.

Figure 3.2 shows predictions of the effect of chain transfer agent on the copolymerization kinetics and copolymer properties. Taking as reference styrene homopolymerization systems where molecular weight, viscosity and identity points were known (Villalobos, 1989), it was estimated that an identity point (in our copolymerization system) occurring at approximately 2 hours (a time considered long enough to monitor particle size distribution evolution) would correspond to a system with gelation time occurring at approximately 4 hours after the start of polymerization. Such a system would be obtained using a concentration of chain transfer agent of 0.125 mole/litre (Fig. 3.2a). As noted on the comments to Figure 3.1(a), the presence of an abrupt change in the slope of the conversion versus time profiles is an indicator of unreliable behaviour past the gelation point. Figure 3.2(a) shows that the higher the concentration of chain transfer agent, the more abrupt the change in slope of the conversion-time profiles. Also noticed in that figure is the fact that the limiting conversion seems to increase as the concentration of CTA is increased, and even a crossover of curves is observed. We believe that these unusual predictions are due to a deficiency of the model during the post-gelation period in the presence of a solvent, and not to a strange physical phenomenon. The unreliable prediction of limiting conversion could be associated to the fact of using an equilibrium free-volume model instead of a more realistic non-equilibrium one, as explained in Vivaldo-Lima et al. (1994a). Figures 3.2b and 3.2c show predictions of gel fraction and accumulated number- and weight-average chain lengths of the sol fraction for the chain transfer concentrations indicated in Figure 3.2a. In Figure 3.2b we observe that the content of gel is predicted to increase very rapidly to

a limiting value when a CTA is used. Previous validation of the model and the subsequent experimental data to be shown in Figure 3.3 seem to indicate that the prediction of limiting gel content is adequate, but the increase should be more gradual. This confirms the previous observation that the transition from sol to gel is not captured sufficiently well by our model. Figure 3.2c also shows this abrupt change at and past the gelation point, but this time the property observed is weight average chain length of the sol fraction, P_w. The abrupt increase of P_w is indicative of gelation taking place, and the model predictions seem to be adequate. What does not seem quite adequate is the very abrupt decrease of P_w right after gelation. The shape of the curve is fine, but the decrease should be more gradual.

The next step was to verify the predictions of the model. To do so, ampoule (batch) copolymerizations at the selected conditions were carried out. In the next section the experimental techniques that were used are described, and comparisons are made in section 3.5.

3.4 Experimental Techniques

3.4.1 Ampoule Batch Copolymerizations

Styrene monomer (Aldrich S 497-2, 99% pure) was washed three times with 5% NaOH solution to remove the inhibitor. Divinyl benzene (Aldrich 41,456-5, technical grade, 80% mixture of isomers) was also washed three times with 5% NaOH solution to remove the inhibitor. Neither styrene nor DVB were distilled, as the presence of isomers (m- and p-DVB) and impurities (ethyl vinyl benzene and di-ethylbenzene, mainly) could be accounted for by the kinetic model. After washing, the monomers were dried over anhydrous calcium chloride. Benzoyl peroxide (Aldrich 17,998-1, 97%) was used as received.

Monomer solutions were prepared shortly before use by weighing the required amounts of styrene, DVB and BPO. Pyrex ampoules of 4, 5 and 8 mm O.D., and 30 cm length were used to study the effect of temperature rise in the measured properties [according to Zhu and Hamielec (1991), the temperature rise in crosslinking reactions carried out in ampoule reactors is significant]. Each of the

Pyrex ampoules was filled with ca. 1.5 g of monomer solution. After degassing by four successive freeze-thaw cycles using liquid nitrogen and a reduced pressure (approximately 10^{-4} torr), the ampoules were torch sealed. The polymerization was initiated by immersing the ampoules in a water bath maintained at 80 °C. The polymerization was stopped by thrusting the ampoules into liquid nitrogen.

3.4.2 Total Monomer Conversion

The ampoules were broken and the contents transferred to a covered flask with toluene and hydroquinone. After being shaken and allowed to dissolve for two to three days, the swollen gel, if present, was vacuum filtered using a combination of filters of different grade (coarse and fine), and then extracted by toluene in a Soxhlet extractor for one day with a coarse grade thimble. The sol-free gel was dried at 80 °C in a vacuum oven for 3 to 5 days until a constant weight was obtained. The sol polymer was precipitated from solution using methanol and dried at 50 °C in a vacuum oven for two days. Conversions to gel and sol were determined gravimetrically.

3.4.3 Copolymer Characterization

To test the predictive power of the kinetic model at least two independent type of measurements are needed. These can be conversion and weight-average chain length, conversion and copolymer composition, or these three properties together with sol and gel fractions. As mentioned before, conversion was measured gravimetrically. Sol and gel fractions were also measured gravimetrically from the weights of dried gel, sol polymer and total initial mass.

Number average molecular weight was measured by gel permeation chromatography (GPC). Weight average molecular weight was measured by GPC and multiple angle laser light scattering (MALLS). Samples for GPC were prepared by dissolving 10 mg of polymer in 2 cc of tetrahydrofuran (THF) in 2 cc vials. Some samples were prepared two weeks before doing the measurements, and others the day before. Each sample solution was filtered with a 0.5 μm micro-filter. A Waters

Associates GPC was used. Three Waters Ultrastyragel columns (10^3, 10^4, and 10^6 Å) were installed in series. THF, degassed and filtered, was used as the eluent. Polymer elution was detected with a Waters R401 differential refractometer (DRI).

Vials for MALLS determination were washed with ethanol, then with unfiltered THF, and finally with filtered THF. The polymer solutions were filtered with a 0.5 μm micro-filter, and four dilutions were prepared from the stock solutions. As with GPC, some stock solutions were prepared two weeks before doing the measurements, and others were prepared the same day of the measurement. A Wyatt Technology DAWN DSP-F laser photometer was used.

Copolymer composition can be determined by residual monomer analysis or copolymer composition measurements on the actual copolymer. Some of the techniques used to determine copolymer composition are chemical analysis, elemental analysis, infrared spectroscopy (IR), nuclear magnetic resonance (NMR), ultraviolet spectroscopy (UV), etc. Chemical and elemental analyses are general techniques that can be applied to almost any polymer. The spectroscopic techniques can be applied depending on the ability of the functional groups present to absorb at specific wavelengths (García-Rubio, 1981). Some experimental techniques applied to measure copolymer composition of styrene-divinylbenzene copolymers are residual monomer measurement by gas chromatography (GC) (Hild and Okasha, 1985; Fink, 1981), radioactivity assay techniques (Wiley et al., 1967; Wiley and Ahn, 1968), and IR spectroscopy (Malinsky et al., 1969, 1971; Cheng et al., 1992).

In this study, copolymer composition was measured by both ^{1}H-NMR (at 300 MHz in a Bruker AM 500 Fourier-Transform spectrometer) and ^{13}C-NMR (at 75 MHz in a Bruker AC 200 Fourier-Transform spectrometer) spectroscopy. Analyses were carried out in deuterated chloroform at room temperature. The relative amounts of monomer bound in the polymer were determined from the areas under the appropriate peaks of the spectra. Interpretation of the spectra was not always straightforward due to the very similar structures of styrene and divinylbenzene. Using two types of analyses assured that the results were consistent.

Zero-shear viscosity measurements for mixtures of copolymer (free of initiator and unreacted

monomers) and styrene (inhibited) were carried out using a Bohlin VOR rheometer with co-axial cylindrical (low conversion) and cone and plate (intermediate conversion) configurations. These measurements were aimed at characterizing the rheological behaviour of the reacting mass at the same degree of conversion of the copolymer samples before being frozen and recovered. Viscosity profiles were measured for two selected samples (one at fairly low conversion and another at a conversion close to the gelation point) at temperatures ranging from 30 to 80 °C, and shear rates in the range of 0.001 to 150 s^{-1}. Repeats for some conditions were obtained for error variance estimation purposes.

3.5 Results and Discussion

Parameter estimation and preliminary validation of the kinetic model used in this study was performed previously by Vivaldo-Lima et al. (1994a, b). A test of the predictive power of the model was one of the objectives of the present study, as stated before. From Figure 3.2(a) ([CTA]=0.125 mole/litre), gelation in the selected system should occur at approximately four hours after polymerization started. Gelation in our experimental system occurred between 5 and 5.5 hours after polymerization was started. This meant that fine-tuning of some of the model parameters was indeed needed.

Based on the analysis presented by Vivaldo-Lima et al. (1994a) it was realized that the value for primary cyclization, k_{cp}, used in our calculations corresponded to a system without solvent. Although the content of CCl_4 used in our recipe was rather low, it was high enough to increase the free volume and subsequently alter the value of the rate constant for primary cyclization [as explained in Vivaldo-Lima et al. (1994a) and Tobita and Hamielec (1989), this constant increases proportionally to solvent concentration in styrene/divinylbenzene copolymerizations]. Therefore, the value for k_{cp} was re-estimated by running several simulations with values of k_{cp} higher than 0.25, and comparing the predicted gelation times with experimental values. Gelation was predicted to occur at 5.05 hr using a value of k_{cp}=0.335 (instead of 0.25 for a system without solvent). No other parameters were modified to produce the predicted profiles shown in Figures 3.3 and 3.4. The profiles of conversion-time, gel

fraction-conversion and average chain lengths versus conversion for [CCl_4]= 0.1 and 0.15 mole per litre shown in Figure 3.2 are dubious due to an anticipated gel formation prediction. To obtain accurate predictions at those conditions experimental gelation times should be measured and k_{cp} evaluated for those concentrations of chain transfer agent from simulated profiles. We did not carry out those additional experiments, since the results obtained at [CCl_4]= 0.125 mole/litre fully fulfilled our objectives.

Figure 3.3(a) shows experimental data and model predictions for monomer conversion for a system without CTA (dotted-dashed line), and for a system with [CTA]=0.125 mole/litre (solid line). Two ampoule diameters were used: 4 and 8 mm OD. It is observed that there is significant increase in polymerization rate at the vicinity of gelation when the larger diameter ampoule was used. This corroborates the conclusions obtained by Zhu and Hamielec (1991) regarding the heat effects in ampoule polymerization reactions. Figure 3.3(a) also corroborates some conclusions obtained by Vivaldo-Lima et al. (1994a) regarding the applicability of their kinetic model to the post-gelation period. They observed that their kinetic model predicted fairly well the behaviour of the copolymerization system during the post-gelation period when there was no solvent or CTA, whereas deviations were obtained when CTA, solvent or inhibitor were present.

Figure 3.3(b) shows experimental data and model predictions for gel fraction for a system without CTA and for a system with [CTA]=0.125 mole/litre. As observed, the agreement seems to be fairly good (although the onset of gelation is predicted to be more abrupt than it actually is in the experimental system).

Figure 3.4(a) shows experimental data (for a system with CTA) and model predictions (for systems with and without CTA) of number and weight average chain length of the sol fraction (the whole system during the pre-gelation period). The agreement between model predictions and experimental data seems to be good. The samples at conversions of 0.04, 0.25 and 0.5 were prepared two weeks before the measurements by GPC and MALLS were made, whereas the other samples were prepared a day before (GPC) or the same day (MALLS). For the samples that were prepared two

weeks in advance, the agreement between experimental data and model predictions is very good. For the samples prepared the day before or the same day, the experimental values are lower that the model predictions (of weight average chain length). The reason for this may be that the polymer fraction with high molecular weight in the samples prepared the day before or the same day did not dissolve completely and could have been retained in the micro-filter when the samples were filtered. It is also observed that the predictions of number average chain length are systematically slower than the experimental data. This seems to indicate that the semi-empirical relationship between k_{tw} and conversion proposed by Vivaldo-Lima et al. (1994b) (eq. 82 of that paper) may not be exact, although it can be considered adequate for practical calculations. Experimental data and model predictions of copolymer composition are shown in Figure 3.4(b). Once again, the agreement between model predictions and experimental data seems to be very satisfactory.

At the time the experiments reported in this paper were being carried out, a paper reporting experimental data for the free-radical crosslinking copolymerization of styrene and divinylbenzene became available (Sajjadi et al., 1996). To further test the predictive power of our kinetic model, we attempted to simulate all the conditions reported in that paper. In the paper it was reported that BPO at 0.1 wt% was used as initiator. Our simulations using that initial initiator concentration of BPO predicted much slower rates of polymerization than those observed experimentally. Experimental data for another system obtained at very similar conditions of temperature and crosslinker concentration (Storey, 1965), but using 1 wt% of BPO and a DVB which contained close to 100% of p-DVB (instead of a mixture of isomers), showed polymerization rates not much faster than those reported by Sajjadi et al. (1996) . Simulations of the copolymerization system studied by Storey (1965) were carried out using our kinetic model and the agreement with his experimental data and other experimental data from other research groups was very good (1994a). We repeated our simulation of the system studied by Sajjadi and coworkers (1996) using 1 wt% of BPO instead of 0.1 wt%. The agreement with their experimental data was quite good for the pre-gelation period. This led us to believe that the concentration of BPO reported in the paper by Sajjadi et al. (1996) was incorrect.

Therefore, we contacted the corresponding author of that paper and he confirmed to us that there was a typographical error on the reported concentration of BPO, and that the correct concentration was indeed 1 wt%.

Figures 3.5 to 3.7 show some of the experimental data reported by Sajjadi et al. (1996) with our model predictions. It is observed that our (isothermal) model agrees fairly well with their experimental data during the pre-gelation period (which occurs at conversion levels around 0.1 -see Figure 3.6a-), but large discrepancies are observed during the post-gelation period (see Figures 3.5a, 3.6a and isothermal predictions in figure 3.7). Since they used 9 mm ID ampoules, it is very likely that temperature did not remain constant (at the centre of the ampoules) in their experiments, thus causing very strong auto-acceleration. In figures 3.5(b), 3.6(b), 3.7 (non-isothermal predictions) and 3.8 we present non-isothermal simulations of their polymerization system, using a non-isothermal model [the energy balance is incorporated by using equation (82) from Vivaldo-Lima et al. (1994a)]. Figure 3.8 shows predicted temperature profiles. It is interesting to note that the maximum temperature increments calculated with our model are similar to the experimental profiles measured by Zhu and Hamielec (1991) for methyl methacrylate/ethylene glycol dimethacrylate (MMA/EGDMA) copolymerizations in ampoule reactors. The simulated profiles for non-isothermal copolymerization shown in Figures 3.5 to 3.8 were obtained using a value of UA= 0.75 cal $^{o}C^{-1}s^{-1}$ (close to adiabatic polymerization), where U is a combined heat transfer coefficient and A is heat transfer area. It can be observed that when non-isothermal polymerization is considered, the predicted profiles for conversion, gel fraction and crosslinking density (Figures 3.5b and 3.6b) are in much better agreement with the experimental data of Sajjadi et al. (1996).

The experiments that we carried out for styrene/divinylbenzene copolymerization without chain transfer agent (circles and dotted-line profiles in Figures 3.3a and 3.3b) in 4 mm OD ampoules were designed to verify that this heat effect causes indeed the deviations from isothermal model simulations. It is noticed that our isothermal simulations are in good agreement with experimental data even at high conversions and after gelation time (i.e., during the post-gelation period) when ampoules of small

diameter are used. This further confirms that heat effects are likely present in the results of Sajjadi et al. (1996). Even our own experimental results using ampoules of 8 mm OD seem to show the presence of non-isothermal effects (see Figure 3.3a).

Figure 3.9 shows viscosity versus shear rate profiles for mixtures of styrene and poly(styrene/divinylbenzene) at conditions that represent conversion levels of 0.25 (Fig. 3.9a, coaxial cylinder configuration) and 0.5 (Fig. 3.9b, cone and plate configuration). Most of the profiles at low conversion levels seem to overlap and show a linear relationship of the logarithm of viscosity with the logarithm of shear rate, as observed in Figure 3.9(a).

Figure 3.9(b) shows the viscosity-shear rate profiles for a monomer/polymer mixture representing 50% monomer conversion. The measurements from 27.3 to 60 °C were obtained from a single sample in the same day. The other measurements for 60 (repeat), 70 and 80 °C were obtained on another sample (same conversion) in a different day. A clear shear-thinning effect is observed at this conversion level, although the temperature effect is rather unclear and different from what would be expected for a homopolymer (lower viscosity at higher temperature). It should also be considered that some monomer could have evaporated from the sample while the measurements where made, so that the polymer concentration may have changed (increased).

Zero shear viscosities were estimated from Figure 3.9 (by extrapolating to zero shear rate) and compared with predictions from a correlation used for polystyrene [equation (36) in the paper of Vivaldo-Lima et al. (1997)]. There was disagreement between our estimates and the predictions using the correlation. Using experimental data (viscosity-shear rate profiles) for polystyrene from the literature (García-Sandoval, 1993) and our results, we attempted to develop a single correlation valid for polystyrene and poly(styrene/divinylbenzene). Equation (1) represents a correlation obtained from combined experimental data [homopolymerization (styrene polymerization) and copolymerization]. The estimated parameters are all significantly different from zero. However, the absolute errors for some of the individual viscosity measurements were significantly large.

$$\ln(\eta_0) = 14.16 - 13.41\ln(C) - 2.29\ln(Mw) + \frac{1259.15}{T} - 11442.2\ln(1 - f_{DVB}^0) \qquad (10)$$

η_0 in equation (1) represents zero-shear viscosity in (Pa s), C is total monomer mass fraction, Mw is weight average molecular weight in (g mol^{-1}), T is temperature in degrees Kelvin, and f_{DVB}^0 is initial mole fraction of crosslinker.

3.6 Concluding Remarks

The polymerization conditions required to conduct a study on breakage and coalescence of droplets in a suspension copolymerization of styrene and divinylbenzene were designed using a single set of experiments. This was possible because of previous knowledge on the studied system, and the availability of a sound mathematical model which had been used to model similar systems. The factors that were determined using this approach were: temperature, initiator concentration, chain transfer agent concentration, and crosslinker concentration. If a full factorial design in 4 factors had been used (if we did not know much about the system), 16 sets of experiments would have been required. Using a half fraction would have required 8 sets of experiments. Even using an optimal Bayesian design might have required about 4 sets of experiments [e.g., Dubé et al. (1996)].

The kinetic model developed by Vivaldo-Lima et al. (1994a) can be used with confidence to simulate the behaviour of a styrene/divinylbenzene copolymerization system during the pre-gelation period. The key requirement is to ensure that experimental and predicted gelation times are in agreement, in order to get reliable estimates of conversion, weight average molecular weight, gel fraction, and copolymer composition.

This paper illustrates how useful a mathematical model can be in studying and designing the operating conditions in polymer production processes.

Acknowledgement

We wish to acknowledge financial support from the Science and Technology National Council (CONACYT) of Mexico, and the Natural Sciences and Engineering Research Council (NSERC) of Canada.

3.7 Nomenclature

A Effectiveness factor to account for overlap of free-volume and separation of reactive radicals (or heat transfer area, m^2, in Table 3.1).

C Total monomer mass fraction.

C_1 Empirical parameter to account for initiator efficiency decrease during the post-gelation period.

C_2 Empirical parameter to account for propagation kinetic constant decrease during the post-gelation period.

C_3 Empirical parameter to account for termination kinetic constant decrease during the post-gelation period.

Cp Heat capacity, J/K.

C^0_{rd} Parameter for reaction-diffusion termination.

D Effectiveness factor to account for overlap of free-volume and separation of fragment-radical molecules.

f, f^0 Initiator efficiency (superscript "0" accounts for initial conditions).

f_2, f_{20} Divinyl monomer molar fraction (also shown as f^0_{DVB}).

F_2 Instantaneous relative composition of monomer 2 in the polymer (accumulated composition if shown with an overline).

$(-\Delta H)_r$ Heat of reaction, J/mol.

[I] Initiator concentration, mol/L.

k_{ij} Effective (diffusion-controlled) propagation kinetic constant for radical type I (I= 1, 2, or 3) and adding monomer unit j (j=1, 2), L mol^{-1} s^{-1}.

k^*_{i3} Effective (diffusion-controlled) propagation kinetic constant for addition of a pendant double bond (macromonomer) into a radical with end unit of monomer I, L mol^{-1} s^{-1}.

k_{cp} Proportionality constant between primary cyclization density and mole fraction of divinyl monomer bound in the polymer chains.

k_{cs} Proportionality constant between the average number of secondary cycles per crosslink and the fraction of "free" pendant double bonds in the primary polymer molecule.

k_d Initiator decomposition kinetic constant, s^{-1}.

k_{fI} Pseudo-kinetic rate constant for chain transfer to initiator, L mol^{-1} s^{-1}.

k_{fm} Pseudo-kinetic rate constant for chain transfer to monomer, L mol^{-1} s^{-1}.

k_{fp} Pseudo-kinetic rate constant for chain transfer to polymer, L mol^{-1} s^{-1}.

k_{fT} Pseudo-kinetic rate constant for chain transfer to a small molecule T, L mol^{-1} s^{-1}.

k_{fTi} Kinetic constant for chain transfer of radical type i (i= 1,2 or 3) to a small molecule T, L mol^{-1} s^{-1}.

k_p Pseudo-kinetic propagation rate constant, L mol^{-1} s^{-1}.

k_p^* Pseudo-kinetic rate constant for crosslinking reaction, L mol^{-1} s^{-1}.

k^0_{tc} Intrinsic chemical kinetic constant for termination by combination, L mol^{-1} s^{-1}.

k^0_{td} Intrinsic chemical kinetic constant for termination by disproportionation, L mol^{-1} s^{-1}.

k_{tn} Number average pseudo-kinetic rate constant for termination, L mol^{-1} s^{-1}.

k_{tw} Weight average pseudo-kinetic rate constant for termination, L mol^{-1} s^{-1}.

m- Accounts for meta isomer.

[M] Total monomer concentration, mol/L.

Mw Molecular weight, g mol^{-1}.

n Molar mass, mol.

p- Accounts for para isomer.

Q_i i-th moment of the dead polymer distribution, mol/L.

r_1 Reactivity ratio, k_{11}/k_{12}.

r_2 Reactivity ratio, k_{22}/k_{21}.

[R˙] Total polymer radical concentration (also shown as Y_0), mol/L.

T, T_w Temperature ("w" accounts for cooling water), ^{0}C or ^{0}K.

[T] Concentration of small molecule (either solvent of chain transfer agent), mol/L.

Tg_i Glass transition temperature for species I, ^{0}C.

U Combined heat transfer coefficient, $W\ m^{-2}\ K^{-1}$.

V Volume, L.

V_{fcr2} Critical fractional free volume for glassy effect.

x Total monomer conversion.

Y_i I-th moment of the polymer radical distribution, mol/L.

Greek symbols

α_i Expansion coefficient for species I, $^0C^{-1}$.

η_0 Zero-shear viscosity, Pa s.

3.8 References

Balakrishnan, T. and W.T. Ford, *J. Appl. Polym. Sci.*, **27**, 135 (1982).

Bamford, C.H. and C.F.H. Tipper, *Comprehensive Chemical Kinetics*, Vol. 14A, 1976, p. 153.

Batch, G.L. and C.W. Macosko, *J. Appl. Polym. Sci.*, **44**, 1711 (1992).

Cheng, C.W., J.W. Vanderhoff, and M.S. El-AAsser, *J. Polym. Sci., Polym. Chem.*, **30**, 245 (1992).

Dubé, M.A., A. Penlidis, and P.M. Reilly, *J. Polym. Sci., Polym. Chem.*, **34**, 811 (1996).

Fink, J.K., *J. Polym. Sci., Polym. Chem.*, **18**, 195 (1981).

García-Rubio, L.H., Ph.D. Thesis, Department of Chemical Engineering, McMaster University, Hamilton, Ontario, Canada, 1981.

García-Sandoval, E., M.Eng. Thesis (in Spanish), Unidad de Ciencias Básicas e Ingeniería, Universidad Autónoma Metropolitana, Plantel Iztapalapa, Mexico D.F., Mexico, 1993.

Hamielec, A.E. and J.F. MacGregor, in *Polymer Reaction Engineering*, K.-H. Reichert and W. Geiseler, Eds., Hanser Publishers, New York, 1983, p.21.

Hild, G. and R. Okasha, *Makromol. Chem.*, **186**, 93 (1985).

Hild, G., R. Okasha, and P. Rempp, *Makromol. Chem.*, **186**, 407 (1985).

Leng, D.E. and G.J. Quarderer, *Chem. Eng. Commun.*, **14**, 177 (1982).

Malinsky, J., J. Klaban, and K. Dušek, *Collect. Czechoslov. Chem. Commun.*, **34**, 711 (1969).

Malinsky, J., J. Klaban, and K. Dušek, *J. Macromol. Sci.-Chem.*, **A5**(6), 1071 (1971).

Okasha, R., G. Hild, and P. Rempp, *Eur. Polym. J.*, **15**, 975 (1979).

Sajjadi, S., S.A.M. Keshavarz, and M. Nekoomanesh, *Polymer*, **37**(18), 4141 (1996).

Sandler, S.R. and W. Karo, *Polymer Syntheses*, Vol. I, 2nd. Ed., 1992, chap. 14, p. 547.

Storey, B.T., *J. Polym. Sci., Part A*, **3**, 265 (1965).

Tobita, H. and A.E. Hamielec, in *Polymer Reaction Engineering*, K.-H. Reichert and W. Geiseler, Eds., VCH Publishers, New York, 1989, p. 43.

Villalobos, M.A., M.Eng. Thesis, Department of Chemical Engineering, McMaster University, Hamilton, Ontario, Canada, 1989.

Vivaldo-Lima, E., M.Eng. Thesis, Department of Chemical Engineering, McMaster University, Hamilton, Ontario, Canada, 1993.

Vivaldo-Lima, E., A.E. Hamielec, and P.E. Wood, *Polym. React. Eng.*, **2**(1&2), 87 (1994a).

Vivaldo-Lima, E., A.E. Hamielec, and P.E. Wood, *Polym. React. Eng.*, **2**(1&2), 17 (1994b).

Vivaldo-Lima, E., P.E. Wood, A.E. Hamielec, and A. Penlidis, *Ind. Eng. Chem. Res.*, **36**(4), 939 (1997).

Vivaldo-Lima, E., P.E. Wood, A.E. Hamielec, and A. Penlidis, *Can. J. Chem. Eng.*, **76**, 495 (1998).

Watters, J.C. and T.G. Smith, *Ind. Eng. Chem. Process Des. Dev.*, **18**(4), 591 (1979).

Wiley, R.H. and T.-O. Ahn, *J. Polym. Sci., Part A-1*, **6**, 1293 (1968).

Wiley, R.H., W.K. Mathews, and K.F. O'Driscoll, *Macromol. Sci. (Chem.)*, **A1**(3), 503 (1967).

Winslow, F.H. and W. Matreyek, *Ind. Eng. Chem.*, **43**(5), 1108 (1951).

Zhu, S. and A.E. Hamielec, *Macromolecules*, **22**(7), 3093 (1989).

Zhu, S. and A.E. Hamielec, *Polymer*, **32**(16), 3021 (1991).

Zhu, S. and A.E. Hamielec, *Macromolecules*, **26**, 3131 (1993).

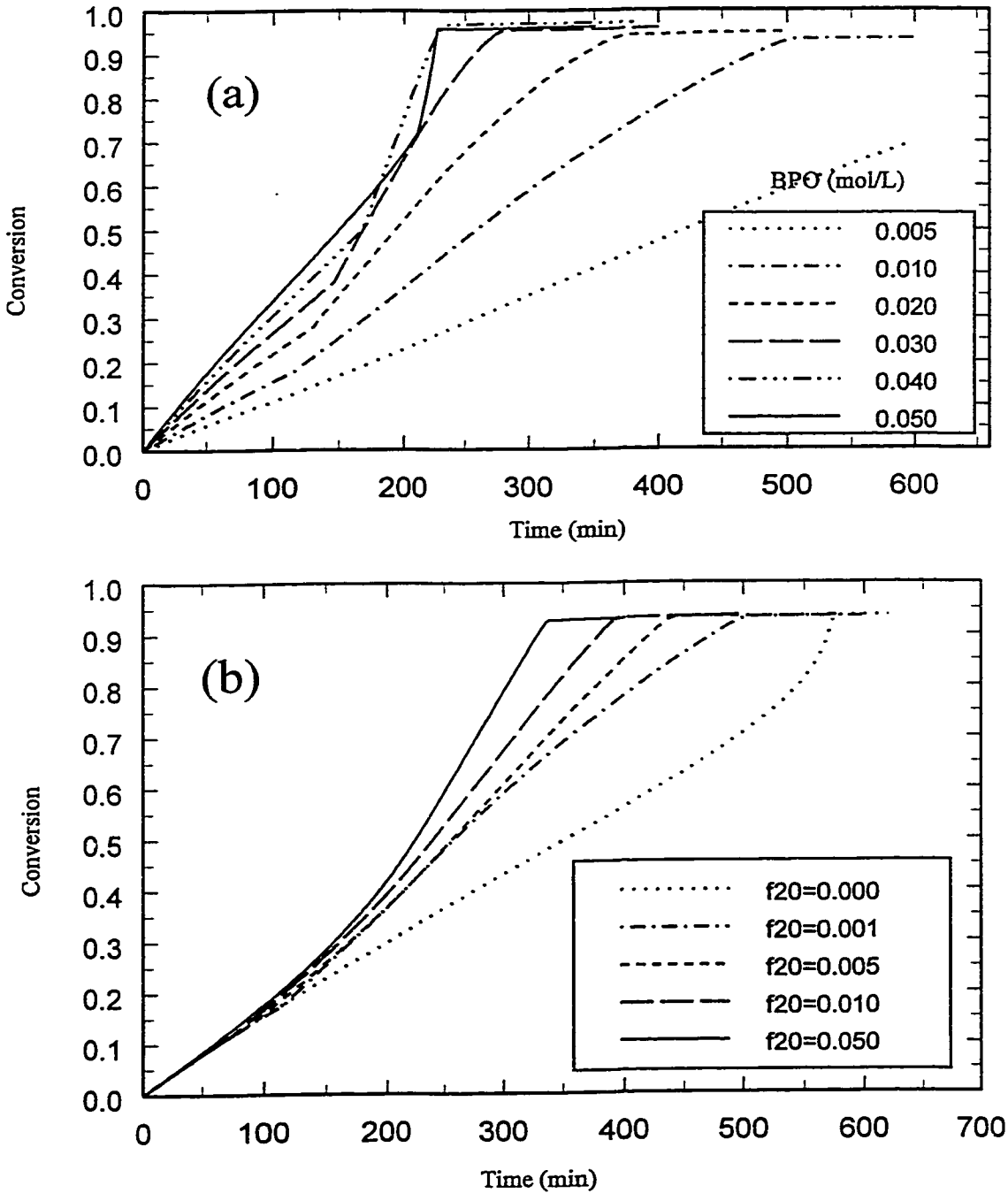

Figure 3.1 Selection of copolymerization conditions. (a) Effect of initial initiator concentration. Concentrations of BPO in mole/litre, T= 80 °C, f^0_{DVB}= 0.001, [CTA]= 0. (b) Effect of initial crosslinker mole fraction at [BPO]=0.02 mole/litre, [CTA]= 0, and T= 80 °C.

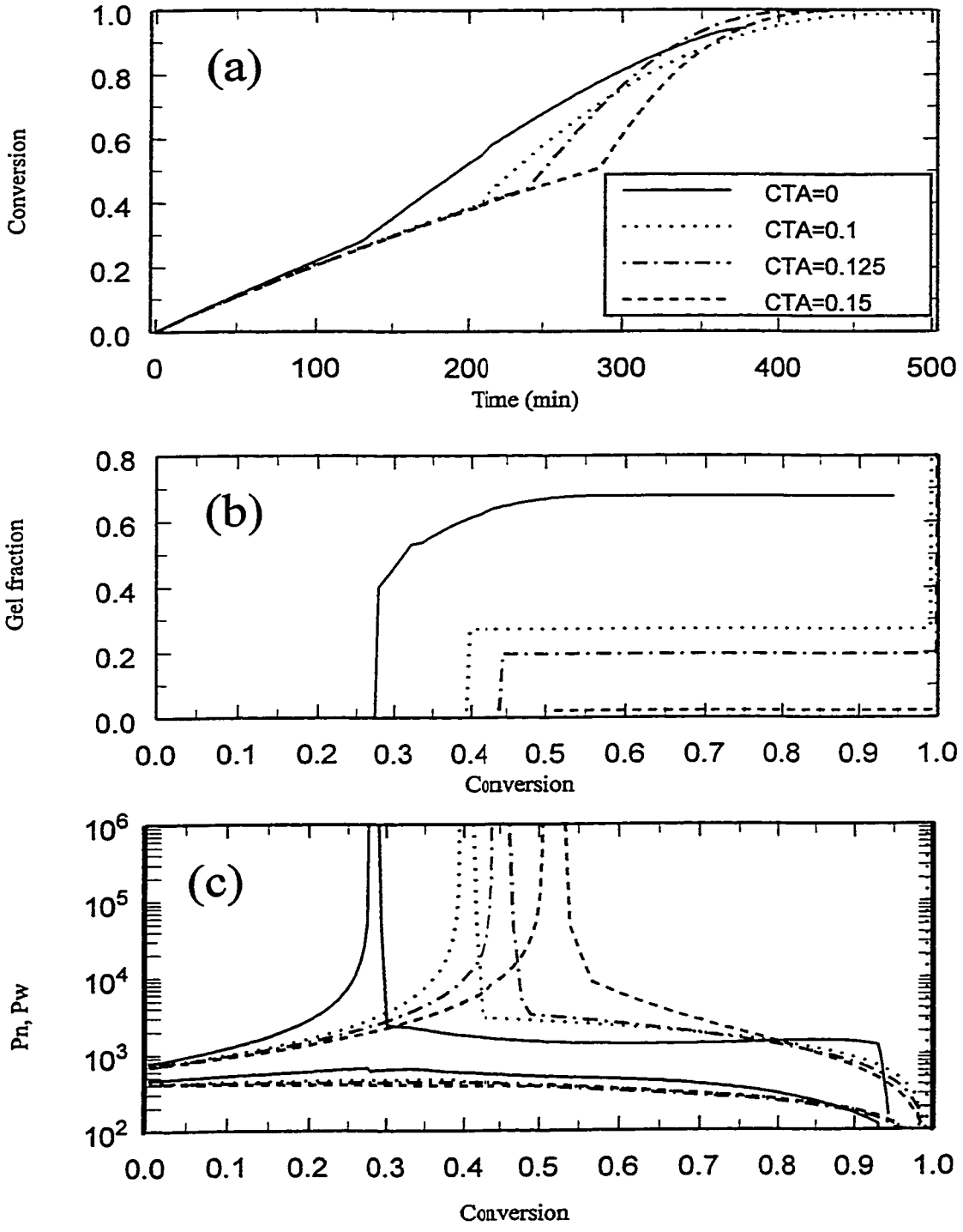

Figure 3.2 Effect of chain transfer agent (CTA), CCl_4, on copolymerization kinetics at T= 80 °C, [BPO]= 0.02 mole/litre, and f°_{DVB}= 0.001. Concentrations of CTA in mole/litre. (a) Conversion versus time. (b) Gel-fraction versus conversion. (c) Chain length versus conversion.

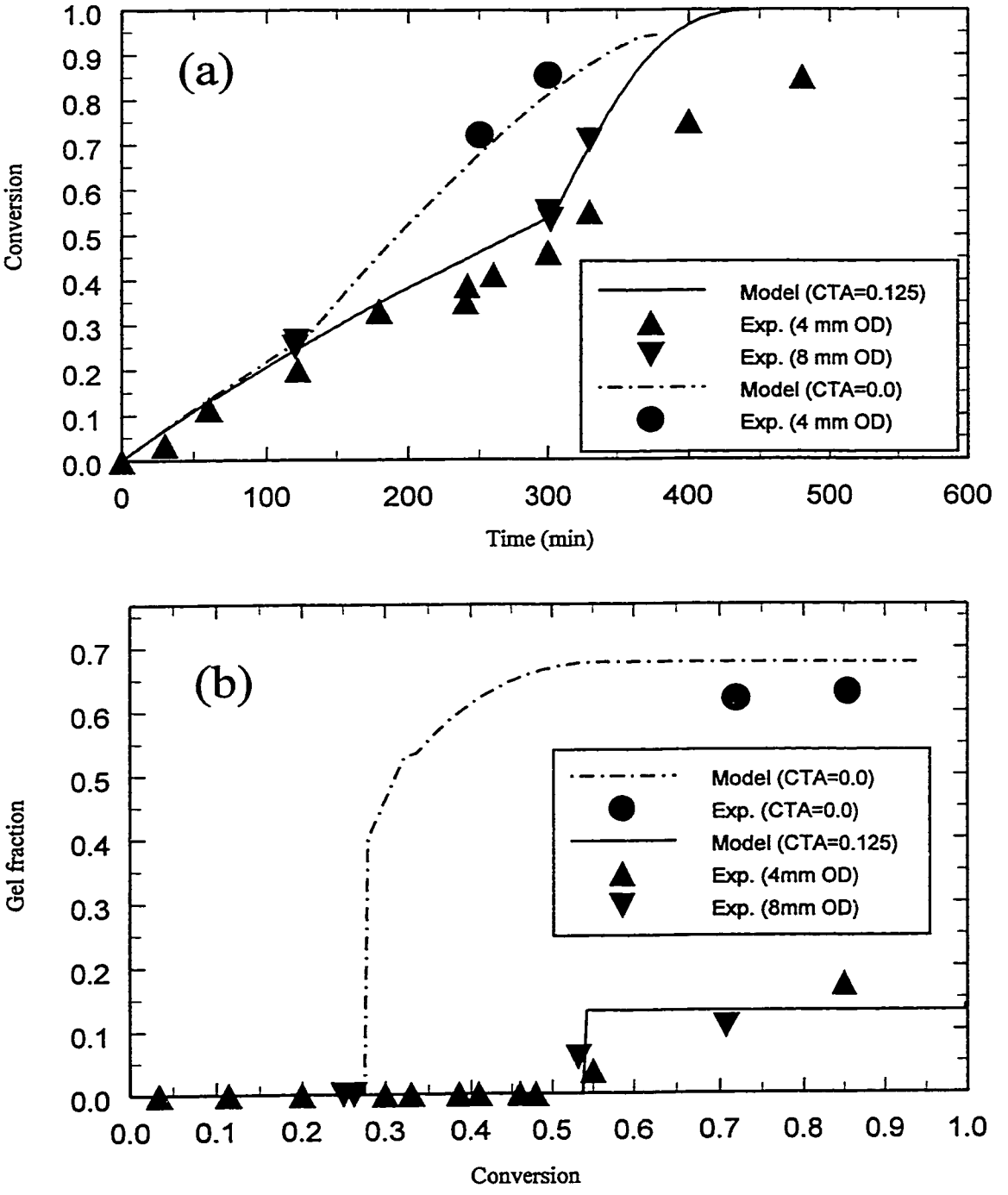

Figure 3.3 Characterization of copolymer synthesized at designed conditions: [BPO]= 0.02 mole/litre, T= 80 °C, and f^0_{DVB}= 0.001. (a) Conversion versus time. (b) Gel fraction versus conversion.

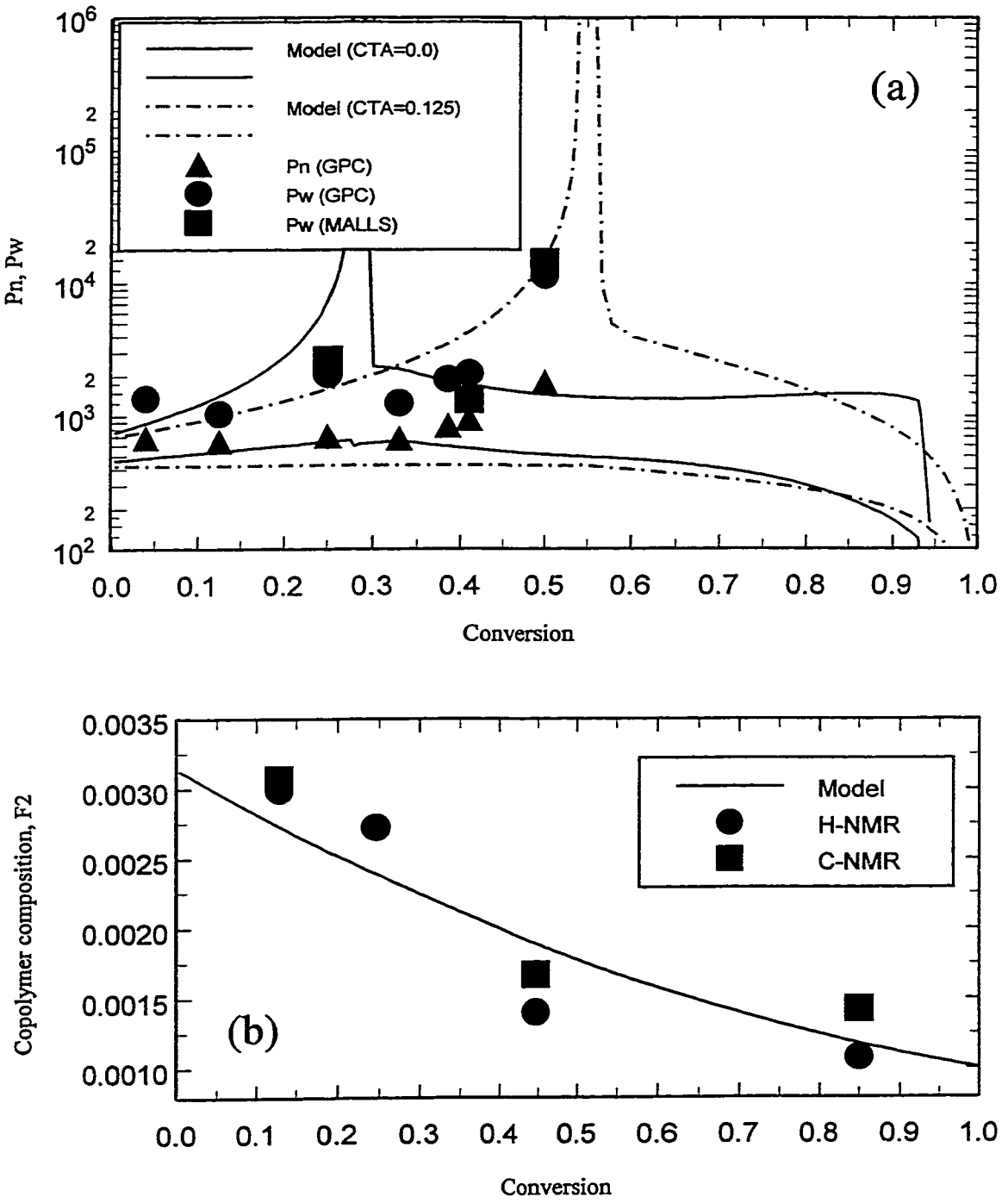

Figure 3.4 Characterization of copolymer synthesized at designed conditions: [BPO]= 0.02 mole/litre, T= 80 °C, and f^{o}_{DVB}= 0.001. (a) Average chain lengths versus conversion. (b) Copolymer composition (F_2) versus conversion.

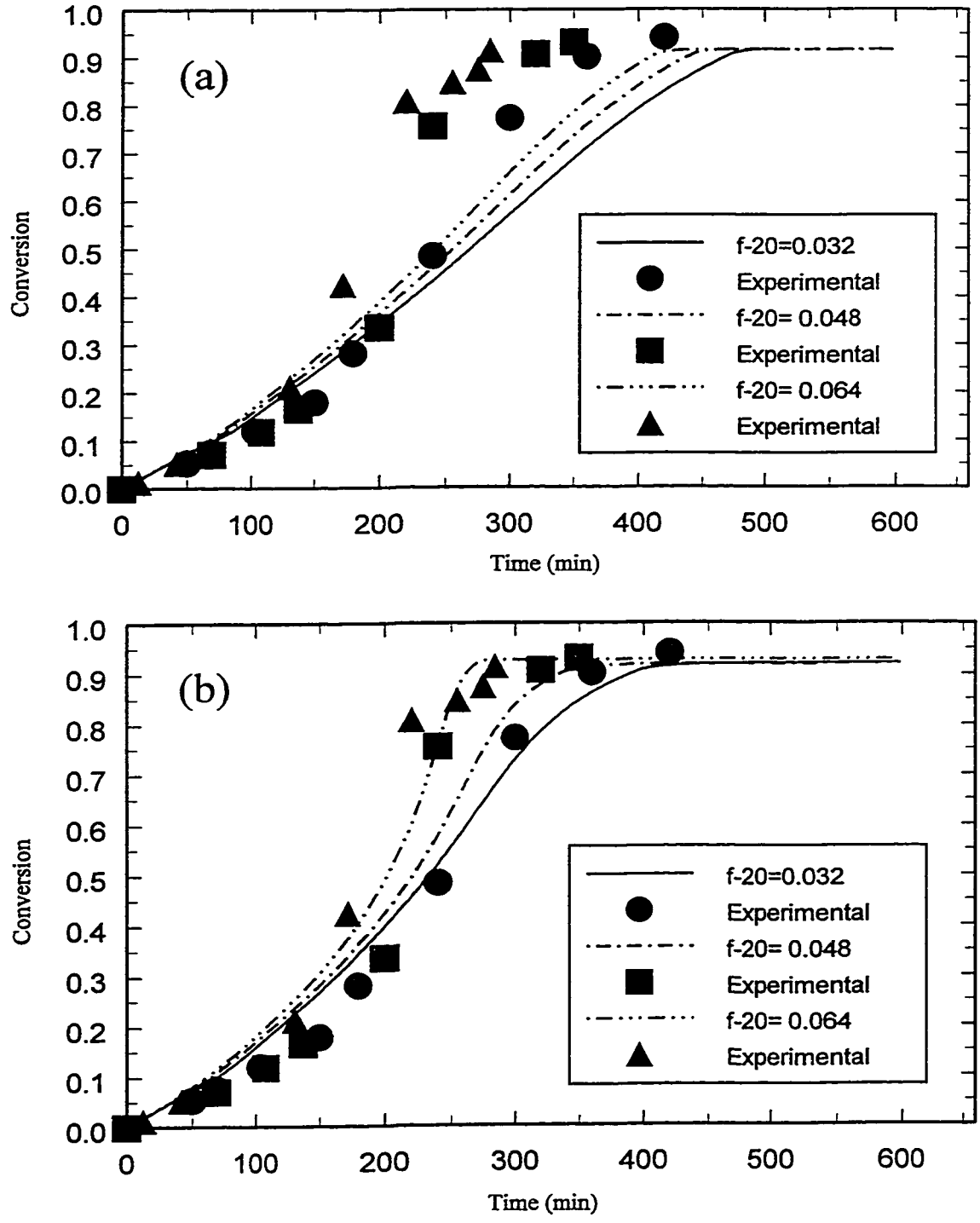

Figure 3.5 Conversion versus time profiles for the copolymerization of styrene and divinylbenzene at conditions (and experimental data) from Sajjadi et al. (1996). [BPO]= 0.036 mol/L, T=70°C. (a) Isothermal modelling. (b) Non-isothermal modelling (see text).

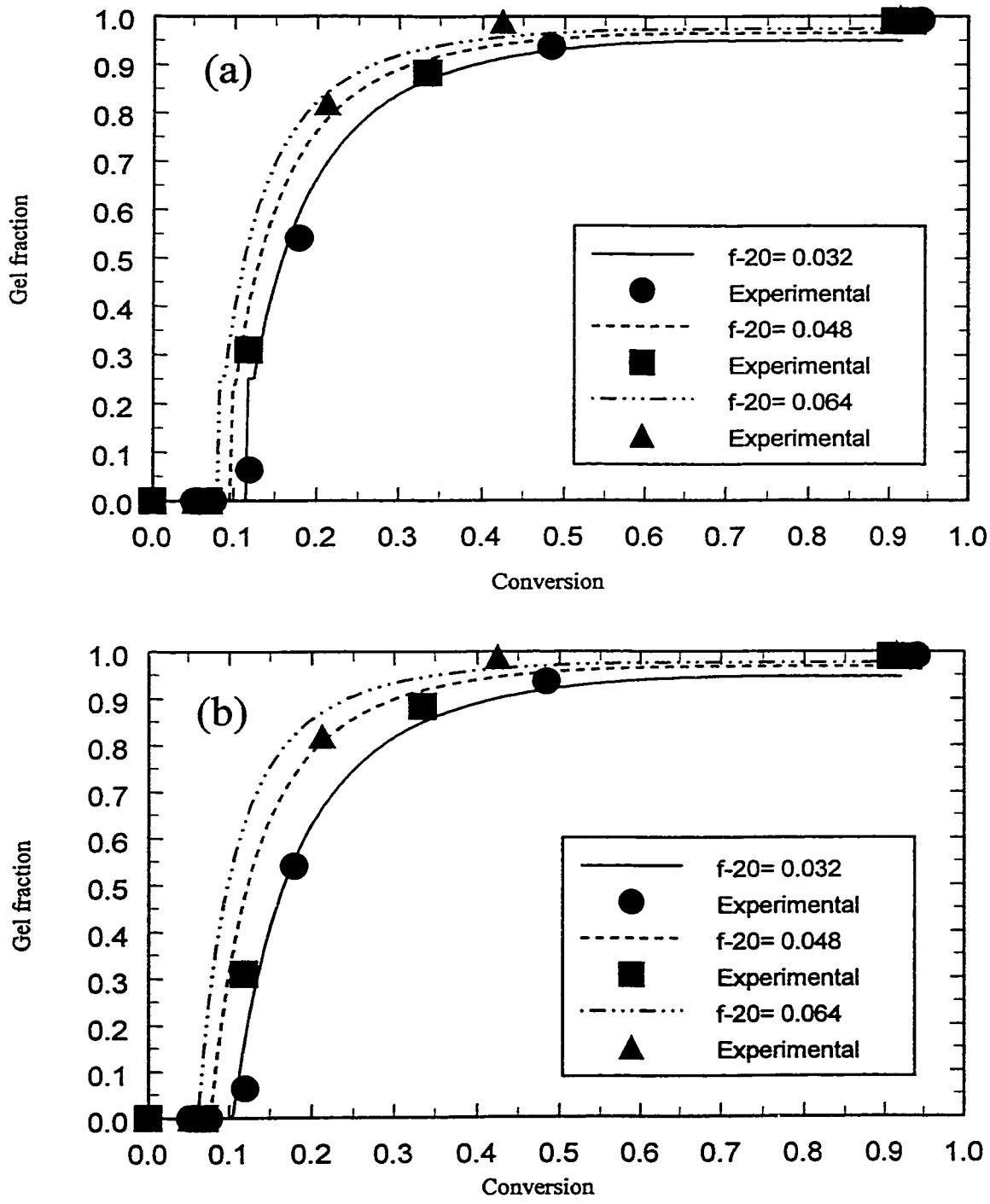

Figure 3.6 Gel fraction versus conversion profiles for the copolymerization of styrene and divinylbenzene at conditions (and experimental data) from Sajjadi et al. (1996). [BPO]= 0.036 mol/L, T= 70 °C. (a) Isothermal modelling. (b) Non-isothermal modelling (see text).

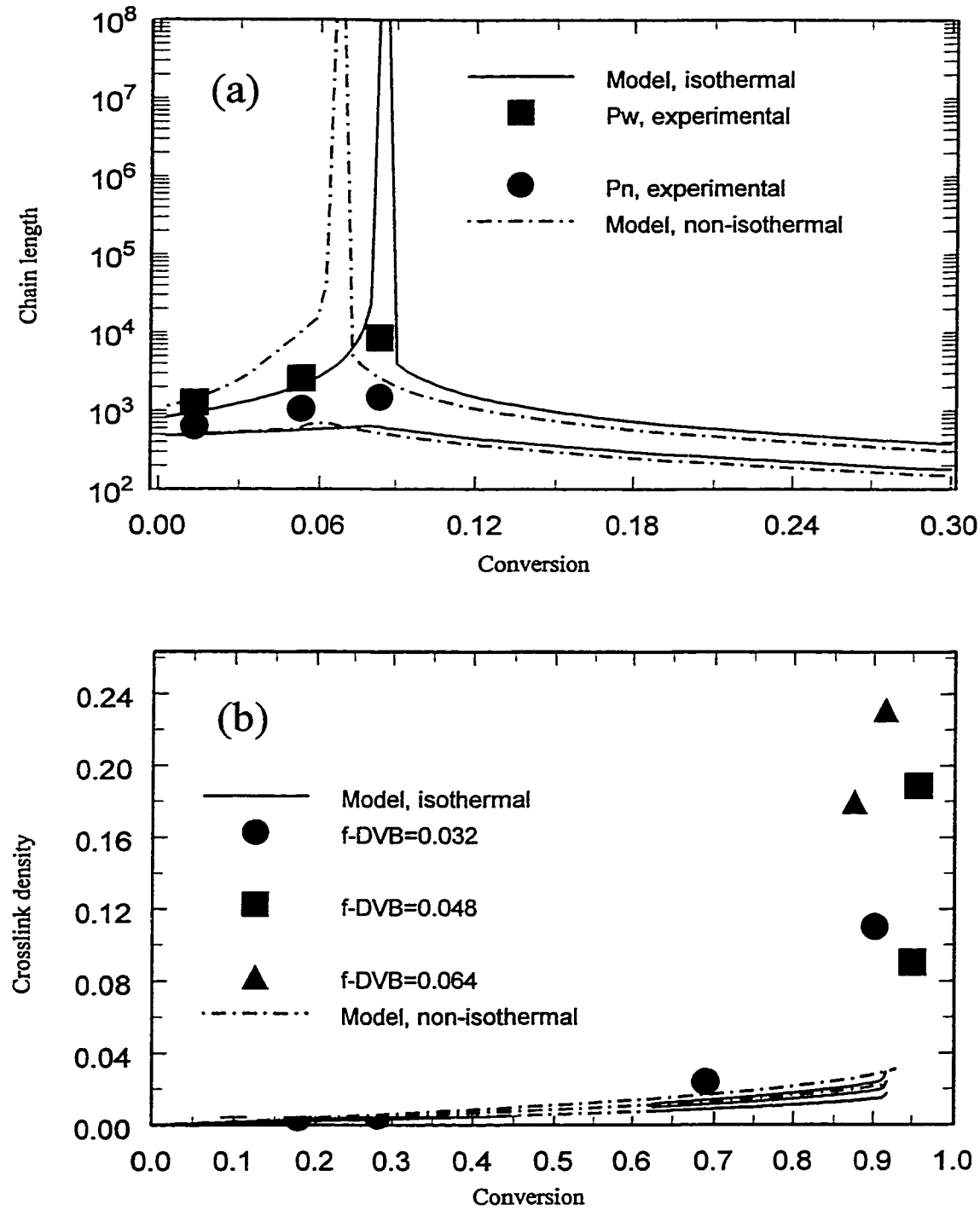

Figure 3.7 Copolymerization of styrene and divinylbenzene at conditions (and experimental data) from Sajjadi et al. (1996). [BPO]= 0.036 mol/L, T= 70 °C, and f^0_{DVB}= 0.064. (a) Average chain lengths versus conversion. (b) Crosslink density versus conversion.

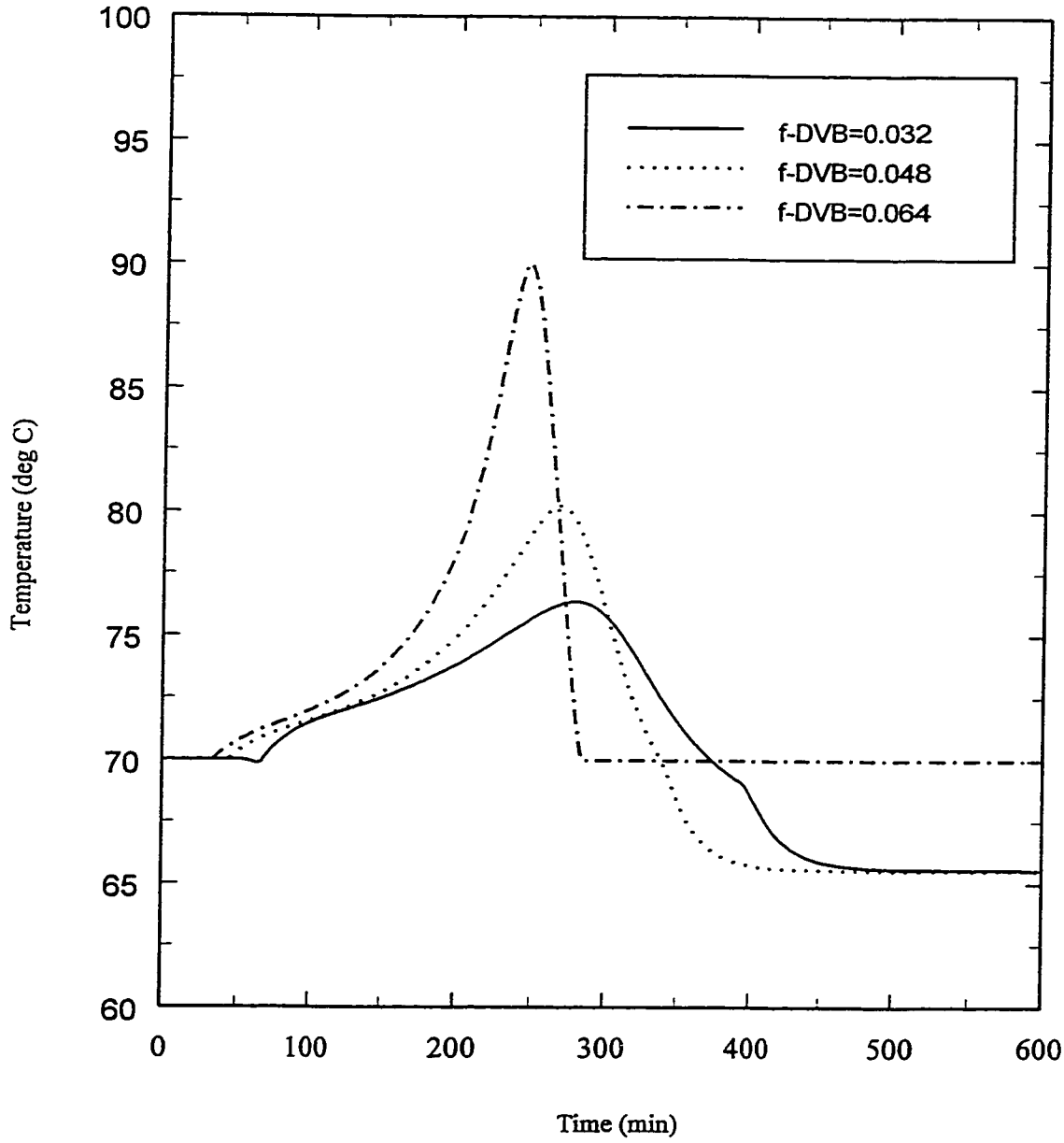

Figure 3.8 Temperature variation (from non-isothermal model) in the copolymerization of styrene and divinylbenzene at conditions from Sajjadi et al. (1996). [BPO]= 0.036 mol/L, and T= 70°C.

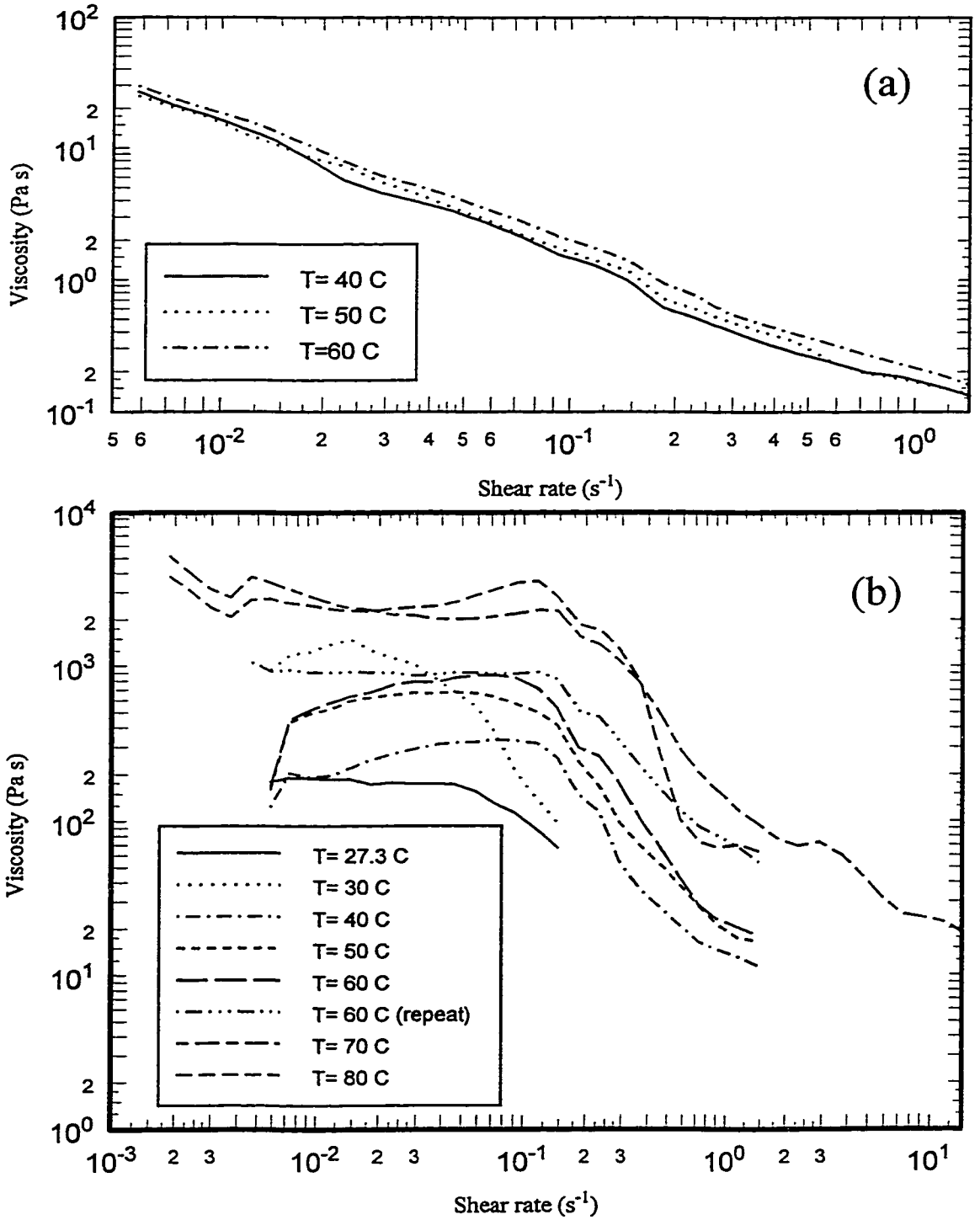

Figure 3.9 Rheological characterization (viscosity versus shear rate measured in a Bohlin rheometer) of mixtures of styrene and poly(styrene/divinylbenzene) (synthesized at different conversions of a copolymerization under the designed conditions). (a) Conversion= 0.25, coaxial cylinder configuration. (b) Conversion= 0.5, cone and plate configuration.

Chapter 4

Calculation of the Particle Size Distribution in Suspension Polymerization using a Compartment-Mixing Model[1]

Eduardo Vivaldo-Lima[†], Philip E. Wood[†*], Archie E. Hamielec[†], and Alexander Penlidis[‡]
[†] McMaster Institute for Polymer Production Technology, Department of Chemical Engineering, McMaster University, Hamilton, Ontario, Canada, L8S 4L7.
[‡] Institute for Polymer Research, Department of Chemical Engineering, University of Waterloo, Waterloo, Ontario, Canada, N2L 3G1.

Abstract

A modelling strategy for effective estimation of the particle size distribution (PSD) in suspension polymerization is presented. The strategy consists of coupling a population balance equation (PBE) and a compartment-mixing (CM) model to account for the non-homogeneous mixing in the tank reactor. The values for the rate of energy dissipation of each compartment are estimated from Computational Fluid Dynamics (CFD) calculations and experimental reports on systems with the same agitator and geometric characteristics. Model predictions using the CM model are compared with predictions that assume homogeneous mixing and experimental data on PSD from styrene and divinylbenzene pilot-plant suspension polymerization reactors of 1 and 5 litres with Rushton and PBT impellers.

Keywords: Particle size distribution, suspension polymerization, non-homogeneous mixing, polystyrene-divinylbenzene, crosslinking.

4.1 Introduction

Suspension polymerization is an old and relatively simple process to produce polymers and copolymers for insulation and chromatographic applications, among others. In the past, this process was used to produce commodity homopolymers (such as polystyrene), but nowadays it is mainly used to produce copolymers of high added value (specialty copolymers) and low volume demand. Controlling the particle size distribution of the polymer is one of the main issues for the manufacturing industries that use this process. Even though the process has been widely studied for more than five decades, our understanding of the factors that affect the PSD and the several physical phenomena that occur inside the vessel is still limited. A review on this process that summarizes the most recent contributions for modelling purposes was presented recently by our group (Vivaldo-Lima et al., 1997).

---

[1]Reprinted with permission from *Can. J. Chem. Eng.*, **76**, 495-505, 1998.

At present, there are sound models for prediction of the PSD in suspension polymerization that take into consideration important effects such as the high viscosity of the monomer/polymer mixture and viscoelasticity of the droplets (e.g., Alvarez et al., 1991, 1994), or the satellite daughter droplet breakage mechanism for bimodal distributions used by Chatzi and Kiparissides (1992, 1995). However, because of the kinetic and viscoelastic models used by Alvarez et al. (1994), both of which are qualitatively adequate but quantitatively uncertain as explained in Vivaldo-Lima et al. (1997), and the assumption of homogeneous mixing in the tank reactor (assumption made in most suspension polymerization models reported in the literature), the predictions obtained using these models are expected to be uncertain if used for actual applications. On the other hand, the modelling of mixing in stirred tanks has reached a very mature state in the last decade (reviewed in Vivaldo-Lima et al., 1997). The ultimate goal of our group in dealing with suspension polymerization is to develop an effective model for PSD. To be effective the model has to be sound, yet reasonably simple to solve with average computing resources, and the predictions should be reliable. Validation with experimental data and a test for extrapolated performance are required to assure reliability. This paper constitutes a step forward towards the achievement of that goal.

The models for breakage and coalescence used in this paper were proposed by Valadez (1988), who used a power law viscosity model. They can be considered as a first approximation to realistic polymerization behaviour. Also, a preliminary approach to the actual behaviour of the polymerizing system is the assumption of a quasi-steady state condition for the PSD. These simplifications, which make these aspects of the model less rigorous than the model of Alvarez et al. (1994) but more powerful than most other empirical and semi-empirical models, were used in order to focus on the implementation of a compartment-mixing model, without losing much on the other phenomena that occur during the polymerization. In future publications these limitations will be removed to create a model of reasonable complexity and better performance (for quantitative applications) than those presently available.

4.2 Modelling

4.2.1 Description

Most mathematical models for calculation of the PSD in suspension polymerization are either semi-empirical (based on dimensionless correlations) or make use of a population balance equation where mixing is assumed to be homogeneous. As suggested and supported in our review (Vivaldo-Lima et al., 1997), this homogeneous mixing approach is clearly unrealistic. A more rigorous way to approach the problem would be to couple the equations of motion in three dimensions with a space dependent population balance equation. Although feasible in principle, this approach would lead to a system of equations very difficult and computationally intensive to solve. To avoid deriving and solving a model of such characteristics, without failing to recognize the importance of non-homogeneous mixing in the tank reactor, an intermediate approach is proposed and used in this paper. The approach consists of dividing the vessel into two or more homogeneous regions, but different in intensity of mixing (regions with different values of rate of energy dissipation). Each region is assumed to be represented by a continuous stirred tank reactor (CSTR) with input and output streams that feed into or are fed by other zones.

Because of the operational problems associated with the transport of highly viscous droplets in suspension, there are basically no commercial continuous suspension polymerization processes in operation. Therefore, our analysis will focus on modelling a batch tank reactor. The different regions in the batch reactor will be modelled as CSTRs connected among themselves. A simplified schematic representation of suspension polymerization in a batch reactor is shown in Figure 4.1.

The calculations reported in this paper were obtained using a two-zone mixing model (two-compartment model). A schematic representation of this model is shown in Figure 4.2. The small tank reactor of volume V_i represents the mixing zone surrounding the impeller (impeller region), whereas the other tank reactor of volume V_b represents the mixing zone for the remaining of the tank (bulk region). The PSD for the "impeller" region, F_i (or f_i if the PSD function is normalized), is characterized by a high intensity of mixing (high rate of energy dissipation), whereas the PSD of the

bulk zone, F_2 (or f_2), is characterized by a lower intensity of mixing (lower rate of energy dissipation).

Figure 4.3 shows two different representations for a three-zone mixing model. In this case V_i is again the volume of the impeller region, V_b is the volume of the bulk region (excluding the baffles zone), and V_3 is the volume of the zone surrounding the baffles. In case (A) it is assumed that the flow goes from the impeller region to the bulk region and then back to the impeller region. In case (B) the flow goes from the impeller to the bulk region, but it is then divided in two streams. One stream goes back to the impeller region, and the other to the baffles region. The flow from the baffles zone in (B) goes to the bulk zone and not to the impeller region, as in case (A).

4.2.2 Model Equations

4.2.2.1 Homogeneous mixing situation

For a population uniformly distributed in physical space of constant volume, V_t, the population balance equation (PBE) that describes the PSD in a (continuous) stirred tank reactor is given by equation (1) (Ramkrishna, 1985).

$$\frac{\partial F}{\partial t} + \frac{\partial}{\partial v}\left(\frac{\partial v}{\partial t}F\right) - \frac{Q}{V_t}(F - F_{in}) = B - D \qquad (1)$$

In order to simplify the numerical calculations, the following assumptions were made:

(a) Quasi-steady-state assumption (QSSA) for the PSD. This means that the dynamics of the PSD evolution are considered to be much faster than the dynamics of reaction. Under these circumstances, the breakage and coalescence terms are at equilibrium during any change in the reaction conditions. This can be considered valid at low conversion levels, before the increase in polymerization rate due to the "auto-acceleration effect" takes place, or after the particle identity point is reached (when the PSD gets "frozen").

(b) Droplet volume contraction is negligible.

(c) The PBE to be solved numerically is expressed in terms of a normalized PSD density

distribution function, f.

(d) The birth and death terms (right hand side of equation (1)) are modelled using the Valadez (1988) models for breakage and coalescence of increasingly viscous drops.

Therefore, the equation used in this paper to obtain the PSD in the homogeneous mixing case was equation (2), shown below.

$$\int_{u}^{\infty} g(v)\,\zeta(v)\,\beta(u,v)\,f(v)\,dv + N\int_{0}^{\frac{u}{2}} h(u-v,v)\,f(u-v)\,f(v)\,dv - Nf(u)\int_{0}^{\infty} h(u,v)f(v)dv - g(u)f(u) = 0 \qquad (2)$$

4.2.2.2 Two-zone (compartment) model

Assume that our batch stirred tank reactor of Figure 4.1 can be modelled as a series of two CSTRs, as shown in Figure 4.2 (three or more CSTRs can be used to obtain a multi-zone compartment model, as shown in Figure 4.3). Writing down the PBE for each CSTR of Figure 4.2 and a conservation of mass equation for that configuration, equations (3) to (5) are obtained.

$$\frac{\partial F_1}{\partial t} + \frac{\partial}{\partial v}\left(\frac{\partial v}{\partial t}F_1\right) - \frac{Q_i}{V_i}(F_1 - F_2) = B_1 - D_1 \qquad (3)$$

$$\frac{\partial F_2}{\partial t} + \frac{\partial}{\partial v}\left(\frac{\partial v}{\partial t}F_2\right) - \frac{Q_b}{V_b}(F_2 - F_1) = B_2 - D_2 \qquad (4)$$

$$F_3 = \frac{V_i}{V_t}F_1 + \frac{V_b}{V_t}F_2 \qquad (5)$$

where:

$$V_t = V_i + V_b \qquad (6)$$

$$F_1 = \frac{N_1}{V_i} \quad , \qquad F_2 = \frac{N_2}{V_b} \qquad (7)$$

The density distribution functions (normalized PSD) for each zone are given by equations (8) and (9). The overall density distribution function, f_3, is given by equation (10).

$$f_1(x,t) = \frac{F_1(x,t)}{\int_0^\infty F_1(x,t)dx} = \frac{F_1(x,t)}{N_1(t)} \tag{8}$$

$$f_2(x,t) = \frac{F_2(x,t)}{\int_0^\infty F_2(x,t)dx} = \frac{F_2(x,t)}{N_2(t)} \tag{9}$$

$$f_3 = \frac{N_1\frac{V_i}{V_t}f_1 + N_2\frac{V_b}{V_t}f_2}{N_1 + N_2} \tag{10}$$

Using again assumptions (a) through (d), the equations that describe the PSD in the two-zone model are given by equations (11), (12), and (10). These equations constitute an approximation to the actual situation. Using assumption (a) (QSSA) makes it possible to transform an integro-differential equation into an integral equation, which is much easier to solve. It also makes it possible to decouple the ordinary differential equations (ODEs) that describe the (co)-polymerization kinetics from the PBE. The ODEs that describe the copolymerization kinetics are listed in Table 4.1. The details about their derivation, limitations, and the definition of variables and parameters not shown in this paper are explained in Vivaldo-Lima et al. (1994). In order to follow the particle size evolution in time it is only required to know the viscosity of the dispersed phase and the monomer conversion at different times, and then solve equations (10) to (12) for each case. The viscosity of the dispersed phase can be estimated at any time from independent simulations of the kinetic behaviour of the polymerization system, provided that a correlation between viscosity and molecular weight is available.

Table 4.1 Free-radical copolymerization kinetics of vinyl/divinyl monomers.

Initiation	$\frac{d(V[I])}{Vdt} = -k_d[I]$
Overall conversion	$\frac{dx}{dt} = (k_p + k_{fm})(1-x)[R^\bullet]$
Moment equations for polymer radicals	$\frac{d(VY_0)}{Vdt} = 2fk_d[I] - (\bar{k}_{tcn} + \bar{k}_{td})Y_0^2$ $\frac{d(VY_1)}{Vdt} = 2fk_d[I] + (k_{fm}[M] + k_{fT}[T]) + k_p^\bullet Y_0 Q_2 + k_p[M]Y_0$ $-\{k_{fm}[M] + k_{fT}[T] + (\bar{k}_{tcn} + \bar{k}_{td})Y_0 + k_{fp}([Y_1 + Q_1] - Y_1)\}Y_1$
Moment equations for total polymer concentration	$\frac{d(V[Y_0 + Q_0])}{Vdt} = 2fk_d[I] + (k_{fm}[M] + k_{fT}[T])Y_0 - k_p^\bullet Y_0([Y_1 + Q_1] - Y_1) - \frac{1}{2}\bar{k}_{tcn}Y_0^2$ $\frac{d(V[Y_1 + Q_1])}{Vdt} = 2fk_d[I] + (k_{fm}[M] + k_{fT}[T])Y_0 + k_p[M]Y_0$ $\frac{d(V[Y_2 + Q_2])}{Vdt} = 2fk_d[I] + (k_{fm}[M] + k_{fT}[T])Y_0 + k_p[M]Y_0 + 2k_p[M]Y_1$ $+2k_p^\bullet Y_1[Y_2 + Q_2] + \bar{k}_{tcw}Y_1^2$
Divinyl monomer consumption	$\frac{df_2}{dt} = \frac{f_2 - F_2}{1-x}$
Accumulated copolymer composition	$\overline{F_2} = \frac{f_{20} - f_2(1-x)}{x}$
Crosslink density	$\frac{d[x\bar{\rho}(x)]}{dt} = \frac{k_p^{\bullet 0}[2\overline{F_2}(x)(1-k_{cp}) - \bar{\rho}(x)(1+k_{cp})]x}{k_p(1-x)}\frac{dx}{dt}$
Transfer to small molecule	$\frac{d(V[T]_i)}{Vdt} = -k_{fTi}[T_i][R^\bullet]$
Temperature	$\frac{dT}{dt} = \frac{(-\Delta H)_r R_p}{n_m Cp_m} - \frac{n_w Cp_w}{n_m Cp_m}\frac{dT_w}{dt} - \frac{UA}{n_m Cp_m}(T - T_w)$

$$\frac{Q_1}{V_i}(N_1 f_1 - N_2 f_2) + N_1 \int_u^{\infty} g_1(v)\zeta_1(v)\beta_1(u,v) f_1(v)dv + N_1^2 \int_0^{\frac{u}{2}} h_1(u-v,v) f_1(u-v) f_1(v)dv$$
$$- N_1^2 f_1(u) \int_0^{\infty} h_1(u,v) f_1(v)dv - N_1 g_1(u) f_1(u) = 0 \qquad (11)$$

$$\frac{Q_2}{V_b}(N_2 f_2 - N_1 f_1) + N_2 \int_u^{\infty} g_2(v)\zeta_2(v)\beta_2(u,v) f_2(v)dv + N_2^2 \int_0^{\frac{u}{2}} h_2(u-v,v) f_2(u-v) f_2(v)dv$$
$$- N_2^2 f_2(u) \int_0^{\infty} h_2(u,v) f_2(v)dv - N_2 g_2(u) f_2(u) = 0 \qquad (12)$$

Assuming that the phase holdup (ratio of volume of water to volume of monomer) remains constant in all the compartments, the number of droplets in each compartment, N_1 and N_2, are given by equation (13). It was also assumed that the volumetric flow for each compartment was the same, and given by equation (14).

$$N_1 = \frac{\phi V_i}{\int_0^{\infty} v f_1(v)dv} \quad , \quad N_2 = \frac{\phi V_b}{\int_0^{\infty} v f_2(v)dv} \qquad (13)$$

$$Q_1 = Q_2 = Q = N_Q M D_{imp}^3 \qquad (14)$$

4.2.2.3 Breakage and Coalescence

Very few models for breakage and coalescence of droplets in liquid-liquid dispersions take into consideration the effects of increasing viscosity and elasticity inherent to a polymerization system. As mentioned in Vivaldo-Lima et al. (1997), one such model is that proposed by Alvarez et al. (1994),

where these characteristics of the fluid behaviour are modelled with a Maxwell model for viscoelasticity. However, the Maxwell model, although illustrative of polymer behaviour and widely used in the rheology area for testing of numerical procedures (due to its simplicity when compared with other models) is known to be a poor model for quantitative prediction of actual polymer behaviour (Vlachopoulos, 1994). A previous model from the group of Alvarez (Valadez, 1988), which considered the effect of viscosity with a power-law model, was used in the calculations presented in this paper. The derivation of the Valadez model is presented elsewhere (Valadez, 1988; Vivaldo-Lima, 1989). Equations (15) to (19) show the final expressions of the model, as used in our solution to the PBE, for the homogeneous mixing situation.

$$g[u(y)] = C_1 \left[\frac{D}{y}\right]^{\frac{2}{3}} \frac{M}{1+\phi} \exp\left\{-(1+\phi)^2 \left[C_2 \left(\frac{D}{y}\right)^{\frac{5}{3}} \frac{1}{We} + C_3 \left(\frac{D}{y}\right)^{\frac{2}{3}} \frac{1}{Re} + C_4 \left(\frac{D}{y}\right)^{\frac{4}{3}} \frac{1}{(1+\phi)} \frac{\sqrt{\frac{\rho_c}{\rho_d}}}{Re_d} + C_5 \frac{1}{(1+\phi)} \left(\frac{D}{y}\right)^{\frac{4}{3}} \frac{1}{Re_d}\right]\right\} \tag{15}$$

$$h(y,z) = C_6 (y^2+z^2) \sqrt{y^{\frac{2}{3}}+z^{\frac{2}{3}}} \frac{MD^{\frac{2}{3}}}{1+\phi} exp\left[-C_9 \frac{(z^3+y^3)^2}{(yz)^3 (y+z)^{\frac{2}{3}}} \frac{\rho_c}{\rho_d} \frac{(1+\phi)^2 D^{\frac{2}{3}}}{Re} - C_{10} \frac{(y^2+z^2)(y^3+z^3)}{(yz)^3 (y+z)^{\frac{2}{3}}} \frac{\rho_c}{\rho_d} \frac{(1+\phi)^2 D^{\frac{5}{3}}}{We}\right] exp\left[-Max(C_7\tau_1, C_8\tau_2)\right] \tag{16}$$

where:

$$\tau_1 = \left[\frac{4N_p D^3}{\pi H T^2}\right]^{\frac{4}{3}} \frac{\eta_c \rho_c M^3 D^2}{\sigma^2} \frac{(yz)^4}{(y+z)^4} \tag{17}$$

$$\tau_2 = 8\left[\frac{4N_p D^3}{\pi H T^2}\right]^{\frac{2}{3}} \frac{(1+\phi)^2 D^{\frac{4}{3}}}{Re_d} \frac{yz}{(y+z)^{\frac{10}{3}}} \tag{18}$$

$$Re = \frac{\rho_c M^2 D^2}{\tau_0} \quad , \quad Re_d = \frac{\rho_c M D^2}{\eta_d} \quad , \quad We = \frac{\rho_c M^2 D^3}{\sigma} \tag{19}$$

Equations (15) and (16) describe the breakage and coalescence rate distributions, g and h, respectively. As explained in Vivaldo-Lima et al. (1997), the structure of equation (15) is given by the product of a collision frequency and two types of breakage efficiencies (contained in the exponential term). Likewise, equation (16) is given by the product of a coalescence frequency and three types of coalescence efficiencies (deformation, film drainage and time for deformation efficiencies).

In the models of Valadez (1988) the rate of energy dissipation, ϵ, is given by equation (20). In our compartment model we use the same expression for each compartment, but the constant k in equation (20) is different for each compartment. The ratio of rate of energy dissipation at the impeller zone to the rate of energy dissipation at the bulk zone, represented by "a" and given by equation (21), can be estimated from experimental measurements or CFD calculations of the distribution of rate of energy dissipation inside the tank reactor. The ratio of volume of the impeller zone to the volume of the bulk zone can also be estimated from such sources, as explained in the "Results and Discussion" section.

$$\epsilon = kM^3 D^2 \tag{20}$$

$$a = \frac{\epsilon_{impeller}}{\epsilon_{bulk}} \quad , \quad a' = \frac{\epsilon_{average}}{\epsilon_{bulk}} \tag{21}$$

Since the rate of energy dissipation in equations (15) and (16) is expressed in terms of equation (20) (constant k is contained in constants C_1 to C_{10}), there should be a correction made depending on the zone under consideration. If constants C_1 to C_{10} are known from parameter estimation using the homogeneous mixing model (based on $\epsilon_{average}$), the difference for the rate of energy dissipation for each zone can be made by adequate calculation of sets of parameters for each zone from parameters known (or estimated) in one region. For the models of Valadez that relationship is given by equations (22) and (23) (the derivation of these equations is a simple algebraic exercise not shown in this paper).

$$\begin{aligned} C_{\alpha,imp} &= a^{\frac{1}{3}} C_{\alpha,bulk} \quad , \quad \alpha=1, 5, 6, 7 \\ C_{\beta,imp} &= a^{-\frac{2}{3}} C_{\beta,bulk} \quad , \quad \beta=2, 3, 4, 8, 9, 10 \end{aligned} \tag{22}$$

$$\begin{aligned} C_{\alpha,bulk} &= (a')^{-\frac{1}{3}} C_{\alpha,average} \quad , \quad \alpha=1, 5, 6, 7 \\ C_{\beta,bulk} &= (a')^{\frac{2}{3}} C_{\beta,average} \quad , \quad \beta=2, 3, 4, 8, 9, 10 \end{aligned} \tag{23}$$

4.2.2.4 Solution Procedure

To solve the PBE under QSSA a set of N non-linear algebraic equations for the homogeneous model and 2N non-linear algebraic equations for the two-zone model, (where N is the number of collocation points) a collocation with the cubic splines technique was used. Two types of meshes were used to solve the equations, evenly and unevenly spaced. Best results were obtained with the unevenly distributed mesh (collocation points concentrated on the small droplet size range of the distribution), and 30 (26 in some cases) collocation points. The PBE was solved using scaled variables in order to reduce numerical problems. The scale factor was chosen based on *a priori* estimate of the mean volume of the PSD. Because of the QSSA, it was not necessary to solve the kinetic equations and the PBE simultaneously, although it was necessary to know the results for conversion and weight average molecular weight (or viscosity) prior to solving the PBE.

The selection of the initial estimates for the density distributions, f_1 and f_2 at each collocation point, was a crucial step. If these estimates were not good enough, convergence would be very difficult or even impossible to achieve. Four types of estimates were used in our calculations: (i) estimation of the PSD for each zone assuming that f_1 and f_2 are given by a Gamma distribution function (mean and variance estimates were required), (ii) same as (i), but assuming normal (instead of Gamma) distribution functions, (iii) providing rough estimates of f_1 and f_2 at each collocation point from experimental PSD measurements, and (iv) providing the output solution from a different case or a non-converged one.

4.3 Results and discussion[2]

To test the implementation of our model and the effect of non-uniform mixing, two different polymerization systems were chosen. The first system was a styrene suspension homopolymerization and the second one a suspension copolymerization of styrene and divinylbenzene. The conditions of polymerization and reactor dimensions are reported in Table 4.2. The experimental data for the homopolymerization system was taken from Sánchez and García (1993). For the copolymerization system we generated our own experimental data.

A tank and agitator configuration very similar to the one used by Sánchez and García (1993) for the homopolymerization system reported in Table 4.2, was studied in detail by Kresta (1991). Based on experimental measurement of the rate of energy dissipation in the tank reactor, which agreed very well with the CFD calculations, Kresta and Wood (1991, 1993) reported profiles of variation of rate of energy dissipation in the radial and axial directions of the tank for both Rushton and pitched blade turbine (PBT) impellers. From these profiles the ratio of rate of energy dissipation at the impeller zone to the rate of energy dissipation at the bulk zone was estimated to be equal to 50. The impeller zone volume was calculated as the volume of a cylinder with diameter 1.45 times larger than

---

[2]The PSDs shown in Figures 4.4 to 4.8 are normalized with respect to particle volume, but plotted against particle diameter. The area under the curve will be one if particle size is represented as volume.

the impeller diameter and with a height equal to the width of the impeller blade (Kresta and Wood, 1991). The ratio of the impeller zone volume to the total volume of the tank was then found to be equal to 0.0353.

Table 4.2 Vessel dimensions and polymerization conditions.

Parameter	Homopolymerization	Copolymerization
Temperature, °C	70	80
Initiator type and concentration, mol/litre	AIBN, 0.05	BPO, 0.02
Divinylbenzene, mole fraction	0	0.001
CTA type and concentration, (mol/litre)	None, 0	CCl_4, 0.125
Stabilizer type and concentration (g/litre-water)	Polyvinyl alcohol (PVA), 0.3	Polyvinyl pyrrolidone, 5
Impeller type	Rushton, 6 blades	Two-impeller 45° pitched blade turbine, 4 blades
Impeller diameter, cm	4.59	9.1
Tank diameter, cm	11.2	15.8
Z/T	1	1.2
W/T	1/10	1/12
Bottom clearance, cm	Not reported	3
Separation between impellers, cm	N/A	8.5
Agitation speed, rps	5	9.717
PSD conditions and technique	PSD at different conversion levels, sample-imaging technique (Sánchez and García, 1993).	PSD at final conversion, Coulter Counter (present paper).
Viscosity, η, Pa·s	0.008 (@ x=0.12), 0.2 (@ x=0.4), 100 (@ x=0.7) (García, 1993).	Taken as 1000, but not measured at final conversion.
Interfacial tension, σ, g/s^2	18.875 (Valadez, 1988)	4.5

Table 4.3 Values for model parameters.

Parameter	Value	Reference or comments
$C_{1,average}$	0.035	Valadez (1988), order of magnitude analysis (OMA)
$C_{2,average}$	0.0625	Valadez (1988), OMA
$C_{3,average}$	10^{-5}	Valadez (1988), OMA
$C_{4,average}$	$6.0x10^{-7}$	OMA
$C_{5,average}$	$6.0x10^{-7}$	OMA
$C_{6,average}$	10^{-6} (all cases, homogeneous mixing model) 10.4195, 0.10249, 0.0484 (@ x=0.7, 0.4, 0.12, two-zone model, homopolymerization) 3.0 (two-zone model, copolymerization)	Present study (dependent on dispersed phase viscosity)
$C_{7,average}$	10^{8}	Valadez (1988), OMA
$C_{8,average}$	$6.0x10^{-7}$	OMA
$C_{9,average}$	10^{-7}	Valadez (1988), OMA
$C_{10,average}$	0	Valadez (1988)
a	50	See text
a′	5 (33 if calculated as the ratio of ϵ_{imp} to ϵ_{av}, with $\epsilon_{av}=N_p V_t M^3/D$)	Sensitivity analysis
N_p	5 (Rushton impeller) 1.4 (PBT impeller)	Kresta (1991) Zhou and Kresta (1996)
N_Q	0.745 (Rushton impeller) 0.776 (PBT impeller)	Kresta (1991)
V_{imp}/V_t	0.0353 (for tank reactor used in the homopolymerization) 0.06-0.2 (for tank reactor used in the copolymerization)	See text
τ_0, $g \cdot s^{-2} \cdot cm^{-1}$	5	Valadez (1988)

Parameter sensitivity analyses for the copolymerization system showed that the values of a and a′ used for the Rushton impeller (homopolymerization system) were equally good for the two-PBT impeller (copolymerization system). These values and the parameters of the Valadez model used in our calculations are summarized in Table 4.3.

Before proceeding with the comparison of simulation results and experimental data, it is important to make some comments about the reliability of the experimental data used in this paper. The range of particle sizes obtained in conventional suspension polymerization applications is very broad, typically from a fraction of a micron (fine particles, latex portion) up to 1 or 2 mm. Therefore, few experimental techniques are capable of adequately capturing the whole PSD. Perhaps only laser light scattering instruments can successfully achieve this goal (e.g., Hildebrand and Row, 1995; Vivaldo-Lima et al., 1997). Another problem with samples of very broad PSD is that of getting a representative sample. This means that repeatability and reproducibility are important issues in the measurement of particle size distributions in suspension polymerization.

The information that we had about the experimental data of Sánchez and García (1993) did not include error analyses, and repeats were not available. The distributions were obtained using an image analysing technique. If one looks at these data (e.g., experimental data on Figures 4.4 to 4.7), the distributions seem bimodal. However, the bimodality is manifested by only one point in the three different experimental conditions shown in these figures (three levels of conversion), and that being the case, it could be argued that the profiles are tri- or tetra-modal. Although we included only three profiles here, they made several more measurements at other conversion levels. In all the eight distributions measured at different times of the polymerization carried out at the conditions reported in Table 4.2, the point that defines the first two peaks of the PSD is always present. The other points that seem to indicate the possibility of other peaks in the PSD do not appear consistently and seem to be due to experimental error. We were therefore inclined to believe that their distributions are bimodal.

The experimental data for the copolymerization system, shown in Figure 4.8, were obtained using a Coulter size counter (electrical sensing method). We run two batches at the same conditions to address the issue of reproducibility, and measured 5 different samples of batch 1, and two of batch 2 to address the issue of repeatability. Although the polymerization and the PSD measurements were carried out carefully, it was found that both types of error are significant, yet acceptable. Our experimental data clearly show a bimodal distribution, although the first peak of the distribution is not complete due to the fact that the aperture of the cell that we used was not able to sense the whole range of the distribution.

It is well known that bimodal distributions in suspension polymerization are frequently obtained when small reactors (pilot-plant scale) are used (e.g., Vivaldo-Lima et al., 1997). It is believed that the bimodality is associated to the non-homogeneous mixing in the tank reactor which causes most of the breakage events to occur in the vicinity of the impeller, and most coalescence events taking place in the low shear regions of the tank. When the system is well stabilized (e.g., latex size particles in a emulsion), the bimodality can be associated to the satellite daughter drop distribution breakage mechanism, as Chatzi and Kiparissides (1992, 1995) have proposed.

Even though the experimental error on the PSD measurements of Sánchez and García (1993) was unknown, the distributions seemed to be bimodal. Our experimental data also produced a bimodal distribution. Since accounting for non-homogeneous mixing was a major component of our model, having experimental data with bimodal behaviour was desirable. We therefore decided to use both sources of data.

Figure 4.4 shows PSD predictions using the two-zone mixing model for the homopolymerization system at 420 minutes (x=0.7, η_d=100 Pa·s). Since convergence was very difficult to achieve, it was decided to study the effect of volume of the impeller zone on the solution. It is observed that the best agreement with experimental data of Sánchez and García (1993) is obtained when the volume calculated with the methodology of Kresta and Wood (1991) is used, thus confirming the utility of having detailed information on the flow field inside the tank. Although the agreement is

good and the model predicts a bimodal distribution, the lower size range of the distribution is not captured sufficiently well. Although the two peaks predicted by the model can be distinguished, they are too close to one another. Given the broad spread of the distribution, more collocation points would be needed to improve the resolution of the distribution in all the size ranges.

A comparison of the predictions between the homogeneous and the two-zone model for the conditions used in Figure 4.4 is shown in Figure 4.5. Also shown in that figure is the experimental PSD reported by Sánchez and García (1993). It is seen that the homogeneous model predicts a unimodal PSD of narrower dispersion than that observed for the experimental data.

The evolution of the PSD with reaction time is presented in Figure 4.6. Experimental data and predictions using the homogeneous mixing model are shown in that figure. It is clearly seen that the predictions are poor at low and intermediate conversions. This may be due to the use of a QSSA in solving the PBE. As previously stated, this assumption may be adequate at low (before the "auto-acceleration effect") or high (after the "identity point") conversion levels, but it may be inappropriate at intermediate conversion levels. Recall that the identity point occurs when the distribution stops changing due to an equilibrium between breakage and coalescence of droplets.

Figure 4.7 shows the same profile, but using predictions obtained with the two zone model. It is clearly seen that the two-zone model produces bimodal distributions for the three cases presented in the figure, which agrees with the experimental data. The resolution in the first peak of the distributions at 0.008 and 0.2 Pa·s is rather poor. This may be caused by the fact of not having enough collocation points at the very low region of the distribution, as pointed out in our analysis for Figure 4.4.

Figure 4.8 shows a comparison of predictions of the final PSD for the copolymerization system using the two-zone model, and experimental data. It is observed that the experimental error is rather large, particularly for the second peak of the (bimodal) distribution. The first successful attempt to model this system produced a bimodal distribution with a mean diameter close to the experimental one (solid line in Figure 4.8). However, the first peak is not well resolved, and it occurs at a larger droplet

diameter than the experimental data. We tried to improve the simulation results by using more collocation points in the lower end of the distribution and less in the larger size range, as well as changing the ratio of the volume of the impeller zone to total volume. The lower end of the distribution was improved, although the solution did not converge to an adequate tolerance, and the large range of the distribution was not adequately captured (dotted line in Figure 4.8). It was observed that the initial estimate of the PSD was very important to get a converged solution. Also critical were the amount and distribution of the collocation points.

The simulations shown in this paper, as well as the values of the parameters a, a′, and V_{imp}/V_t, show that, depending on the difference of intensities of mixing and volume of the mixing compartments, bimodal distributions of different characteristics can be generated. Providing accurate estimates for these parameters permits the generation of particle size distributions with characteristics similar to the ones observed experimentally. This fact seems to corroborate the importance that non-homogeneous mixing has on the shape and parameters (mean and spread) of the PSDs obtained in suspension polymerization.

It is important to point out that the model for breakage and coalescence used in this paper has several adjustable parameters. However, from all these parameters, only one was found to have a strong effect on the predictions of the PSD, namely C_6 (a proportionality constant for the frequency of collision used in the coalescence model). This is an indication that coalescence plays a dominant role in the PSD obtained in suspension polymerization. Alvarez and his group (1991,1994; Martínez, 1990; Hernández, 1993) were aware of the limitations of the Valadez (1988) model and the use of a QSSA. They removed the QSSA and developed another model for breakage and coalescence. However, their choice of kinetic and viscoelastic models is not adequate for practical applications (see Vivaldo-Lima et al., 1997), and the effect of non-uniform intensity of mixing is ignored in their models. This paper is a first attempt at considering non-homogeneous mixing in the modelling of PSD in suspension polymerization tank reactors. However, the idea of a two-zone model has been used in other applications of liquid-liquid dispersions, as reviewed in Vivaldo-Lima et al. (1997).

In our analysis of Figures 4.4 to 4.8 it was mentioned that better profiles could have been obtained if more collocation points and different initial estimates had been used. We decided not to perform additional calculations for several reasons. First, the number of collocation points that we used was already large (around 30) and the computations were time consuming. Further increasing the computation time would compromise the effectiveness of the model by reducing its ease of solution with average computing resources. Second, it was also mentioned that the breakage and coalescence models used in this paper have several limitations that do not justify complicating the numerical analysis. Third, it was explained that the reliability of the experimental data was not high, so that it was not worth trying to replicate a result to a degree of precision higher than its uncertainty. Finally, this was an intermediate stage of our systematic approach towards the development of an effective model (outlined in Vivaldo-Lima et al. , 1997). The generation of additional carefully designed experimental data, and refinement of the mathematical model, are subsequent stages of this approach that are currently in progress.

Once a more reliable model is developed, important issues such as the design of operation conditions that reduce coalescence and promote the formation of more stable particles could be addressed. The use of more effective stabilizers, faster polymerization rates, different impellers, etc. could be evaluated by using a mechanistic model based experimental design technique.

4.4 Concluding Remarks

It has been suggested here that the effect of non-homogeneous mixing on PSD in suspension polymerization is more important than most researchers in this area realize. An important step forward towards the develpment of an effective model for PSD has been taken. Even when otherwise non-rigorous models for breakage and coalescence and strong assumptions such as the QSSA for the dynamics of the PSD are used, coupled to a simple compartment mixing model, predictions of the PSD in suspension polymerization which are in fairly good agreement with experimental data, are possible to obtain.

One effect that few groups have been able to reproduce is that of getting bimodal PSDs when pilot-plant scale tank reactors are used. Chatzi and Kiparissides (1992, 1995) have predicted bimodal PSD in liquid-liquid dispersions of low viscosity assuming homogeneous mixing and a satellite daughter drop distribution formation as one of the breakage mechanisms. That phenomenon, which is observed in the experimental data shown in this paper, can be adequately modelled with a two-zone mixing model.

A model of fairly low degree of complexity and balanced importance of factors (in terms of mixing, polymerization kinetics, and changing rheological behaviour) has been obtained. It is now possible to improve different aspects of the model. To do so, carefully designed experiments are needed. Refinements to the mathematical models should take into account the identification and recognition of the relative importance of the different factors that determine the characteristics (mean, spread and possible multi-modal character) of the PSD. How to design these experiments and how to guide the refinement of the models are the scope of future publications from our group.

Acknowledgements

The authors wish to acknowledge financial support from the Science and Technology National Council (CONACYT) of Mexico, and the Natural Sciences and Engineering Research Council (NSERC) of Canada.

4.5 Nomenclature

A = heat transfer area, m^2 (Table 4.1)

B = birth term of the PBE, Number·mL·s^{-1}

C_α = parameters of the Valadez (1988) model (α= 1, 2, ..., 10)

Cp = heat capacity, J/K

D = death term of the PBE, Number·cm^{-3}·s^{-1}, or impeller diameter, mL

f =normalized droplet volume distribution (also used to represent initiator efficiency)

f_2 = relative divinyl monomer concentration (Table 4.1)

F = droplet volume distribution, number of particles per litre

F_2 = instantaneous relative composition of monomer 2 in the polymer (Table 4.1)

g = breakage rate distribution, s^{-1}

h = coalescence rate distribution, s^{-1}

H = tank height (also represented as Z in Table 4.2), cm

ΔH = heat of reaction, J/mol

[I] = initiator concentration, mol/L

k_{cp} = constant for primary cyclization

k_{cs} = constant for secondary cyclization

k_d = initiator decomposition kinetic constant, s^{-1}

k_{fm} = pseudo-kinetic rate constant for chain transfer to monomer, L·mol^{-1}·s^{-1}

k_{fp} = pseudo-kinetic rate constant for chain transfer to polymer, L·mol^{-1}·s^{-1}

k_{fr} = pseudo-kinetic rate constant for chain transfer to small molecule, L·mol^{-1}·s^{-1}

k_p = pseudo-kinetic propagation rate constant, L·mol^{-1}·s^{-1}

k_p^* = pseudo-kinetic rate constant for crosslinking reaction, L·mol^{-1}·s^{-1}

k_{td} = pseudo-kinetic rate constant for termination by disproportionation, L·mol^{-1}·s^{-1}

k_{tcn} = number average pseudo-kinetic rate constant for termination by combination, L·mol^{-1}·s^{-1}

k_{tcw} = weight average pseudo-kinetic rate constant for termination by combination, L·mol^{-1}·s^{-1}

M = speed of agitation, rps

[M] = total monomer concentration, mol/L

n = molar mass, mol (Table 4.1)

N = number of droplets

N_P = power number

N_Q = flow number

Q = volumetric flow, mL/s (defined by equation (14))

Q_0 = zeroth moment of the dead polymer distribution, mol/L

Q_1 = first moment of the dead polymer distribution, mol/L

Q_2 = second moment of the dead polymer distribution, mol/L

$[R^{\cdot}]$ = overall polymer radical concentration, mol/L

Re = Reynolds number

R_p = polymerization rate, $mol \cdot L^{-1} \cdot s^{-1}$

t = time, s

T = tank diameter, cm (also used to represent temperature in Table 4.1, ^0C)

[T] = concentration of small molecule species (either solvent or chain transfer agent), mol/L

u, v = droplet volume, mL

U = combined heat transfer coefficient, $W \cdot m^{-2} \cdot K^{-1}$

V = volume, L

W = blade width, cm

We = Weber number

x = total monomer conversion

y, z = droplet diameter, cm

Y_0 = zeroth moment of the polymer radical distribution (polymer radical concentration), mol/L

Y_1 = first moment of the polymer radical distribution, mol/L

Y_2 = second moment of the polymer radical distribution, mol/L

Greek letters

β = normalized daughter drop distribution, $\beta(u,v)=\frac{2.4\exp[-4.5\frac{(2v-u)^2}{u^2}]}{u}$

ϵ = rate of energy dissipation, cm^2/s^2

ζ = number of daughter drops after breakage of a mother drop (assumed equal to two)

η = viscosity, Pa·s

ρ = density, g/cm^3 (also used to represent crosslink density in Table 1)

σ = interfacial tension, g/s^2

τ_0 = yield stress, $g \cdot s^{-2} \cdot cm^{-1}$

ϕ = phase holdup (volume of water to volume of monomer)

Subscripts

1 = impeller zone

2 = bulk zone

3 = overall distribution (equation 10), or zone 3

b = bulk zone (also indicated as 2)

c = continuous phase

d = dispersed phase

i = impeller zone (also indicated as 1, or "imp")

in = inlet stream

m = monomer/polymer mixture

r = reaction

t =overall or total

w = cooling water

Abbreviations

AIBN = Azo-bis-isobutironitrile

BPO = Benzoyl peroxide

CFD = computational fluid dynamics

CM = compartment model

CSTR = continuous stirred tank reactor

CTA = chain transfer agent

ODE = ordinary differential equation

PBE = population balance equation

PSD = particle size distribution

QSSA = quasi-steady-state assumption

References

Alvarez, J., J.J. Alvarez and R.E. Martínez, "Conformation of the particle size distribution in suspension polymerization. The role of kinetics, polymer viscosity and suspension agent", J. Appl. Polym. Sci.: Appl. Polym. Symp. **49**, 209-221 (1991).

Alvarez, J., J.J. Alvarez and J.M. Hernández, "A population balance approach for the description of particle size distribution in suspension polymerization reactors", Chem. Eng. Sci. **49**, 99-113 (1994).

Chatzi, E.G. and C. Kiparissides, "Dynamic simulation of bimodal drop size distributions in low-coalescence batch dispersion systems", Chem. Eng. Sci. **47**, 445-456 (1992).

Chatzi, E.G. and C. Kiparissides, "Steady-state drop-size distributions in high holdup dispersion systems", AIChE J. **41**, 1640-1652 (1995).

García-Sandoval, E., "Determinación experimental de los parámetros del modelo para la descripción de la DTP en reactores de polimerización en suspensión", M. Eng. Thesis (in Spanish), Unidad de Ciencias Básicas e Ingeniería, Universidad Autónoma Metropolitana, Plantel Iztapalapa, México D.F., Mexico (1993).

Hernández-Valdez, J.M., "Dinámica de reactores de polimerización en suspensión", M. Eng. Thesis (in Spanish), Unidad de Ciencias Básicas e Ingeniería, Universidad Autónoma Metropolitana, Plantel Iztapalapa, México D.F., Mexico (1993).

Hildebrand, H. and G. Row, "Laser light scattering in particle size analysis", Am. Ceram. Soc. Bull. **74**, 49-52 (1995).

Kresta, S.M., "Characterization, measurement and prediction of the turbulent flow in stirred tanks", Ph.D. Thesis, Department of Chemical Engineering, McMaster University, Hamilton, ON (1991).

Kresta, S.M. and P.E. Wood, "Prediction of the three-dimensional turbulent flow in stirred tanks", AIChE J. **37**, 448-460 (1991).

Kresta, S.M. and P.E. Wood, "The mean flow field produced by a 45° pitched blade turbine: changes in the circulation pattern due to off bottom clearance", Can. J. Chem. Eng. **71**, 45-53 (1993a).

Kresta, S.M. and P.E. Wood, "The flow field produced by a pitched blade turbine: characterization of the turbulence and estimation of the dissipation rate", Chem. Eng. Sci. **48**, 1761-1774 (1993b).

Martínez-Gómez, R.E., "Conceptualización y modelado de la polimerización en suspensión", M. Eng. Thesis (in Spanish), Unidad de Ciencias Básicas e Ingeniería, Universidad Autónoma Metropolitana, Plantel Iztapalapa, México D.F., Mexico (1990).

Ramkrishna, D., "The status of population balances", Rev. Chem. Eng. **3**, 49-95 (1985).

Sánchez-Vázquez, L. and García-Corichi, B., B.Sc. Thesis (In Spanish), Universidad Autónoma de Tlaxcala, Tlaxcala, Mexico (1993).

Valadez-González, A., "Evolución de la distribución de tamaños de partículas en una polimerización en suspensión", M. Eng. Thesis (In Spanish), Unidad de Ciencias Básicas e Ingeniería, Universidad Autónoma Metropolitana, Plantel Iztapalapa, México D.F., Mexico (1988).

Vivaldo-Lima, E., "Simulación del proceso de polimerización de estireno via suspensión", B.Sc. Thesis (in Spanish), Facultad de Química, Universidad Nacional Autónoma de México (UNAM), Ciudad Universitaria, México D.F., Mexico (1989).

Vivaldo-Lima, E., A.E. Hamielec and P.E. Wood, "Batch reactor modelling of the free radical copolymerization kinetics of styrene/divinylbenzene up to high conversions", Polym. React. Eng. **2**, 87-162 (1994).

Vivaldo-Lima, E., P.E. Wood, A.E. Hamielec and A. Penlidis, "An updated review on suspension polymerization", Ind. Eng. Chem. Res. **36**, 939-965 (1997).

Vlachopoulos, J., "Chem. Eng. 772 Polymer Rheology Course Notes", Department of Chemical Engineering, McMaster University, Hamilton, Ontario, Canada (1994).

Zhou, G. and S.M. Kresta, "Distribution of energy between convective and turbulent flow for three frequently used impellers", Trans. Inst. Chem. Eng. **74**, Part A, 379-389 (1996).

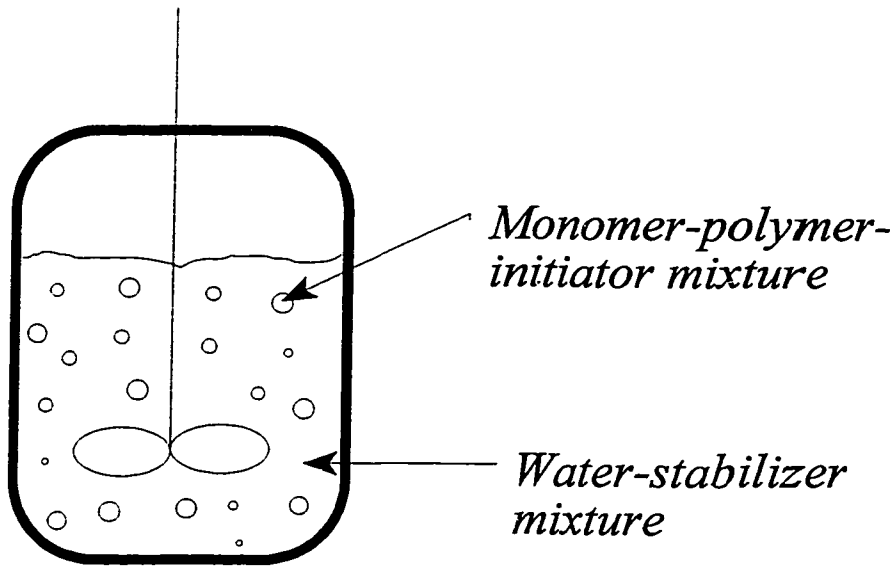

Figure 4.1 Suspension polymerization in a stirred, batch reactor (baffles not shown).

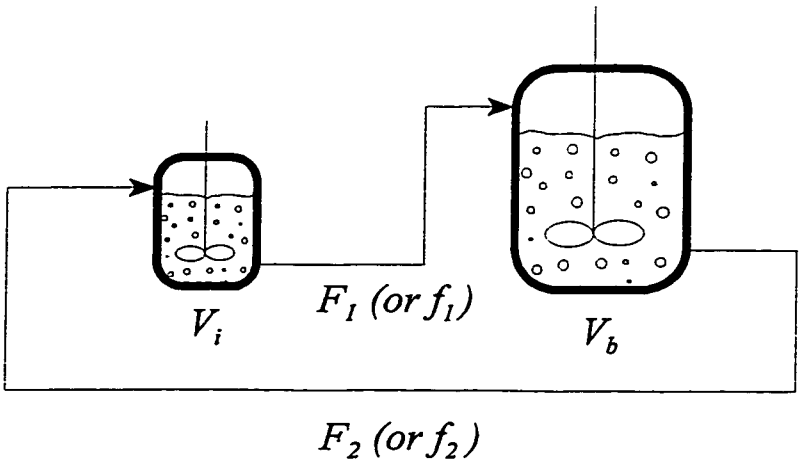

Figure 4.2 Modelling of a suspension polymerization reactor with two interconnected CSTRs (two zone model).

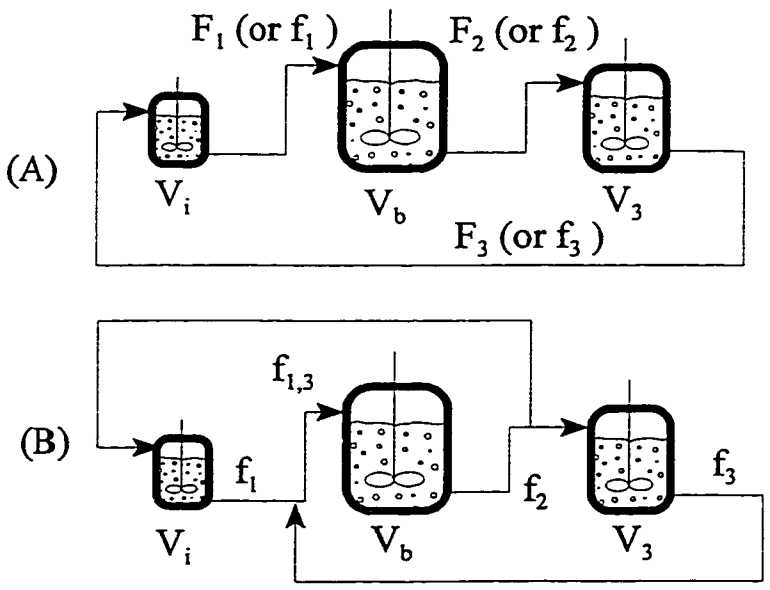

Figure 4.3 Modelling of a suspension polymerization reactor using a three-zone model.

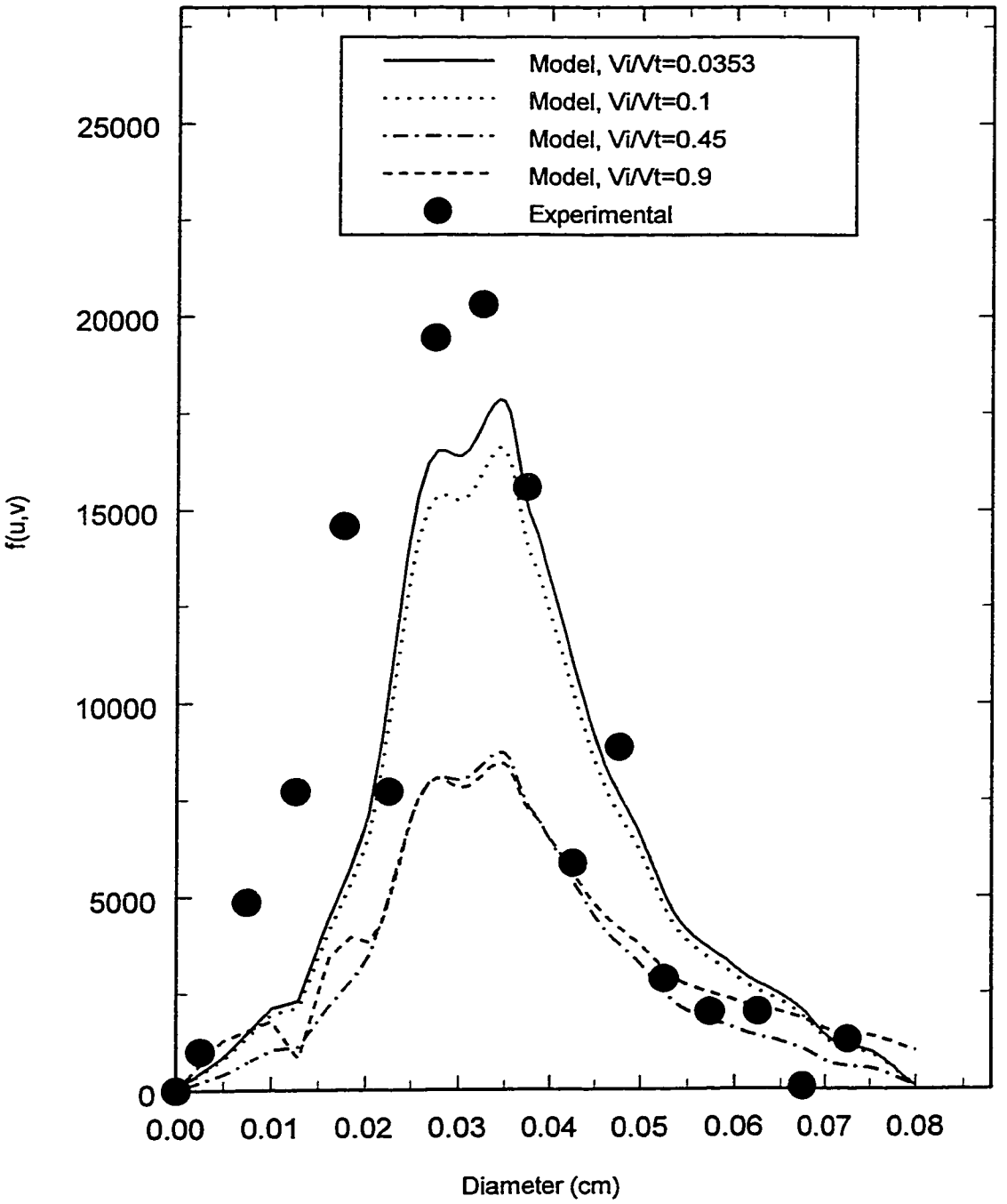

Figure 4.4 Effect of volume of the impeller zone on the PSD in suspension homopolymerization of styrene.

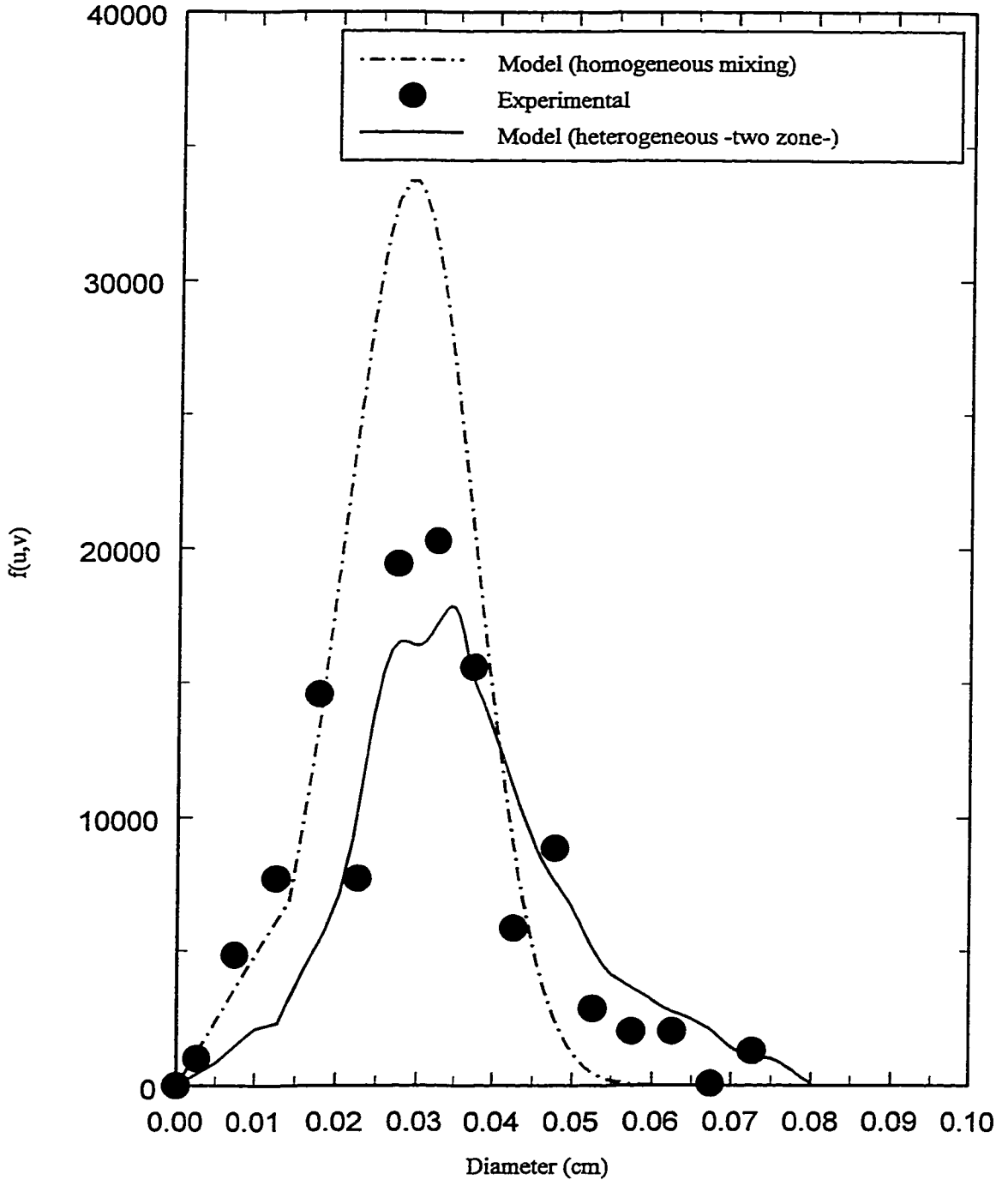

Figure 4.5 Comparison of homogeneous and non-homogeneous (compartment-mixing) model predictions of PSD against experimental data for suspension polymerization of styrene.

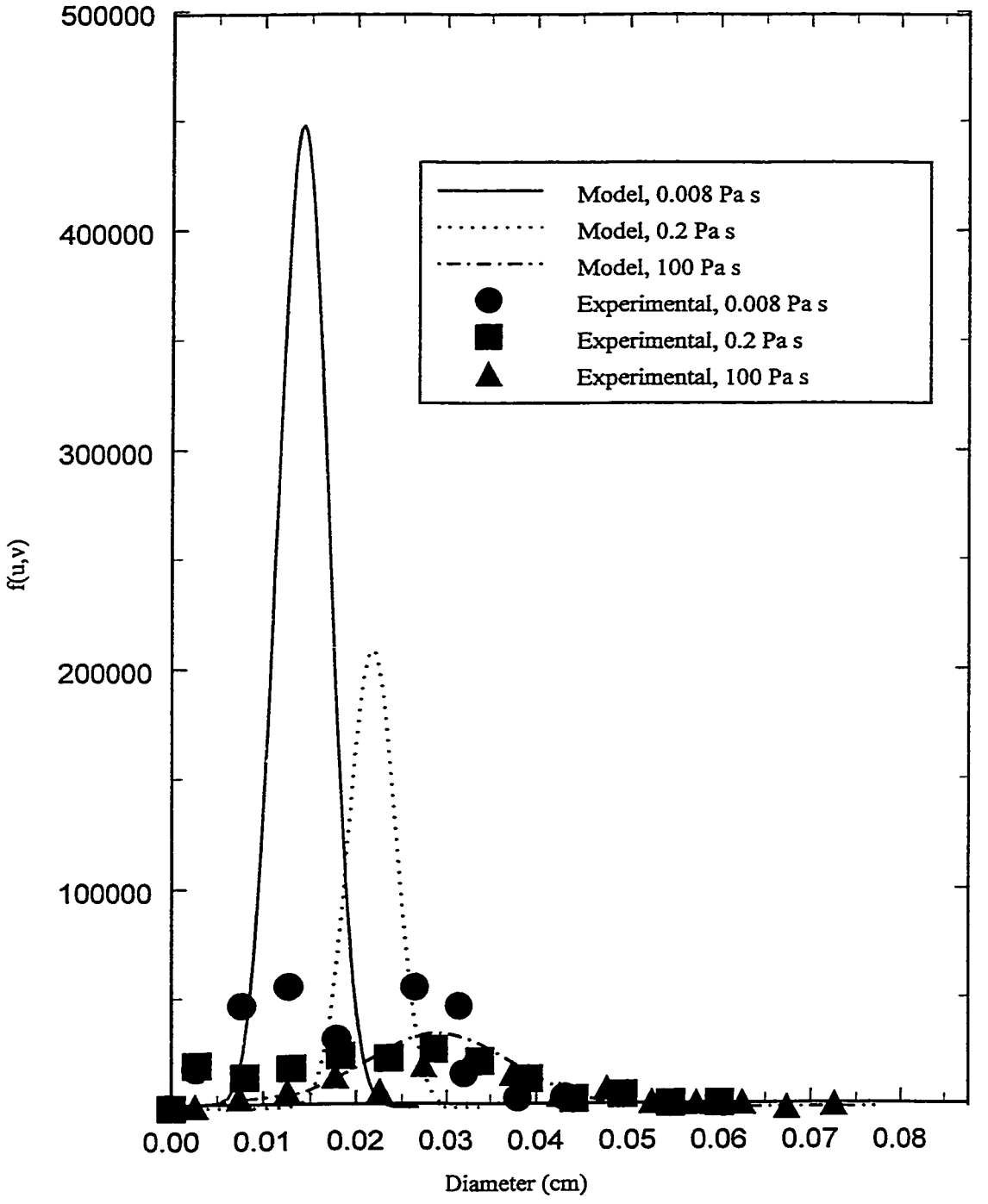

Figure 4.6 Evolution of the PSD in suspension polymerization of styrene. Comparison of homogeneous model predictions of PSD against experimental data.

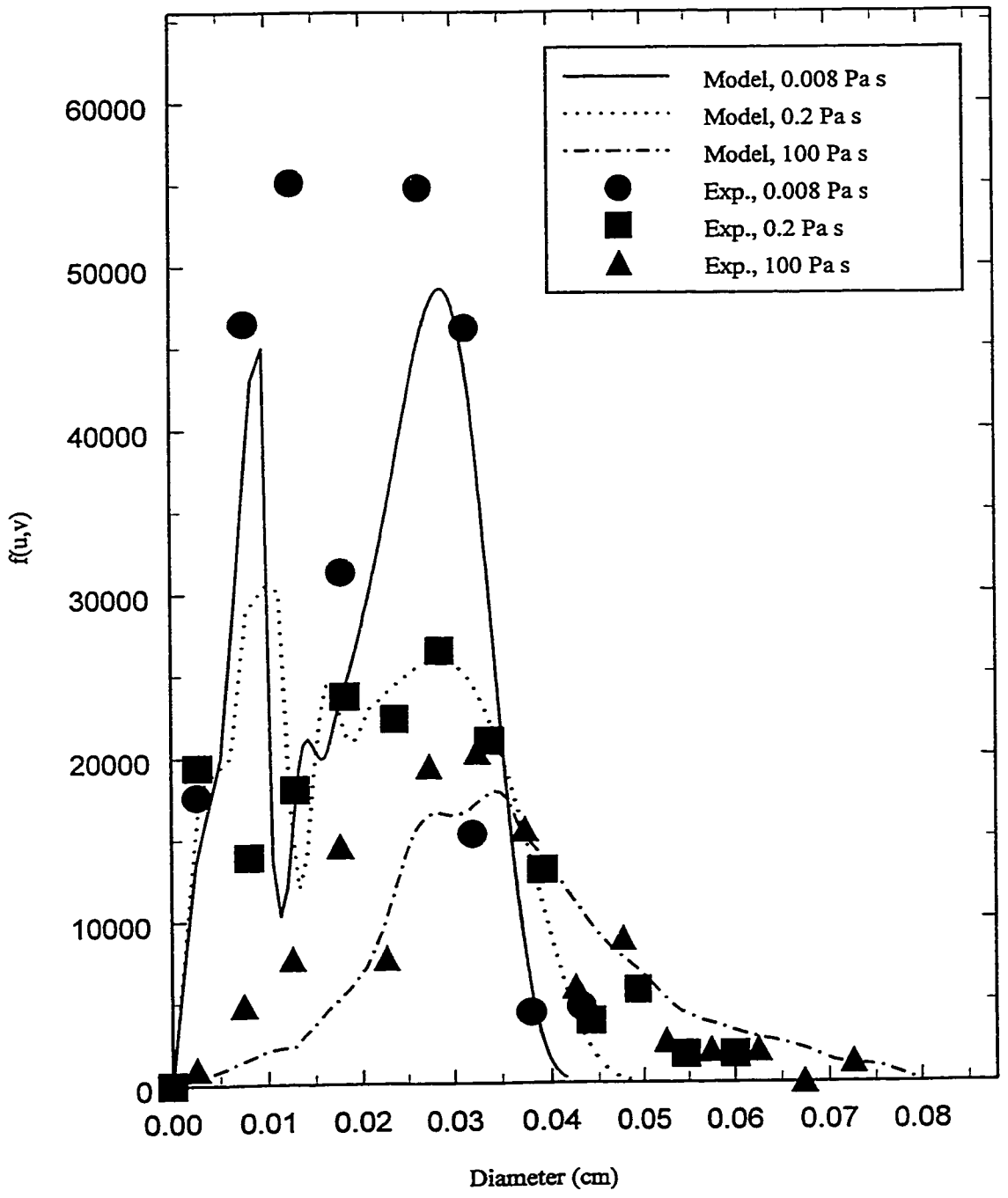

Figure 4.7 Evolution of the PSD in suspension polymerization of styrene. Comparison of non-homogeneous (CM) model predictions of PSD against experimental data.

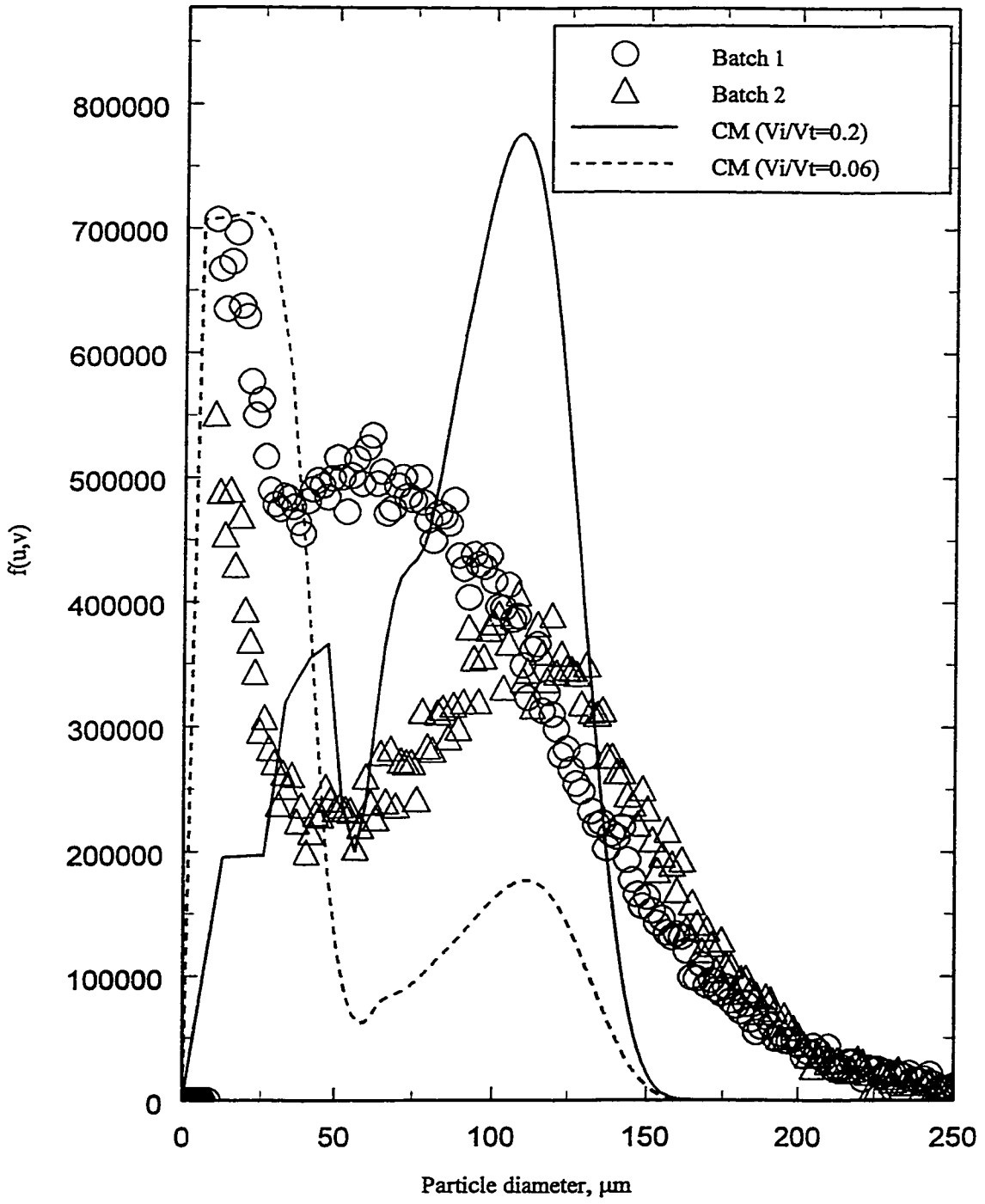

Figure 4.8 Final PSD in suspension copolymerization of styrene and divinylbenzene. Comparison of CM model predictions against (replicated) experimental data.

Chapter 5

Importance of Process Factors on Particle Size Distribution in Suspension Polymerization[1]

Eduardo Vivaldo-Lima[†], Alexander Penlidis[‡*], Philip E. Wood[†], and Archie E. Hamielec[†]
[†]McMaster Institute for Polymer Production Technology, Department of Chemical Engineering, McMaster University, Hamilton, Ontario, Canada, L8S 4L7.
[‡]Institute for Polymer Research, Department of Chemical Engineering, University of Waterloo, Waterloo, Ontario, Canada, N2L 3G1.

Abstract

The use of a Bayesian experimental design technique to determine the relative importance of factors that control particle size distribution (PSD) in suspension copolymerization of styrene and divinylbenzene is reported. Six factors and two responses are considered in this study. The experimental trials are of the two-level factorial type designed with a Bayesian method. The experiments were carried out in a 5 litre pilot plant reactor. The matrix of variances of the parameter means (the prior knowledge) was estimated with the use of a preliminary compartment-mixing (CM) model for PSD in suspension polymerization and our subjective judgement (process understanding). The responses, mean particle size (MPS) and coefficient of variation (CV), were calculated from distributions obtained with a Coulter particle counter. The results of this study provided the criteria needed to guide the future improvement of our CM-PSD model in a balanced and effective way.

Keywords: suspension polymerization, copolymerization, crosslinking, particle size distribution.

5.1 Introduction

Suspension polymerization is a rather old process that presently is aimed at producing specialty resins. Although many studies on particle size distribution (PSD) in suspension polymerization have been published in the last few decades, the understanding of the influence and importance that the known key factors have on the shape and spread of the PSD is still unclear and incomplete. A critical review on suspension polymerization was recently presented by our group (Vivaldo-Lima et al., 1997). There, we proposed a systematic approach to the study of PSD in suspension polymerization. The ultimate goal of this study is to develop an effective mathematical model for the calculation of the

---

[1]Preliminary version of a manuscript in preparation for submission to *Polym. React. Eng.*

PSD. Some of the stages of this approach include the development of an effective model for crosslinking free-radical copolymerization kinetics (Vivaldo-Lima et al., 1994), the selection of the polymerization conditions using a mechanistic model-based experimental design technique (Vivaldo-Lima et al., 1998a), and the development of a preliminary mathematical model for the PSD using a compartment-mixing (CM) model approach to account for the non-homogeneous mixing in the tank reactor (Vivaldo-Lima et al., 1998b).

In the present paper, a Bayesian experimental design technique is used to determine the relative importance that the different factors of the process have on the PSD. This Bayesian technique was chosen for two main reasons: first, the possibility of easily incorporating the prior knowledge about the process into the design and, second, its flexibility to change the levels of the factors with relative ease. Although the Bayesian design of experiments used in this study is still a factorial type of design, the technique is not restricted to a linear model. A detailed explanation of the technique and a step by step illustration of its application to the systematic study of an emulsion terpolymerization system was presented by Dubé et al. (1996).

The experimental data obtained from this design were used to calculate the contributions of the main factors and their two and three factor interactions on the mean values of mean particle size (MPS) and the coefficient of variation (CV) of the PSD. The knowledge of the relative importance of the factors and their interactions not only indicate how good (or bad) our prior knowledge is, namely how good our preliminary mathematical model is for PSD, but they also provide valuable information as to which aspects of the model are poorly explained. This will serve as a measure of how much greater a degree of complexity is needed about the different phenomena that affect the PSD in order to improve the mathematical model. The development of an improved model, guided by the results of this study, is the objective of a future publication from our group (Vivaldo-Lima et al., 1998c). This interplay of models, experimentation and statistical design techniques represents the most systematic approach one can follow in order to clarify complex processes.

5.2 Experimental

Styrene monomer (Aldrich S 497-2, 99% pure), divinylbenzene crosslinker (DVB) (Aldrich 41,456-5, technical grade, 80% mixture of isomers), benzoyl peroxide initiator (BPO) (Aldrich 17,998-1, 97%), carbon tetrachloride (CTA) (Caledon Laboratories LTD, Ontario, Code 2700-1, 99.9%) and polyvinylpyrrolidone stabilizer (PVP) (Aldrich 85,647-9, Mw= 360,000) were used as received. Water was filtered and deionized to 0.2 megohm-cm using a Nanopure ion-exchange system.

The polymerization conditions were designed using a kinetic model-based experimental design technique (Vivaldo-Lima et al., 1998a). The selected conditions for monomer concentration, crosslinker mole fraction, initiator concentration and temperature are listed in Table 5.1. The concentration of CTA was one of the factors studied with the Bayesian experimental design. The lower limit was 0 mol/L, and the upper limit was 0.125 mole/L (of the organic phase). The initial levels for the remaining factors are listed in Table 5.2 (symbols are defined either in Table 5.1 or later under the section on "Selection of Design Factors and Levels"). As it will be explained later, the levels of some of the factors were changed at different points of the experimental stages.

The experiments were carried out in a 5 litre pilot plant reactor. The configuration and dimensions of the vessel are shown in Figure 5.1 and Table 5.1, respectively. Either one or two 4-bladed 45^0 pitched bladed turbine (PBT) impellers were used, depending on the design conditions. For each batch, the PVP in water solution would be prepared a day before the polymerization was carried out. The pH of the PVP solution was adjusted to 8.0 for every batch, except for the first one, by adding a small amount of ammonium hydroxide solution. The reagents were added to the reactor in the following order: PVP solution, styrene monomer, DVB (in 50 mL of styrene), the CTA (if present), and finally the initiator, previously dissolved in 50 mL of styrene. Oxygen would be removed from the reactor by repeatedly pressurizing with liquid nitrogen and then drawing a vacuum. This would be done three times. The contents of the reactor would be stirred for 15 minutes at 20 ^{0}C prior to starting the heating cycle. The reactor would be pressurized with nitrogen to 3 atm. The temperature in the reactor was controlled with a West 3300 PID controller.

Table 5.1 Polymerization conditions and vessel dimensions.

Parameter	Value
Temperature, °C	80
[BPO], mol/L	0.02
f_{DVB}^{0}	0.001
[CTA], mol/L	Variable (see Tables 5.2, 5.5 and 5.6)
[PVP], g/(L-water)	Variable (see Tables 5.2, 5.5 and 5.6)
Tank diameter (T), cm	15.8
Tank height (H_t), cm	28.0
H_2, cm	21.3 (see Figure 5.1)
Impeller diameter, cm	Variable (see Tables 5.2, 5.5 and 5.6)
Z_2, cm	20.1 (see Figure 5.1)
Z_1, cm (= Z_2 - Sep)	Variable (see "Sep" in Tables 5.2, 5.5 and 5.6) If Sep=0, only one impeller is being used
Z/T	1.2 (see Figure 5.1 for Z)
Agitation speed (N), rps	Variable (see Tables 5.2, 5.5 and 5.6)

Table 5.2 Factors and their initial levels

Factor	Low level	High level
(1) N, rps	5	9.717
(2) ϕ	0.37	0.47
(3) [PVP], g/(L-water)	2.0	5.0
(4) D, cm	5.9	9.1
(5) Sep (Z_2 - Z_1), cm	0 (1 impeller)	8.5 (2 impellers)
(6) [CTA], mol/L	0	0.125

Once the reactor was discharged, the polymer was washed three times with methanol (Caledon laboratories LTD, reagent grade) and rinsed thoroughly with distilled water in a Buchner funnel. It was then transferred to a large flat container and left to dry overnight. A sample of about 3 grams would be prepared, by taking small portions of polymer from different zones of the flat container.

The PSDs were measured with a Coulter particle counter. A cell with an aperture size of 560 μm was used. Particle sizes lower than 20 μm could not be detected with this cell. The maximum expected drop diameter was in the order of 400 μm.

5.3 Bayesian Design of Experiments

5.3.1 Background

Dubé et al. (1996) presented a brief theoretical background on the Bayesian approach to experimentation which was based on a preliminary report by Reilly (1993). In this subsection we will include the equations required to use the technique.

The technique requires a model equation for the process response(s) as a function of the factors or variables under study, and a distribution function which contains the prior knowledge about the process. In our study, as in Dubé's study, we will use a linear regression model and a multivariate normal distribution for the prior knowledge, although a non-linear model could also be used. The model is then represented by equation (1), and the prior knowledge by equation (2).

In equations (1) through (6), $\underline{y}$ is an $n \times 1$ vector of observations, $\underline{X}$ is an $n \times p$ matrix of the coefficients of the parameters, and $\underline{\theta}$ is the $p \times 1$ vector of parameters (note that the effect is defined as twice the parameter value). The superscript * denotes the true value of the parameter θ and a "hat" denotes the posterior mean of the parameter θ. ε is the error, $\underline{I}$ is the identity matrix, σ^2 is the variance of the response(s), $\underline{\alpha}$ is a $p \times 1$ known vector of the parameter means, $\underline{U}$ is a positive definite $p \times p$ known matrix of the variances of the parameter means, n is the number of trials, and p is the number of parameters or effects.

$$\underline{y} = \underline{X}\underline{\theta}^* + \underline{\varepsilon} \tag{1}$$

$$\underline{\theta}^* : N[\underline{\alpha}\,;\underline{U}] \tag{2}$$

The posterior distribution of $\underline{\theta}^*$, after application of Bayes' theorem, is given by equation (3).

$$(\underline{\theta}^*/\underline{y}) : N\{[\underline{U}^{-1} + (\tfrac{1}{\sigma^2})\underline{X}'\underline{X}]^{-1}[\underline{U}^{-1}\underline{\alpha} + (\tfrac{1}{\sigma^2})\underline{X}'\underline{y}];[\underline{U}^{-1} + (\tfrac{1}{\sigma^2})\underline{X}'\underline{X}]^{-1}\} \tag{3}$$

The "best" set of experiments represents an n-trial fraction of a full factorial experiment. The search for the best set of trials involves maximizing the determinant shown in equation (4).

$$H = |\underline{I} + (\tfrac{1}{\sigma^2})\underline{X}\underline{U}\underline{X}'| \tag{5}$$

After the completion of a set of experiments (design sequence), the vector of parameter means α and the matrix U of variances of the parameter means are updated using equation (3) or, more explicitly, equations (5) and (6).

$$\hat{\underline{\theta}} = [\underline{U}^{-1} + (\tfrac{1}{\sigma^2})\underline{X}'\underline{X}]^{-1}[\underline{U}^{-1}\underline{\alpha} + (\tfrac{1}{\sigma^2})\underline{X}'\underline{y}] \tag{5}$$

$$\underline{U} = [\underline{U}^{-1} + (\tfrac{1}{\sigma^2})\underline{X}'\underline{X}]^{-1} \tag{6}$$

5.3.2 Selection of the Design Factors and Levels

Six factors and two responses were considered in this study. The factors were: speed of agitation (N), disperse phase hold-up, ϕ (defined as the ratio of volume of the dispersed phase, V_d, to the total volume of the dispersion, V_J), concentration of stabilizer ([PVP]), diameter of the impeller (D), distance of separation between impellers (Sep), and concentration of chain transfer agent ([CTA]). The responses were: mean particle size (MPS), and coefficient of variation (CV). The selection of these factors and their low and high level values was based on a detailed and critical analysis of the literature (e.g., Vivaldo-Lima et al., 1997), combined with some of our previous experience about the process. The initial levels for each factor are listed in Table 5.2.

5.3.3 Incorporation of Previous Knowledge

The prior knowledge about the process is incorporated into the design through the initial estimates of the vector of parameter means, $\underline{\alpha}$, and the matrix of the variances of the means, $\underline{U}$. The initial values of $\underline{\alpha}$ and $\underline{U}$ will depend on the selected response. As mentioned before, we decided to use MPS (measured as mean particle volume) and CV (σ_{Vol}/MPS) as the responses.

The prior information about the mean and the various effects was obtained from a mechanistic model-based 2^{6-1} conventional fractional factorial design. The 32 trials were simulated with a computer program based on the preliminary CM-PSD model developed by Vivaldo-Lima et al. (1998b). Calculated values for MPS and CV were recorded for each one of the 32 trials. The vectors of means of the parameters, $\underline{\alpha}_{MPS}$ and $\underline{\alpha}_{CV}$, were obtained by performing linear regression on the data of MPS and CV calculated with the CM-PSD model. The regression calculations were made using an electronic spreadsheet. The regression analyses provided estimates of the coefficients (means of the parameters), standard error of the mean, and standard error of the coefficients. The calculation of the standard error of the coefficients was possible due to the intentional omission of some of the three factor interactions during the regression procedure.

Some of the standard error estimates were altered based on our knowledge of the characteristics and assumptions of the CM-PSD model. Since the CM-PSD model had been developed putting emphasis on non-homogeneous mixing, we felt that the effects of speed of agitation, impeller diameter and impeller separation (accounted for by the volume of the compartments and the rate of energy dissipation at the impeller zone) on PSD were better explained by the model than the other effects. Therefore, we assumed the magnitudes of the means of these parameters to be equal to 6σ on a normal distribution curve. For [PVP] and some of the two factor interactions we assumed the magnitude of the parameters to be equal to 3σ. For the remaining factors and two- and three-factor interactions we assumed their standard deviations to be the higher of the magnitude of the parameter representing 3σ or the standard deviation estimated during the linear regression calculations. Squaring σ gave the diagonal elements of $\underline{U}$; the off-diagonal elements were initially all set to zero. Table 5.3 shows the

initial estimates of $\underline{\alpha}$ and $\underline{U}$ for the mean and the main factors for each of the two measured responses.

The error variance of the responses [the variance of ε in equation (1)] was calculated from a previous set of experiments (Vivaldo-Lima et al., 1998b). The PSD of seven samples from two different batches at the same polymerization conditions were measured (five samples from one batch and two from the other), and the corresponding MPS and CV values calculated from the experimental data. From these data, the variance for MPS was estimated to be $\sigma^2_{MPS,Vol} = 5.26 \times 10^{-14}$ cm^6, whereas variance for CV was $\sigma^2_{CV} = 2.902 \times 10^{-3}$.

Table 5.3 Elements of initial α and U: mean and main effects.

Effect	$\alpha_{i,MPS} \times 10^5$, cm^3	$U_{i,MPS} \times 10^{10}$, cm^6	$\alpha_{i,CV}$	$U_{i,CV} \times 10^6$
Mean	3.5	2.958	0.3273	11906.52
N	-2.63	0.192	0.0146	23.73
ϕ	0.124	0.092	0.0057	100.0
[PVP]	-2.27	0.572	0.0161	79.21
D*	-1.79 (-0.447)	0.089	0.0096 (0.0024)	79.21
Sep	-1.1	0.034	0.0071	79.21
[CTA]	0.001	0.092	0.0001	100.0

*Numbers in brackets will be explained later, in the "Results and Discussion" section.

5.4 Results and Discussion

It was decided to run a total of eight experiments in two sequences of four experiments each. The reason for running only eight experiments was that we wanted to improve our knowledge about a fairly old process, and we did not expect to uncover striking new phenomena about the process. We just wanted to quantify the relative importance that the already known key factors have on the characteristics of the PSD. The decision to run two sequences of four trials each, instead of running a single eight trial sequence, was made because we were not certain that the chosen factor levels were the most adequate (optimal). It should be emphasized that the Bayesian technique allows one to design

any number of trials per sequence, and any number of sequences. We chose four trials per sequence in two sequences for convenience. In the following paragraphs, the sequence of chronological events to design and run the two design sequences is documented. This will serve to illustrate some important aspects related to the implementation, flexibility and interpretation of results with the Bayesian experimental design technique.

As explained in Dubé et al. (1996), the methodology for selecting an optimal set of experimental trials involves generating several sub-optimal designs (> 500) and choosing the one with the highest value of H from equation (4). We varied the number of designs from 500 to 10000, and ran the program 20 times for MPS and 15 times for CV. We noticed that the sub-optimal designs for CV did not change the H value much, whereas the sub-optimal designs for MPS did show significant differences in H. We therefore chose the best sub-optimal design for MPS (the one which produced the largest H value using equation 4) as the one to be executed, which was indeed nearly optimal for CV. The first sequence of 4-trials that resulted from the previous procedure is shown in Table 5.4.

Table 5.4 First sequence of 4-trial experiments (original coding).

Run	N	ϕ	[PVP]	D	Sep	[CTA]
1	-1	1	-1	1	1	1
2	-1	-1	-1	1	-1	-1
3	1	1	-1	1	-1	-1
4	-1	1	1	-1	-1	-1

The first run of the first design sequence resulted in a suspension set-up (massive agglomeration of the dispersed droplets). After careful analysis of the chronological events for this run, we found some possible explanations for this incident. An undetected nitrogen leak had occurred through one of the feed lines to the reactor. So, it was possible that oxygen was present during the reaction. Another abnormality was that although the pH was measured (pH= 4.5), it was not raised to 8.0, as recommended by Villalobos (1989). It has been demonstrated that lowering the pH of the stabilizer

solution increases the coalescence rate (Tobin and Ramkrishna, 1992). It was also noticed that several of the factors were at levels promoting large beads and possible suspension instability. Namely, the speed of agitation was at its low level, the dispersion phase hold-up at its high level, and the concentration of stabilizer at its low level. All these conditions favour the formation of large beads, and the possibility of massive agglomeration.

Table 5.5 Factors and their updated levels after first run.

Factor	Low level	High level
(1) N, rps	10	14.717
(2) ϕ	0.27	0.37
(3) [PVP], g/(L-water)	3.5	6.5
(4) D, cm	5.9	9.1
(5) Sep (Z_2 - Z_1), cm	0 (1 impeller)	8.5 (2 impellers)
(6) [CTA], mol/L	0	0.125

Some changes were made based on the previous analysis. The recipe was modified by adding ammonium hydroxide to control the pH at a value of 8.0. The lower and upper levels for N, ϕ and [PVP] were modified. The speed of agitation was increased to assure operation in the turbulent region for the two impeller diameters used in the design, the dispersion phase hold-up was decreased to reduce the risk of agglomeration, and the stabilizer concentration was increased to promote better suspension stability. The new levels of these factors are listed in Table 5.5. Since the differences between the upper and lower levels were not altered, it was not necessary to update the values of the means of the parameters and their variances at this point and, therefore, it was not necessary to generate a new design for this sequence.

The four trials of the first design sequence were carried out in the pilot plant reactor described previously. Runs 1, 2 and 3 did not show any problem. In all three cases, well-formed, white beads of

small (latex size) and medium size (less than 300 microns) particles were obtained. Run 4, however, behaved differently. Although the samples taken from the reactor at different times of reaction for run 4 showed that the particles were small (latex size and beads no larger than 100 microns), when the reactor was opened, it was noticed that a partial set-up had occurred. What happened was very interesting. Run 4 had been produced using the upper level of stabilizer concentration, but low speed of agitation, and a single impeller with a small diameter. The impeller was positioned in the lower third section of the reactor (see Z_2 in Figure 5.1). As observed in Figure 5.2 (a photograph of the shaft and the impeller after the reactor was opened), a cone-shaped "block" of polymer was attached to the shaft of the impeller. Medium size (mostly smaller than 1 mm in diameter) and small size (polymer latex in the order of microns) beads were formed at the bottom of the reactor. What this photograph shows is that there were at least three populations of polymer particles. The populations with the medium and small particle sizes had been formed in the lower third of the reactor, in the surroundings of the impeller, and the single, large cone-like "bead" had been obtained in the upper section of the reactor. The small section of the cone started right at the impeller position in the shaft, and it increased in diameter up to almost the reactor diameter at the top of the suspension volume, as we moved further away from the impeller. This photograph is an indication that the compartment-mixing approach for modelling of the PSD in suspension polymerization (Vivaldo-Lima et al., 1998b) can be considered as a realistic approach. The CM modelling approach divides the tank into two or more regions of different intensities of mixing. The fact that latex size particles are also obtained when the concentration of stabilizer is high could be considered as an indication that the mechanism of satellite daughter drop distribution breakage mechanism of Chatzi and Kiparissides (1992, 1995) is also a plausible mechanism for bimodal PSD formation under these conditions.

Based on the partial suspension set-up result obtained in run 4, likely caused by the poor mixing under those conditions, we decided to change the lower level of the impeller diameter. Therefore, two new impellers of 8.2 cm in diameter were built. The final levels used in this study are listed in Table 5.6. This change in diameter modified the difference between the upper and lower levels for this

factor. It was therefore necessary to recalculate the means for this parameter (elements α_4 and all the α_{4i} or α_{i4} of the $\underline{\alpha}_{MPS}$ and $\underline{\alpha}_{CV}$ vectors) and all its interactions in order to design the second 4-trial sequence and calculate the updated $\underline{\alpha}_{MPS}$ and $\underline{\alpha}_{CV}$ vectors. The new values for this parameter are shown in brackets in Table 5.3. The means for the two- and three-factor interactions that contain factor 4 (impeller diameter) are not shown in the tables of this paper, but were also recalculated.

Table 5.6 Factors and their updated levels after first design sequence.

Factor	Low level	High level
(1) N, rps	10	14.717
(2) ϕ	0.27	0.37
(3) [PVP], g/(L-water)	3.5	6.5
(4) D, cm	8.3	9.1
(5) Sep (Z_2 - Z_1), cm	0 (1 impeller)	8.5 (2 impellers)
(6) [CTA], mol/L	0	0.125

In order to determine the second 4-trial design sequence we needed the "posterior" variance matrix, $\underline{U}$, of the first design sequence. The "posterior" $\underline{U}$ of the first design would become the "prior" $\underline{U}$ for the second design. Since the values of the means for parameter 4 and its interactions had been changed, it was necessary to recalculate the posterior $\underline{U}$ of the first design. To do so, equation (6) was used. The prior $\underline{U}$ in this calculation was the original matrix of variances used when the first sequence was designed, and matrix $\underline{X}$ was the matrix of coefficients of the parameters in terms of the revised coding system (the values of -1 and +1 in the $\underline{X}$ matrix are defined by the lower and upper levels of the parameters, shown in Table 5.6). Table 5.7 shows the first 6 columns of the $\underline{X}$ matrix in terms of the revised coding system. The remaining columns are formed by taking the corresponding products indicated by the interactions. For instance, the column of elements for the N×ϕ interaction is obtained by multiplying the elements of the column associated to N times the corresponding elements of the column associated to ϕ.

Table 5.7 Modified first 4-trial design (revised coding).

Run	N	ϕ	[PVP]	D	Sep	[CTA]
1	-1	1	-1	1	1	1
2	-1	-1	-1	1	-1	-1
3	1	1	-1	1	-1	-1
4	-1	1	1	-3.5	-1	-1

With the corrected "prior" $\underline{U}$ (calculated in terms of the revised coding), the second 4-trial sequence was designed. The computer program was executed 17 times for MPS and 7 times for CV. Once again it was observed that the sub-optimal designs for CV were equally good, and the best design for MPS was also nearly optimal for CV. The conditions for the second design sequence are shown in Table 5.8.

Before running the second 4-trial sequence, we decided to calculate the updated vectors of means of the parameters, $\underline{\alpha}_{MPS}$ and $\underline{\alpha}_{CV}$, based on the results from the first 4-trial sequence, using equation (5). The initial and updated values of the main and two-factor interaction elements of the vectors $\underline{\alpha}_{MPS}$ and $\underline{\alpha}_{CV}$ are listed in the second and third columns of Tables 5.11 and 5.12, respectively. These vectors are called $\underline{\theta}_{MPS}$ and $\underline{\theta}_{CV}$ once updated. It is observed that the mean MPS and mean CV values are underestimated by the CM-PSD model. However, the estimated relative contributions to the mean of each effect do not change significantly for MPS, and the change is moderate for CV.

Table 5.8 Second (final) sequence of 4-trial experiments (revised coding).

Run	N	ϕ	[PVP]	D	Sep	[CTA]
5	-1	-1	-1	-1	1	1
6	1	-1	1	-1	-1	-1
7	1	-1	-1	-1	-1	-1
8	1	1	-1	1	1	1

In a preliminary (screening) stage of our systematic study on suspension polymerization, we had measured the PSD of three batches at the conditions described in Table 5.9 (two repeats at conditions of run "a" and one at conditions of run "b"). Runs "a" (two batches at the same conditions) were used to estimate the MPS and CV variances, and run b was the result of an earlier training session. In order to decide if it was worth running the second 4-trial sequence, namely, if running the second sequence would provide substantial additional information, we decided to update once more the vector of means of the effects using the experimental data from runs a and b, and carry out a full analysis. The experimental data of MPS and CV for runs a, b, and 1 to 4 are listed in Table 5.10.

Table 5.9 Conditions for preliminary (screening) experimental data (revised coding).

Run	N	ϕ	[PVP]	D	Sep	[CTA]
a	-1.12	1	0	1	1	1
b	1	1	0	1	1	-1

Tables 5.11 and 5.12 show the results for MPS and CV, respectively. The second column shows the initial values of the means of the parameters (mean, main factors and two-factor interactions), and the third column shows the updated values of the means of the parameters after the first design sequence was completed. Column 4 shows the newly updated values with the results from runs "a" and "b" as well. To quantify the relative importance of the parameters and their interactions, as well as the adequacy of the model used to generate the "prior knowledge", we carried out a series of statistical tests (columns 5 to 7 in Tables 5.11 and 5.12).

Test 1 is defined as the ratio of the prior means to the prior standard deviations of the means $[\alpha_i/(U_i)^{1/2}]$ and tests the null hypothesis that $\alpha_i = 0$ purely in the opinion of the "expert" (the person who assigned the values for the prior effects and variances). It is a measure of the uncertainty of the "expert". A value greater than 2 or less than -2 is considered significant (this is equivalent to a 95.44% confidence interval). Test 2 is a measure of the actual significance of an effect. It is equal to the last

updated estimate of the effect, divided by the square root of the diagonal element of the last posterior variance/covariance matrix. Once again, a value greater than 2 or less than -2 implies significance. Finally, test 3 is equal to $(\theta_i - \alpha_i)$ divided by the square root of the diagonal element of the last posterior variance/covariance matrix. Test 3 is a measure of the quality of the expert's opinion. A significant value ($> |2|$) for test 3 implies that the portion(s) of the mechanistic model (the CM-PSD model in our case) related to the response and the effect in question may need refinement. As explained in Dubé et al. (1996), caution should be exercised in the interpretation of this test, since correlation and nonlinearity in the model equations could also cause the results of test 3 to become significant.

Table 5.10 Experimental data for first sequence and preliminary (screening) runs.

Run	MPS×10^5, cm^3	CV
1	0.085	0.4761
2	0.0607	0.2442
3	0.00825	0.3632
4	5.0	0.8
a	0.0257	0.5355
b	0.1044	0.4873

The results from test 1 for MPS (Table 5.11) indicate that in the "expert's opinion" (the predictions from the CM-PSD model), the factors and interactions that control the MPS are D×[CTA], N, Sep, N×Sep, N×D, D×Sep, [PVP], N×[PVP], [PVP]×Sep, and [PVP]×D, in that order of importance. Although not shown, the three-factor interactions showed no significance at all in either of tests 1 and 2. The results from test 2 confirm that the expert's opinion was correct in most instances (the order of importance changes somewhat, though). It is important to note that the factors (either pure or interactions) that have a major quantitative effect on the MPS are mostly related to the mixing environment in the tank (D, N and Sep). The results from test 3 show that the CM-PSD model is

adequate for MPS. The only effect which showed a value close (but still lower) to the decision criterion of test 3 was [PVP].

Table 5.11 Results for main effects and two-factor interactions for MPS.

Effect Name	$\alpha_i \times 10^5$, cm^3	$\theta_{i1} \times 10^5$, cm^3	$\theta_{i2} \times 10^5$, cm^3	Test 1	Test 2	Test 3
Mean	3.5	4.5076	4.548	2.035	11.47	2.643
N	-2.63	-2.8169	-2.797	-6.0	-9.87	-0.589
ϕ	0.124	0.2127	0.2159	0.408	0.814	0.346
[PVP]	-2.27	-1.5556	-1.52	-3.0	-3.93	1.939
D	-0.4475	-0.7042	-0.7019	-1.5	-2.77	-1.004
Sep	-1.11	-1.1099	-1.1048	-6.0	-6.51	0.0306
[CTA]	0.001	0.001	0.0003	0.01	0.003	-0.007
N×ϕ	-0.101	-0.2481	-0.2404	-0.332	-1.0	-0.5799
N×[PVP]	1.69	1.4947	1.5086	3.0	4.63	-0.5567
N×D	1.2	1.3025	1.3067	5.625	7.07	0.5773
N×Sep	0.76	0.7701	0.773	6.0	6.45	0.1085
N×[CTA]	0.001	0.0073	0.0069	0.01	0.07	0.0598
ϕ×[PVP]	-0.206	-0.1479	-0.1441	-0.677	-0.559	0.2401
ϕ×D	0.0757	-0.1336	-0.1294	0.249	-0.541	-0.5645
ϕ×Sep	0.0172	-0.0397	-0.0281	0.056	-0.1082	-0.1744
ϕ×[CTA]	0.001	-0.0051	-0.0061	0.01	-0.062	0.0722
[PVP]×D	0.8822	0.6877	0.695	2.81	2.69	-0.7246
[PVP]×Sep	0.495	0.4516	0.45	3.0	2.944	-0.2944
[PVP]×[CTA]	0.001	-0.0149	-0.0155	0.01	-0.1592	-0.1695
D×Sep	-0.148	-0.1457	-0.1457	-5.62	-5.547	0.0876
D×[CTA]	0.0937	0.094	0.094	9.37	9.405	0.03
Sep×[CTA]	0.001	0.001	0.001	0.1	0.1	0.0

Table 5.12 Results for main effects and two-factor interactions for CV.

Effect Name	$\alpha_i \times 10^3$	$\theta_{i1} \times 10^3$	$\theta_{i2} \times 10^3$	Test 1	Test 2	Test 3
Mean	327.35	749.3739	911.3834	3.0	37.66	24.133
N	14.61	13.3483	14.7475	3.0	3.077	0.0287
ϕ	5.74	17.9043	27.262	0.574	2.8505	2.2503
[PVP]	16.07	23.4917	34.4836	1.806	3.99	2.1306
D	2.4	-15.5539	-7.7534	0.2697	-0.9573	-1.2536
Sep	7.17	7.9974	26.2012	0.8056	3.102	2.2531
[CTA]	1.0	2.0395	7.0683	0.1	0.7498	0.6437
N×ϕ	11.87	0.8152	-0.849	1.334	-0.101	-1.513
N×[PVP]	13.63	12.0669	11.1517	3.0	2.4786	-0.551
N×D	12.7	16.9464	16.4194	2.816	3.7438	0.8481
N×Sep	-0.85	-0.6176	0.1727	-0.17	0.0352	0.2084
N×[CTA]	0.1	0.1749	-1.3042	0.0316	-0.4146	-0.4464
ϕ×[PVP]	4.54	5.1316	9.7891	0.51	1.1396	0.6111
ϕ×D	6.11	-5.022	9.1131	0.6865	1.1324	0.3732
ϕ×Sep	15.61	8.0298	23.014	1.561	2.4457	0.7868
ϕ×[CTA]	0.1	-0.6578	-0.9546	0.0316	-0.304	-0.3358
[PVP]×D	7.36	6.2052	7.7371	2.812	2.968	0.1415
[PVP]×Sep	7.67	6.7576	6.798	3.0	2.666	-0.342
[PVP]×[CTA]	0.1	-1.2951	-1.2334	0.0316	-0.3919	-0.4237
D×Sep	9.19	12.1025	13.65	2.812	4.233	1.3831
D×[CTA]	0.09	2.8188	2.4729	0.0285	0.7927	0.7638
Sep×[CTA]	0.1	0.4545	-1.2047	0.0316	-0.3828	-0.4146

In the case of CV, the situation was rather different. The results from test 2 show that the factors and interactions that control the spread of the distribution are, in order of importance: D×Sep, [PVP], N×D, Sep, N, [PVP]×D, ϕ, [PVP]×Sep, N×[PVP], and ϕ×Sep. In this case there is a more balanced weight on the importance of effects. The effects of stabilizer, mixing and dispersion concentration are

equally significant on the spread of the PSD. The fact that most of the mean values of the effects and their interactions are positive, is an indication that broad particle size distributions are inherent to suspension polymerization processes. The results of test 3 suggest that the CM-PSD model needs improvement. The effects of ϕ, [PVP] and Sep on CV are not sufficiently well captured by our CM-PSD model in its present form. Any attempt to improve this model should pay special attention to these factors.

Given the fact that the second 4-trial sequence was designed based on MPS as the response (the information content about CV from different additional 4-trial combinations was not expected to improve significantly, as explained before), and considering that the analysis on MPS showed that the CM-PSD model (the source of "prior knowledge") was already effective enough to explain the importance of factors on MPS, we decided not to run the second 4-trial sequence. With the information gathered from the first sequence and the additional experimental data that we had available, we managed to successfully achieve our objectives. We were able to determine the relative importance of the factors that control the PSD, and also identify which aspects of the CM-PSD model need improvement.

If more experiments were to be designed, it would be better to use a mechanistic model-based experimental design technique with an improved version of our CM-PSD model. We have used this experimental design technique before, when our copolymerization kinetic model was validated (Vivaldo-Lima et al., 1998a). An alternate way to generate a more effective design is to use an improved version of the CM-PSD model to replace equation (1) of this paper, and still use a Bayesian approach (but based on a non-linear model).

5.5 Concluding Remarks

A Bayesian experimental design technique whose prior knowledge was generated with a preliminary CM-PSD model was successfully used to determine the relative importance of the factors that control the PSD in suspension copolymerization of styrene and divinylbenzene. The combination

of the mechanistic nature of the CM-PSD model, the versatility of the Bayesian technique, and our engineering judgement, allowed to obtain valuable information about the effect of six factors on two responses of the PSD with only six experiments.

It was corroborated that the effect of mixing on the PSD is more important than most researchers that do modelling in this area realize. The photograph shown in this paper seems to indicate that different mixing zones are present in the vessel, and that each zone promotes the formation of different particle size populations. Therefore, it seems to be inadequate to assume that the intensity of mixing is homogeneously distributed in the tank reactor, as most models in the literature for PSD in suspension polymerization assume.

The MPS of the PSD seems to be heavily influenced by the mixing parameters (N, D and Sep). The spread of the distribution (CV), on the other hand, is equally affected by interfacial ([PVP]), mixing (N, D, and Sep) and dispersion (ϕ) parameters. The effects of ϕ, [PVP] and Sep on CV are not sufficiently well explained by the CM-PSD model in its present state. Further efforts to improve the PSD model will have to put emphasis on these factors. This means that the degree of sophistication about polymerization kinetics and mixing in our present CM-PSD model is adequate and that more sound theoretical models that explain the effects of the stabilizer and the dispersion concentration (dispersed phase hold-up) on the spread of the distribution are needed.

Acknowledgements

Financial support from the Science and Technology National Council (CONACYT) of Mexico and the Natural Sciences and Engineering Research Council (NSERC) of Canada is gratefully acknowledged. The assistance of professor Harald Stöver and Ms. Wen-Hui Li (Chemistry Dept., McMaster University) with the PSD measurements is greatly appreciated. Also, many thanks go to Loui Polic (Chem. Eng. Dept., Waterloo) for providing the FORTRAN code of the computer program for the Bayesian design.

5.6 Literature Cited

Chatzi, E.G. and C. Kiparissides, "Dynamic Simulation of Bimodal Drop Size Distributions in Low-Coalescence Batch Dispersion Systems," *Chem. Eng. Sci.*, **47**, 445 (1992).

Chatzi, E.G. and C. Kiparissides, "Steady-state Drop-size Distributions in High Holdup Dispersion Systems," *AIChE J.*, **41**, 1640 (1995).

Dubé, M.A., A. Penlidis, and P.M. Reilly, "A Systematic Approach to the Study of Multicomponent Polymerization Kinetics: the Butyl Acrylate/Methyl Methacrylate/Vinyl Acetate Example. IV. Optimal Bayesian Design of Emulsion Terpolymerization Experiments in a Pilot Plant Reactor," *J. Polym. Sci., Polym. Chem.*, **34**, 811 (1996).

Reilly, P.M., "A Bayesian Approach to Experimentation," Internal Report, Department of Chemical Engineering, University of Waterloo, Waterloo, Ontario, Canada (1993).

Tobin, T. and D. Ramkrishna, "Coalescence of Charged Droplets in Agitated Liquid-Liquid Dispersions", *AIChE J.*, **38**, 1199 (1992).

Villalobos, M.A., "Suspension Polymerization of Styrene through Bifunctional Initiators," M. Eng. Thesis, Department of Chemical Engineering, McMaster University, Hamilton, Ontario, Canada (1989).

Vivaldo-Lima, E., A.E. Hamielec and P.E. Wood, "Batch Reactor Modelling of the Free Radical Copolymerization Kinetics of Styrene/Divinylbenzene up to High Conversions," *Polym. React. Eng. J.*, **2**, 87 (1994).

Vivaldo-Lima, E., P.E. Wood, A.E. Hamielec and A. Penlidis, "An Updated Review on Suspension Polymerization," *Ind. Eng. Chem. Res.*, **36**, 939 (1997).

Vivaldo-Lima, E., P.E. Wood, A.E. Hamielec and A. Penlidis, "Kinetic Model-based Experimental Design of the Polymerization Conditions in Suspension Copolymerization of Styrene/Divinyl-benzene," *J. Polym. Sci., Polym. Chem.*, **36**, 2081-2094 (1998a).

Vivaldo-Lima, E., P.E. Wood, A.E. Hamielec and A. Penlidis, "Calculation of the Particle Size Distribution in Suspension Polymerization using a Compartment-Mixing Model," *Can. J. Chem. Eng.*, **76**, 495-505 (1998b).

Vivaldo-Lima, E., P.E. Wood, A.E. Hamielec and A. Penlidis, "An Improved Model for Particle Size Distribution in Suspension Polymerization", in preparation, 1998c.

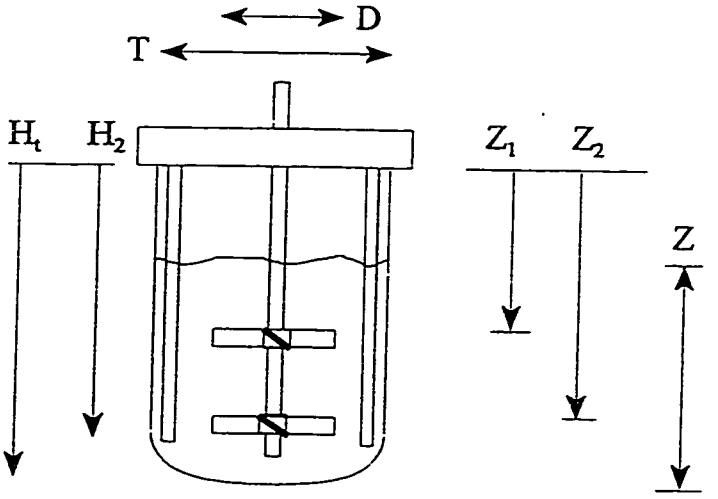

Figure 5.1 Tank reactor configuration.

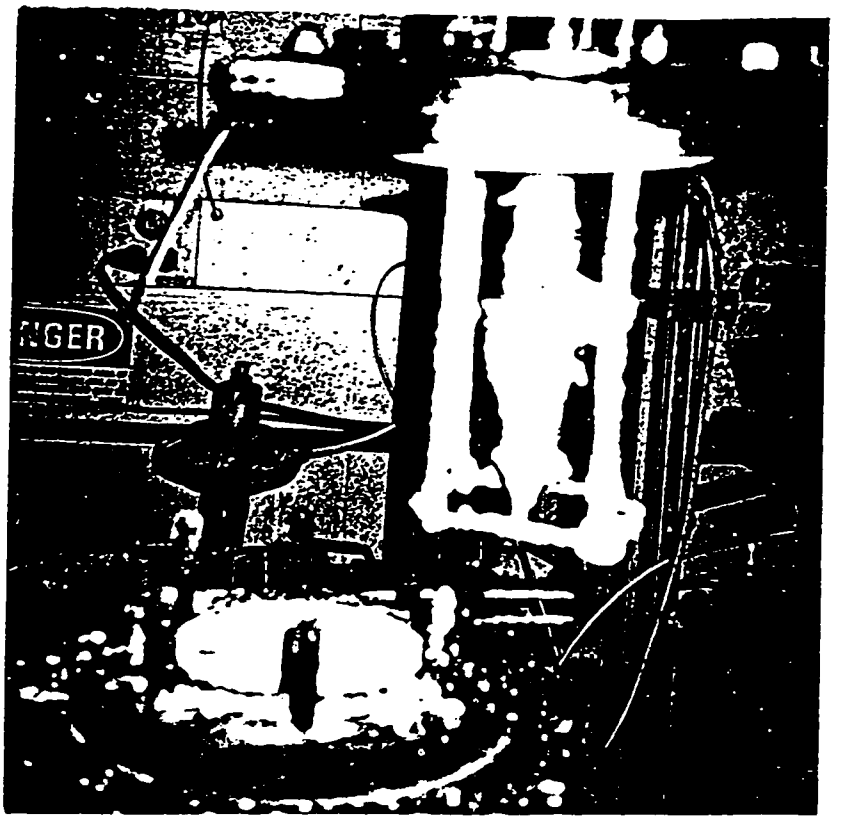

Figure 5.2 "Single bead" obtained at the poor mixing zone in Run # 4. At least two other populations of medium and small sizes were obtained in the lower half of the tank reactor.

Chapter 6

An Improved Model for Particle Size Distribution in Suspension Polymerization[1]

Eduardo Vivaldo-Lima[†], Philip E. Wood[†*], Archie E. Hamielec[†], and Alexander Penlidis[‡]
[†] McMaster Institute for Polymer Production Technology, Department of Chemical Engineering, McMaster University, Hamilton, Ontario, Canada, L8S 4L7.
[‡] Institute for Polymer Research, Department of Chemical Engineering, University of Waterloo, Waterloo, Ontario, Canada, N2L 3G1.

Abstract

An effective model for particle size distribution (PSD) in suspension polymerization is presented. The model was developed by building on a previous compartment-mixing (CM) model from our group (Vivaldo-Lima et al., *Can. J. Chem. Eng.*, **76**, 495-505, 1998b) and guiding the changes with the results obtained from an experimental study designed to highlight the process factors that were not explained sufficiently well with the CM-PSD model (Vivaldo-Lima et al., in preparation, 1998c). Special attention was paid to properly account for the effects of dispersed phase holdup (ϕ), stabilizer concentration ([PVP]), and volume of the high intensity of mixing zone (which is related to the dimensions and separation (Sep) between the impellers of a two-impeller 45° pitched bladed turbine (PBT) agitator), on the coefficient of variation (CV) of the PSD. Experimental data of final PSD in suspension copolymerizations of styrene/divinylbenzene carried out in a 5 litre pilot plant reactor were used to test the performance of the model.

Keywords: Particle size distribution, suspension polymerization, breakage, coalescence, liquid-liquid dispersions, polystyrene-divinylbenzene, crosslinking.

6.1 Introduction

A systematic study on the modelling of particle size distribution (PSD) in suspension polymerization reactors has been under way in our laboratories at McMaster and Waterloo for the last few years. A critical review on this process that summarizes the most recent contributions for modelling purposes was presented recently (Vivaldo-Lima et al., 1997). Some of the previous stages of this study include the development of an effective model for free-radical crosslinking copolymerization kinetics of styrene/divinylbenzene (Vivaldo-Lima et al., 1994), the design of the

[1]Preliminary version of a manuscript in preparation for submission to *Polym. React. Eng.*

polymerization conditions for an experimental study on PSD using a mechanistic model-based experimental design technique (Vivaldo-Lima et al., 1998a), the development of a mathematical model for PSD in suspension polymerization with emphasis on non-homogeneous mixing in the stirred tank reactor (Vivaldo-Lima et al., 1998b), and the design and implementation of an experimental study aimed at determining the relative importance of the process factors on the mean particle size (MPS) and spread of the PSD (Vivaldo-Lima et al., 1998c).

The ultimate goal of our group in dealing with suspension polymerization is to develop an effective model for PSD. To be effective the model has to be sound, yet reasonably simple to solve with average computing resources, and the predictions should be reliable. Validation with experimental data and a test for extrapolated performance are required to assure reliability.

Our previous experimental study showed that the mean particle size (MPS) of the PSD is predicted well with the CM-PSD model, but the spread of the distribution is underpredicted. Our statistical analyses showed that the effects of stabilizer concentration, dispersed phase hold-up and separation between impellers on the spread of the distribution were not captured sufficiently well (Vivaldo-Lima et al., 1998c). The main objective of the present paper is to improve the breakage and coalescence models used in the CM-PSD model of Vivaldo-Lima et al. (1998b), paying special attention to these factors.

As explained in Chapter 1 of Vivaldo-Lima (1998), the different factors that affect the PSD in suspension polymerization can be classified in four groups: (i) those related to the polymerization kinetics (which determine the dispersed phase viscosity, η_d), (ii) mixing in the stirred tank reactor (represented by the rate of energy dissipation, ϵ), (iii) surface phenomena (interfacial tension, σ), and (iv) suspension concentration (dispersed phase hold-up, ϕ). In our previous papers we concentrated on groups (i) (Vivaldo-Lima et al., 1994, 1998a) and (ii) (Vivaldo-Lima et al., 1998b). In this paper we will concentrate on groups (iii) and (iv). An important issue still missing in our model is the effect of drop electrical charges on the coalescence rate (Tobin and Ramkrishna, 1992). This aspect should be considered in future improvements to the PSD model.

6.2 Experimental

The details about the reactor configuration, polymerization conditions and operation procedure have been documented elsewhere (Vivaldo-Lima et al., 1998c). A total of six batches were prepared and the polymer PSD was measured with a Coulter counter particle sizer. Tables 6.1, 6.2 and 6.3 show the factor levels, the polymerization conditions for each batch, and the experimental results for MPS and coefficient of variation (CV), respectively. The experimental PSDs for each batch are shown in the plots of the "Results and Discussion" section of this paper.

Table 6.1 Process factors and their levels.

Factor	Low level (-1)	High level (1)
(1) N, rps	10	14.717
(2) ϕ (V_d/V_l)	0.27	0.37
(3) [PVP], g/(L-water)	3.5	6.5
(4) D, cm	8.3	9.1
(5) Sep (Z_2 - Z_1), cm	0 (1 impeller)	8.5 (2 impellers)
(6) [CTA], mol/L	0	0.125

Table 6.2 Coded values of the process factors for each batch.

Run	N	ϕ	[PVP]	D	Sep	[CTA]
a	-1.12	1	0	1	1	1
b	1	1	0	1	1	-1
1	-1	1	-1	1	1	1
2	-1	-1	-1	1	-1	-1
3	1	1	-1	1	-1	-1
4	-1	1	1	-3.5	-1	-1

Table 6.3 Experimental data for MPS and CV.

Run	MPS×10^5, cm^3	CV
1	0.085	0.4761
2	0.0607	0.2442
3	0.00825	0.3632
4	5.0	0.8
a	0.0257	0.5355
b	0.1044	0.4873

6.3 Modelling

Most mathematical models for calculation of the PSD in suspension polymerization are either semi-empirical (based on dimensionless correlations) or make use of a population balance equation where mixing is assumed to be homogeneous. As suggested (and supported) in our review (Vivaldo-Lima et al., 1997), this homogeneous mixing approach is clearly unrealistic. A more rigorous way to approach the problem would be to couple the motion equations in three dimensions with a space dependent population balance equation. Although feasible in principle, this approach would lead to a system of equations very difficult (and computational intensive) to solve. To avoid deriving and solving a model of such characteristics, without failing to recognize the importance of non-homogeneous mixing in the tank reactor, an intermediate approach was proposed and used in Vivaldo-Lima et al. (1998b). The approach consisted of dividing the vessel into two or more homogeneous regions, but different in intensity of mixing (regions with different values of rate of energy dissipation). Each region was assumed to be represented by a continuos stirred tank reactor (CSTR) with input and output streams that feed to or are fed by the streams of other zones. These ideas are illustrated in Figures 6.1 and 6.2.

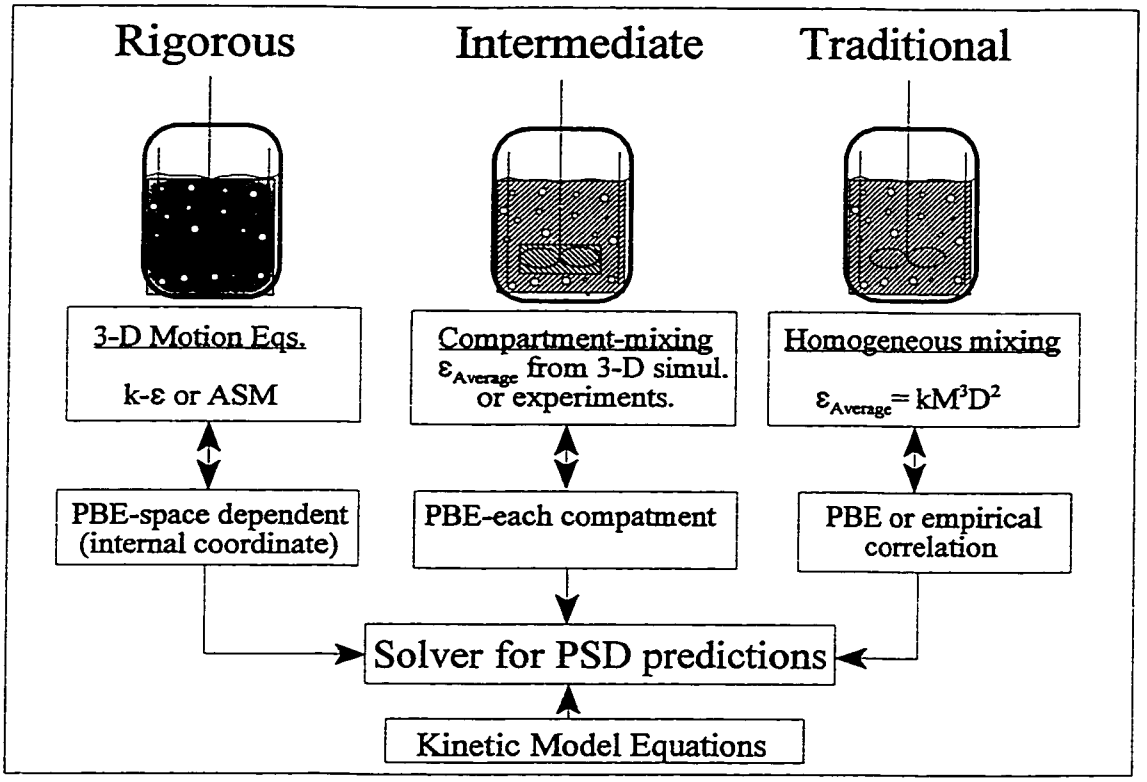

Figure 6.1 Modelling of Mixing in Stirred Tank Reactors.

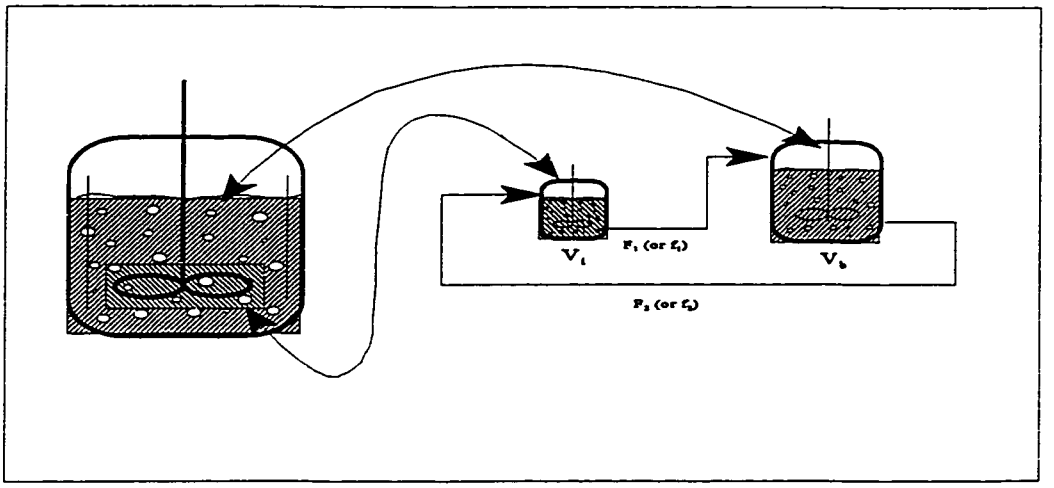

Figure 6.2 Modelling of non-homogeneous mixing in suspension polymerization using two compartments.

6.3.1 Population Balance Equations

For a population uniformly distributed in physical space of constant volume, V_t, the transient population balance equation (PBE) that describes the PSD in suspension polymerization for a (continuous) stirred tank reactor is given by equation (1) (Vivaldo-Lima et al., 1998b), where the chain rule of calculus has been used to evaluate the term $\partial F(u,t)/\partial u$. In the case of a batch stirred tank reactor, the flow term [first on the right hand side of equation (1)] would not be present.

$$\frac{\partial F(u,t)}{\partial t} = \frac{1}{2}\left[\frac{Q}{V_t}[F(u,t) - F_{in}(u,t)] + k_p[R^{\cdot}]F(u,t) + \int_u^{\infty} g(v)\ \zeta(v)\ \beta(u,v)\ F(v,t)\ dv \right.$$
$$\left. + \int_0^{\frac{u}{2}} h(u-v,v)\ F(u-v,t)\ F(v,t)\ dv - F(u,t)\int_0^{\infty} h(u,v)F(v,t)dv - g(u)F(u,t) \right] \quad (1)$$

F(u,t) can be divided by the total number of particles at time t, N(t), to provide a normalized PSD density distribution function, f(u,t), defined by equation (2) (Vivaldo-Lima et al., 1998b). The PBE in terms of f(u,t) is then given by equation (3).

$$f(u,t) = \frac{F(u,t)}{\int_0^{\infty} F(v,t)dv} = \frac{F(u,t)}{N(t)} \quad (2)$$

$$\frac{\partial f(u,t)}{\partial t} = \frac{1}{2}\left[\frac{Q}{V_t}[f(u,t) - \frac{N_{in}(t)}{N(t)} f_{in}(u,t)] + k_p[R^{\cdot}]f(u,t) + \int_u^{\infty} g(v)\zeta(v)\beta(u,v)f(v,t)\,dv \right.$$
$$\left. + N(t)\int_0^{\frac{u}{2}} h(u-v,v)f(u-v,t)f(v,t)\,dv - f(u,t)N(t)\int_0^{\infty} h(u,v)f(v,t)dv - g(u)f(u,t) \right] \quad (3)$$

6.3.2 Compartment-Mixing Model

The calculations reported in this paper were obtained using a two-zone mixing model (two-compartment model) to represent a batch stirred tank reactor. A schematic representation of this model

is shown in Figure 6.2. The small tank reactor of volume V_i represents the mixing zone surrounding the impeller (impeller region), whereas the other tank reactor of volume V_b represents the mixing zone for the remaining of the tank (bulk region). The PSD for the "impeller" region, F_1 (or f_1 if the PSD function is normalized), is characterized by a high intensity of mixing (high rate of energy dissipation), whereas the PSD of the bulk zone, F_2 (or f_2), is characterized by a lower intensity of mixing (lower rate of energy dissipation).

Assuming that our batch stirred tank reactor of Figure 6.2 (left) can be modelled as a series of two CSTRs, as shown in the same figure (right), equations (4) to (6) are obtained after writing down the PBE for each CSTR and a conservation of mass equation for that configuration. The overall PSD function is given by $f_3(u,t)$.

$$\frac{\partial f_1(u,t)}{\partial t} = \frac{1}{2}\left[\frac{Q_1}{V_i}[f_1(u,t) - \frac{N_2(t)}{N_1(t)}f_2(u,t)] + k_p[R^-]f_1(u,t) + \int_u^{\infty} g_1(v)\zeta(v)\beta(u,v)f_1(v,t)\,dv \right.$$
$$\left. + N_1(t)\int_0^{\frac{u}{2}} h_1(u-v,v)f_1(u-v,t)f_1(v,t)\,dv - f_1(u,t)N_1(t)\int_0^{\infty} h_1(u,v)f_1(v,t)dv - g_1(u)f_1(u,t)\right] \quad (4)$$

$$\frac{\partial f_2(u,t)}{\partial t} = \frac{1}{2}\left[\frac{Q_2}{V_b}[f_2(u,t) - \frac{N_1(t)}{N_2(t)}f_1(u,t)] + k_p[R^-]f_2(u,t) + \int_u^{\infty} g_2(v)\zeta(v)\beta(u,v)f_2(v,t)\,dv \right.$$
$$\left. + N_2(t)\int_0^{\frac{u}{2}} h_2(u-v,v)f_2(u-v,t)f_2(v,t)\,dv - f_2(u,t)N_2(t)\int_0^{\infty} h_2(u,v)f_2(v,t)dv - g_2(u)f_2(u,t)\right] \quad (5)$$

$$f_3(t) = \frac{N_1(t)\frac{V_i}{V_t}f_1(u,t) + N_2(t)\frac{V_b}{V_t}F_2(t)}{N_1(t) + N_2(t)} \quad (6)$$

where:

$$V_t = V_i + V_b \quad (7)$$

$$N_1(t) = \frac{\phi V_i}{\int_0^{\infty} v f_1(v,t)dv} \quad , \quad N_2(t) = \frac{\phi V_b}{\int_0^{\infty} v f_2(v,t)dv} \tag{8}$$

$$Q_1 = Q_2 = Q = N_Q M D_{imp}^{\ 3} \tag{9}$$

$$V_i = \frac{\pi}{4}(1.4D)^2 W N_{imp} \tag{10}$$

In the previous equations it has been assumed that (i) the dispersed phase hold-up is the same for all the compartments, (ii) the overall PSD is a linear combination of the PSDs of each compartment, (iii) the flow between compartments is constant, and (iv) the volume of the impeller zone is calculated as that of a cylinder with diameter equal to 1.4 times the impeller diameter. If it is further assumed that the dynamics of evolution of the PSD are much faster than the dynamics of reaction, then the transient PSD equations can be approximated with a quasi-steady-state approximation (QSSA). Using a QSSA makes it possible to transform integro-differential equations (4) and (5) into integral equations (11) and (12), which are easier to solve. It also makes it possible to decouple the ordinary differential equations (ODEs) that describe the (co)-polymerization kinetics from the PBEs. The ODEs that describe the copolymerization kinetics are listed in Table 6.4. The details about their derivation, limitations, and the definition of variables and parameters not shown in this paper are explained in Vivaldo-Lima et al. (1994). In order to follow the particle size evolution in time it is only required to know the viscosity of the dispersed phase and the monomer conversion at different times, and then solve equations (11), (12) and (6) for each case. The viscosity of the dispersed phase can be estimated at any time from independent simulations of the kinetic behaviour of the polymerization system, provided that a correlation between viscosity and molecular weight is available. Equation (1) from Vivaldo-Lima et al. (1998a) can be used for this purpose.

$$\frac{Q_1}{V_i}[f_1(u) - \frac{N_2}{N_1}f_2(u)] + k_p[R^-]f_1(u) + \int_u^{\infty} g_1(v)\zeta(v)\beta(u,v)f_1(v)dv$$
$$+ N_1\int_0^{\frac{u}{2}} h_1(u-v,v)f_1(u-v)f_1(v)dv - f_1(u)N_1\int_0^{\infty} h_1(u,v)f_1(v)dv - g_1(u)f_1(u) = 0 \quad (11)$$

$$\frac{Q_2}{V_b}[f_2(u) - \frac{N_1}{N_2}f_1(u)] + k_p[R^-]f_2(u) + \int_u^{\infty} g_2(v)\zeta(v)\beta(u,v)f_2(v)dv$$
$$+ N_2\int_0^{\frac{u}{2}} h_2(u-v,v)f_2(u-v)f_2(v)dv - f_2(u)N_2\int_0^{\infty} h_2(u,v)f_2(v)dv - g_2(u)f_2(u) = 0 \quad (12)$$

6.3.3 Breakage and Coalescence

6.3.3.1 Breakage

In our previous paper on CM-PSD modelling (Vivaldo-Lima et al., 1998b), we used the model of Valadez (1988) to represent the breakage and coalescence of droplets, but no details about its derivation were provided then. In this paper we will analyse these phenomena in some detail. As explained before, the idea behind this analysis is to ensure that the effects of the variables that were found to be inadequately explained by our CM-PSD model (dispersed phase hold-up, concentration of stabilizer and separation between impellers) are modelled in a more realistic way, thus producing a CM-PSD model of better performance.

The breakage rate distribution, g(u), can be expressed as the product of a breakage frequency and a breakage efficiency, as shown in equation (13). The breakage frequency for liquid-liquid dispersions in turbulent stirred tank reactors has been modelled using equation (14) [Valadez, 1988; Chatzi et al., 1989 (Cases 1 and 2 of that paper); Vivaldo-Lima, 1989; Alvarez et al., 1991, 1994].

Table 6.4 Model equations for free-radical copolymerization kinetics with crosslinking.

Initiation	$\frac{d(V[I])}{Vdt} = -k_d[I]$
Overall conversion	$\frac{dx}{dt} = (k_p + k_{fm})(1-x)[R^\bullet]$
Moment equations for polymer radicals	$\frac{d(VY_0)}{Vdt} = 2fk_d[I] - (\bar{k}_{tcm} + \bar{k}_{td})Y_0^2$ $\frac{d(VY_1)}{Vdt} = 2fk_d[I] + (k_{fm}[M] + k_{fT}[T] + k_p^\bullet Y_0 Q_2 + k_p[M]Y_0$ $-\{k_{fm}[M] + k_{fT}[T] + (\bar{k}_{tcm} + \bar{k}_{td})Y_0 + k_{fp}([Y_1 + Q_1] - Y_1)\}Y_1$
Moment equations for total polymer concentration	$\frac{d(V[Y_0 + Q_0])}{Vdt} = 2fk_d[I] + (k_{fm}[M] + k_{fT}[T])Y_0 - k_p^\bullet Y_0([Y_1 + Q_1] - Y_1) - \frac{1}{2}\bar{k}_{tcm}Y_0^2$ $\frac{d(V[Y_1 + Q_1])}{Vdt} = 2fk_d[I] + (k_{fm}[M] + k_{fT}[T])Y_0 + k_p[M]Y_0$ $\frac{d(V[Y_2 + Q_2])}{Vdt} = 2fk_d[I] + (k_{fm}[M] + k_{fT}[T])Y_0 + k_p[M]Y_0 + 2k_p[M]Y_1$ $+ 2k_p^\bullet Y_1[Y_2 + Q_2] + \bar{k}_{tcw}Y_1^2$
Divinyl monomer consumption	$\frac{df_2}{dt} = \frac{f_2 - F_2}{1-x}$
Accumulated copolymer composition	$\overline{F_2} = \frac{f_{20} - f_2(1-x)}{x}$
Crosslink density	$\frac{d[x\bar{\rho}(x)]}{dt} = \frac{k_p^{*0}[2\overline{F_2}(x)(1-k_{cp}) - \bar{\rho}(x)(1+k_{cp})]x}{k_p(1-x)}\frac{dx}{dt}$
Transfer to small molecule	$\frac{d(V[T]_d)}{Vdt} = -k_{fT}[T_d][R^\bullet]$
Temperature	$\frac{dT}{dt} = \frac{(-\Delta H)_r R_p}{n_m Cp_m} - \frac{n_w Cp_w}{n_m Cp_m}\frac{dT_w}{dt} - \frac{UA}{n_m Cp_m}(T - T_w)$

$$g(u) = \omega_b(u)\lambda_b(u) \tag{13}$$

$$\omega_b[u(y)] = C_1\left[\frac{D}{y}\right]^{2/3}\frac{M}{DF(\phi)} \tag{14}$$

The term DF(ϕ) in equation (14) is a correction factor to account for the effect of the dispersed phase on the flow properties of the continuous phase, mostly its effect on the rate of energy dissipation, ϵ. Most authors have used DF(ϕ) as defined in equation (15), with C_ϕ= 1.0 (e.g., Coulaloglou and Tavlarides, 1977; Valadez, 1988; Alvarez et al., 1991, 1994).

$$DF(\phi) = 1 + C_\phi \cdot \phi \tag{15}$$

The change in the rate of energy dissipation of a fluid-liquid dispersion with respect to the corresponding value for the pure liquid depends on the ratio of the viscosity of the dispersion to the viscosity of the pure liquid. This relationship is given by equation (16) (Doulah, 1975; Tsouris and Tavlarides, 1994).

$$\epsilon_s = \epsilon_c\left[\frac{\eta_c}{\eta_s}\right]^3 \tag{16}$$

From the derivation steps of former models for breakage and coalescence available in the literature (e.g., Coulaloglou and Tavlarides, 1977; Valadez, 1988; Tsouris and Tavlarides, 1994) and equations (15) and (16), it can be shown that the correction factor used in equation (14) is defined as shown in equation (17).

$$DF(\phi) = \frac{\eta_s}{\eta_c} \tag{17}$$

There are several correlations available in the literature to calculate the ratio of viscosity of the dispersion to viscosity of the pure liquid (e.g., Hunter, 1993). Most of these correlations are based on Einstein's equation for calculation of the viscosity of a diluted dispersion of solid, non-interacting spheres in a liquid medium. Just by visual comparison of Einstein's equation [$DF(\phi)=1+2.5\phi$] with equation (15) when $C_\phi = 1.0$, we notice that the effect of ϕ on the PSD is underestimated, and the deviation increases with ϕ. Since the Valadez model uses $C_\phi = 1.0$ in equation (15) for breakage and coalescence, this may explain why our previous analysis of the CM-PSD model showed that ϕ was not explained adequately by that model (Vivaldo-Lima et al., 1998c). For our suspension polymerization application we found that an adequate correlation for $DF(\phi)$ was Mooney's equation for viscosity of a suspension (Hunter, 1993), given by equation (18). In all the following model equations, $DF(\phi)$ is given by equation (15) with $C_\phi = 1.0$, when reference to either the models of Valadez (1988) or Alvarez et al. (1991, 1994) is made. In all the final expressions for breakage and coalescence derived for use in this paper, $DF(\phi)$ is given by equation (18).

$$DF(\phi) = \left\{1 - \frac{\phi}{\phi_m}\right\}^{-[\eta]\phi_m} \approx \left\{1 - \frac{\phi}{0.631}\right\}^{-2} \qquad \textbf{(18)}$$

Valadez (1988) assumed that the overall breakage efficiency was given by the product of two other efficiencies: an energy efficiency, λ_{be}, and a time efficiency λ_{bt}, as shown in equation (19). The energy efficiency was calculated as the fraction of turbulent eddies with energy content greater than the energy required to break a droplet, as shown in equation (20), where the energy terms are defined by equations (21) and (22).

$$\lambda_b(u) = \lambda_{be}(u)\lambda_{bt}(u) \qquad \textbf{(19)}$$

$$\lambda_{be}(u) = \exp\left\{-\frac{E_{required}}{E_{available}}\right\} \qquad \textbf{(20)}$$

$$E_{required} = E_{surface} + E_{yield} + E_{deformation} \tag{21}$$

$$E_{available} \propto \rho_c(\bar{\epsilon}y)^{2/3} \tag{22}$$

Assuming that the droplets follow a power-law flow behaviour and after proper estimation of the energy terms in equation (21), Valadez (1988) obtained equation (23).

$$\lambda_{be}[u(y)] = \exp\left\{-DF(\phi)^2\left[C_2\left(\frac{D}{y}\right)^{\frac{5}{3}}\frac{1}{We} + C_3\left(\frac{D}{y}\right)^{\frac{2}{3}}\frac{1}{Re} + C_4\left(\frac{D}{y}\right)^{\frac{4}{3}}\frac{1}{DF(\phi)}\frac{\sqrt{\frac{\rho_c}{\rho_d}}}{Re_d}\right]\right\} \tag{23}$$

The time efficiency term of equation (19), λ_{bt}, is defined in equation (24), where t_b is the characteristic (available) breakage time, and t_v is the characteristic time for viscous flow (time required to elongate a distance equal to the drop diameter). After proper estimation of these times, according to equation (25), equation (26) is obtained.

$$\lambda_{bt} = \exp\left\{-\frac{t_v}{t_b}\right\} \tag{24}$$

$$t_b \propto y^{2/3}\bar{\epsilon}^{-1/3}, \quad t_v \propto \frac{8\eta_d}{\rho_c(\bar{\epsilon}y)^{2/3}} \tag{25}$$

$$\lambda_{bt} = \exp\left\{-\frac{C_5}{Re_d\sqrt{DF(\phi)}}\frac{\rho_d}{\rho_c}\left[\frac{D}{y}\right]^{4/3}\right\} \tag{26}$$

Equations (14), (23) and (26) are the ones used for breakage in our previous model (Vivaldo-Lima et al., 1998b). In these equations, Re, Re_d and We are defined by equation (27).

$$Re = \frac{\rho_c M^2 D^2}{\tau_0}, \quad Re_d = \frac{\rho_c M D^2}{\eta_d}, \quad We = \frac{\rho_c M^2 D^3}{\sigma} \tag{27}$$

Alvarez et al. (1994) considered only an energy efficiency. The required energy to overcome the resistance to deformation was modelled as the addition of the surface and viscoelastic energies. Assuming that the monomer/polymer mixture behaves as a Maxwell fluid, they obtained equation (28), whose parameters are defined by equations (29) through (31).

$$\lambda_b = \exp\left\{-a_b\left[\frac{6}{Re(y)[1+Re(y)V_e(y)]} + \frac{1}{We(y)}\right]\right\} \tag{28}$$

$$Re(y) = \frac{y u_v(y)}{\nu_{susp}}, \quad We(y) = \frac{\rho_{susp} y u_v^2(y)}{\sigma} \tag{29}$$

$$V_e(y) = \frac{Y_0}{\alpha(1-\alpha)}\left[1+\alpha-\frac{(1-\alpha)^2}{1+\alpha}\exp\left(-\frac{1-\alpha}{2Y_0 Re(y)}\right)\right]\exp\left(-\frac{1-\alpha}{2Y_0 Re(y)}\right) - \frac{1}{12} \tag{30}$$

$$Y_0 = \frac{\tau_{elastic}}{\tau_{viscous}} = \frac{E_s}{\rho_{susp} y^2}, \quad \alpha = \sqrt{1-48Y_0} \tag{31}$$

In their "case 3", Chatzi et al. (1989), considered another possible breakage mechanism, namely, that breakage is due to a droplet oscillation resulting from the relative velocity fluctuations. In this case, the breakage rate distribution is given by the product of the number of eddies arriving on the surface of a drop per unit time, and the probability that the arriving eddy will have an energy content greater than the surface energy. Proper estimation of these quantities leads to equation (32), where the number of satellite drops, N_{sa}, and the ratio of volume of daughter to volume of satellite drops, x, are defined by equation (33) (Chatzi et al., 1989; Chatzi and Kiparissides, 1992).

$$g[u(y)] = C_{VII} erfc\left\{\frac{C'_{VIII}\sqrt{\frac{\sigma}{\rho_d}}}{y^{5/6} MD^{2/3}}\left[\frac{N_{da}x^{2/3}+N_{sa}}{(N_{da}x+N_{sa})^{2/3}}-1\right]^{1/2}\right\} \tag{32}$$

$$N_{sa} = 1 + Int[S_{N_{sa}} v_{pa}], \quad x = 1 + S_x v_{pa} \tag{33}$$

Chatzi et al. (1989) selected their breakage and coalescence models based on the best possible overall fit to experimental data of the full PSD in a liquid-liquid dispersion under different conditions of M, η_{susp}, σ, ϕ, and temperature. This approach is perfectly valid and recommended for engineering applications, but it is not enough to judge the theoretical bases and validity of the competing models.

In this paper, the breakage frequency will be calculated using equation (14) with DF(ϕ) defined by equation (20). It will be assumed that $\lambda_{bt} \approx 1$ and $E_{yield} < E_{deformation}$. This last assumption implies that the yield stress is low, which is reasonable at low and intermediate conversions. Under these assumptions, the breakage efficiency is simplified from equation (23) to the expression shown in equation (34).

$$\lambda_b[u(y)] = \exp\left\{-DF(\phi)^2\left[\frac{C_2}{We}\left(\frac{D}{y}\right)^{\frac{5}{3}} + \frac{C_4}{DF(\phi)Re_d}\left(\frac{D}{y}\right)^{\frac{4}{3}}\sqrt{\frac{\rho_c}{\rho_d}}\right]\right\} \tag{34}$$

We found before that our CM-PSD model needed improvement in order to adequately explain the effects of [PVP], ϕ and Sep on the spread of the PSD (Vivaldo-Lima et al., 1998c). The spread of the PSD was underestimated with that model, and the predicted maximum particle sizes were also smaller than the experimental values. This is an indication that the coalescence kernel of the CMD-PSD model may be responsible for these inadequate results. The fact that the effects of the process variables on MPS were adequately explained by the model, seems to indicate that the breakage model is good enough for our application. Therefore, it was decided not to increase the degree of complexity of the breakage model. On the contrary, it was simplified by removing two terms from equation (23) and, thus, decreasing in two the number of fitting parameters.

Depending on the value of the number of daughter drops after breakage of a mother drop, $\zeta[u(y)]$, the breakage kernel is called binary (ζ=2), ternary (ζ=3), or multiple (ζ>3). The multiple breakage case is studied in some detail by Hill and Ng (1996). The daughter drop distribution, $\beta(u,v)$,

has been modelled as a normal distribution function (e.g., Valentas and Amundson, 1966; Coulaloglou and Tavlarides, 1977; Alvarez et al., 1991, 1994), a beta function (Hsia and Tavlarides, 1983), a U-shaped breakage kernel (Hesketh et al., 1991; Kumar et al., 1991; Tsouris and Tavlarides, 1994), and other mathematical functions, as reviewed by Kostoglou et al. (1997). Since we concluded previously that it was the coalescence model which needs improvement, we decided to keep our previous models for ζ and β, namely, equation (35).

$$\zeta[u(y)] = 2\,,\ \beta[u(y),v(z)] = \frac{2.4}{u}\exp\left[-4.5\frac{(2v-u)^2}{u^2}\right] \tag{35}$$

6.3.3.2 Coalescence

The coalescence rate distribution, h[u(y),v(z)], can be expressed as the product of the collision frequency and a coalescence efficiency, as indicated in equation (36). The collision frequency can be estimated using equation (37) (Alvarez et al., 1994; Chatzi and Kiparissides, 1995; Vivaldo-Lima et al., 1998b). As in the case of breakage, the term DF(ϕ) in the coalescence models of Valadez (1988), Alvarez et al. (1991, 1994) and Vivaldo-Lima et al. (1998b) is given by equation (15).

$$h[u(y),v(z)] = \omega_c(u,v)\lambda_c(u,v) \tag{36}$$

$$\omega_c[u(y),v(z)] = C_6(y^2+z^2)\sqrt{y^{\frac{2}{3}}+z^{\frac{2}{3}}}\,\frac{MD^{\frac{2}{3}}}{DF(\phi)} \tag{37}$$

Valadez (1988) assumed that the coalescence efficiency is given by the product of two efficiencies, as indicated in equation (38). The energy efficiency, λ_{ce}, accounts for the efficiency associated to having a collision energetic enough to overcome the resistance to deformation, which is characterized by the yield stress of the droplet. The time efficiency, λ_{ct}, is associated to the slower of two events: (time for) deformation and flow of the droplets, or (time for) liquid film drainage. The energy efficiency used by Valadez (1988) is shown in equation (39).

$$\lambda_c(y,z) = \lambda_{ce}(y,z)\lambda_{ct}(y,z) \tag{38}$$

$$\lambda_{ce}(y,z) = exp\left\{-C_9\frac{(y^3+z^3)^2}{(yz)^3(y+z)^{2/3}}\frac{\rho_c}{\rho_d}\frac{[DF(\phi)]^2D^{2/3}}{Re}\right\} \tag{39}$$

Saldivar et al. (1989) included an energy barrier associated to the interfacial energy in the coalescence energy efficiency, transforming equation (39) into equation (40). This modification to the Valadez model was based on a model developed by Sovova (1981). However, in their calculations they neglected the interfacial energy term by setting $C_{10}= 0$ (Saldivar et al., 1989; Vivaldo-Lima, 1989; Vivaldo-Lima et al., 1998b). Tsouris and Tavlarides (1994) pointed out that the exact representation of the ratio of the interfacial energy to the collision energy leads to an expression somewhat different from the one obtained by Sovova (1981). Equation (41) is equivalent to equation (40) with the correction of Tsouris and Tavlarides (1994).

$$\lambda_{ce}(y,z)=exp\left\{-C_9\frac{(y^3+z^3)^2}{(yz)^3(y+z)^{2/3}}\frac{\rho_c}{\rho_d}\frac{[DF(\phi)]^2D^{2/3}}{Re}-C_{10}\frac{(y^2+z^2)(y^3+z^3)}{(yz)^3(y+z)^{2/3}}\frac{\rho_c}{\rho_d}\frac{[DF(\phi)]^2D^{5/3}}{We}\right\} \tag{40}$$

$$\lambda_{ce}(y,z)=exp\left\{-C_9\frac{(y^3+z^3)^2}{(yz)^3(y+z)^{2/3}}\frac{\rho_c}{\rho_d}\frac{[DF(\phi)]^2D^{2/3}}{Re}-C'_{10}\frac{(y^2+z^2)}{(y^{11}+z^{11})}\frac{\rho_c}{\rho_d}\frac{[DF(\phi)]^2}{WeD^{1/3}}\right\} \tag{41}$$

The coalescence time-efficiency is defined by equation (42), and is determined by the ratio of required time to drain and break the liquid film among colliding drops to the available coalescence time. This time efficiency is the one used in the conventional theoretical approaches to address coalescence of droplets in fluid-liquid dispersions. A very good review on the modelling of coalescence of droplets in fluid-liquid dispersions was presented by Chesters (1991). A numerical study on the drainage and rupture of the liquid film between two drops was carried out by Abid and Chesters (1994).

$$\lambda_{ct} = e^{-\tau_c} = \exp\left\{-\frac{t_{required}}{t_{available}}\right\} \tag{42}$$

Equation (43) shows the coalescence time-efficiency model developed by Valadez (1988) and used by Saldivar et al. (1989) and Vivaldo-Lima et al. (1998b). The droplets in a suspension can be modelled as rigid spheres or as deformable drops, and the continuous phase film as fully mobile, partially mobile, or immobile, depending on the dispersed phase viscosity (Chesters, 1991). Although not explicitly mentioned by Valadez (1988), the development of equation (43) is based on the assumption that the drops are deformable and the interface is immobile. This assumption may be adequate at high conversions in a suspension polymerization, but not at intermediate and low conversions.

$$\lambda_{ct}(y,z) = \exp\left\{-Max\left[\frac{C_7\eta_c\rho_c M^3 D^2 (yz)^4}{[DF(\phi)]^3\sigma^2(y+z)^4}, \frac{C_8[DF(\phi)]^2 D^{4/3} yz}{Re_d(y+z)^{10/3}}\right]\right\} \tag{43}$$

The reason why Valadez (1988) used an energy efficiency (λ_{ce}) was to take into account the resistance for deformation. The equations for film drainage proposed by Chesters (1991) already consider the deformable nature of the droplets. Therefore, in this paper, only a coalescence time-efficiency will be used. Our model for coalescence will be developed building on the film drainage models of Chesters (1991).

Based on the film drainage models of Chesters (1991), Calabrese et al. (1993) developed several expressions for the coalescence efficiency when pairs of drops of equal size collide. For the case of deformable drops when the interface is fully mobile, partially mobile, or immobile, they developed equations (44), (45) and (46), respectively.

$$\lambda_{ct}(y,y) = e^{-\tau_{fm}} = \exp\left\{-\frac{C_c\rho_c y^{5/3}\epsilon^{2/3}}{\sigma}\right\} \tag{44}$$

$$\lambda_{ct}(y,y) = e^{-\tau_{pm}} = \exp\left\{-\frac{C_c\sqrt{\rho_c}\eta_d y^{13/6}\epsilon^{2/3}}{\sigma^{3/2}}\right\} \tag{45}$$

$$\lambda_{ct}(y,y) = e^{-\tau_{im}} = \exp\left\{-\frac{C_c\rho_c\eta_c y^4\epsilon}{\sigma^2}\right\} \tag{46}$$

Equations (44) to (46) can be extended to the non-equal drop size situation by using an equivalent diameter, which can be calculated using equation (47) (Chesters, 1991).

$$y_{eq} = \frac{2yz}{y+z} \tag{47}$$

In order to account for the fact that the viscosity of the droplets changes with time due to polymerization, thus changing the nature of the interface film, we propose to model the coalescence efficiency as a conversion-weighted combination of partially mobile and immobile interfaces, as shown in equation (48), where x is monomer conversion. It should be noted that at low and intermediate conversions the partially mobile mechanism controls the coalescence process, whereas at high conversions the controlling mechanism is that of an immobile interface.

$$\lambda_{ct} = \exp\{-[(1-x)\tau_{pm} + x\tau_{im}]\} \tag{48}$$

Combining equations (45) through (48), a final expression for coalescence efficiency, equation (49), is obtained. The final model for coalescence rate distribution used in this paper consists of equations (36), (37) and (49). As in our previous paper on the CM-PSM model, the intensities of mixing for each zone are estimated using equations (50) to (53), where a and a' are obtained from experimental data or CFD calculations on rate of energy dissipation for the impeller and reactor configuration being used, or as fitting parameters when this information is not available.

$$\lambda_c(y,z)=\exp\left\{-C_7 x \rho_c \eta_c \left(\frac{D}{\sigma}\right)^2 \left(\frac{M}{DF(\phi)}\right)^3 \left(\frac{yz}{y+z}\right)^4 - C_8'(1-x)\frac{\sqrt{\rho_c} D^{4/3} \eta_d}{\sigma^{3/2}} \left(\frac{M}{DF(\phi)}\right)^2 \left(\frac{yz}{y+z}\right)^{13/6}\right\} \quad \textbf{(49)}$$

$$\epsilon = kM^3D^2 \quad \textbf{(50)}$$

$$a = \frac{\epsilon_{impeller}}{\epsilon_{bulk}} \quad , \quad a' = \frac{\epsilon_{average}}{\epsilon_{bulk}} \quad \textbf{(51)}$$

$$\begin{aligned} C_{\alpha,imp} &= a^{\frac{1}{3}} C_{\alpha,bulk} \quad , \quad \alpha = 1,\ 6,\ 7 \\ C_{\beta,imp} &= a^{-\frac{2}{3}} C_{\beta,bulk} \quad , \quad \beta = 2,\ 4,\ 8 \end{aligned} \quad \textbf{(52)}$$

$$\begin{aligned} C_{\alpha,bulk} &= (a')^{-\frac{1}{3}} C_{\alpha,average} \quad , \quad \alpha = 1,\ 6,\ 7 \\ C_{\beta,bulk} &= (a')^{\frac{2}{3}} C_{\beta,average} \quad , \quad \beta = 2,\ 4,\ 8 \end{aligned} \quad \textbf{(53)}$$

6.3.4 Solution Procedure

To solve the PBE under QSSA, a set of N non-linear algebraic equations for the homogeneous model and 2N non-linear algebraic equations for the two-zone model (where N is the number of collocation points), a collocation with the cubic splines technique was used. Unevenly distributed meshes were used (collocation points concentrated on the small droplet size range of the distribution), with 10 to 30 collocation points. The PBE was solved using scaled variables in order to reduce numerical problems. The scale factor was chosen based on *a priori* estimate of the mean volume of the PSD. Because of the QSSA, it was not necessary to solve the kinetic equations and the PBE simultaneously, although it was necessary to know the results for conversion and weight average molecular weight (or viscosity) prior to solving the PBE.

The selection of the initial estimates for the density distributions, f_1 and f_2, at each collocation point, was a crucial step. If these estimates were not good enough, convergence would be very difficult or even impossible to achieve. In our previous papers, four types of estimates were used in our calculations: (i) estimation of the PSD for each zone assuming that f_1 and f_2 are given by a Gamma distribution function (mean and variance estimates were required), (ii) same as (i), but assuming normal (instead of Gamma) distribution functions, (iii) providing rough estimates of f_1 and f_2 at each collocation point from experimental PSD measurements, and (iv) providing the output solution from a different case or a non-converged one. In addition to these initial estimates, in this present paper we tried using lognormal distribution functions, and a combination of normal (for the impeller zone) and lognormal (for the bulk zone) distribution functions, which provided better results.

For the transient solution to the PBE, an adequate integration method for stiff systems should be used (e.g., Gear's method). Alvarez et al. (1991, 1994) used an implicit Euler method with variable integration step. When the transient solution to the PBE is sought, the ODEs that describe the polymerization kinetic model (shown in Table 6.4) should be solved simultaneously. Our model copolymerization system includes crosslinking reactions, which lead to a stiff system of ODEs (Vivaldo-Lima et al., 1994). Considering in addition that the QSSA solution to the PBE with the present model and 30 collocation points consumed a significant amount of computing time, and that a converged solution was not always possible (a very good estimate of the solution was needed to obtain a converged solution), no transient calculations were carried out in this paper.

6.4 Results and discussion[2]

The experimental data obtained to determine the relative importance of the process factors on the PSD in suspension copolymerization of styrene/divinylbenzene in a previous paper of our group (Vivaldo-Lima et al., 1998c), are also used here to evaluate the performance of our improved CM-PSD

[2]The PSDs shown in Figures 6.3 to 6.7 are normalized with respect to particle volume, but plotted against particle diameter. The area under the curve will be one if particle size is represented as volume.

model. Only final PSDs were measured due to the difficulty associated to the manipulation of samples with high monomer content. The values of the model parameters are reported in Table 6.5.

Table 6.5 Values for model parameters.

Parameter	Value	Comments
a	50	Vivaldo-Lima et al. (1998b)
a'	35	Sensitivity analysis (SA)
$C_{1,\,average}$	1.0	Alvarez et al. (1994)
$C_{2,\,average}$	0.0625	SA
$C_{4,\,average}$	6×10^{-3}	SA
$C_{6,\,average}$	1×10^{-3}	Alvarez et al. (1994)
$C_{7,\,average}$	1×10^{3}	SA
$C_{8,\,average}$	6×10^{-3}	SA
N_p	1.4	Zhou and Kresta (1996)
N_Q	0.776	Kresta and Wood (1993)
V_{imp}/V_t	Equation (10)	See text
η_d, Pa·s	1000	Set to a reasonable value (not measured)
σ, g/s^2	40	Horák et al. (1981) for a PVP/GMA:EDMA system (same stabilizer, different monomers)

Figure 6.3 shows experimental (replicated) and simulated PSDs at the conditions of run "a". The broken line was obtained with our original CM-PSD model (Vivaldo-Lima et al., 1998b), and the solid line with the modifications reported in this paper. The simulation line for the improved model shown in this figure converged to a tolerance in the order of 1.0. The specified tolerance of 10^{-8} was not reached. Although the spread of the distribution is captured better with the improved model, it seems as if the number of particles of small size was overpredicted, and the number of particles of larger size underpredicted. However, it is also observed that the lower size range of the PSD is incomplete in the experimental data due to physical constraints. The aperture size of the cell used in

the Coulter counter was not able to cover the whole range of the distribution. In order to compare the distributions, the experimental data were normalized by dividing the area of each channel by the total area under the curve of number of drops versus particle volume. If the full distribution was possible to obtain, then the area of the large particles zone would decrease, thus resembling the shape of the simulated (improved) profile.

In all the remaining figures, two experimental profiles are shown. The reason is that two samples of the same batch were measured in each case for batches b, 1, 2, and 3. This is different from the case of run a, where the independent measurements of several samples of the same batch were lumped and the run was replicated (Vivaldo-Lima et al., 1998b).

Figure 6.4 shows the results for run "b". Although the experimental PSD looks unimodal, there was also a significant portion of small particles not counted. What seems surprising in this case, given the fact that run b was obtained at higher speed of agitation and faster polymerization rate than run a, is the much broader PSD obtained for run b, in comparison with run a. The records for run b showed that there was an unusual temperature oscillation possibly caused by a fluctuation in the flow of cooling water. This temperature fluctuation could have caused the broadening of the distribution by promoting unusual variation in the polymerization rate.

Figures 6.5, 6.6 and 6.7 show the results obtained for runs 1, 2 and 3. Run 1 is clearly bimodal, run 2 looks unimodal, and run 3 seems to be bimodal. As mentioned before for run b, it is likely that run 2 is also bimodal. Given the difficulty in obtaining converged solutions to the PBEs with our solution procedure, no simulations were included in Figures 6.4 to 6.7, although similar results to those shown in Figure 6.3 would be expected.

A further consideration in the evaluation and validation of our CM-PSD model would be to simulate the evolution of the PSD with conversion, and make a comparison of the calculated Sauter diameter (d_{32}) using this model with experimental data from the literature (e.g., Konno et al., 1977). The result of this analysis would indicate if the solution of the transient model is indeed needed, or if the QSSA is good enough for engineering calculations.

6.5 Concluding Remarks

An improved model for PSD in suspension polymerization was obtained with the aid of a previous Bayesian experimental design study, which indicated what aspects of the model were still poor. The changes that we made were indeed simple, but unnecessary refinements to other aspects of the model might have been attempted, had we not known these results.

The effect of the disperse phase hold-up on the spread of the PSD was improved by using an adequate correlation for viscosity of a suspension [equation (18)]. The effect of separation between impellers in a single shaft was refined by using equation (10) to estimate the volume of the impeller zone. Although this approximation was considered in our former version of the model (Vivaldo-Lima et al., 1998b), the estimated value was changed during the generation of the "prior knowledge" needed for the Bayesian experimental design technique (Vivaldo-Lima et al., 1998c), in an attempt to obtain faster converging solutions. The importance of the stabilizer was enhanced by using more sound models for liquid film drainage between two colliding drops [equations (44) to (48)].

If one compares our final model equations and the models of Valadez (1988) or Alvarez et al. (1994), it can be noticed that the generalized Newtonian rheology model of Valadez (1988), or the Maxwell fluid model of Alvarez et al. (1994) were transformed into a much simpler (and certainly more unrealistic for polymer flow) Newtonian rheology model. Experts in the rheology field (e.g., Tanner, 1992; Vlachopoulos, 1994) agree with the fact that the choice of constitutive models for engineering problems needs only be the adequate one for the purpose at hand, and not the most complex (no matter how realistic) one. Tanner (1992) has provided guidelines to choose constitutive models for different applications, depending on the characteristics of the flow. Several classes of flows have been defined and the different constitutive equations "graded" for performance in actual applications. Among those categories, the cases of steady viscosity and elongation in polymer flow should be of interest for our application. For these two properties, both the Maxwell and the Newtonian models are classified as "P" (possible or poor). The generalized Newtonian is "E" (excellent) for steady viscosity, but also poor for elongation. In other words, although the Maxwell

model is excellent for illustrating the viscoelastic behaviour of polymers under flow, it is a poor model for actual engineering applications (where precision and reliability are important). Therefore, although much simpler in terms of the rheological equations, our model is not inferior to the one of Alvarez et al. (1994).

More than the model itself, an important aspect that needs to be enhanced in our case, is the solution procedure for the population balance equations. The group of Alvarez (1991, 1994) has developed a more robust and effective solution procedure than ours. In our review (1997), more references to work done by other research groups that have made significant contributions to the solution of population balance equations are offered.

Acknowledgements

The authors wish to acknowledge financial support from the Science and Technology National Council (CONACYT) of Mexico, and the Natural Sciences and Engineering Research Council (NSERC) of Canada. The assistance of Ms. Wen-Hui Li and Professor Harald Stöver (Chemistry Dept., McMaster University) with the PSD measurements is greatly appreciated.

6.6 Nomenclature

a, a' = compartment-mixing parameters, defined by equation (51)

A = heat transfer area, m^2 (Table 6.4)

a_b = constant in the model of Alvarez et al. (1994)

C_α, C_ϕ= model parameters (α= 1, 2, ..., 10)

Cp = heat capacity, J/K

D = impeller diameter, cm

DF(ϕ)= damping factor, defined by equation (17)

E = energy term, $g \cdot cm^2 \cdot s^{-2}$

E_s = suspension elasticity modulus, $g \cdot cm^{-1} \cdot s^{-2}$

f = normalized droplet volume distribution (also used to represent initiator efficiency)

f_2 = relative divinyl monomer concentration (Table 6.4), or "f" at the bulk zone

F = droplet volume distribution, number of particles per litre

F_2 = instantaneous relative composition of monomer 2 in the polymer, or "F" at the bulk zone

g = breakage rate distribution, s^{-1}

h = coalescence rate distribution, s^{-1}

ΔH = heat of reaction, J/mol

[I] = initiator concentration, mol/L

k = kinetic energy, $g \cdot cm^2 \cdot s^{-2}$, or proportionality constant in equation (50)

k_{cp} = constant for primary cyclization

k_{cs} = constant for secondary cyclization

k_d = initiator decomposition kinetic constant, s^{-1}

k_{fm} = pseudo-kinetic rate constant for chain transfer to monomer, $L \cdot mol^{-1} \cdot s^{-1}$

k_{fp} = pseudo-kinetic rate constant for chain transfer to polymer, $L \cdot mol^{-1} \cdot s^{-1}$

k_{fT} = pseudo-kinetic rate constant for chain transfer to small molecule, $L \cdot mol^{-1} \cdot s^{-1}$

k_p = pseudo-kinetic propagation rate constant, $L \cdot mol^{-1} \cdot s^{-1}$

k_p^* = pseudo-kinetic rate constant for crosslinking reaction, $L \cdot mol^{-1} \cdot s^{-1}$

k_{td} = pseudo-kinetic rate constant for termination by disproportionation, $L \cdot mol^{-1} \cdot s^{-1}$

k_{tcn} = number average pseudo-kinetic rate constant for termination by combination, $L \cdot mol^{-1} \cdot s^{-1}$

k_{tcw} = weight average pseudo-kinetic rate constant for termination by combination, $L \cdot mol^{-1} \cdot s^{-1}$

M = speed of agitation, rps

[M] = total monomer concentration, mol/L

n = molar mass, mol (Table 6.4)

N = number of droplets in the PBE, or speed of agitation (Tables 6.1 and 6.2), rps

N_{ds} = number of drops of equal volume from breakage of a parent drop

N_{imp} = number of impellers on the same shaft

N_{ss} = number of satellite drops from breakage of a parent drop

N_Q = flow number

Q = volumetric flow, mL/s (defined by equation (14))

Q_0 = zeroth moment of the dead polymer distribution, mol/L

Q_1 = first moment of the dead polymer distribution, mol/L

Q_2 = second moment of the dead polymer distribution, mol/L

[R˙] = overall polymer radical concentration, mol/L

Re = Reynolds number

R_p = polymerization rate, $mol \cdot L^{-1} \cdot s^{-1}$

S_v, S_{Nss} = parameters (slops) of equation (33) (Chatzi and Kiparissides, 1992)

Sep = separation distance between impellers, cm

t = time, s

T = tank diameter, cm (also used to represent temperature in Table 6.4, °C)

[T] = concentration of small molecule species (either solvent or chain transfer agent), mol/L

u, v = droplet volume, mL

u_v = drop velocity, cm/s

U = combined heat transfer coefficient, $W \cdot m^{-2} \cdot K^{-1}$

V = volume, L

W = blade width, cm

We = Weber number

x = total monomer conversion, or ratio of daughter to satellite droplet volumes

y, z = droplet diameter, cm

Y_0 = zeroth moment of the polymer radical distribution (polymer radical concentration), mol/L

Y_1 = first moment of the polymer radical distribution, mol/L

Y_2 = second moment of the polymer radical distribution, mol/L

Z_1, Z_2 = distance from top of tank to impeller position, cm (see Vivaldo-Lima et al., 1998c)

Greek letters

β = normalized daughter drop distribution

ϵ = rate of energy dissipation, cm^2/s^2

ζ = number of daughter drops after breakage of a mother drop (assumed equal to two)

η = viscosity, Pa·s

λ = efficiency

ν = kinematic viscosity, cm^2/s [equation (29)]

ρ = density, g/cm^3 (also used to represent crosslink density in Table 6.4)

σ = interfacial tension, g/s^2, or standard deviation

τ_0 = yield stress, $g \cdot s^{-2} \cdot cm^{-1}$

ϕ = phase holdup (volume of water to volume of monomer)

ω = frequency, s^{-1}

Subscripts

1 = impeller zone

2 = bulk zone

3 = overall distribution

b = bulk zone (also indicated as 2), or breakage

c = continuous phase, or coalescence

d = dispersed phase

e = energy

i = impeller zone (also indicated as 1, or "imp")

in = inlet stream

m = monomer/polymer mixture

p = polymerization

pa = parent drop

r = reaction

s = suspension (also indicated as "susp")

t = overall (total), or time

v = viscous

w = cooling water

Abbreviations

3-D = three-dimensional

ASM = algebraic stress model

CM = compartment model

CSTR = continuous stirred tank reactor

CTA = chain transfer agent

CV = coefficient of variation (MPS/σ_{vol})

EDMA= ethylene dimethacrylate

GMA = glycidyl methacrylate

MPS = mean particle size, cm^3

ODE = ordinary differential equation

PBE = population balance equation

PBT = pitched bladed turbine

PSD = particle size distribution

PVP = polyvinyl pirrolydone

QSSA = quasi-steady-state assumption

6.7 References

Abid, S. and A. K. Chesters, "The drainage and rupture of partially-mobile films between colliding drops at constant approach velocity", *Int. J. Multiphase Flow*, **20(3)**, 613-629 (1994).

Alvarez, J., J.J. Alvarez and R.E. Martínez, "Conformation of the particle size distribution in suspension polymerization. The role of kinetics, polymer viscosity and suspension agent", *J. Appl. Polym. Sci.: Appl. Polym. Symp.* **49**, 209-221 (1991).

Alvarez, J., J.J. Alvarez and J.M. Hernández, "A population balance approach for the description of particle size distribution in suspension polymerization reactors", *Chem. Eng. Sci.* **49**, 99-113 (1994).

Calabrese, R. V., A. W. Pacek and A. W. Nienow, "Coalescence of viscous drops in a stirred dispersion", pre-prints of *The 1993 I Chem E Research Event*, University of Birmingham, U.K., 642-644, January 1993.

Chatzi, E.G., A.D. Gavrielides and C. Kiparissides, "Generalized model for prediction of the steady-state drop size distributions in batch stirred vessels", *Ind. Eng. Chem. Res.*, **28**, 1704-1711 (1989).

Chatzi, E.G. and C. Kiparissides, "Dynamic simulation of bimodal drop size distributions in low-coalescence batch dispersion systems", *Chem. Eng. Sci.* **47**, 445-456 (1992).

Chatzi, E.G. and C. Kiparissides, "Steady-state drop-size distributions in high holdup dispersion systems", *AIChE J.* **41**, 1640-1652 (1995).

Chesters, A. K., "The modelling of coalescence processes in fluid-liquid dispersions: a review of current understanding", *Trans. Inst. Chem. Eng.*, **69**, Part A, 259-270 (1991).

Coulaloglou, C. A. and L. L. Tavlarides, "Description of interaction processes in agitated liquid-liquid dispersions", *Chem. Eng. Sci.*, **32**, 1289-1297 (1977).

Doulah, M. S., "On the effect of holdup on drop sizes in liquid-liquid dispersions", *Ind. Eng. Chem. Fundam.*, **14**, 137 (1975).

Hesketh, R. P., A. W. Etchells and T. W. F. Russell, "Bubble breakage in pipeline flow", *Chem. Eng. Sci.*, **46**, 1-9 (1991).

Hill, P. J. and K. M. Ng, "Statistics of multiple particle breakage", *AIChE J.*, **42(6)**, 1600-1611 (1996).

Horák, D., Z. Pelzbauer, S. Švec and J. Kálal, "Reactive polymers XXXIII. The influence of the suspension stabilizer on the morphology of a suspension polymer", *J. Appl. Polym. Sci.*, **26**, 3205-3211 (1981).

Hsia, M. A. and L. L. Tavlarides, "Simulation and analysis of drop breakage, coalescence, and micromixing in liquid-liquid stirred tanks", *Chem. Eng. J.*, **26**, 189 (1983).

Hunter, R. J., "Introduction to Modern Colloid Science", Ch. 4, 1st. Edition, Oxford University Press, Oxford, 1993.

Konno, M., K. Arai and S. Sato, "The effect of stabilizer on coalescence of dispersed drops in suspension polymerization of styrene", *J. Chem. Eng. Japan*, **15(2)**, 131-135 (1982).

Kostoglou, M., S. Dovas and A.J. Karabelas, "On the steady-state size distribution of dispersions in breakage processes", *Chem. Eng. Sci.*, **52(8)**, 1285-1299 (1997).

Kresta, S.M. and P.E. Wood, "The flow field produced by a pitched blade turbine: characterization of the turbulence and estimation of the dissipation rate", *Chem. Eng. Sci.* **48**, 1761-1774 (1993b).

Kumar, S., R. Kumar and K. S. Gandhi, "Alternative mechanisms of drop breakage in stirred vessels", *Chem. Eng. Sci.*, **46**, 2483-2489 (1991).

Saldívar-Guerra, E., E. Vivaldo-Lima and L.E. Gómez-Cadena, "Simulación de la distribución de tamaños de partícula en polimerización en suspensión empleando colocación con splines. Comparación con datos industriales" (in Spanish), X Encuentro Nacional AMIDIQ, Universidad de Guadalajara, Guadalajara, Jalisco, Mexico (1989).

Sovova, H., "Breakage and coalescence of drops in a batch stirred vessel. II. Comparison of model and experiments", *Chem. Eng. Sci.*, **36**, 1567 (1981).

Tanner, R. I., "Engineering rheology", Ch. 5, Revised Edition, Oxford University Press, New York (1992).

Tobin, T. and D. Ramkrishna, "Coalescence of charged droplets in agitated liquid-liquid dispersions", *AIChE J.*, **38(8)**, 1199-1205 (1992).

Tsouris, C. and L. L. Tavlarides, "Breakage and coalescence models for drops in turbulent dispersions", *AIChE J.*, **40(3)**, 395-406 (1994).

Valadez-González, A., "Evolución de la distribución de tamaños de partículas en una polimerización en suspensión", M. Eng. Thesis (In Spanish), Unidad de Ciencias Básicas e Ingeniería, Universidad Autónoma Metropolitana, Plantel Iztapalapa, México D.F., Mexico (1988).

Valentas, K. J. and N. R. Amundson, "Breakage and coalescence in dispersed phase systems", *Ind. Eng. Chem. Fundam.*, **5(4)**, 533-542 (1966).

Vivaldo-Lima, E., "Simulación del proceso de polimerización de estireno via suspensión", B.Sc. Thesis (in Spanish), Facultad de Química, Universidad Nacional Autónoma de México (UNAM), Ciudad Universitaria, México D.F., Mexico (1989).

Vivaldo-Lima, E., A.E. Hamielec and P.E. Wood, "Batch reactor modelling of the free radical copolymerization kinetics of styrene/divinylbenzene up to high conversions", *Polym. React. Eng.* **2**, 87-162 (1994).

Vivaldo-Lima, E., P. E. Wood, A. E. Hamielec and A. Penlidis, "An updated review on suspension polymerization", *Ind. Eng. Chem. Res.* **36**, 939-965 (1997).

Vivaldo-Lima, E., "Development of an effective model for particle size distribution in suspension copolymerization of styrene/divinylbenzene", PhD Thesis, Department of Chemical Engineering, McMaster University, Hamilton, Ontario, Canada (1998).

Vivaldo-Lima, E., P. E. Wood, A. E. Hamielec and A. Penlidis, "Kinetic Model-Based Experimental Design of the Polymerization Conditions in Suspension Copolymerization of Styrene/ Divinylbenzene", *J. Polym. Sci., Polym. Chem.* **36**, 2081-2094 (1998a).

Vivaldo-Lima, E., P. E. Wood, A. E. Hamielec and A. Penlidis, "Calculation of the Particle Size Distribution in Suspension Polymerization using a Compartment-Mixing Model", *Can. J. Chem. Eng.* **76**, 495-505 (1998b).

Vivaldo-Lima, E., A. Penlidis, P. E. Wood and A. E. Hamielec, "Importance of Process Factors on Particle Size Distribution in Suspension Polymerization", in preparation, (1998c).

Vlachopoulos, J., "Chem. Eng. 772 Polymer Rheology Course Notes", Department of Chemical Engineering, McMaster University, Hamilton, Ontario, Canada (1994).

Zhou, G. and S. M. Kresta, "Distribution of energy between convective and turbulent flow for three frequently used impellers", *Trans. Inst. Chem. Eng.* **74**, Part A, 379-389 (1996).

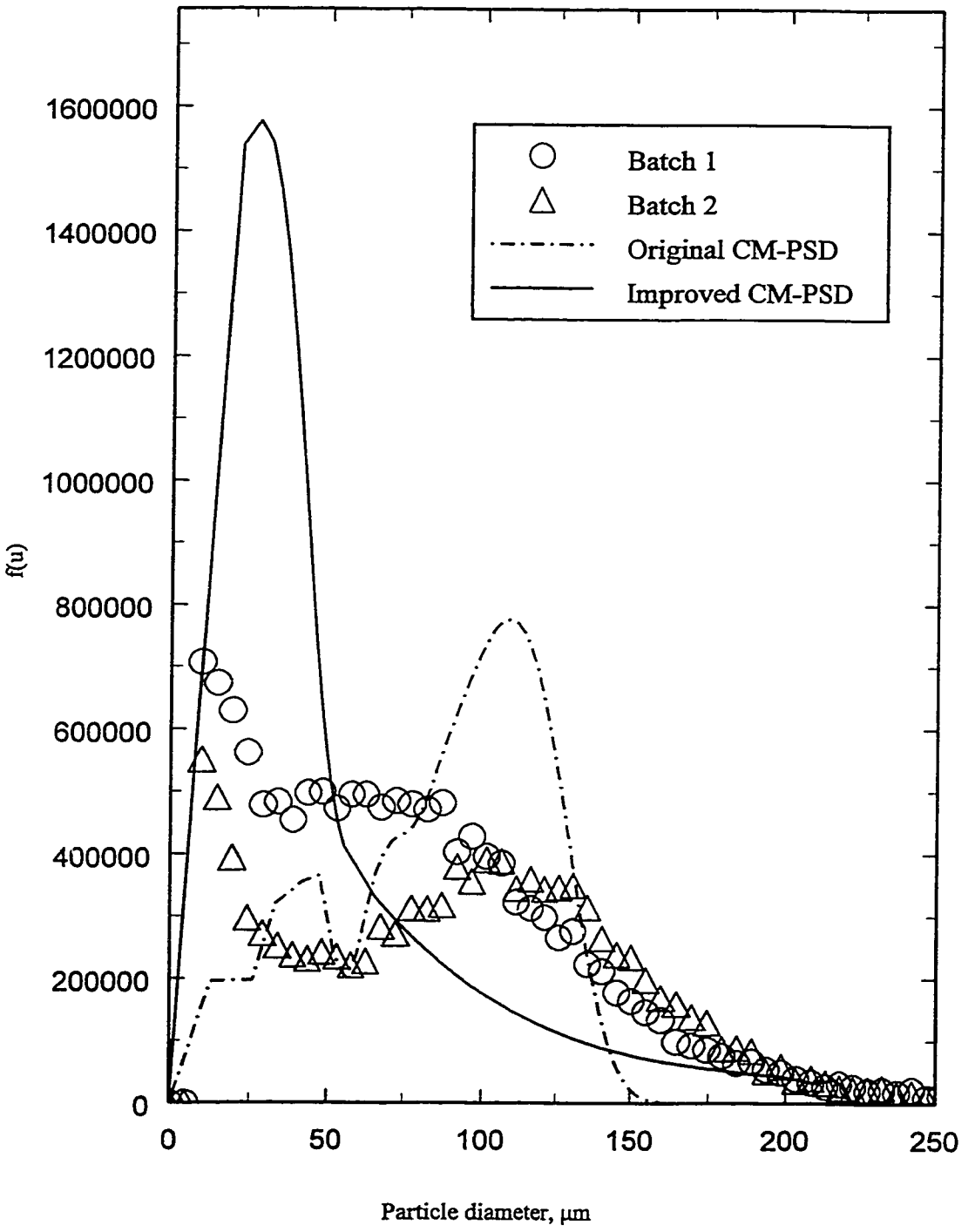

Figure 6.3 Final PSD in suspension copolymerization of styrene and divinylbenzene. Comparison of original and improved CM-PSD model predictions against (replicated) experimental data for run "a".

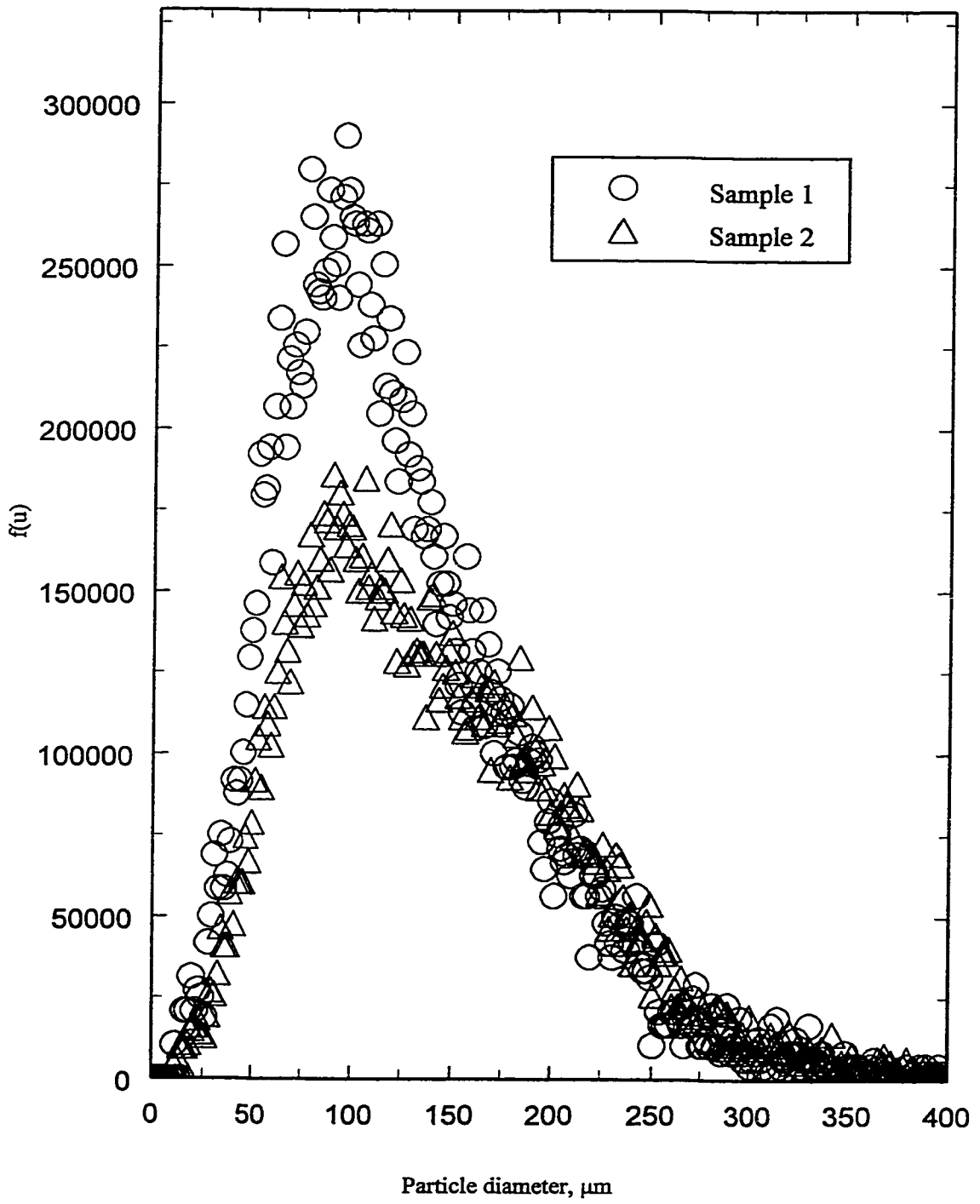

Figure 6.4 Final PSD in suspension copolymerization of styrene and divinylbenzene. Experimental data for run "b".

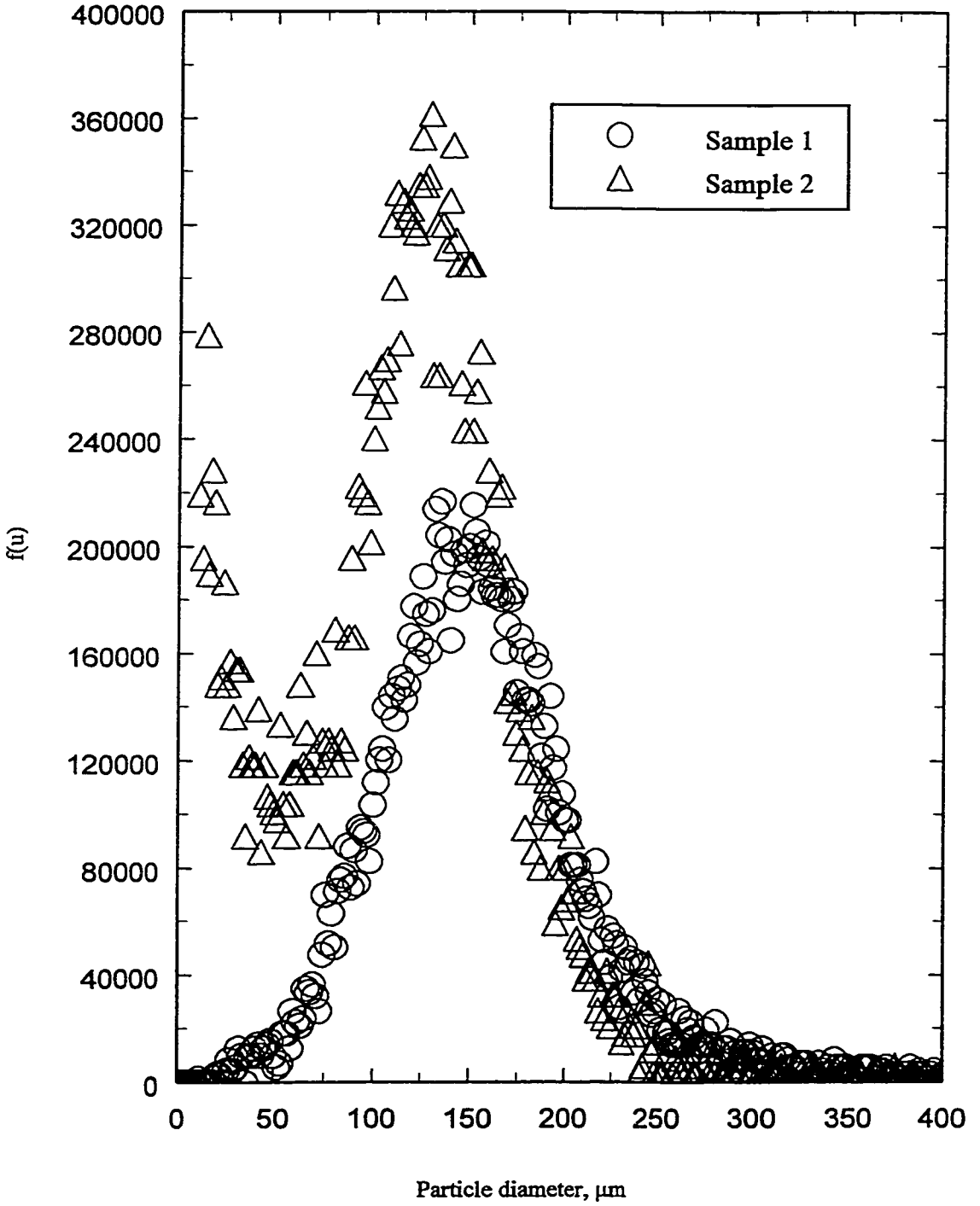

Figure 6.5 Final PSD in suspension copolymerization of styrene and divinylbenzene. Experimental data for run "1".

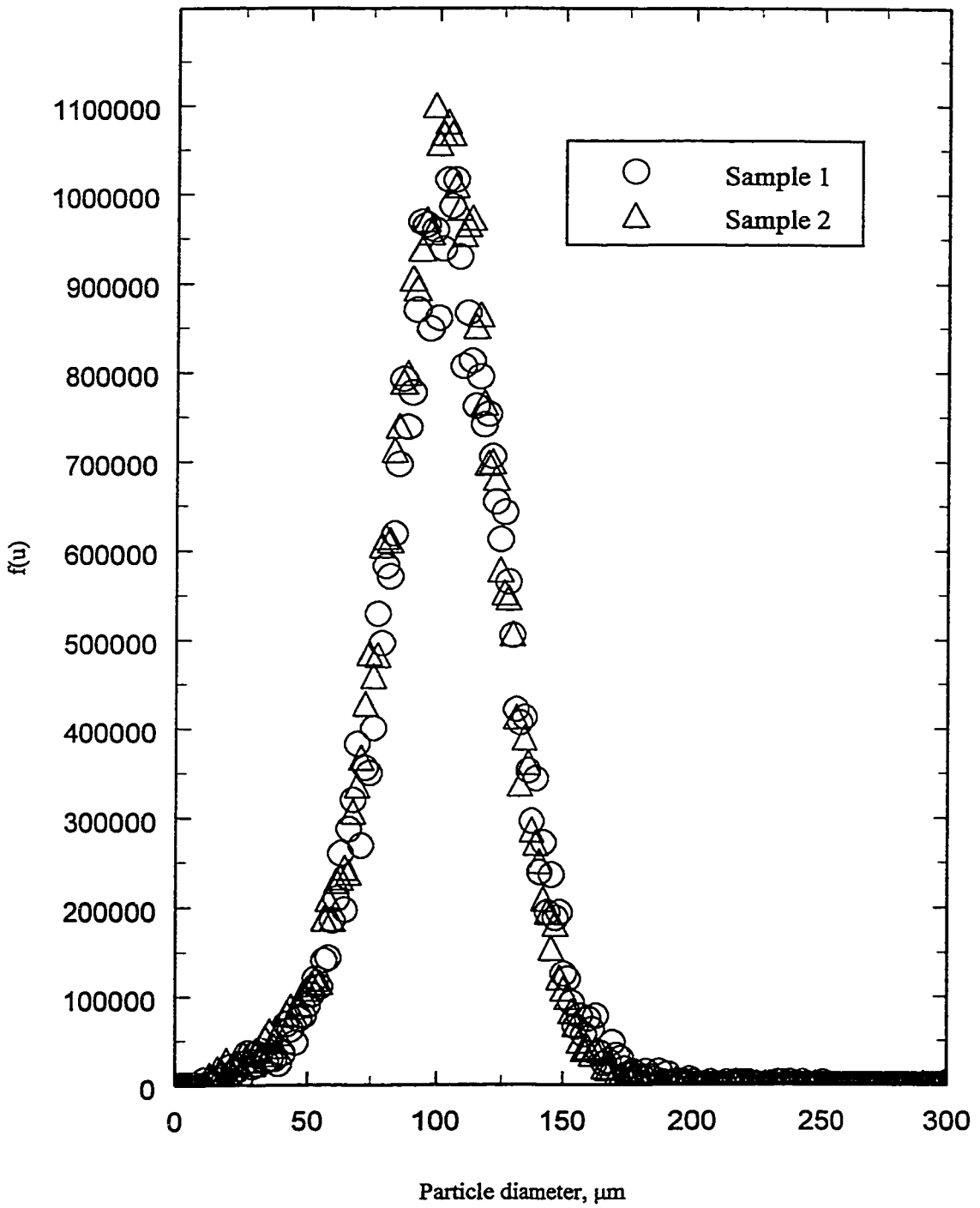

Figure 6.6 Final PSD in suspension copolymerization of styrene and divinylbenzene. Experimental data for run "2".

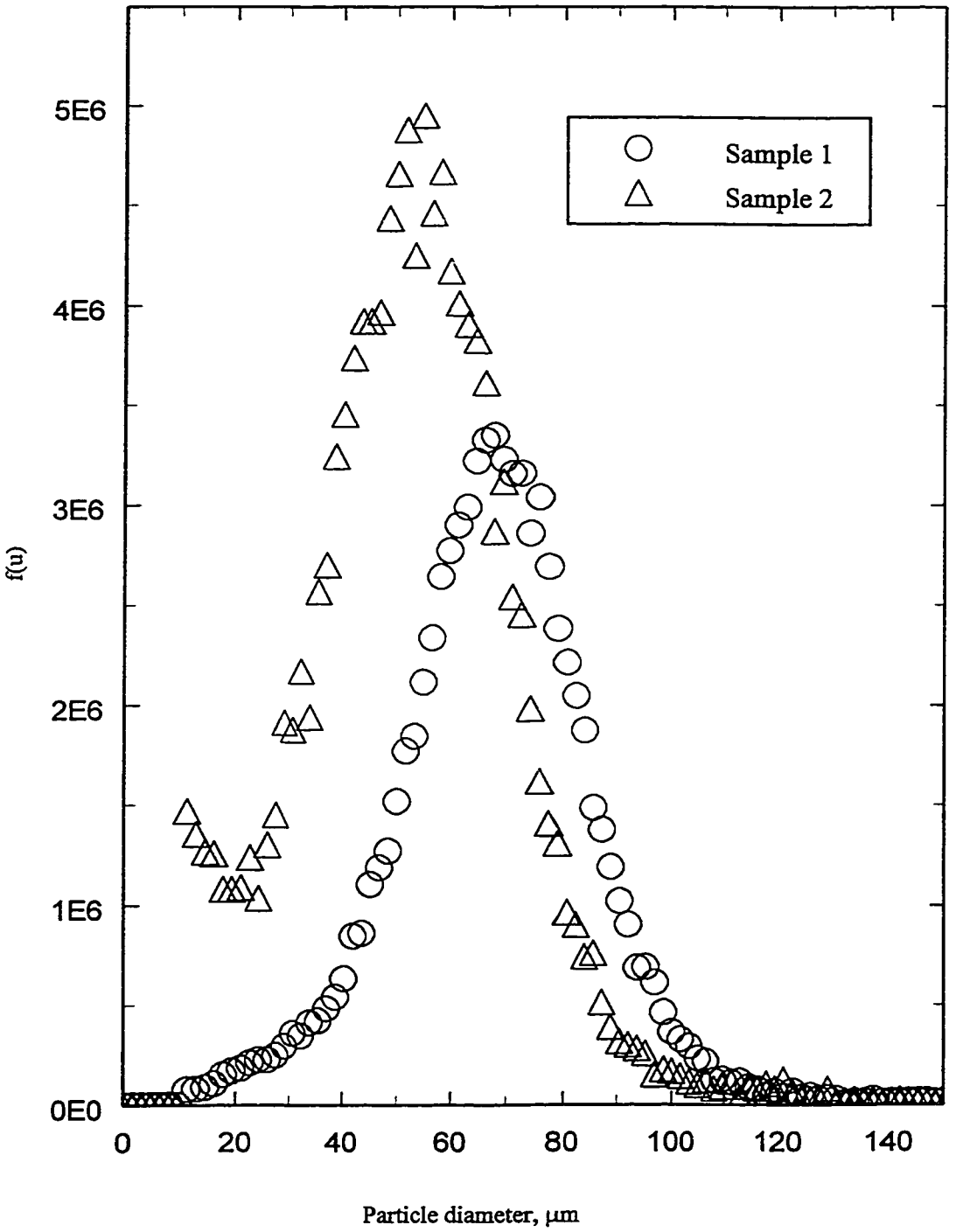

Figure 6.7 Final PSD in suspension copolymerization of styrene and divinylbenzene. Experimental data for run "3".

Chapter 7

General Conclusions and Recommendations for Future Research

7.1 Conclusions and Contributions to Knowledge

The goal of developing an effective mathematical model for estimation of the particle size distribution (PSD) in suspension copolymerization of styrene/divinylbenzene has been accomplished. The model developed herein has the unique characteristics of being reasonably easy to solve, and possessing a solid and balanced theoretical background. All the important phenomena known to affect the PSD were included in the model. To highlight the characteristics of this model and visualize the importance of the contributions to knowledge derived from this thesis, it is instructive to explain them in relation to the objectives defined in Chapter 1.

a) By carrying out a detailed review and critical analysis of the existing literature in the field, the key factors that control the PSD in suspension polymerization were identified (Chapters 1 and 2), and their relative importance quantified, using a Bayesian experimental design technique (Chapter 5). Most previous models for PSD in liquid-liquid dispersions or suspension polymerization are either empirical, or highly biased towards the field of expertise of their originators. Since the phenomena taking place in suspension polymerization in stirred tank reactors are diverse, complex and highly inter-dependent, it is necessary to use mathematical equations at the same level of complexity to model them. An effective methodology consisting of gradual, sequential and alternating implementation of model-development and experimental-validation steps (e.g., analysis of experimental facts/model building/experimental validation/model improvement/model-based experimental design/...) has been successfully implemented. This approach is ideal for analysis of complex processes.

b) An effective (namely, accurate and simple) model for the free-radical crosslinking copolymerization kinetics of styrene/divinylbenzene was developed in the author's Masters of Engineering Thesis (1993). The predictive power of this model was tested in the present thesis. The high reliability of the model predictions made it possible to use the model as an effective design tool. The model developed by the author of this thesis is the only one which has been demonstrated to be useful for actual engineering calculations, providing simultaneous reliable predictions for several properties (conversion, gel content, copolymer composition and molecular weight averages), without having to re-estimate or change the parameters of the model every time a different polymer property is being calculated, or a process condition changed.

c) Effective models for breakage and coalescence in suspension polymerization were selected from the best available in the literature or developed in this thesis. In doing the selection and development, the most important drawbacks of the former models were identified and overcome. This will allow other researchers in this area to avoid using inadequate models and focus their expertise towards the remaining weak aspects about these phenomena.

d) The important effect of non-homogeneous mixing on the PSD was incorporated into the model in a balanced and effective way. This is the first time in modelling of PSD in suspension polymerization reactors that non-homogeneous mixing is considered. It was demonstrated that assuming homogeneous mixing is inadequate. Any refinement made to other PSD models that does not consider this effect will be of limited value and uncertain predictive power capabilities.

e) The mathematical equations that model the different phenomena in suspension polymerization (polymerization kinetics, surface phenomena, mixing and dispersion concentration) were incorporated into a population balance equation. Although several simplifications were made to solve the equations (such as the QSSA), the selection of the mechanistic models was so effective, that adequate predictions of actual copolymerizations could be obtained.

f) The predictive power of the PSD model developed in this thesis is still limited. Nonetheless, it can be considered as one of the most reliable models presently available in the open literature. The limitations and deficiencies still present in the PSD model have been identified and a strategy to improve it has been designed and its implementation is already under way.

As explained in Chapter 1, most of the results of this thesis have been published or accepted for publication in highly prestigious technical journals of the polymer and chemical engineering areas. The fact that none of the papers has been rejected serves as an indication of the value that the reviewers have put in their content.

Although this thesis dealt with a specific problem (PSD in suspension polymerization) and a specific system (styrene/divinylbenzene), the research approach undertaken here to accomplish our objectives is very much applicable and recommended for other processes and situations where many complex phenomena simultaneously affect the responses of interest.

7.2 Suggested Guidelines for Future Research.

There are several ways in which the model for PSD in suspension polymerization developed in this thesis can be improved, and our understanding of the involved phenomena increased. The proposed guidelines described next are related to the important factors described in Figure 1.2 and Table 1.1 of Chapter 1, as well as the authors's critical literature review in Chapter 2.

7.2.1 Polymerization Kinetics.

There is no real need to introduce changes to our model for crosslinking free-radical copolymerization kinetics in order to model PSDs in suspension copolymerization. However, that does not mean that the model is perfect.

Our kinetic model can provide different averages of the molecular weight distribution (MWD), but not the full distribution. Teymour and Campbell (1994) proposed a gelation model based on the "numerical fractionation" technique, which can provide the full MWD. Their model is fairly easy to

solve and their ideas appealing. Tobita (1995, 1997) has severely criticized the model of Teymour and Campbell, particularly because of its "obscure validity" due to their "unproven" assumptions (regarding the assumption of representing each fraction with a Schulz-Zimm distribution). He himself has proposed to model the full MWD using a "Monte Carlo sampling technique" [e.g., Tobita (1995, 1996, 1997a, 1997b)]. Without disregarding Tobita's views, it is the author's belief that a combination of the model of Vivaldo-Lima (1993) (which is indeed based on the Tobita-Hamielec model) and the one of Teymour and Campbell (1994) could lead to a powerful practical model capable of providing reliable enough estimates (for engineering applications) of the full MWD.

As explained in Vivaldo-Lima (1993), the author's model for crosslinking free-radical copolymerization should be tested with other systems [e.g., copolymerization of methyl methacrylate (MMA)/ethylene glycol dimethacrylate (EGDMA)], and other conditions (e.g., semi-batch reactors, variable temperature intervals, etc.), in order to generalize further.

7.2.2 Mixing in Stirred Tank Reactors

As explained in Chapter 2, the state of the art in modelling of mixing in stirred tank reactors is much more advanced and sophisticated than what is needed for modelling of PSD in suspension polymerization. CFD simulations or experimental measurement of turbulence quantities (e.g., rate of energy dissipation) in stirred tank reactors should be carried out whenever changes in the reactor configuration or the agitator design take place. Having this information available can increase tremendously the reliability of the model predictions obtained with our CM-PSD model.

Our model for PSD and the detailed characterization of the turbulent flow for different agitators and vessel configurations can be used to design the polymerization conditions required to produce a product of narrower PSD. These two tools can also be used to simplify the procedures in place to carry out studies on scaling up (or down) of suspension polymerization reactors.

7.2.3 Breakage and Coalescence Models

Breakage and coalescence are complex phenomena with many variables into play. This situation makes it difficult to discriminate among different theoretical models. From the author's point of view, there are two approaches that should be followed in order to validate a proposed mechanism. The first one is to design experiments where the actual breakage and coalescence events can be observed. The second one is to use adequate statistical tools for model building and model discrimination purposes.

Regarding the visual observation of breakage and coalescence, two projects were designed and tried during the development of this thesis. Using laser sheet illumination (LSI) and high speed video-filming techniques, dilute dispersions of (dyed) mineral oil in water in a 1 gallon plexy-glass vessel with baffles and a pitched blade turbine impeller at turbulent flow were prepared, in an attempt to capture in film the actual breakage and coalescence events taking place inside the vessel. It was possible to observe some breakage events but only at very low Reynolds numbers (laminar flow). It was not possible to observe these events at high Reynolds numbers with the resources available. In the other project, we tried to calculate PSDs in different zones of the acrylic vessel for the same mineral oil dispersion system from the corresponding images obtained with a high speed video camera. This second visualization study was aimed at proving that non-uniform mixing promotes the formation of bimodal (or multi modal) PSDs. Time restrictions and insufficient familiarity of the author with the laser equipment and the image analysis software caused the second project to be aborted. These two projects could be carried out by other researchers interested in these phenomena.

Regarding the use of adequate statistical techniques for model building and model discrimination, Chapters 5 and 6 of this thesis are an example of the former. Using a Bayesian experimental design technique we guided the model building for the improvement of our PSD model. We used a linear model to determine the relative importance of the process factors. A more efficient approach would be to use the Bayesian method with a non-linear model. In order to compare our model against others, statistical model discrimination techniques can be used [e.g., Burke et al. (1994a, 1994b), or Stewart et al. (1996, 1998)].

7.2.4 Surface Phenomena and Other Aspects.

Much of this thesis was focused on developing sound models for copolymerization kinetics and non-homogeneous mixing. Although we chose the most comprehensive, yet simple enough, models available in the literature to model the effect of stabilizer concentration and disperse phase hold-up on the PSD, our results from Chapter 5 indicated that these aspects were captured rather weakly in our PSD model. In Chapter 6 we enhanced significantly the breakage and coalescence models in order to overcome these weaknesses. From our analysis of Chapter 6, the following aspects should be considered in future research:

a) Improvement of the numerical technique and optimization of the computer code used to solve the PBE, and test of the transient case to compare with the steady-state solution.

b) Incorporation of charge effect into the coalescence model (effect of pH).

c) Test of the predictive power of the model against experimental data obtained at conditions outside the ranges used for the parameter estimation.

d) Test of the predictive power of the model with other polymerization systems and different vessel sizes and impeller designs.

e) Development or improvement of experimental techniques for visualization of breakage and coalescence events in turbulent flow, and measurement of PSDs over wider size ranges.

REFERENCES FOR CHAPTERS 1 AND 7

Burke, A. L., T. A. Duever and A. Penlidis, "Model Discrimination via Designed Experiments: Discriminating between the Terminal and Penultimate Models on the Basis of Composition Data", *Macromolecules*, **27**, 386-399 (1994a).

Burke, A. L., T. A. Duever and A. Penlidis, "Model Discrimination via Designed Experiments: Discriminating between the Terminal and Penultimate Models Based on Triad Fraction Data", *Macromol. Theory Simul.*, **3**, 1005-1031 (1994b).

Stewart, W. E., T. H. Henson and G. E. P. Box, "Model Discrimination Criticism with Single-Response Data", *AIChE J.*, **42**, 3055-3062 (1996).

Stewart, W. E., Y. Shon and G. E. P. Box, "Discrimination and Goodness of Fit at Multiresponse Mechanistic Models", *AIChE J.*, **44(6)**, 1404-1412 (1998).

Teymour, F. and J. D. Campbell, "Analysis of the Dynamics of Gelation in Polymerization Reactors using the 'Numerical Fractionation' Technique", *Macromolecules*, **27**, 2460-2469 (1994).

Tobita, H., "Simulation Model for the Modification of Polymers via Crosslinking and Degradation", *Polymer*, **36**, 2585-2596 (1995).

Tobita, H., "Random Sampling Technique to Predict the Molecular Weight Distribution in Nonlinear Polymerization", *Macromol. Theory Simul.*, **5**, 1167-1194 (1996).

Tobita, H., "Molecular Weight Distribution in Nonlinear Emulsion Polymerization", *J. Polym. Sci., Polym. Phys.*, **35**, 1515-1532 (1997a).

Tobita, H., "Copolymerization with Chain Transfer Monomer. 2. Molecular Weight Distribution", *Macromolecules*, **30**, 1693-1700 (1997b).

Vivaldo-Lima, E. "Free-Radical Copolymerization Kinetics of Styrene/Divinylbenzene", M.Eng. Thesis, Department of Chemical Engineering, McMaster University, Hamilton, Ontario (1993).